TECHNICKÁ UNIVERZITA V LIBERCI
Fakulta textilní

Pletené distanční textilie pro multifunkční aplikace

Disertační práce

Studijní program: P3106 – Textile Engineering
Studijní obor: 3106V015 – Textile Technics and Materials Engineering

Autor práce: **Veerakumar Arumugam, M.Tech.**
Vedoucí práce: doc. Rajesh Mishra, Ph.D.

Liberec 2017

TECHNICAL UNIVERSITY OF LIBEREC
Faculty of Textile Engineering

Knitted Spacer Fabrics for Multi-Functional Applications

Dissertation

Study programme: P3106 – Textile Engineering
Study branch: 3106V015 – Textile Technics and Materials Engineering

Author: **Veerakumar Arumugam, M.Tech.**
Supervisor: doc. Rajesh Mishra, Ph.D.

Liberec 2017

Prohlášení

Byl jsem seznámen s tím, že na mou disertační práci se plně vztahuje zákon č. 121/2000 Sb., o právu autorském, zejména § 60 – školní dílo.

Beru na vědomí, že Technická univerzita v Liberci (TUL) nezasahuje do mých autorských práv užitím mé disertační práce pro vnitřní potřebu TUL.

Užiji-li disertační práci nebo poskytnu-li licenci k jejímu využití, jsem si vědom povinnosti informovat o této skutečnosti TUL; v tomto případě má TUL právo ode mne požadovat úhradu nákladů, které vynaložila na vytvoření díla, až do jejich skutečné výše.

Disertační práci jsem vypracoval samostatně s použitím uvedené literatury a na základě konzultací s vedoucím mé disertační práce a konzultantem.

Současně čestně prohlašuji, že tištěná verze práce se shoduje s elektronickou verzí, vloženou do IS STAG.

Datum:

Podpis:

Acknowledgement

This dissertation has been completed with the guidance and mentorship of many people. I would like to gratefully acknowledge their support on conclusion of this thesis.

Firstly, I would like to thank my supervisor and mentor, Associate Professor doc. Rajesh Mishra, for his encouragement at the onset of this project all the way through to the last days of it. The completion of this project was solely due to his strong commitment to my future and success. I am extremely grateful to my Supervisor-specialist, Professor Jiri Militky, who suggested that I take the challenge of undertaking PhD in the Technical University of Liberec. His enthusiasm, experience and expertise have been truly invaluable. In addition to being a supervisor specialist to me, he also committed his expertise and knowledge to assist in the completion of this work.

I would like to express my special gratitude to Associate Professors, Dr. Dana Kremenakova and Dr. Maros Tunak, for motivating and guiding me immensely through numerous stages throughout the project. My special thanks to Professor. Antonian Havelka, Prof. Lubos Hes, Dr. Jan Novak and Dr. Jana Salacova for their technical support and allowing me to use their instruments. I thank and appreciate all the technical staff of TUL for their accessibility and openness to make this research a wonderful experience. My special thanks to the Dean of Faculty of Textile Engineering, Dr. Jana Drasarova and Vice Dean Dr. Gabriela Krupincova for their continuous support. I also thank our HOD Dr. Blanka Tomkova, Secretary Katerina Struplova, Katerina Nohynkova, Hana Musilova, Bohumila Keilova for their seamless coordination and efficiency. My hearty thanks to management of Technical University of Liberec for the sustained support to pursue Ph.D degree in this esteemed institution. I really endear the relationship that we have established over the years and the support and availability to use the research facilities in TUL. Finally, I would like to thank my father and my mother, Arumugam and Indira Devi, for the foundation built for me to stand upon, and my success is proof of their commitment to building a strong person and family. Also I thank my brothers and their family, my sister and her family who have always believed and supported me with their continuous availability for help. My final appreciation goes to my wife, Dhivya, the person who supported me the most the last few years through thick and thin. She believed in me even during times when I lost faith in myself and gratitude cannot be expressed just by words. Thank you, my dear wife, for your support and patience. This thesis is especially dedicated to my beautiful daughter, Hanshitha who was born during this PhD journey and who is missing me a lot.

I look forward to starting and successfully finishing more new chapters in life.

Veerakumar Arumugam
Technical University of Liberec

Synopsis

The objective of this thesis was to examine multi-functional properties of both warp and weft knitted 3-dimensional spacer fabrics which could be used to replace the existing cushion materials in the mattress, pillows, in-sole, car seat and back supports. It presents an experimental and analytical investigation on intra-ply shear properties of 3D knitted spacer fabrics conducted using picture frame shear fixture. The nonlinear behavior of shear stress versus shear angle and the deformation mechanism were analyzed. The curves for shear stress versus shear angle and position of buckling for in-plane shear test are recorded by considering two different frame lengths in order to compare with each other. Load–displacement curves of inter-ply shear tests are also analyzed. In addition to this, a program was developed in MATLAB using Hough transform to analyze the shear angle in the real-time image taken during displacement of specimen at various positions. The results of image analysis were compared with the actual experimental results. Also, the shear stress was predicted using finite element model and compared with experimental results.

This study also determines the influence of different structural characteristics of knitted a spacer fabric on the compressive behavior and energy absorption capability. The potential compression mechanism of the fabric was identified with support of the compression stress-strain curve, work done and efficiency at different compression stages. Third order polynomial regression model was used to establish the elastic deformation properties used to obtain the compression results.

Spacer textile fabrics have superior thermal and acoustic characteristics compared to conventional woven/knitted structures, foams or nonwovens due to their wonderful 3D sandwich pattern and porous nature. Hence this research work also investigates the influence of different structural parameters of spacer fabrics e.g. areal density, porosity, thickness, stitch density etc. on thermo-physiological and acoustic performance. The sound absorption coefficient (SAC) was evaluated using two microphone impedance tube. Moreover, tortuosity of the spacer fabrics was calculated analytically and compared with experimental results. This study also discusses the influence of material parameters and structural characteristics on acoustic properties of 3D spacer knitted fabrics.

Advanced statistical evaluation and two-way analysis of variance are used to analyze the significance of various factors such as thickness, type of spacer yarn, surface structures and raw materials on specific properties. These findings are important requirements for designing knitted spacer fabrics which could be used as suitable cushioning material in the applications such as car mattress, seats, shoe insole, pillows, back supports etc.

Keywords: - 3D Spacer fabrics; in-plane shear; compression stress; energy absorption; efficiency; thermo-physiology; sound absorption

Abstrakt

Cílem této práce bylo prověřit multifunkční vlastnosti osnov a útků 3D distančních pletených textilií, které by mohly být použity jako náhrada existujících vycpávkových materiálů v matracích, polštářích, vložkách do bot, autosedačkách a podpěrách zad. To představuje experimentální a analytické šetření vlastností na vnitřních vrstvách 3D distančních textilií smykem prováděných pomocí upnutí ve fixačním rámečku (The Picture-frame shear test). Bylo analyzováno nelineární chování smykového napětí oproti úhlu smyku a deformačnímu mechanismu. Křivky smykového napětí vůči úhlu smyku a pozici vzpěry pro zkoušku smyku v rovině jsou zaznamenány pro dvé různé délky rámu pro účely dalšího porovnávání s ostatními. Jsou analyzovány zátěžové-posunuté křivky smykového testu ve vnitřních vrstvách. Kromě toho byl v prostředí MATLAB vytvořen program s využitím Houghovy transformace pro analýzu snímání obrazu smykového úhlu v reálném čase při posunutí vzorku v různých polohách. Výsledky obrazové analýzy byly porovnány se skutečnými experimentálními výsledky. Rovněž i smykové napětí bylo predikováno s použitím modelu konečných prvků a porovnáno s experimentálními výsledky.

Tato práce se také zabývá určením vlivu různých strukturních charakteristik pletených distančních textilií na chování tlaku a absorpční schopnosti energie. Potenciál tlakového mechanismu textilie byl identifikován s podporou kompresní křivky napětí/deformace, práce a účinnosti při různých stupních komprese. Třetí stupeň polynomické regrese byl použit pro stanovení vlastností pružné deformace k získání výsledků komprese.

Distanční textilie mají vynikající tepelné a akustické vlastnosti ve srovnání s konvenčními tkanými či pletenými strukturami, pěnami nebo netkanými textiliemi oproti jejich nádherné 3D struktuře sendviče a porézní povaze. Proto tato práce rovněž zkoumá vliv různých strukturních parametrů distančních pletenin,jako jsou plošná hustota, porozita, tloušťka, hustota očekatd. na termo-fyziologické a akustické vlastnosti. Absorpční koeficient zvuku (SAC) byl hodnocen pomocí dvou mikrofonové impedanční trubice. Kromě toho, křivolakost textilie byla vypočítána analyticky a porovnána s experimentálními výsledky. Tato práce také popisuje vliv materiálových parametrů a strukturních charakteristik na akustické vlastnosti 3D distančních textilií.

Pokročilé statistické vyhodnocení a dvoufaktorová analýza rozptylu jsou použity k analýze významu různých faktorů, jako je tloušťka, typ distanční nitě, povrchové struktury a surovin, na specifické vlastnosti.Tyto poznatky jsou důležitými požadavky pro navrhování pletených distančních textilií, které by mohly být použity jako vhodný fixační materiál v aplikacích pro automobilový průmysl, matrace, sedačky, vložky do bot, polštáře, podpěry zad atd.

Klíčová slova: 3D distanční textilie, smyk ve vnitřní vrstvě, komprese-napětí, absorpce energie, účinnost, termo-fyziologie, zvuková pohltivost

Table of Contents

List of Figures

List of Tables

Chapter 1 Introduction

This chapter outlines the objectives and foundation of the work described in the thesis. The first section describes the motivation for performing the experimental and analytical work included, followed by the sub-objectives and approach of the study. Finally, an overall outline is given that summarizes the contents of the thesis followed by a section that discusses the potential contribution of this work to the field of multifunctional light weight material for car seats, mattress, shoe insole, golf hitting mats, compressive bandage etc.

1.1 Motivation

The customer requirement for above mentioned applications depends on various factors, mainly shearing, excellent cushioning and conditioned air and heat (breathability) etc. There are a number of materials and structures with the above mentioned features for those applications. Airbags, bubble films, rubberized fibre cushioning, and polymer-based foams are just a few typical examples. The use of foamed materials results in a significant improvement in the passive safety, owing to their excellent energy dissipation properties. In addition, they have low apparent density and are relatively cheap; allow great design flexibility as they can be easily modeled in complex geometric parts. However, despite their promising applications, these materials are not suitable for many critical applications due to inferior comfort properties and environmental hazards both in terms of production and recycling. Hence, in order to overcome all these drawbacks in car interior application, 3-dimensional spacer fabrics has attracted attention of researchers in recent times. Spacer fabrics are a class of material with unique properties and applications. They have two outer surfaces connected to each other with spacer yarns; they provide light weight and bulkier structure. They are lightweight and designed to undergo very large deformations. Their properties are the results of the spacer fabrics microstructure, a complex three-dimensional network, low density and possibly high thickness, which undergo larger deformations during mechanical loading. Their compression and comfort characteristics are also better than conventional textile structures.

Hence, the current study relies entirely on objective measures of 3D spacer fabrics for evaluating the multi-functional properties like in-plane shear, compressibility, thermal comfort, also in addition to that acoustic performance for the replacement of foam for cushioning applications. This research aims to provide a new material and design strategy for the replacement of existing cushioning materials with 3D spacer fabrics. For better performance, different materials and methods were used to aid in the determination of the best material parameters for the improvement of functional properties. A thorough study of the properties of the processed materials was performed.

1.2 Objectives

The goal of the current study was to characterize the 3-Dimensional knitted spacer fabrics for the multi-functional application. This research mainly involves investigating the effect of various

structural and material characteristics on multi-functional properties of both warp and weft knitted spacer fabrics. The major sub-objectives of this research work are as follows:

1.2.1 To study the effect of structural parameters on advanced characteristics of spacer fabrics

The aim of this work was to investigate various structural parameters of 3D knitted spacer fabrics such as knit structure, thickness, type of spacer yarn, stitch density, porosity and volume density on mechanical and functional properties. This study specially focuses on spacer fabric behavior such as in-plane shear deformation, compressibility, air and water flow, thermal behavior and acoustic properties due to their structural variations. Due to the advanced characteristics of spacer fabrics such as bulkiness, lower density and air layer in the middle part, spacer fabric might be a proper selection for various applications according to its suitability.

1.2.2 Theoretical and experimental analysis of in-plane shear behavior of 3D spacer knitted fabrics

The objective of this study was to study the shear behavior of 3D spacer knitted fabrics by using a picture frame fixture. Three different methods were used to find the shear angle during loading rate of 10mm/min. All the tests were recorded by a CCD monochrome camera. The images acquired during loading process were used for analysis in order to obtain the full-field displacement and shear angles at chosen points on the surface of test specimen. To determine its suitability for measuring intra-ply shear properties of 3D knitted spacer fabrics, an experimental and analytical investigation of picture frame shear fixture was conducted. In this work, a fixture was designed to analyze the in-plane shear behavior of these fabrics. The nonlinear behavior of shear force versus shear angle and the deformation mechanism were analyzed. The curves for shear force versus shear angle and position of buckling for in-plane shear test were recorded by considering two different frame lengths in order to compare with each other. Load–displacement curves of intra-ply shear tests were also analyzed. In addition, a MATLAB program was developed using Hough transform to analyze the shear angle in the real-time image taken during displacement of specimen at various positions. The image analysis results were compared with the actual experimental results.

1.2.3 Study of compressibility and related behavior of 3D spacer fabrics

The aim of this study was to determine the influence of different structural characteristics of knitted spacer fabrics on the compressive behavior and energy absorption capability. The potential compression mechanism of the fabric was identified with support of the compression stress-strain curve, work done and efficiency at different compression stages. Third order polynomial regression model was used to establish the elastic deformation properties used to obtain the compression results. Advance statistical evaluation and two-way analysis of variance was used to analyze the significance of various factors such as thickness, spacer yarn diameter and surface structures on energy absorption at maximum compression load and deformation. These findings are important requirements for designing warp and weft knitted spacer fabrics for

cushioning applications.

1.2.4 Thermo-physiological characteristics of knitted 3D spacer fabrics

In recent years, mattress, shoe-insole, automobile interiors etc. play an important role in improving thermal comfort. This research was to evaluate the thermal comfort properties of 3-Dimensional knitted spacer fabrics which could be used to replace the existing polyurethane foams in the functional applications. This study was to determine the influence of different characteristics of spacer fabrics like structure, areal density, thickness, density on thermo-physiological performance. The potential thermal behavior was identified with the support of the thermal conductivity and resistance evaluation. The air and water vapour permeability were measured and analyzed in order to study the breathability performance of spacer fabrics. Advanced statistical evaluation and two-way analysis of variance was used to analyze the significance of various factors on desired properties. These findings are important requirements for designing the cushioning materials with required thermal comfort properties using 3D spacer fabrics.

1.2.5 Study of acoustic behavior of 3D knitted spacer fabrics with respect to permeability

This study also focussed on finding the suitability of 3D porous spacer fabrics for the interior applications by improving acoustic performance. Hence, an experimental investigation on the sound absorption behavior of 3D knitted spacer fabrics was conducted. The sound absorption coefficient (SAC) was measured using two microphone impedance tube. Moreover, tortuosity of the spacer fabrics was calculated analytically and compared with experimental results. This study deeply discusses the influence of material parameters and characteristics on acoustic properties of 3D spacer knitted fabrics.

1.3 Research approach and outline

The research work has covered different aspects of manufacturing of a lightweight material for cushioning applications as well as the study of different characteristics that should be considered in mattress, car seats, insole, mats etc. The content of this thesis is organized into five chapters. They are as follows;

- **Chapter** 1 begins by discussing general introduction of this research work such as motivation and detailed research objectives of this thesis.

- **Chapter 2** provides the detailed discussion of the requirements for mattress, insole, car seats and mattress materials, spacer fabrics and its suitability. This chapter contains literature review and detailed study of previous articles and understanding of studies conducted, limitations in past research.

- **Chapter 3** describes the methodology, which includes experimental materials, test equipments and data acquisition used for all experiments performed in this study.

This chapter also has elaborate explanation about methods and techniques used for characterization of shear, compression, thermal and acoustic experiments conducted.

- **Chapter 4** presents a detailed analysis of the results derived from various experiments. The results were tabulated, suitable graphical representations made and detailed statistical analysis was performed. Various interpretations were drawn from the analysis.

- **Chapter 5** contains the broad conclusions drawn from the result and analysis of the research. An additional section discussing future research and recommendation has been included. The outputs are in the form of scientific papers, book chapters and conference proceedings.

Chapter 2 Literature review

2.1 Introduction

The purpose of this chapter is to provide a background for the research conducted in this thesis. The first part of this literature deals with the cushioning materials and the required properties to make the customer more comfortable. The later parts contain details of 3-dimensional knitted spacer fabrics and its special characteristics which are suitable to replace the existing material for mattress, insole, car seats and mats. Finally, the existing literature and the highlighted research gaps relevant to the various objectives of this research work have been summarized.

2.2 Cushioning materials

Foam is an important engineering material used in cushions of mattress, car seats, insole, pillows, packaging, acoustic absorption and upholstery. Foams are typically used under compression, but it is very likely that also shear loading will occur in the foam components of the cushions. It is the primary means used in most modern seats, mattress and insole to achieve static comfort and vibration isolation which also happens to be the application area. It is non-linear and viscoelastic in nature. Its increasing importance as an engineering material has led to a detailed study of its structure and properties [1,2]. The foam has a relatively complex geometry, with curved surfaces and varying thickness in order to provide the desired properties for support and cushioning. The foam material is uniform over the thickness. This means that the thickness is the only parameter to the mechanical cushioning behavior of the foam components. The behavior of foams in general can be described as highly non-linear and strain rate dependent with high energy dissipation characteristics and hysteresis in cyclic loading. For low levels of stress, high levels of strain can be obtained. Low density combined with high energy dissipation capacity make foams attractive for energy absorbing functions in cushioning applications. However, the three-dimensional mechanical response of foam materials is quite difficult to capture in a mathematical model. At small strains, the mechanical behavior is close to linear elastic, followed by a large order of magnitude reduction in slope. Then, there is a long region in which the slope changes gradually. This stage corresponds to the collapse of cells. In this stage, the air is gradually pressed out of the foam. After the cells have collapsed, the final stage of densification is reached in which the cells come in contact with one another causing a sharp increase in the stress [3, 4]. The polyurethane foam (PUF) is characterized by its strongly non-linear and compressible feature. It is a hyper-elastic cellular elastomeric that presents a significant visco-elastic behavior (Figure 2.1). A few studies have analyzed the PUF performance in terms of distribution of human-cushioning material interface pressure under static loading. These have established that softer PUF provides the occupant with greater comfort sensation since the contact pressure is more evenly distributed over the contact area of the human body with the seat pan as well as the backrest. Soft foams, however, tend to bottom easily and could thus cause considerable discomfort. Alternatively, relatively harder PUF protect the heavier subjects against bottoming and yield enhanced sensation of stability; but cause

concentrated pressure zones for the lighter subjects. Blair et al. [5] investigated the effect of chemical structure of PUF on dynamic and static characteristics of the seat cushions and concluded that cushions with moderate hardness and high thickness yield lowest vibration transmissibility at low frequencies and near the resonance frequency. It has been further shown that thick PUF cushions yield lower stiffness and higher deflections [6]. However, the hysteresis loss for a thicker PUF sample was observed to be less than that of the thin foam, which led to higher vibration transmissibility.

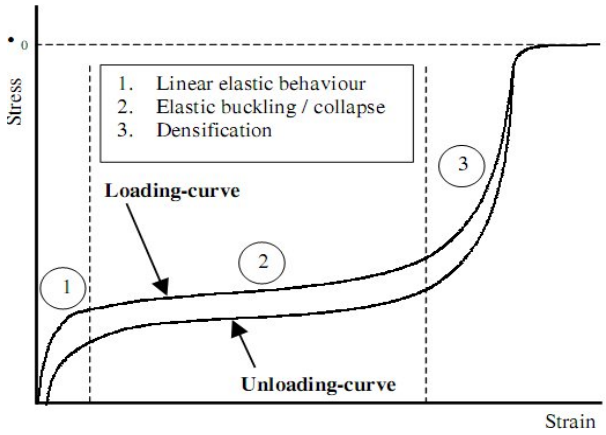

Figure 2.1 Compressible feature of polyurethane foam [4]

2.2.1 Problems and replacement of PU foam for cushions

The PU foam, thanks to its specific characteristics, is the key element of the multilayer fabric in terms of comfort and mechanical behavior especially for the compression ones. The main issue with PU foam is partly the toxic gases it generates during its manufacturing process and recycling [7]. In fact, the recycling processes of such products require a delamination step of the different layers (PET, PU, PA). This operation is not optimal because some PU foam remains on the textile fabrics. It is also important to note that the machines used for the recycling are very expensive. The PU foam has many serious drawbacks such as flammability and gases emissions due to the laminating processes. These problems lead to the question of its replacement by a new product. A key requirement of this new product is not to alter the product functionality. It means that the new product should present at least mechanical properties, especially compression properties close or equal to the actual multilayer fabric. Another key aspect is to propose an environmentally friendly solution for complex fabric composed of a mono material product. This new product should comply with the cushioning application specifications in terms of weight, formability and cost. In this context, industries and researchers all around the world are developing new products which could substitute the PU foam [8, 9]. Analyses of the existing solutions have been carried out by textile industrialists and the obtained results show that the 3D textile technologies offer the best solution in terms of product quality and cost. 3D textiles offer a good solution to the recycling issue of the multilayer products using PU foam because of their specific structure as spacer fabric. In fact, they present a vertical orientation of the yarns

(weaving and knitting technologies) or a vertical orientation of the fibres (nonwoven technology) [10]. This vertical orientation will provide a good mechanical behavior especially in term of compression. It appears that the knitted spacer fabric provides the most interesting solution in terms of mechanical properties, cost and productivity.

2.2.2 Design parameters of cushions in mattress, seats, insole and mats

Design parameters that affect the local sensation of comfort at the interface between the occupant and cushion are called “Feel” parameters. The effects of “Feel” parameters are detected by nerve receptors in the skin and superficial underlying tissues. Four stimuli applied to the skin surface are important contributors to local tissue discomfort [11].

2.2.2.1 Compression pressure

It is the force generated directly normal to the skin surface whenever the tissue bears external load. Of course, the skin is continually under hydrostatic pressure from the atmosphere, but this pressure does not cause discomfort. In fact, the skin and underlying tissues are remarkably impervious to hydrostatic pressure (equal components in all directions) as when submerged in water. The physiological effects of surface pressure in seating are due to deformation of the skin and underlying tissues, resulting in occlusion of blood vessels and compression of nerves. Pressure on nerves can cause discomfort immediately, while loss of blood circulation leads to discomfort as cell nutrition is interrupted and metabolites build up in the tissues. The state of stress in body tissues produced by application of external pressure can be decomposed into a combination of hydrostatic and shear stresses. Chow and Odell (1978) point out that since body tissue is relatively impervious to hydrostatic stress; it is the shear stress and accompanying deformation that are harmful [12].

2.2.2.2 Shear stress

Shear stress results internally whenever a uniaxial load is applied to the skin, as is the case in sitting when pressure is applied to the dorsal surfaces of the buttocks and thighs. The primary cause of discomfort associated with external pressure is the shear stress and deformation that result internally. Shear stresses applied externally (surface friction) have a compounding effect, producing larger tissue deformations than the surface pressure alone. External shear stress often occurs in seating, particularly under the buttock area when the torso is reclined.

2.2.2.3 Temperature

The temperature can affect the local feeling of discomfort, with both high and low temperatures being perceived as uncomfortable. Both the foam padding and surface material of the mattress, seats, insole and mats affect the skin temperature at the interface [13].

2.2.2.4 Humidity

Humidity interacts with temperature to influence discomfort. Perspiration that is trapped against

the skin by the upholstery can produce a sticky feeling if the skin is warm or a clammy feeling if it is cold. Both the foam padding and the surface covering of the cushion are important determinants of local humidity on the seat [14]. The Feel parameters of compression pressure and shear stress are considered together because their discomfort causing mechanisms are closely related. Similarly, local temperature and humidity are usually measured simultaneously and are discussed together.

2.3 Spacer fabrics – a brief Introduction

Spacer fabrics can be defined as fabrics which have two outer surfaces connected to each other with spacer yarns. Since the middle layer comprised of monofilaments or yarns, the fabrics possess special characteristics. Figure 2.2 illustrates a kind of spacer fabric in which its third dimension (thickness) is significant. Components in spacer fabrics differ depending on the yarn type and production method [15]. It has excellent compression elasticity and breathability is the greatest advantages of spacer fabric [16]. Admirable compressibility indicated that, crush resistant property and bending performance are excellent. Spacer fabric possesses excellent cushioning and shock absorbing properties [16]. It is because spacer fabric is able to absorb and dissipate kinetic mechanical energy when it is subjected to compression at regular stress over a large extent of displacement [17]. In spacer fabric construction, the two separate outer fabric layers are kept apart by spacer yarns through the thickness direction. A through-thickness property is developed in this 3D textile composite [18]. The spacer yarns act as linear springs, yarn loops are deformed under impact loading and hence created a high damage tolerance characteristic [16]. Besides, the hollow structure created by the spacer yarns between two outer layers resulted in outstanding moisture transmission property since moisture vapour is allowed to transmit freely [19]. Thermal comfort is improved and the chance of skin maceration is reduced in this moisture free environment created by the spacer fabric. The major application areas are automotive textiles, medical textiles, geotextiles, protective textiles, sportswear and composites [20]. This part of review is mainly focuses on knitted spacer fabrics and their production technique, properties and applications.

2.4 State of art – spacer fabrics

The three dimensional knitted fabric can be produced in different methods. The classifications of 3D knitted fabrics are given below (Figure 2.3). In particular, this review mainly focuses on to discuss about knitted spacer fabrics and their production methods, properties and applications. Spacer fabrics are special types of 3D fabrics which are characterized by two outer fabric surfaces connected with pile yarns. Warp knitting, weft knitting and weaving technologies are suitable for producing this kind of 3D structures [21, 22]. The knitted spacer fabrics can be produced by using either warp or weft knitted technologies.

2.4.1 Warp knit spacer fabric

Warp knitting spacer fabric is usually knitted on a rib Raschel machine with two needle bars and a number of guide bars (Figure 2.4). The warp knitting spacer fabric has a higher thickness [23]. There are two major classes of warp knitting machines: raschel and tricot. Fabric on raschel machines is drawn downward from the needles almost parallel to the needle bar, at an angle of 120-160 degrees. This angle creates a high take-up tension, particularly suitable for open fabric structures such as laces and nets. The warp beams are arranged above the needle bar and centered over the top of the machine so that the warp yarns pass down to the guide bars on either side of them. The guide bars are numbered from the front of the machine. Raschel machines can accommodate at least four 32-inch diameter beams or a large number of small diameter beams. Raschel machines typically knit with latch needles or compound needles. Machine gauge is expressed as needles per inch. The gauge range can be from 1 to 32. The simple knitting action and the strong and efficient take-down tension makes the raschel machine well suited for the production of coarse gauge open work structures using pillar stitch, inlay lapping variations and partly threaded guide bars (Figure 2.5). Raschel sinkers perform the function of holding down the loops while the needles rise [24].

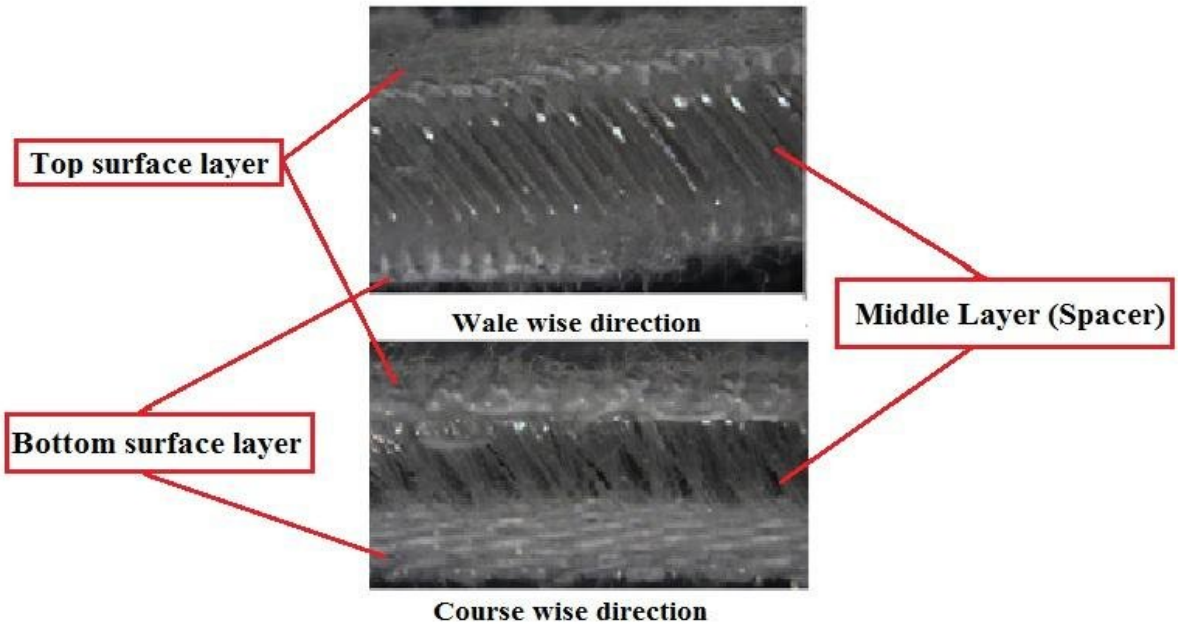

Figure 2.2 Structure of spacer fabric [48]

On the other hand, fabric on tricot warp knitting machines is drawn towards the batching roller, almost at right angles to the needle bar. This creates a gentle and lower tension on the fabric being knitted. The maximum number of beams and guide bars on tricot warp knitting machines is limited to four, and the majority of tricot warp knitting machines operate with only two guide bars [25]. The machines have a simple construction and a short yarn path from the beams. Guide bars are numbered from the back of the machine towards the front of the machine. This makes it

ideal for the high speed production of simple, fine gauge (28-44 needles per inch), close-knitted, plain and pattern work. For that reason, many lingerie and apparel fabrics are knitted using two guide bar structures with both bars overlapping and under lapping.

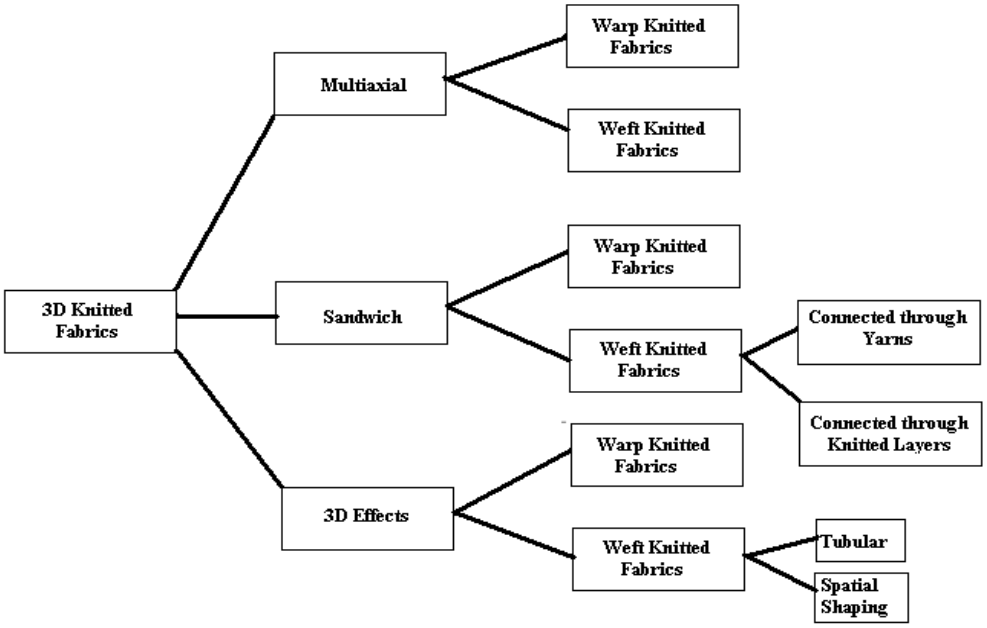

Figure 2.3 Classifications of 3D knitted fabrics [21]

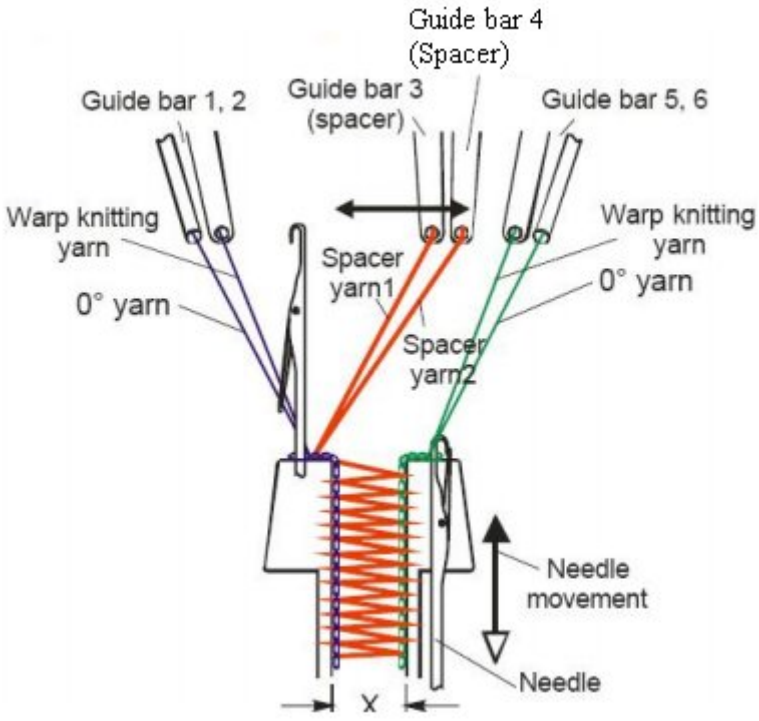

Figure 2.4 Warp knitted spacer fabrics in raschel machine [27]

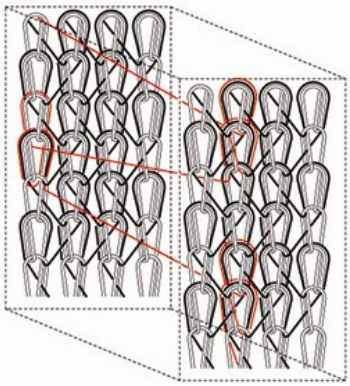

Figure 2.5 Structure of warp knitted spacer fabrics [26]

2.4.1.1 Mechanism of double needle bar raschel

Double needle bar raschel produced as a plain or semi plain pile structure which utilize up to 48 guide bars and follows the double plush woven model. Two fabrics are knitted at the same time but one behind the other. One is on the front needle bar and one on the back needle bar and they are joined by warp moving between the two and controlled by the guide bars, thus creating double cloth comprising two single cloths with the centre composed of yarn floating between the two cloths. It is possible to refer to the gauge of each needle bar separately or together. The accessibility of the raschel machine is the simple knitting action, and its strong and efficient take down motion [26, 27].These double needle bar fabrics popularly known as warp knitted spacer fabrics (Figure 2.6). Double needle bed Raschel machines designed for spacer fabric are built with varying numbers of guide bars one for each yarn supply beam. The needle bars are operated independently in an up-and-down movement, while the guide bars "shog" alternately back and forth across the needles of each bar. The warp knit fabric design and lapping sequence is controlled by the links, whose height is defined between each course and directs the shogging (back and forth) movement on each of guide bar independently. The shogging movements of the guide bars control different warp knit designs. "Different shogging movements are initiated by varying the radius of a continuously turning pattern shaft, either in the form of different heights of pattern links that pass over a pattern drum attached to the shaft, or in the form of carefully shaped solid metal circular cams, termed pattern wheels. Figure 2.7 shows a pattern drum that can be rotated with links of different heights controlling the shogging movements of an associated guide bar [28]. The movement of each guide bar is controlled by a separate sequence of chain links whose height is different in certain order according to the pattern. The height difference produces a thrust against the end of the push rod, resulting in movement of the associate guide bar. An increase in height from one link to the next produces a positive shog in a direction away from the pattern device while a decrease in height produces a negative shog. A constant height will produce no shog and the guide bar will continue to swing through the same needle space, producing a pillar stitch [28 - 31]. The guide bars swing or shog in front and at back of needs at the mean while the needles move up and down to form continuous loops. The

different structures of face side warp knitted spacer fabrics are shown in Figure 2.8.

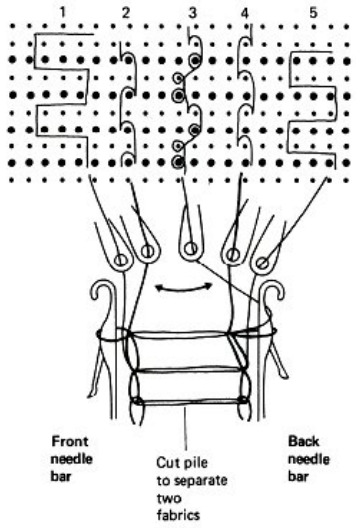

Figure 2.6 Structure of the needle bars and guide bars on a double needle bed machine [27]

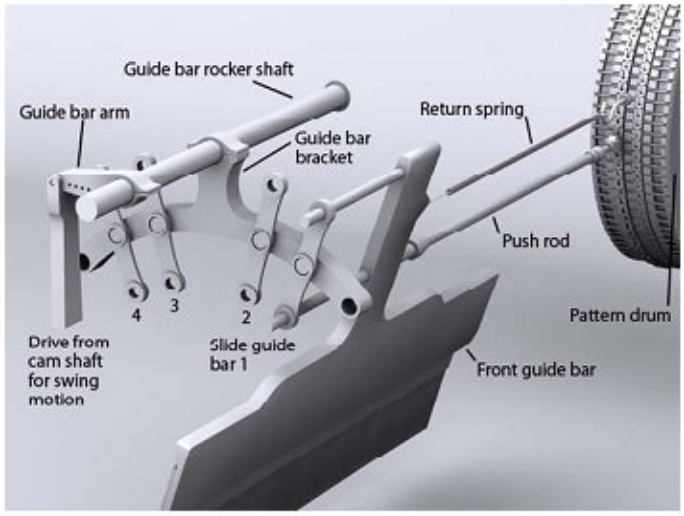

Figure 2.7 Design mechanism of pattern drum [28]

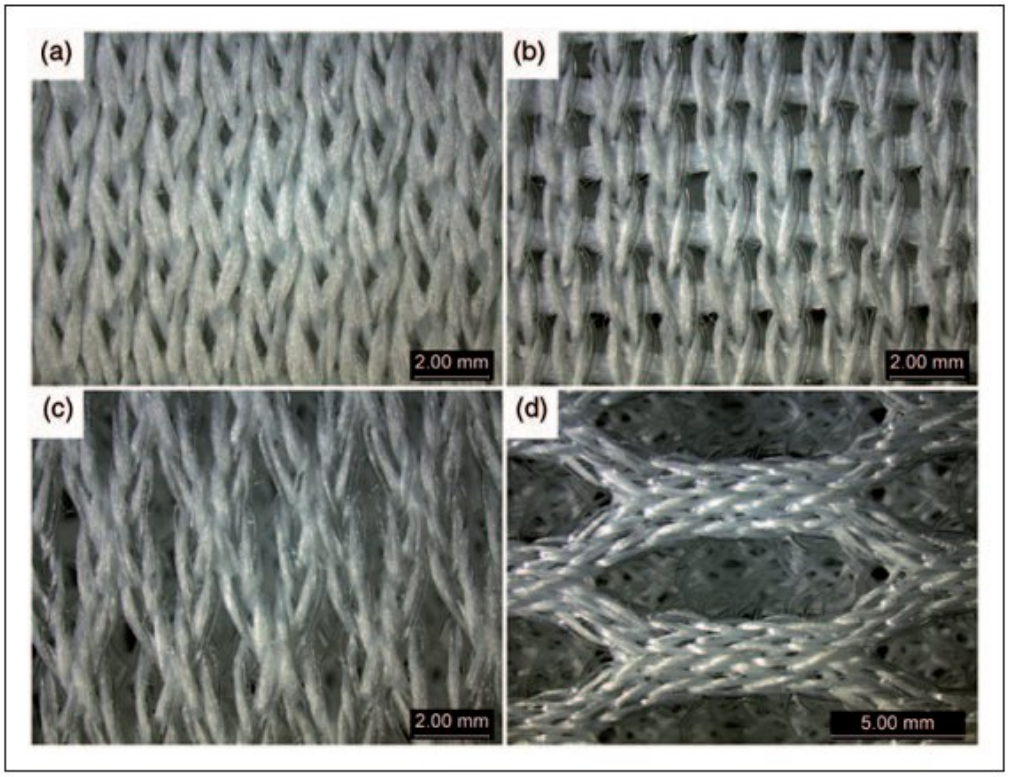

Figure 2.8 (a) locknit; (b) chain plus inlay; (c) rhombic mesh and (d) hexagonal mesh [27]

2.4.2 Weft knit spacer fabrics

Weft knitting spacer fabric is usually knitted on a double jersey circular machine, and fabric width is limited by the needle cylinder in Figure 2.9 [32 -34]. The two primary forms of weft knitting machines are circular knitting machine and flat knitting machine. Circular machines can be subdivided into single jersey, dial and cylinder, and double cylinder purl machines according to the needle set used and the fabrics made [33]. Weft knitting machines with two sets of needles have the potential to produce two separate covering layers that are held together by tucks. It is considered that dial and cylinder, and purl machines are able to produce spacer fabric. Flat knitting machines can be divided into two types- the V-bed machine and flat Purl machine. V-bed machine is useful in the manufacture of spacer fabrics while flat purl machine is rarely used in today's applications. The dial and cylinder machine can connect two separate layers of fabric together by the use of various combinations of stitches. To produce a dial and cylinder spacer fabric, at least three different yarns are required to form each course of the fabric including yarn for dial needles; yarn for cylinder needles; and spacer yarn [34, 35]. Dial height determines the amount of pile yarn being fed between two surface layers. By adjusting the dial height, producer can alter the distance between the two layers [33 - 34]. Spacer fabrics can also be produced with a V-bed flat knitting machine as shown in Figure 2.10. A tubular knitted fabric is connected with mainly mono filament pile connections. Pile yarns are inserted with a zigzag movement between two fabric layers. Angle of connections can be varied, which enables a construction with a

localized adjustment of compression stiffness. The distance between the two needle beds determines the spacer fabric thickness. Unlike circular knitting machine, the distance between the two needle beds of a flat knitting machine fixed around 4 mm. By using computerized flat knitting machine with elastomeric yarn, the spacer fabric thickness can vary in a wide range. But the productivity is very low while knitting the thicker spacer fabrics. The mechanism of tucking on two sets of needles leads to ineffective constraints on spacer yarn provided by outer fabric layer stitches. So, The distance between two needle beds is the cause of limited dimensions [35]. By the use of a V-bed machine, two independent covering layers are knitted on the front and back needle beds respectively. Spacer fabric is created by tucking a pile yarn to link the two separate fabrics together [35, 36].

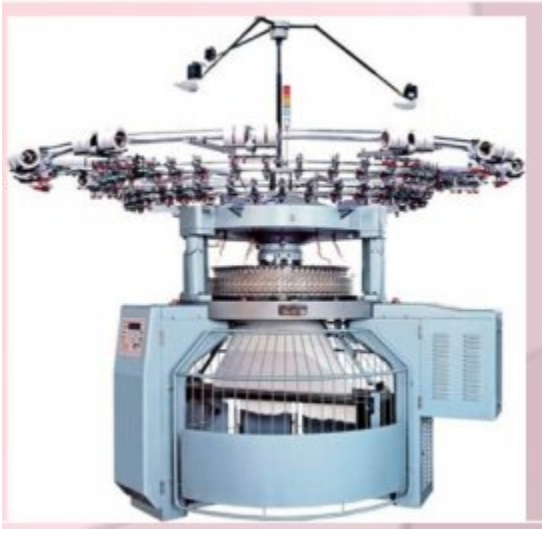

Figure 2.9 Double jersey circular knitting machine

2.4.3 Spacer (middle) layer

There are two types of connecting layers [36]:

1. **Single layers** – the layer is produced on one bed (jersey) or on both beds (rib, interlock) and can have a perpendicular or an inclined disposition between the separate fabrics.
2. **Double layers** - two layers are knitted separately on the beds, connected at a certain point with a rib evolution; if a specified amount of rib courses will be produced also in the exterior fabrics, then the connection will be "X" shaped, with possibilities to extend more the rib dimensions or to alternate the disposition of the two layers. Figure 2.11 shows the types of connecting layer (spacer).

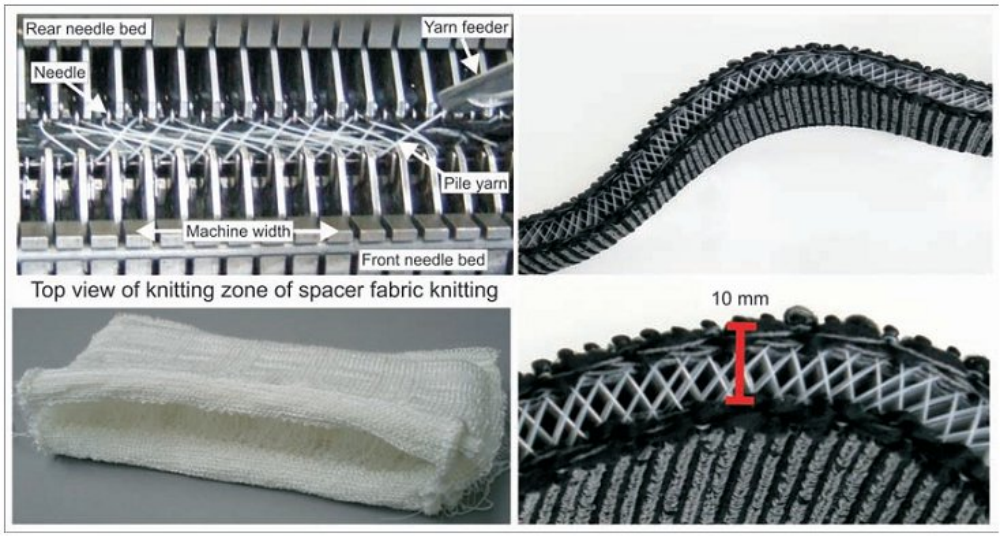

Figure 2.10 Flat knitted spacers [35]

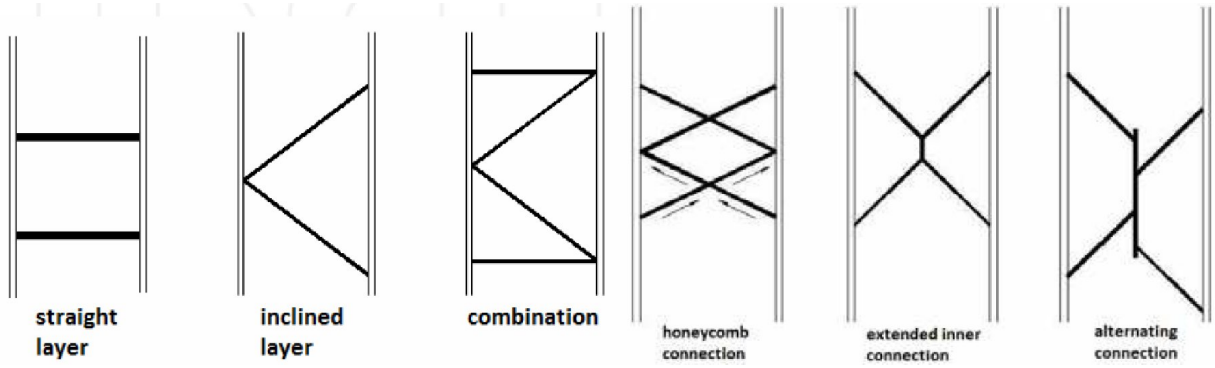

Figure 2.11 Types of spacer layers [36]

2.4.4 Properties of knitted spacer fabrics

2.4.4.1 Mechanical properties

The critical mechanical properties of spacer fabrics are those related to tensile strength, tear strength and stiffness. Tensile strength of spacer fabrics measures the fabric's ability to resist the tensile forces resulting from pre-stress in combination with external loads and it measures the level of direct pull force required to rupture the fibre of material [37, 38]. Stiffness is of course related to modulus of elasticity of the material and the area of fibres employed, which may vary in the warp and fill directions of the material. In addition, the type of weave employed and the manufacturing process will both effect stiffness variation under load due to crimp interchange.

2.4.4.2 Impact properties

The structural parameters of a spacer fabric have significantly effect on its protective performance [39]. Among a group of spacer fabrics, the spacer fabric knitted with higher inclination and coarser spacer monofilaments, a bigger fabric thickness, and a more stable outer

layer structure will have a better force attenuation capacity, Liu et. al., have studied the impact properties of warp knitted spacer fabric by varying different parameters. First, the thickness and outer layer stitch density of the two fabrics are also kept nearly the same. As shown in Figure 2.12, it can be seen that the spacer fabric with the coarser spacer monofilament has a lower peak transmitted force and a longer time to the peak point and, therefore, has a better impact force attenuation property [39, 40]. They also investigated, the group of three fabrics with the same outer layer structure (chain plus inlay) and the same spacer monofilament yarn but with different spacer monofilament inclinations (under lapping one needle, two needles, and three needles between the front- and back-needle bars) is used to analyze the effect of the spacer inclination on the impact force attenuation properties of warp-knitted spacer fabrics (Figure 2.12). The fabric thickness and stitch density of the outer layers are kept nearly the same. The number of the needles under lapped determines the spacer monofilament inclination and length. The higher the number of the needles under lapped, the longer and more inclined the spacer monofilaments.

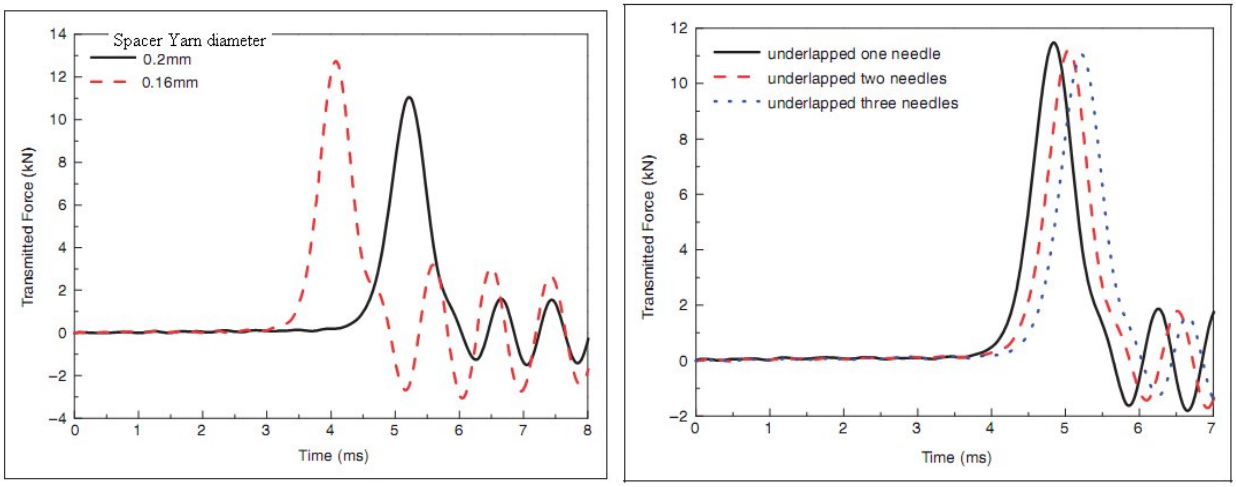

Figure 2.12 Effect of spacer yarn characteristics on transmitted force–time curves (fabric layer: 1; impact energy y: 5 J) [39, 40]

As shown in Figure, the transmitted force–time curves of these fabrics in single layer under impact at a kinetic energy of 5Joules are used as an example for discussing the effect of the spacer monofilament inclination with the same impact energy. It can be seen that while the duration from the beginning point where the striker contacts the fabric upper surface to the peak point where the transmitted force reaches the maximal value increases as the spacer monofilament inclination increases; the peak transmitted force decreases as the spacer yarn inclination increases. This means that the spacer fabric with a higher spacer monofilament inclination and a longer spacer monofilament length more electively resists the impact due to a lower peak transmitted force [39, 40].

2.4.4.3 Bending rigidity

Machova et. al., have studied the bending properties of both warp and weft-wise spacer fabrics.

It appears that the bending rigidity of a spacer fabric is greatly related to the fabric type. Thus, a weft-knitted spacer fabric has a higher bending rigidity in the weft-wise direction, while a warp-knitted spacer fabric has a higher bending rigidity in the warp-wise direction (Figure 2.13). This behavior is mainly due to the directionality of the incorporated yarn [41]. When the samples are of the same fabric type (weft-knitted spacer fabric for example), we can further conclude that the bending rigidity is closely related to the fabric's density, spacer structure and spacer type [38] They also found that weft-knitted spacer fabrics using interlock structure, monofilament spacer yarn and a higher fabric density have a higher bending rigidity.

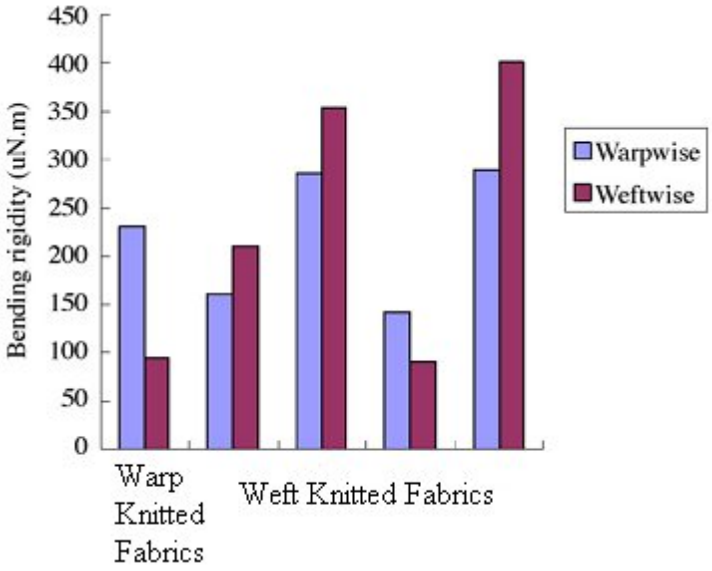

Figure 2.13 Bending rigidity of spacer fabrics [38]

2.4.4.4 Stretch and recovery

Yip and Ng have found and suggest that the stretchability of the spacer fabrics is closely related to their fabric type [47]. The results shown in Figure 2.14 reveal that the stretchability of a warp-knitted spacer fabric has a high stretchability only in the weft-wise direction, while the stretchability in the warp-wise direction is very low (below 50%). On the other hand, weft-knitted spacer fabrics have similar and high stretchability in both the weft-wise and warp-wise directions. As the spacer fabric is composed of two separate surface fabrics and linked together by a spacer yarn, it can therefore be concluded that spacer fabrics carry the same fabric stretchability as their fabric types (i.e. warp-knitted or weft-knitted). When the results of the weft-knitted spacer samples were compared, the stretchability in the weft-wise direction of samples 2 and 3 were found to be higher than those of samples 1 and 4. This is due to samples 3 and 4 using multifilament spacer yarns, which have higher stretchability than those corresponding to samples using monofilament spacer yarns [38].

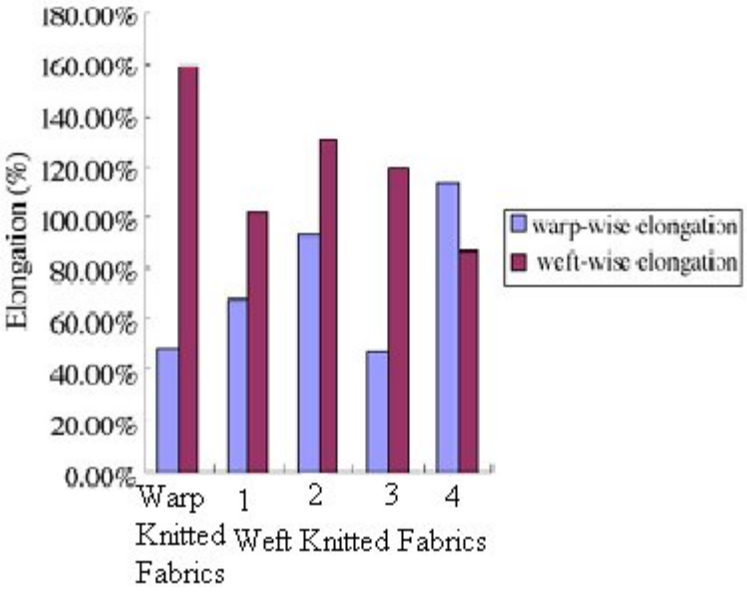

Figure 2.14 Elongation of different spacer samples [38]

2.4.4.5 Compressibility

Spacer fabrics are very resilient and will resist and recover from pressure that may be applied on them thus deformation is not a problem in apparel made using spacer fabrics and this may increase the life of the garment. The stress-strain curve of the spacer fabric reported in article [42] is given in Figure 2.15. Three distinct regions in this curve can be observed: modulus, collapse and densification regions. The modulus of elasticity is defined as the initial slope in the linear elastic part of the stress-strain curve (modulus region). The initiation of collapse region is characterized by a relatively large deformation that occurs with a constant stress. During this stage, the monofilaments bend, so the thickness of the spacer fabric will decrease. This constant stress is referred to a collapse stress or a collapse plateau. The most compressibility behavior and deformation of 3D fabrics occurs in this region, this is why this region is the subject of many investigations in the cushion fabric mechanical behavior. In the densification region, monofilaments are engaged to each other and the deflection change decreases; the slope of stress-strain curve will decrease [37, 43, 44, 49].

2.4.4.6 Shear properties

The shearing behavior of a fabric determines its performance properties when subjected to a wide variety of complex deformations during its use. The ability of a fabric to be deformed by shearing distinguishes it from other thin sheet materials such as paper or plastic films. This property enables fabric to undergo complex deformations and to conform to the shape of the body [42]. Shear properties influence draping, flexibility and also the handle of fabric. The shear behavior of 3D spacer fabrics was investigated by using a picture frame fixture. The image analysis procedure can provide much more information about the shear behavior of the fabric than stroke measurement. The displacement data, and shear angles change during loading

process can aid in the understanding of the shear behavior of the fabric. It is found that shear deformations depend very much on the type of spacer yarn and the fabric stitch density. The non-linearity of shear deformation increases after limiting locking angle which initiates the buckling of the sample [42].

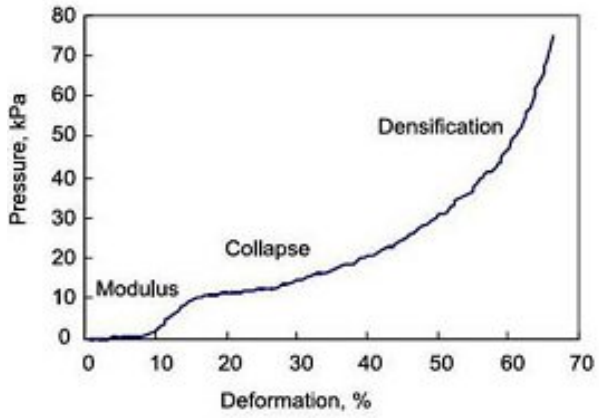

Figure 2.15 Stress-strain curves for spacer fabric during compression [37]

2.4.4.7 Sound absorption

The properties of spacer fabrics such as 3D fibre disposition, possibility to use different materials and single step production system, enable them in different application areas. Dial et al. introduced fabric with spacer fabric structure to improve sound absorption performances. Their studies analyzed and reported that acoustic performance of plain weft knitted spacer is good in middle and high frequency range [45]. Liu and Hu analyzed and compared the effects of different fabric layers and arrangement sequences of both warp and weft knitted spacer fabrics on the noise absorption coefficient [46]. They suggested that sound absorption behavior of spacer fabrics are effective with multilayer arrangements backed up with air cavity. There is only few research studies conducted on acoustic performance of spacer fabrics. Erhan Sancak determined that three factors have a major impact on the sound absorbance behaviour; thickness of fabric, micro porosity between fabric surfaces and yarn linear density in the interconnection of the fabrics (Figure 2.16) [47]. Arumugam et al deeply discusses that the spacer fabrics have too much air in the pores, hence, sound energy dissipation may weaken when the porosity is higher than 0.9. The air flow resistivity is inversely proportional to the porosity of the fabrics; therefore, the sound absorption can increase with decrease in porosity and increases with air flow resistivity. The 3D spacer fabrics have more tortuous path but still lower sound absorption because incident sound energy may get reflected away from the top layer and does not penetrate in to the fabric. The thickness of the porous material layer has also a great influence on the position of the peak value in the frequency spectrum. But the effect of density is more predominant in terms of sound absorbency as compared to effect of thickness [48].

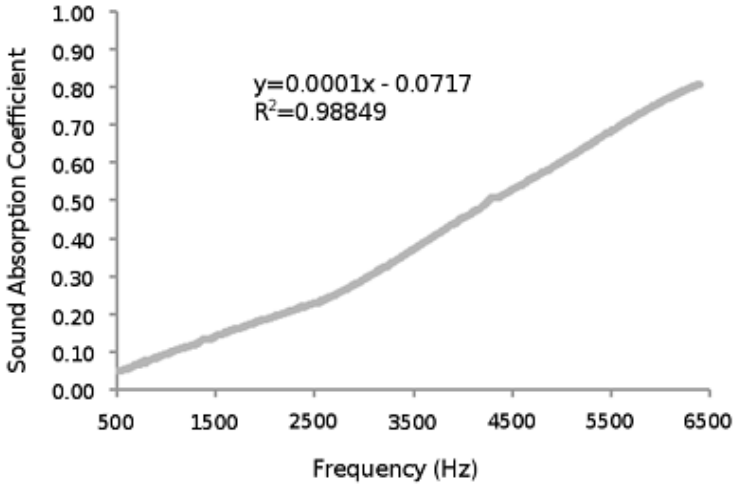

Figure 2.16 Sound absorptive knitted spacer fabrics [47]

2.4.4.8 Air permeability and moisture management

Air permeability is another important factor that should be taken into account when choosing fabrics for certain applications. In this regard, weft knitted spacer fabrics have significantly better air permeability ratings, and are thus more able to resist air penetration, than the warp knit fabric [44]. Although, it should be noted that the density of the fabric, regardless of whether it is a warp knit or a weft knit will have a substantial impact on the air permeability and thermal regulation properties. A spacer fabric that is quite dense will have a higher thermal conductivity value, but a low air permeability value; therefore end use must be taken into consideration to find an optimum density for the fabric [49, 50]. In regard to breathability, moisture wicking, and insulation of spacer fabrics, research at the Institute for Textile and Clothing Technology at the Hohenstein Institutes was conducted in regard to the insertion of a hydrophilic weft yarn on the face of the spacer fabric that is closest to the body, and it s effect on the body's microclimate. Using a spacer fabric made of polyester (PES), monofilament for the pile and multifilament for the faces, and various inserted weft yarns, which accounted for about 5% of the total fabric, in the face of the fabric closest to the body, which also had a ribbed construction Machova, Hoffmann, and Cherif found that the inserted weft yarns increased the density of the fabric, and thus lowered the air permeability [50]. It was also found that viscose weft yarns increase heat transport by 14.2% when compared to spacer fabrics without inserted weft yarns. The inserted weft yarn, while increasing the thermal insulation properties of the fabric, also can increase the dimension stability of the fabric. Moisture management behavior is a vital factor in evaluating thermal and physiological comfort of functional textiles. Air and water vapour permeability, vertical wicking and moisture management of spacer fabrics with different fibre properties (fibre cross section profile) have been studied quantitatively by various authors. They suggested that these spacer fabrics can be used for protective vest to absorb a user's sweat, to reduce the

humidity and improve user's thermal comfort [51]. For this reason, Bagherzadeh et. al., have investigated the different 3D warp knitted spacer fabrics were produced with functional fibre yarns in the back layer of the fabric (close to the body) and polyester in the front and middle layers (outer surface). Comfort properties such as air and water vapour permeability and wicking and other moisture management properties (MMP) of different fabric samples were measured. It is demonstrated that by using profiled fibres such as Coolmax fibre, moisture management properties of spacer fabrics can be improved significantly (Figure 2.17). It is expected that these properties of 3D functional spacer fabrics, beside their good ventilation property, enable them to be used as a snug-fitting shirt worn under protective vests to feel lower humidity and to be dry and comfort [51].

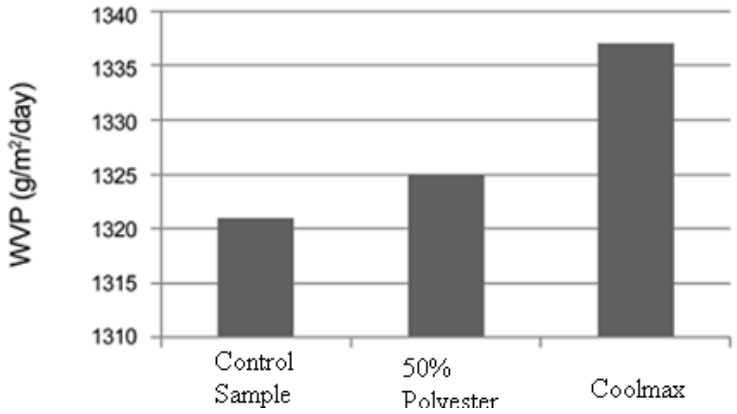

Figure 2.17 Comparisons of water vapour permeability [51]

2.4.5 Applications of knitted spacer fabrics

2.4.5.1 Cushioning applications

Cushioning materials are used to dissipate the kinetic energy of the impacting mass while keeping the maximum load (or acceleration) below some limit [52]. They generally absorb kinetic mechanical energy under compression actions at a relatively constant stress over a large range of displacement. The works done by compressing these kinds of materials are equivalent to the kinetic energies of a mass that might impact on them. There are a number of materials and structures with the above mentioned feature for cushioning applications. Airbags, bubble films, rubberized fibres cushioning, and polymer-based foams are just a few typical examples. However, despite their promising cushioning properties and low cost, the inferior comfort property makes these materials and structures unsuitable for human body protection. A combination of excellent transversal compressibility and high permeability makes spacer fabrics very suitable for multifunctional clothing and technical applications. Some efforts have already been made to investigate the compression properties of warp-knitted spacer fabrics, and most of the studies have reported that the overall compression load-displacement relationship of these fabrics can be split into three main stages, i.e., linear elasticity, plastic plateau, and densification

[53, 54]. This is the typical behavior required by a cushioning material in compression.1In the published results, relatively constant loads at the plastic plateau stage were observed. These results have proved that warp-knitted spacer fabrics are a new class of alternative candidate materials for cushioning applications. However, the plateau stage found in literature is not notable and the zone of the plateau stage reported in literature is too short as well. In other words, the total energy absorbed in the plateau zone by these reported fabrics is not sufficient to identify them as good cushioning materials [52-56].

2.4.5.2 Spacer fabrics for composites

Spacer fabrics are three dimensional textiles. Properties of spacer fabrics such as 3D fibre location, possibility to use different materials and production in one step, provide the spacer fabrics to use in different application areas. Due to inferior mechanical properties, such as elasticity and deformability under applied loads, conventional spacer fabrics are not suitable for high-performance composite applications. Moreover, the restricted distance between the plane layers contributes to the drawbacks of such spacer fabrics. One solution is to connect the planes by means of vertical fabric layers instead of pile yarns. This type of 3D spacer fabric with multi-layer reinforcements in the fabric structures is expected to show superior mechanical properties and be especially suitable as textile preforms for lightweight composite applications [57,58]. Future applications of composites made from 3D multi-layer spacer fabrics involve the replacement of conventional panel structures that are being used for aircraft, transport vehicles, marine applications and infrastructures, lift cabins, and ballistic protection for buildings and combat vehicles, etc. Verpoest was investigated knitted spacer fabrics as reinforcement material in composite structures [59]. Philips et al., investigated the knitted spacer fabric reinforced composite materials produced with monofilament and multifilament spacer yarns. As a result of the study it was concluded that multifilament spacer yarns provide better resin distribution although it is necessary to use monofilament spacer yarn to provide better compression resistance [60]. Philips and Verpoest, focused on the bending behavior of warp knit spacer fabric reinforced composite materials [61]. Mecit and Marmarali studied on application of spacer fabrics in composites [62]. Flat knitted spacer fabrics offer a strong potential for complex shape preforms, which could be used to manufacture composites with reduced waste and shorter production times. A reinforced spacer fabric made of individual surface layers and joined with connecting layers shows improved mechanical properties for lightweight applications such as textile-based sandwich preforms.

2.4.5.3 Protective applications

Over the past few decades a wide range of personnel protective equipment (PPE) has been developed to protect wearers from various types of risks or hazards to their health and safety [63]. Impact protectors, which are the most commonly used PPE, are normally manufactured to include energy-absorbing material in the form of pads. They are integrated or inserted into

protective clothing or equipment specially designed for protecting the human body from impact, blows or falls. A number of different types of impact protectors are on the market for protecting different areas of the body in a variety of circumstances [64]. The use of warp-knitted spacer fabrics in clothing and equipment providing protection against impact has attracted great attention in recent years due to their combination of protection and comfort in use. The static and dynamic compression behavior of a series of warp-knitted spacer fabrics has been investigated in our previous studies, and the energy absorption performance and force attenuation capability of these fabrics under flat wise static and impact compression has been analyzed in detail [65]. These studies indicate that these fabrics have the key feature of behaving as cushioning materials, providing three distinct stages in static and dynamic compression, described as linear elasticity, plateau and densification. However, in order to offer an adequate combination of protection and comfort, the protective material must conform to the shape and curvature of the body part being protected. There is no doubt that the impact properties of a protective material of curved shape are different from those of a planar shape, due to the change in boundary conditions during loading. Most recently, Guo et al. have reported an experimental investigation into the impact behavior of warp-knitted spacer fabrics of hemispherical shape [66]. The impact energy and weight of the striker were kept constant, and only the contact forces were measured. The tests were quoted as having been carried out according to European Standard BS EN 1621–1:1998. However, this standard specifies that protectors should be impacted using a striker of 5 kg weight at a kinetic energy of 50 J, and the transmitted forces then measured. Furthermore, their study did not pay attention to the relationship between energy absorption capacity and force attenuation properties, which is very important in designing fabrics to satisfy protective requirements.

2.4.5.4 Spacer fabrics for thermo-physiological clothing

In last few years, extensive research has been carried out on knitted fabrics for thermo – physiological comfort clothing [67, 68]. Spacer fabrics have ability to trap and hold air and insulate the body because of its nature of spacer yarns between two surface layers. This, along with the ability to wick away moisture, maintains the body's microclimate, and thus keeps the person dry and comfortable. There are many outdoor/ active apparel manufacturers who still employ the layering concept in order to achieve all the desirable properties in active apparel [69]. Warp knitted spacer fabrics tend to have a higher thermal insulation value than weft knitted spacer fabrics regardless to whether the fabric is wet or dry, an important feature for those who may utilize this fabric in the snow. Warp knitted spacer fabrics also have a higher thermal absorptivity value than weft knitted spacer fabrics, and thus the warp knitted will be warmer to touch than weft knitted [64, 70]. Yip and Ng found that warp knit spacer fabrics have a lower thermal conductivity rating than the weft knit fabric, which means the excess heat from the body would not be as quickly transferred if a warp knit spacer fabric is being utilized than if a weft knit fabric is to be utilized with warp knitted spacer fabrics [38].

Spacer fabrics that have a rib construction, and are flocked during the finishing process, have shown to provide better insulation, and better heat and moisture transference, both of which will help maintain the body's micro climate [71]. The ribs of the face fabrics are what actually aid in the movement of heat and moisture; the channels created by ribbed fabric faces thus are better suited to control the microclimate and keep the wearer cool and dry. In regard to the water vapour permeability properties of spacer fabrics, weft knitted spacer fabrics have been found to have better evaporative heat loss properties and water vapour permeability properties than warp knitted spacer fabrics, thus making the weft knit more comfortable when worn close to the skin of a person who is exerting energy and perspiring. When choosing a fibre type to aid in microclimate regulation, viscose can absorb the perspiration of the wearer and delay the moment at which the air in the spacer layer becomes saturated with moisture [38]. This means that a person who is perspiring heavily, or has varying perspiration levels with high peaks, will remain drier for a longer period of time, and have a more level microclimate, if wearing a garment utilizing spacer fabrics with a viscose inserted weft yarn [72]. An inserted weft yarn, that is hydrophobic, will maintain the body's microclimate more effectively than an inserted weft yarn that is hydrophilic because the hydrophilic yarn will hold the moisture and inhibit it from being transported away from the body [73]. Another, not commonly realized, important factor of spacer fabrics for certain types of active wear is compressibility. Many outdoor activities of athletes are seasonal (i.e. skiing), therefore during the off-season it is likely that the garments are stored away in containers, or other means, where they under a heavy load. During the in season, these garments are packed in suitcases for traveling. The athlete or outdoor enthusiast expects the garments to not be distorted in any way when they are removed from storage, as they should be ready to be utilized for the new season.

2.4.5.5 Spacer fabrics for medical applications

As a 3D structure, the spacer fabric contains a considerable amount of space inside the fabric, and the spacer yarns oriented in the Z or thickness direction provide superior compression and recovery properties 24. In addition to having the well-known advantages of knitted structures, such as high bursting strength, high elongation, low Young' s modulus and high porosity, the 3D spacer fabric stands out as a one piece multi-layered structure with high volume to weight ratio, softness, breathability, moisture conductivity, compression resistance and excellent recovery properties [74, 75]. This unique architecture with its impressive physical and mechanical performance has been discovered by medical textile researchers and applied to both internal and external end-uses. In various external applications, the spacer layer allows consistent air circulation to reduce heat build-up and increase moisture transfer. Under applied pressure, it shows sustained graduated compression and uniform pressure distribution. So it is ideally suited for use as a compression bandage, for comfort cushioning and shock absorbency [74 - 76].When used as a compression bandage, for example, the spacer fabric provides lightweight, non-fraying and breathable support with enhanced thermo-physiological properties and protective cushioning. In addition, spacer shows excellent transference of pressure and the sub-bandage

compression applied to the limb does not appear to be as severely influenced by the number of layers as it is with the traditional 2D bandages (Figure 2.18). For internal applications, spacer yarns can provide a layered surface area for cell attachment and guide the cell migration through the thickness of the fabric. The numerous interconnecting pores will allow fluids carrying nutrients and waste by-products to flow through the entire structure, hence providing superior fluid transport performance. However, there is no published research data to support this claim at the present time. Another key advantage of using a spacer fabric as a tissue engineering scaffold is that it is a one-piece multilayer structure with different pore size distributions in the layers but without an inter face. This means that it success fully avoids thermal bonding, toxic organic solvents or chemical adhesives that would be used to assemble traditional foams and combine multi-layer fabrics. The spacer fabric may also facilitate different cell lines so as to generate separate types of tissue in the different layers [86, 88]. The engineered pore size distribution and porosity gradient could also provide physical guidance for the differentiation of progenitor and stem cells. In summary, the future possibilities of applying knitted spacer fabrics to a wide range of different tissue engineering end-uses looks promising, since various properties can be incorporated into the scaffold structure by changing the type of polymer, changing the type of yarns, modifying manufacturing process or activating the fibres with a surface treatment. For instance, the total porosity and the pore size distribution can be controlled by a number of manufacturing parameters, such as the gauge of the needle bed, the number of or the yarn guides, the type or combination of yarns, the gap between the needle beds and the orientation of the spacer yarns to parallel or crossed [77, 80].

(a) (b)

Figure 2.18 a) Commercial two layer bandage b) 3D spacer bandage [78]

2.4.5.6 Other applications of knitted spacer fabrics

The other applications of knitted spacer fabrics and their products which are available in the market are shown below (Table 2.1) [81 - 84].

Table 2.1 Applications of knitted spacer fabrics

Application Fields	Spacer Fabric Products
Automotive	Car seat , door paneling, dash board cover, car boot liners, car window shelf, car seat heating, etc.
Medical	Bandage, knee braces, thermal mats, wheelchair cushions, absorbent fleece, neck supports, etc.,
Industrial	Textile antenna, sound absorption, solar thermal collectors, concrete reinforcement, etc.
Sports	Sports shoe, sports protectors, sportswear, mattress, pillows, etc.
Safety &Protection	Cycle helmets, body armor, bullet proof jackets, hip protector, etc.

2.5 Summary

Since spacer fabrics have two outer surfaces connected to each other with spacer yarns, they provide light weight and bulkier structure. So, the properties of spacer fabrics such as 3D fibre disposition, possibility to use different materials and single step production system, enable them in different application areas. Components in spacer fabrics differ depending on the yarn type and production method. It has excellent compression elasticity and breathability is the greatest advantages of spacer fabric. Admirable compressibility indicated that, crush resistant property and bending performance are excellent. Spacer fabric possesses excellent cushioning and shock absorbing properties. It is because spacer fabric is able to absorb and dissipate kinetic mechanical energy when it is subjected to compression at regular stress over a large extent of displacement. The above discussion clearly stated that the potential of knitted spacer fabrics in a number of technical applications and hold promises for more applications. Also the spacer fabrics are still under active research for a number of advanced functional applications especially in mattress, insole, automobile upholsteries, mats etc.

Chapter 3 Methodology

3.1 Materials

3.1.1 Warp knitted spacer fabrics

Twelve different spacer fabrics made up of polyester filament yarn were knitted using Raschel warp knitting machine with gauge of E22 and 6 guide bars. The surface layer of spacer fabrics were produced with polyester multifilament yarn with same linear density, the spacer layer (connecting) was knitted using polyester monofilament with different diameters and linear densities. By adjusting guide bar movements, the fabrics were produced with two different surface structures. The first group (6 samples) was knitted using lock-knit on both the surfaces and the second group (6 samples) was produced with face layer hexagonal net and base with lock-knit structure. Among these samples, spacer fabrics with different thickness were manufactured by adjusting two needle bars. In each group, former set was developed with 1.5, 2.5 and 3.5 mm thickness and spacer yarn diameter of 0.055 mm, latter set was constructed with same thickness with different spacer yarn diameter (0.1mm). The loop length of the all twelve warp knit spacer fabrics were kept at 2.12 mm. The samples classification is clearly presented in Table 3.1. The structure and knit pattern of both lock knit and hexagonal net warp knit structures are given in Figure 3.1.

Table 3.1 Description of warp knitted spacer fabrics

<table>
<tr><th>S.No.</th><th>Structure</th><th>Fibre Composition (%)</th><th>Face Layer (dtex)</th><th>Middle Layer (Spacer) (dtex)</th><th>Back Layer (dtex)</th><th>Spacer Yarn Dia (mm)</th></tr>
<tr><td>WAS 1</td><td rowspan="6">Lock knit</td><td rowspan="12">100% Polyester</td><td rowspan="12">83f36 (linear density – 83 dtex, number of filaments – 36)</td><td rowspan="3">33f1</td><td rowspan="12">83f36 (linear density – 83 dtex, number of filaments – 36)</td><td rowspan="3">0.055</td></tr>
<tr><td>WAS 2</td></tr>
<tr><td>WAS 3</td></tr>
<tr><td>WAS 4</td><td rowspan="3">108f1</td><td rowspan="3">0.1</td></tr>
<tr><td>WAS 5</td></tr>
<tr><td>WAS 6</td></tr>
<tr><td>WAS 7</td><td rowspan="6">Hexagonal net</td><td rowspan="3">33f1</td><td rowspan="3">0.055</td></tr>
<tr><td>WAS 8</td></tr>
<tr><td>WAS 9</td></tr>
<tr><td>WAS 10</td><td rowspan="3">108f1</td><td rowspan="3">0.1</td></tr>
<tr><td>WAS 11</td></tr>
<tr><td>WAS 12</td></tr>
</table>

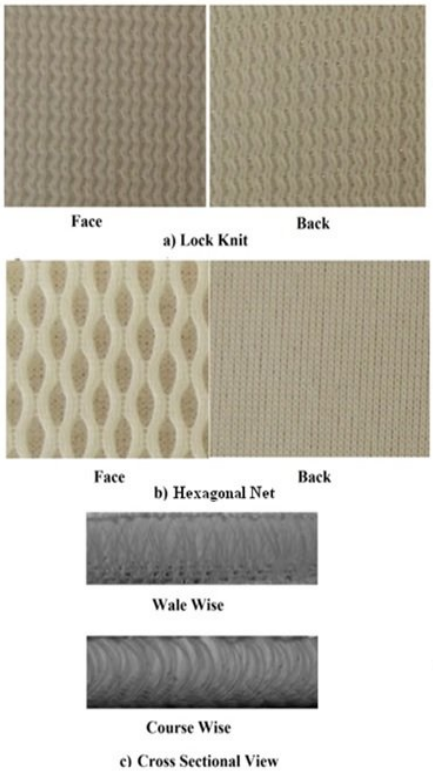

Structures	Lock knit	Hexagonal Net

Knit Notation	Face Side
	Bar 1 : 1-0 0-0/ 3-2 3-3// Fully threaded
	Bar 2 : 2-1 1-1/ 1-0 0-0// Fully threaded
		Face Side
		Bar 1 : (1-0 3-3/ 3-2 1-1)x2/(1-0 3-3/3-2 4-4)/ (5-4 3-3/ 3-2 4-4)x2/(5-4 3-3/3-2 2-2)// 2 Empty 2 Thread
		Bar 2 : (5-4 3-3/ 3-2 4-4)x2/(5-4 3-3/3-2 1-1)/ (1-0 3-3/3-2 1-1)x2/(1-0 3-3/3-2 4-4)// 2 Empty 2 Thread

	Middle (Spacer) Layer Bar 3 : 1-0 2-1/ 2-1 1-0/ 1 Full 1 Empty Bar 4 : 2-1 1-0/ 1-0 2-1/ 1 Full 1 Empty	Middle (Spacer) Layer Bar 3 : 1-0 2-1/ 2-1 1-0/ 1 Full 1 Empty Bar 4 : 2-1 1-0/ 1-0 2-1/ 1 Full 1 Empty
	Back Side Bar 5 : 0-0 2-1/ 1-1 1-0// Fully threaded Bar 6 : 3-3 1-0/ 0-0 3-2// Fully threaded	Back Side Bar 5 : 0-0 2-1/ 1-1 1-0// Fully threaded Bar 6 : 3-3 1-0/ 0-0 3-2// Fully threaded

Figure 3.1 Structure and knit pattern of warp knit spacer fabrics

3.1.2 Weft knitted spacer fabrics

Six different weft knitted spacer fabric samples were developed using computerized Mayer & Cie, circular weft knitting machine with 5 feeders, 14 gauge and 80 cm diameter. These fabrics were developed in co-operation with SINTEX s.r.o., Czech Republic. The first and second feeders were supplied with spacer yarn, third and fourth for technical face side and fifth feeder for technical back. The structure and knit pattern of these samples are given in Figure 3.2. The six fabric samples were classified into two groups for convenient analysis of results, the first group has been developed using Polyester/Polypropylene blend with three different proportions and second group with Polyester/Polypropylene/Lycra blend having another 3 different compositions. As a spacer yarn, three different types of 88 dtex Polyester monofilament yarn and Polyester multifilament yarns (167 dtex and 14.5 tex) were used. 14.5 tex Polypropylene yarn was used on both the surfaces in group 1 samples. In group 2 samples polypropylene (14.5 tex), without and with lycra (44 dtex) were used for the top and bottom surface of the spacer fabrics (Table 3.2). The loop length of the fabric without lycra (WES 1) was 2.46 mm and samples (WES 2 and WES 3) were 2.78. The loop length weft knit spacer fabrics with Lycra on the surface (WES 4) was 1. 28 mm and for samples (WES 5 and WES 6) were 1.52 mm.

Table 3.2 Weft knitted Spacer fabric samples particulars

sample No.	Fabric layers	Technical face	Spacer yarn	Technical back	fibre composition (%)
		Group 1 - Without Lycra			
WES 1		Polypropylene (POP) -14.5 tex	Polyester monofilament) - 88 dtex	Polypropylene (POP) -14.5 tex	58% POP & 42% PES monofilament
WES 2	Type of yarns and linear density	Polypropylene (POP)-14.5 tex	Polyester (PES) - 14.5 tex	Polypropylene (POP) -14.5 tex	45% POP & 55% PES
WES 3		Polypropylene (POP) -14.5 tex	Polyester (PES) - 167 dtex	Polypropylene (POP) -14.5 tex	41%POP & 59% PES
		Group 2- With Lycra			
WES 4		Polypropylene (POP)-14.5 tex Lycra - 44dtex	Polyester monofilament - 88 dtex	Polypropylene (POP) -14.5 tex	55%POP 39%PES monofilament 6% Lycra
WES 5	Type of yarns and linear density	Polypropylene (POP)-14.5 tex Lycra - 44dtex	Polyester (PES) - 14.5 tex	Polypropylene (POP) -14.5 tex	42% POP 52% PES 6% Lycra
WES 6		Polypropylene (POP)-14.5 tex and Lycra - 44dtex	Polyester (PES) - 167 dtex	Polypropylene (POP) -14.5 tex	39% POP 55% PES 6% Lycra

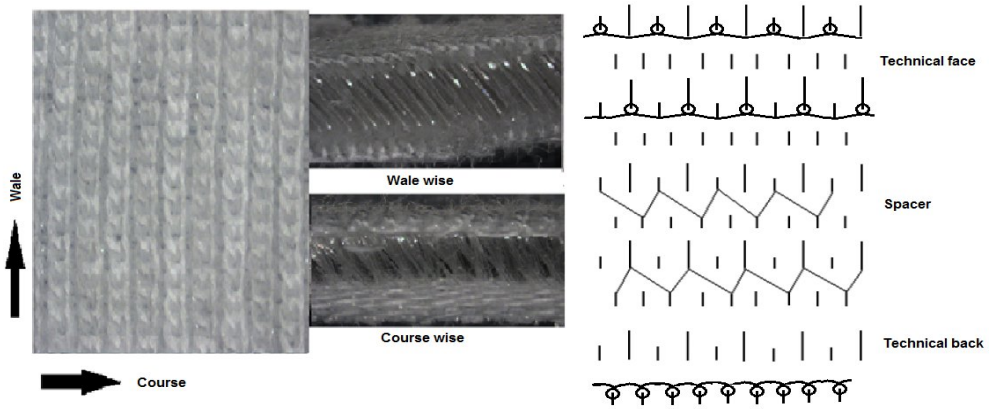

Figure 3.2 Structure and knit pattern of weft knit spacer fabric

3.2 Evaluation of spacer fabric characteristics

Structural properties including the yarn linear density and fabric weights per unit area were determined according to ASTM D1059 standard using electronic weighing scales. The thickness of the fabrics was measured according to ASTM D1777-96 standard with the SDL digital thickness gauge at a pressure of 200 Pa. The stitch density was calculated from Wales per centimetre (WPC) and course per centimetre (CPC) with the help of optical microscope. The density (D) of the fabric was calculated using the relationship in (eqn. 3.1)

$$D = \frac{W}{t} kg / m^3 \tag{3.1}$$

Where, W is areal density (weight per unit area) and t is thickness. Porosity, H, was calculated using the equation 3.2,

$$H = 1 - \frac{\rho_a}{\rho_b} \tag{3.2}$$

where, ρ_b is bulk density of spacer fabrics, ρ_a is weighted average absolute density of fibres in the spacer fabric, expressed in kg/m^3. The structural characteristics of both warp and weft knitted spacer fabrics are presented in the Table 3.3 and 3.4. All the experiments were carried out under standard ambient condition and as per standard testing method.

Table 3.3 Structural characteristics of warp knitted spacer fabrics

Warp Spacer Samples	Stitch Density (Stitches/cm^2)				GSM (g.m^{-2})				Thickness (mm)				Density (Kg.m^{-3})	Porosity (%)
	Mean	ME	LL	UL	Mean	ME	LL	UL	Mean	ME	LL	UL		
WAS 1	120.4	1.1	119.30	121.50	262.3	0.7	261.6	263.1	1.50	0.03	1.47	1.53	174.89	87.33
WAS 2	121	1.4	119.60	122.40	354.3	0.8	353.6	355.1	2.50	0.04	2.46	2.54	141.73	89.73
WAS 3	120.3	1.3	119.00	121.60	446.0	3.1	442.9	449.1	3.50	0.03	3.47	3.53	127.42	90.77
WAS 4	119	1.2	117.80	120.20	573.1	0.7	572.4	573.8	1.50	0.02	1.48	1.52	382.06	72.31
WAS 5	120	1.1	118.90	121.10	871.9	0.6	871.3	872.5	2.50	0.01	2.49	2.51	348.77	74.73
WAS 6	120.5	0.9	119.60	121.40	1174.1	0.7	1173.4	1174.8	3.50	0.01	3.49	3.51	335.47	75.69
WAS 7	119	1.6	117.40	120.60	263.4	2.9	260.6	266.3	1.50	0.03	1.47	1.53	175.63	87.27
WAS 8	120	0.9	119.10	120.90	353.1	0.6	352.5	353.7	2.50	0.03	2.47	2.53	141.25	89.76
WAS 9	119.1	1.2	117.90	120.30	447.1	0.9	446.3	448.0	3.50	0.02	3.48	3.52	127.75	90.74
WAS 10	121	1.3	119.70	122.30	572.3	1.4	570.9	573.7	1.50	0.02	1.48	1.52	381.55	72.35
WAS 11	119.6	1.1	118.50	120.70	872.5	1.0	871.5	873.5	2.50	0.01	2.49	2.51	348.98	74.71
WAS 12	119.5	1.4	118.10	120.90	1173.3	1.4	1171.9	1174.7	3.50	0.03	3.47	3.53	335.23	75.71

Table 3.4 Structural characteristics of weft knitted spacer fabrics

Weft Spacer Samples	GSM ($g.m^{-2}$)				Thickness (mm)				Density ($kg.m^{-3}$)	Stitch Density ($Stitches/cm^2$)				Porosity (%)
	Mean	ME	LL	UL	Mean	ME	LL	UL		Mean	ME	LL	UL	
WES 1	493	0.16	492.84	493.16	4.4	0.88	3.52	5.28	112	200	0.1	199.9	200.1	90.12
WES 2	443	0.12	442.88	443.12	2.62	1.1	1.52	3.72	169.1	150	0.04	149.96	150.04	86.21
WES 3	477	0.2	476.8	477.2	2.74	0.61	2.13	3.35	174.1	150	0.12	149.88	150.12	85.06
WES 4	632	0.1	631.9	632.1	4.4	0.55	3.85	4.95	144.8	350	0.06	349.94	350.06	87.15
WES 5	657	0.12	656.88	657.12	3.5	0.86	2.64	4.36	187.7	280	0.1	279.9	280.1	84.09
WES 6	695	0.22	694.78	695.22	3.4	0.45	2.95	3.85	205.4	280	0.1	279.9	280.1	83.11

3.2.1 In–plane shear behavior

The in-plane shear behavior of both warp and weft kitted spacer fabrics are carefully measured and analyzed using picture frame test and image analysis methods.

3.2.1.1 Picture frame test

The picture frame shear test method achieved some popularity in the early days of composite materials development when few other shear test methods existed. But as the two- and three-rail shear test methods, and later the Iosipescu shear test, were introduced for characterizing basic shear properties, picture frame shear testing became less popular for three reasons: It used a relatively large specimen; test preparation required that a number of holes be drilled in the specimen; and the method required a complex fixture. Despite these disadvantages, the picture frame shear test continued to be an attractive option for composite laminate panel testing because the method accommodates large specimens [85].

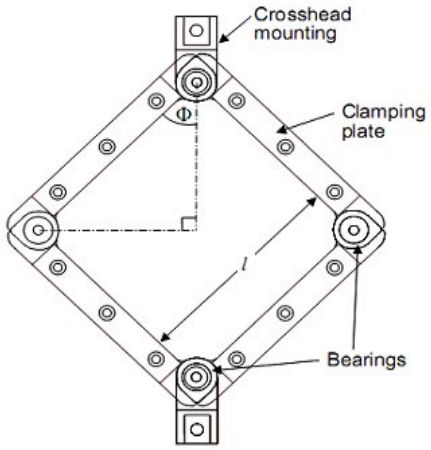

Figure 3.3 Picture frame fixture design

As shown in Figure 3.3, the picture frame is an effective way for characterizing intra-ply shear

property of fabrics. The picture frame test is preferred by many researchers for shear testing since it has pure state of strain which can be imposed on the test specimen. Shearing is induced by restraining the textile reinforcement in a rhomboid deformation frame with fibres constrained to move parallel to the frame edges. The frame is extended at diagonally opposing corners using simple tensile testing equipment. The description of this test method and the modifications done in the frame for this work has been discussed in detail in the following section.

3.2.1.1.1 Description of the test method

A 3-dimensional view of developed picture frame fixture for shear testing is given in Figure 3.4. The apparatus has four legs which are hinged to form a picture frame. Further, there is a rod which runs across one of the diagonal of the frame. It should be noted that this rod is not in the plane of the frame but runs behind the frame. The lower end of the rod is hinged with the common hinge of the two legs meeting in that corner. The other opposite corner hinge is resting in the slot provided in the rod. The slot is about 6 cm long for maximum deformation of frame. Further, at the lower end the rod is again hinged to individual legs of the frame. The lower end of the rod is fixed in crossheads of the loading machine. By adjusting the distance between the upper and lower crossheads, the angles between the arms of fixture reach 90^{o}.

The distance can be set as the original reference value, i.e., the zero displacement position, in computer, so that later on, all the experiments can automatically begin from this zero point. Also, the force can be set to zero at this position. Thus, when the load is applied through the upper end of the rod, it pushes these two legs apart and deforms the frame. These two legs in turn push their adjacent legs making their common hinge to slide in the slot of the rod. The plate deforms into a diamond shape. The spacer fabric is clamped to the frame with the help of clamping plates as shown in Figure 3.5. These clamping plates are 3cm in width and it has diamond knurled surface for better gripping. The empty frame is tested under the same condition to find the frictional effects between bearings and slots, after several trials of this test; the average value of load at each displacement point is calculated. This is to record the load-displacement behavior of the empty fixture under the same condition as in the real shear experiment. So, it is mainly considered and optimized during sample testing. To eliminate the error caused by the weight and inertia of the fixture, the net load obtained was subtracted from the machine-recorded load when the fabric is being deformed in the picture frame. This resultant load is considered and accounted as an actual load. In order to prevent the pressures from imposing on test samples by the fixture during the large deformation, the central area of shear deformation was 100 mm X 100 mm, and the four corner parts were cut off in order to avoid edge buckling. Shear tests were conducted on a TIRA - universal tensile testing machine with a crosshead speed of 10 mm/min. The test was repeated for 5 samples of each type under the same conditions [86].

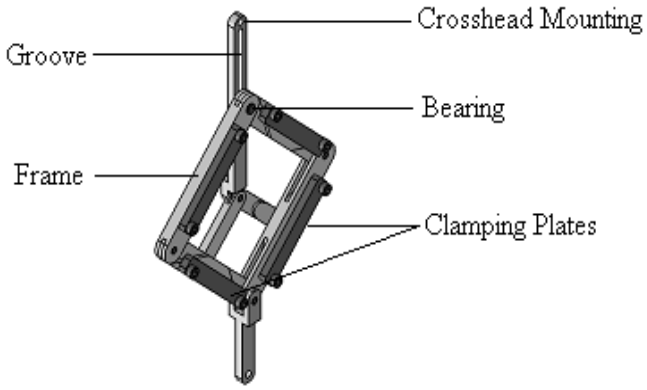

Figure 3.4 3-dimensional view of picture frame shear fixture

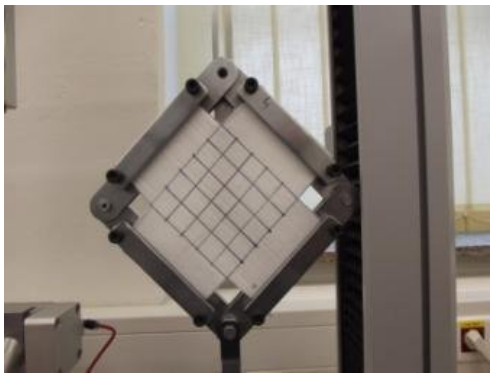

Figure 3.5 Clamping of sample in fixture

3.2.1.1.2 Deformation kinematics of fixture

A tensile force is applied at the crosshead mounting. The rig is jointed at each corner such that its sides can rotate and the interior angle between adjacent sides can change. The initially square frame thus becomes of rhomboid (or diamond) shape as shown in Figure 3.6. Material inside the rig is subjected to pure shear deformation kinematics (Figure 3.6). The force required to deform the material is recorded at the crosshead mounting as a function of crosshead displacement. The 3D spacer fabrics for shear tests were prepared according to the size of the picture frame and the characteristics of samples are described in the Figure 3.7. Direct measurement of axial load and shear angle is possible through the following relationship (eq. 3.3).

$$F_S = \frac{F_x}{2\cos\varphi} \tag{3.3}$$

Shear force (F_s) is determined by the axial force (F_x) frame rig length or sample length (L) and the frame angle (φ). In this study, both sample length and frame length are considered for

calculation of shear angle and to find the correlation with the image analysis method. Meanwhile frame angle can be determined directly from cross head displacement (d). Shear angle (γ) can be obtained from frame angle by using the following equations 3.4 and 3.5.

$$\varphi = \cos^{-1}\left[\frac{L\sqrt{2}+d}{2L}\right] \tag{3.4}$$

$$\gamma = \frac{\pi}{2} - 2\varphi \tag{3.5}$$

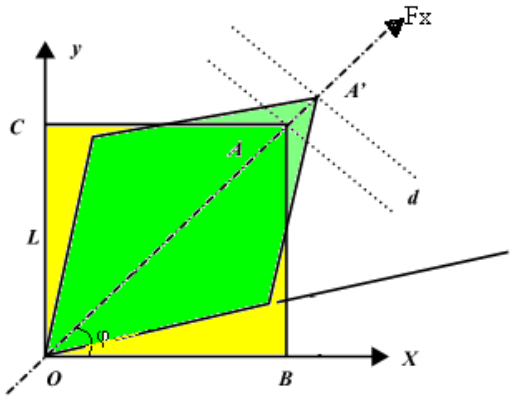

Figure 3.6 Deformation kinematics of picture frame

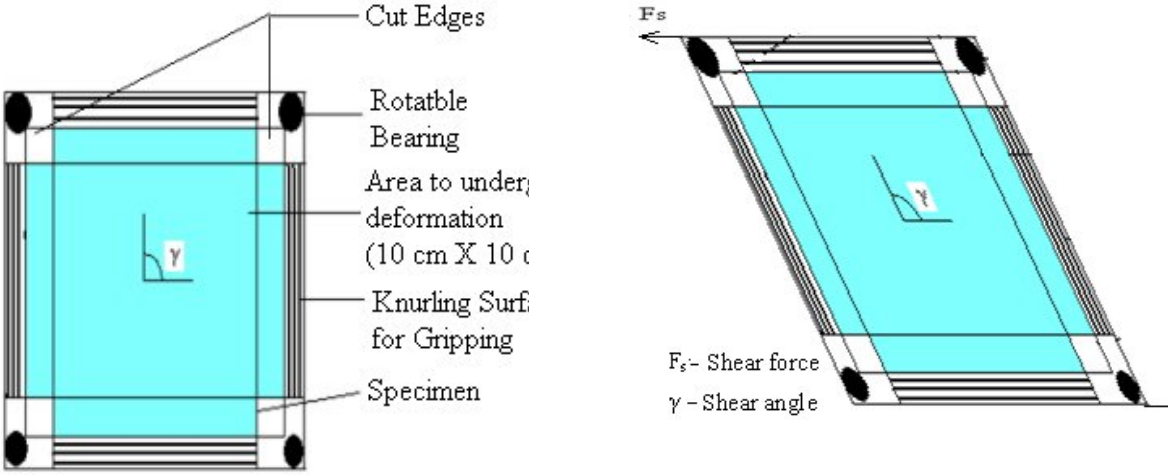

a. Before deformation **b.** After deformation

Figure 3.7 Shear deformation of frame and specimen

3.2.1.1.3 Analysis of in-plane shear stress- strain curve of spacer fabrics

Overall shear stress-strain trend of the spacer fabric samples are presented in the Figure 3.8. Normally the shear behaviour of spacer fabrics are classified into three stages with respect to

changes in the slope. The three stages are surface elongation and lateral compression (1), inter fibre compaction and buckling (2) and densification (3). In the first stage, the surface layer of spacer fabric undergoes elongation; also the inter-fibre slippage takes place in this stage. In this stage, the initial lateral compression occurs in the fabrics due to shearing, a lower slope is observed for loose structures and slope increases with increase in stitch density. Here the spacer yarn has low contribution in constraint during initial compression. Further inter-fibre compaction and extended compression (2^{nd} stage) leads to rapid increase in stress, it might be due to jamming of surface yarns which allows both surface yarn and spacer yarn to buckle to a larger extent. In spacer fabrics, the next stage is quite complex because the compressive stress and strain have been affected by buckling, shearing and locking of spacer yarns. It is also noticed that there is sharp increase in stress in the 3^{rd}stage because the fabric attains a very high density.

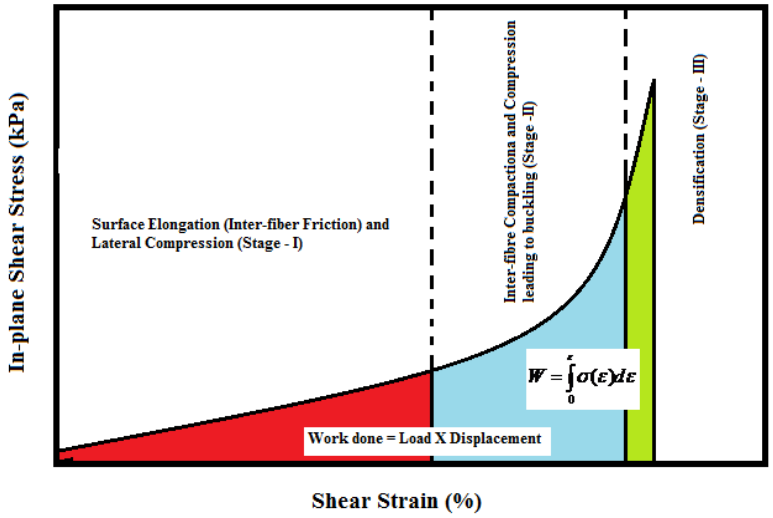

Figure 3.8 In-plane shear behavior of 3D spacer fabrics

3.2.1.1.4 Energy absorption during in-plane shear of spacer fabrics

It is necessary to evaluate and analyze the spacer fabrics energy absorbing ability during shear. It would be more useful to get a better understanding about the applicability of spacer fabric for cushion materials. The shear curve suggests that all spacer fabric samples may potentially be good energy-absorbing materials. The area under the load-displacement curve represents the total energy absorbed and it can be calculated by multiplying the area under the stress-strain curve by the volume of the sample. The energy absorption capacity per unit volume, *W*, can be calculated by integrating the shear stress-strain curve, as given by equation 3.6 [87]:.

$$W = \int_0^{\varepsilon} \sigma(\varepsilon) d\varepsilon \tag{3.6}$$

Where, σ is the shear stress, ε is the shear strain at the end/beginning of densification stage. In order to better understand the energy-absorption capacity of a spacer fabric, the energy-

absorption efficiency E can be used to analyze its energy-absorption process. The efficiency E is expressed by Equation (3.7)

$$E = \frac{Ah\int_0^{\varepsilon}\sigma(\varepsilon)d\varepsilon}{Ah\sigma} \tag{3.7}$$

Where A – area, h – thickness, σ – shear stress at the strain ε. The energy-absorption and efficiency of all the spacer fabrics are compared and analyzed to find the suitable material for hi-end applications.

3.2.1.2 Image analysis using MATLAB

Image analysis can aid in the determination of the shear angle and displacement at any particular point on the surface of fabric specimen. Grid pattern was applied on the specimen surface before the test and used as the reference points of image analysis. The complete displacement of the specimens during loading process was obtained by image analysis method. The images were captured at certain regular interval of time using digital camera. A special program is developed in MATLAB 7.10 (R 2010a) using Hough's transform to find the angle between the lines on the specimens. The results of experimental methods and image analysis were compared with each other.

3.2.1.2.1 Hough Transformation

The Hough Transform patented by Paul Hough in 1962 is basically a feature extraction method used to detect lines and finding position of arbitrary shapes in the image and is widely used in the field of computer vision and image processing. Related to this patent, Richard Duda and Peter Hart in 1972 invented the Hough Transform which is used in modern times and they named it generalized Hough Transform. The simplest case of Hough transform is the linear transform for detecting straight lines. In the image space, the straight line can be described as y = mx + c and can be graphically plotted for each pair of image points (x, y). In the Hough transform, the main idea is to consider the characteristics of the straight line not as image points x or y, but in terms of its parameters, here the slope parameter m and the intercept parameter c. Figure 3.9 shows the main idea in Hough transform. All straight lines passing through point (x, y) satisfy that equation but the values of slope m and intercept c may vary. Now instead of considering the point (x, y), parameters (m, c) are considered to understand the characteristics of straight lines in the image. This is the main idea in Hough Transform. If vertical lines are present in the image the values of m will be infinity, so parameters (ρ, θ) are used. The parameter ρ represents the distance between line and origin, θ is the angle of the vector from origin to this point. So the new rearranged equation becomes (eqn. 3.8),

$$\rho = x\cos\theta + y\sin\theta \tag{3.8}$$

This forms a sinusoidal curve in the (ρ, θ) plane, which is unique for that particular point. Now,

more generally a set of points which form a straight line will produce curves which cross at the (ρ, θ). The result of the Hough transform is stored in a matrix that is often called an accumulator. One dimension of this matrix is the θ values (angles) and the other dimension is the r values (distances), and each element has a value telling how many points/pixel lie on the line with the parameters (ρ, θ). So the element with the highest value tells which line is most represented in the input image. Hough Transform has an advantage that the points need not all be continuous. This can be really helpful if line is broken due to noise. One more factor to be considered is the efficiency which depends on the quality of input data. It also has an importance in the skew correction of documents and characters, finding shapes like rectangle, circle, ellipse etc. in the image. The in-plane shear stress, shear angle, work done and efficiency of both warp and weft knitted spacer fabrics were evaluated and are discussed in chapter 4.

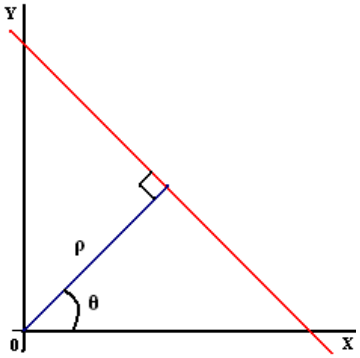

Figure 3.9 Line showing parameters ρ and θ

3.2.1.2 Finite Element Analysis of shear behavior

The spacer fabric geometry was created using solidworks and was imported into ANSYS platform for finite element analysis of shear stress. SOLID45 is used for the 3-D modelling of spacer structures. The element is defined by eight nodes having three degrees of freedom at each node: translations in the nodal x, y, and z directions. The element has plasticity, creep, swelling, stress stiffening, large deflection, and large strain capabilities. The mesh size and number of nodes were determined in order to minimize processing time and yet have accurate results.

3.2.2 Compression behavior

All the compression tests were carried out on a universal testing machine (TIRA) fitted with 5kN load cell. The speed of compression was chosen at 12mm/min in accordance to the ASTM d 575 (Test methods for rubber properties). The compression test was performed on the machine equipped with 2 strictly parallel plates having diameter of 150mm and a smooth surface. The samples were cut with dimensions of 100 mm x 100 mm. All the spacer fabric specimens are compressed up to 80 % of the initial thickness in an atmospheric condition of 20^{o}C and 65% relative humidity. Five tests were carried out for each sample under each testing condition and the average compression stress-strain curves are presented.

3.2.2.1 Analysis of compression stress- strain curve of spacer fabrics

Overall compressive stress-strain trend of the spacer fabric samples are presented in the Figure 3.10. Normally the compression behavior of spacer fabrics are classified into four stages with respect to changes in the slope. The four stages are (1) initial, (2) elastic, (3) plateau and (4) densification (4). In the first stage, the surface layer of spacer fabric undergoes compression, a smaller slope is observed for loose/open structures and slope increases with increase in stitch density. The spacer yarns have very low contribution in constraining the deformation during initial compression. Further compression (2^{nd} stage) leads to rapid increase in stress; it might be due to jamming of surface yarns which allows monofilaments to buckle to a larger extent. In spacer fabrics, third stage is quite complex because the compressive stress and strain have been affected by buckling, shearing and inter-contacting of spacer yarns. A faster increase in stress occurs in 4th stage because the fabric achieves a very high density.

3.2.2.2 Energy absorption during compression of spacer fabrics

To understand the cushioning behavior of the spacer fabrics, it is necessary to evaluate and analyze the spacer fabrics energy absorbing ability during compression. The compression curves reveal long deformation plateaus, suggesting that all spacer fabrics were potentially good energy-absorbing materials. The area under the load-displacement curve represents the total energy absorbed and it can be calculated by multiplying the area under the stress-strain curve by the volume of the sample. The compression efficiency E is defined as the ratio of the energy absorbed by a real cushioning material compressed to a given strain and energy absorbed by an ideal cushioning material that transmits a constant stress of the same value at the same given strain [96]. The compression stress, strain, energy absorption and efficiency of both warp and weft knitted spacer fabrics were evaluated and discussed in Chapter 4.

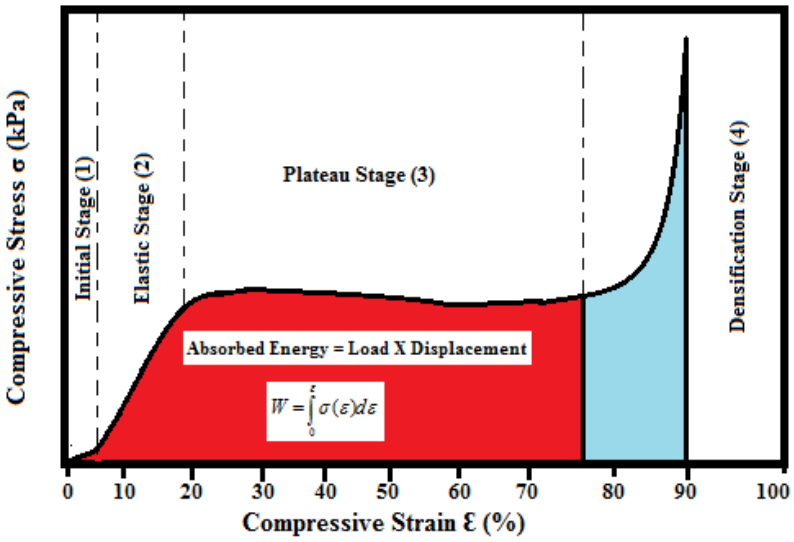

Figure 3.10 Compression behavior of 3D spacer fabrics

3.2.3 Thermo-physiological properties

The air, heat and water transmission behavior of both warp and weft knitted spacer fabrics are measured and analyzed for the advanced applications.

3.2.3.1 Air permeability

Air permeability is described as the rate of air flow passing perpendicularly through a known area, under a prescribed air pressure differential between the two surfaces of a material. Tests were performed according to standard ISO 9237 using a Textest FX-3300 air permeability tester. The air pressure differential between the two surfaces of the material was 200 Pa (Table 3.5 and 3.6).

3.2.3.2 Thermal properties

The measurements of thermal insulation parameters were performed on spacer fabrics with the use of the ALAMBETA device constructed in Czech Republic. Alambeta measuring device was used for fast evaluation of transient and steady state thermo-physiological properties (thermal insulation and thermal contact properties). The instrument measures the sample thickness also. The instrument consists of two measuring heads between which the test specimen was placed. Both measuring heads are equipped with thermocouples and heat flow sensors. The lower measuring head was adjusted to the ambient temperature by suitable cooling means; the upper, heated measuring head was adjusted to a controlled constant differential temperature. The heat flow sensors act at the contact faces of both measuring heads. When upper measuring head was lowered on the measuring specimen, the heat flow at the upper surface and the underside of the test specimen can be measured. The fundamental measuring principle implies the measuring and processing of the heat flows in dependence of time. Six parameters are determined: thermal conductivity λ, thermal diffusion a, thermal absorption b, thermal resistance r, the ratio of maximal to stationary heat flow density υ, and stationary heat flow density q_s at the contact point. The thermal results of both warp and weft knit spacer fabrics are presented in the Table 3.5 and 3.6.

3.2.3.3 Water vapour permeability

The water vapour permeability of the samples has been measured using the PERMETEST. The instrument works on the principle of heat flux sensing. The fabric sample is placed on a measuring head over a semi-permeable foil and exposed to parallel air flow at a velocity of 1m/s. The temperature of the measuring head is maintained at room temperature for isothermal conditions. When water flows into the measuring head, some amount of heat is lost. This instrument measures the heat loss from the measuring head due to the evaporation of water in bare condition and while being covered by the fabric. The relative water vapour permeability (RWVP) of the fabric sample is calculated by the ratio of heat loss from the measuring head with fabric (q_s) and without fabric (q_o) as given in Eqn. (3.9).

$$RWVP = \frac{q_s}{q_o} \times 100\% \tag{3.9}$$

PERMETEST characterizes the capability of the fabric to transfer water vapour, by measuring two parameters, the relative water vapour permeability and the absolute evapourative resistance (*Ret*) and these values are presented in the Table 3.5 and 3.6.

3.2.4 Acoustic properties

3.2.4.1 Determination of tortuosity

The tortuosity is a fundamental parameter which describes complexity of the path of sound wave propagating within a porous material. There are number of methods which have been developed to measure the tortuosity. It is mainly based on high frequency acoustic transmission, ultrasonic pulse transmission, reflection and electric resistivity measurements. In this work the tortuosity of spacer fabrics was determined by both experimental method using ultrasonic waves and by analytical method.

3.2.4.1.1 Experimental determination of tortuosity

In experimental part, the measurements were performed by positioning the samples between two ultrasonic transducers, one is emitter and the other is receiver as shown in figure 3. The emitter provides burst of sine waves with frequency 40 kHz. At higher frequencies the viscous skin depth is very small and viscosity does not influence the velocity very much. The influencing parameter at these frequencies is inertia because compressibility is basically adiabatic. The experimental set up is shown in Figure 3.11. As shown, the computer generates the signal and simultaneously records the received signal via power amplifier.

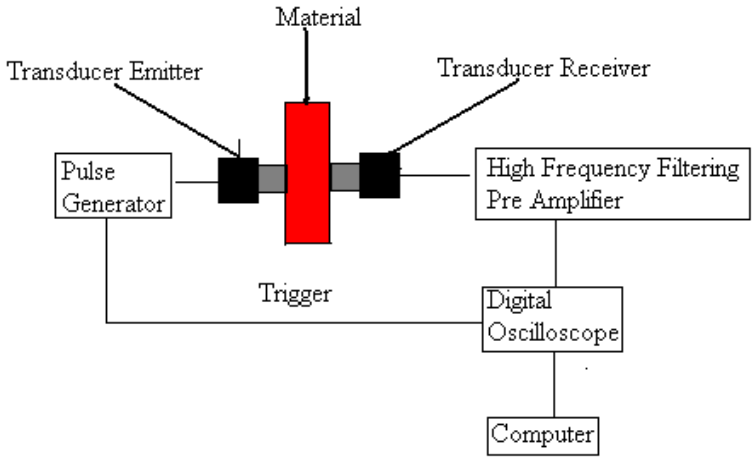

Figure 3.11 Experimental set up to measure tortuosity using ultrasonic method [88]

Table 3.5 Thermo-physiological properties of 3D warp knitted spacer fabrics

Fabric Samples	Air Permeability ($l/m^2.s$)				Thermal Conductivity ($W.m^{-1}k^{-1}$ X 10^{-3}) (λ)				Thermal Resistance (km^2W^{-1} X 10^{-3}) (r)				RWVP (%)				Evoporative Resistance ($Pa.m^2kW^{-1}$) (R_{et})			
	Mean	ME	LL	UL	Mean	ME	LL	UL	Mean	ME	LL	UL	Mean	ME	LL	UL	Mean	ME	LL	UL
WAS 1	3082	6.36	3075.64	3308.41	47.94	0.4	47.54	48.34	64.92	0.67	64.25	65.6	51.12	0.89	50.23	52.01	7.32	0.4	6.92	7.72
WAS 2	3216	9.64	3206.36	3460.05	46.82	0.27	46.55	47.09	66.16	0.24	65.92	66.4	49.62	0.53	49.09	50.15	8.14	1.05	7.09	9.19
WAS 3	3348	15.92	3332.08	3595.17	45.61	0.78	44.83	46.39	68.42	0.39	68.03	68.8	48.7	1.3	47.4	50	8.86	0.9	7.96	9.76
WAS 4	2032	22.79	2009.21	2228.86	53.48	0.51	52.97	53.99	53.98	0.32	53.66	54.3	28.56	1.14	27.42	29.7	18.35	1	17.35	19.35
WAS 5	2134	17.28	2280.72	2373.42	52.27	0.29	51.98	52.56	56.16	0.56	55.6	56.7	27.1	1.11	25.99	28.21	20.12	1.05	19.07	21.17
WAS 6	2298	27.17	2106.83	2555.00	51.96	0.31	51.65	52.27	59.44	0.33	59.11	59.8	25.92	0.33	25.59	26.25	21.98	1.22	20.76	23.2
WAS 7	3290	18.41	3271.59	3088.36	46.78	0.86	45.92	47.64	71.34	1.02	70.32	72.4	61.28	1.64	59.64	62.92	4.92	1.09	3.83	6.01
WAS 8	3432	28.05	3403.95	3225.64	45.64	0.7	44.94	46.34	77.56	0.72	76.84	78.3	58.38	0.42	57.96	58.8	6.04	0.77	5.27	6.81
WAS 9	3568	27.17	3540.83	3363.92	44.38	0.75	43.63	45.13	82.12	0.9	81.22	83	57.16	0.6	56.56	57.76	6.6	0.89	5.71	7.49
WAS 10	2212	16.86	2195.14	2054.79	51.19	0.28	50.91	51.47	60.71	0.32	60.39	61	39.48	0.47	39.01	39.95	12.58	0.96	11.62	13.54
WAS 11	2348	25.42	2322.58	2315.28	50.45	0.2	50.25	50.65	61.13	0.81	60.32	61.9	37.88	0.76	37.12	38.64	14.4	0.74	13.66	15.14
WAS 12	2536	19.00	2517.00	2161.17	49.78	0.38	49.4	50.16	63.45	0.49	62.96	63.9	36.61	0.53	36.08	37.14	15.9	1.1	14.8	17

Table 3.6 Thermo-physiological properties of 3D weft knitted spacer fabrics

Sample Nos.	Air Permeability ($l/m^2/s$)				Thermal Conductivity ($W.m^{-1}k^{-1}$ X 10^{-3}) (λ)				Thermal Resistance (km^2W^{-1} X 10^{-3}) (r)				RWVP (%)				Evaporative Resistance ($Pa.m^2kW^{-1}$) (R_{et})			
	Mean	ME	LL	UL	Mean	ME	LL	UL	Mean	ME	LL	UL	Mean	ME	LL	UL	Mean	ME	LL	UL
WES 1	1806.4	12.6	1793.8	1819	59.98	0.86	59.12	60.84	71.7	1.02	70.63	72.67	47.3	2.48	44.8	49.7	18.61	1.17	17.4	19.78
WES 2	621.8	8	613.8	629.8	61.24	0.7	60.54	61.94	64.4	0.72	63.71	65.15	26.3	1.18	25.1	27.5	7.58	0.31	7.27	7.89
WES 3	545.2	14	531.2	559.2	66.56	0.75	65.81	67.31	61.7	0.9	60.77	62.57	24.2	0.98	23.2	25.2	6.34	1.12	5.22	7.46
WES 4	946.6	13	933.6	959.6	53.42	0.28	53.14	53.70	77.6	0.32	77.23	77.87	37.1	2.74	34.4	39.9	18.45	1.4	17.1	19.85
WES 5	318.8	6.9	311.9	325.7	56.31	0.2	56.11	56.51	69.2	0.81	68.35	69.97	25.8	1.76	24.0	27.5	11.7	2.14	9.56	13.84
WES 6	305.8	7.2	298.6	313	61.72	0.38	61.34	62.10	65.1	0.49	64.60	65.58	24.0	1.2	22.8	25.2	10.31	1.26	9.04	11.57

*ME-Margin of Error, UL – Upper Limit, LL – Lower Limit

The experiment is performed with the sample positioned between two transducers and then compared with reference signal (without sample) to extract the relative time delay and amplitude attenuation (Figure 3.12). From the time delay (τ) and attenuation ratio amplitude (T) with/without sample of signal time, it is possible to calculate tortuosity using the equation (3.10) [88, 89].

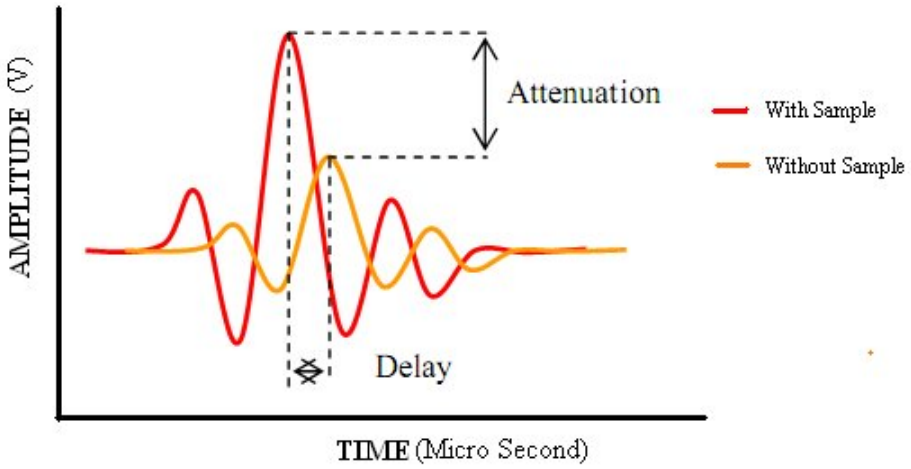

Figure 3.12 Attenuation of ultrasonic waves during testing [89]

$$\text{Tortuosity, } K_S = \left[\left(\frac{\left|\ln(T)\right| c_o}{d\omega} \right) - \sqrt{\left(\frac{\left|\ln(T)\right| c_o}{d\omega} \right)^2 + \left(1 + \frac{c_0 \tau}{d} \right)} \right]^2 \qquad (3.10)$$

Where,

K_S – Tortuosity (no unit)

T – Attenuation ratio amplitude $\left(\left|\ln(T)\right| = a * d\right)$

a - Attenuation per unit length

d – Thickness of material

ω – Ultrasound frequency (40 KHz)

C_0 – Speed of sound in free air (343 m/s)

τ - Time delay in (micro sec)

3.2.4.1.2 Analytical determination of tortuosity

For analytical determination, a few assumptions were made. There are pores in the fabric which are like slits whose walls are bounded by the mesh of yarns and angle of inclination of a pore is same as the angle of inclination of the interconnecting yarn between the front and back surfaces of the fabric. Thus analytical model considers these pores to be inclined at an angle (θ) normal to the surface of the fabric. Also angle θ can be determined using the spacing between tuck loops

on alternate wales on the front and back face of the fabric (*d*) and its thickness (*t*). So tortuosity (k_s) of the fabric and angle of inclination θ can be determined using the equations (3.11, 3.12);

$$K_s = \frac{1}{\cos^2 \theta} \qquad (3.11)$$

$$\theta = \tan^{-1}\left(\frac{d}{t}\right) \qquad (3.12)$$

The spacing *d* can be determined from the number of courses per cm for warp knit and wales per cm (*W*) for weft knitted face of a particular fabric and the number of needle positions between the two alternate courses for warp and wales (*p*) for weft using equation (3.13).

$$d = (p+1) + \frac{10}{(W-1)} \qquad (3.13)$$

Thus, with the use of equations (3.11-3.13), the tortuosity of the spacer fabrics can be calculated approximately. The results are reported and discussed in chapter 4.

3.2.4.2 Air flow resistance

As stated earlier, the viscous resistance of air in the porous material has an important influence on the sound absorption mechanism. Flow resistance has been used as an important parameter in theoretical equations by many researchers. It is therefore important to measure the flow resistance of an acoustic sample.

Air flow resistance of spacer fabric was calculated from air permeability value obtained from Textest FX-3300 air permeability tester. The air permeability is described as the rate of air flow passing perpendicularly through a known area, under a prescribed air pressure differential between the two surfaces of a material (200 Pa). Tests were performed according to standard ISO 9237 for five specimens of each sample and expressed as linear air flow velocity (v) in m/s. This specific flow resistance has been converted to air flow resistivity, R using the equation 3.14 shown below. The results are reported and discussed in chapter 4.

$$\text{Air Flow Resistivity, } R = \frac{\nabla P}{v * d} Pa.m^{-2}.s \qquad (3.14)$$

Where R - air flow resistivity,
∇P - Pressure difference in Pascal,
v -linear air flow velocity in m/s
d- Thickness in meter

3.2.4.3 Sound absorption properties

The frequency of resonance depends on the ratio of elastic modulus to density as both these parameters can be varied independently. Spacer fabrics can be used to eliminate certain frequencies. The damping capacity of spacer fabrics has been shown to be an order of magnitude

higher than that of the other nonwovens and foams. Spacer fabrics have also been used as sound proofing materials. Within porous and three layer structures, sound is attenuated by vibration and friction losses as gas flows between two layers during propagation. Repeated reflections within the spacer structure gives rise to long paths where full absorption is possible. The acoustic properties of the spacer fabrics can be used where sound absorption is vital i.e. auditorium, automotive vehicles etc. There are several techniques to measure sound absorption. They are Reverberant Field Method, Impedance Tube Method and Steady State Method etc [88, 89].

3.2.4.3.1 Measurement of sound absorption coefficient (Impedance tube method)

In this research, the impedance tube method was used to determine the normal incident sound absorption coefficient, SAC (α). A minimum of three specimens for each sample were tested according to ASTM E 1050-07. Standard test method for impedance and absorption of acoustic materials using a tube with two microphones and a digital frequency analysis system was used (Figure 3.13). It uses plane sound waves that strike the material straight and so the sound absorption coefficient is called normal incidence sound absorption coefficient, SAC. In this study, the impedance tube method was used, which is faster and generally reproducible and, in particular it requires relatively small circular samples, both 29 and 100 mm in diameter according to the frequency range (former measures 500 Hz to 6.4 kHz and later 50 Hz to 500 Hz). Thus the method avoids the need to fabricate large test sample with lateral dimensions several times the acoustic wavelength.

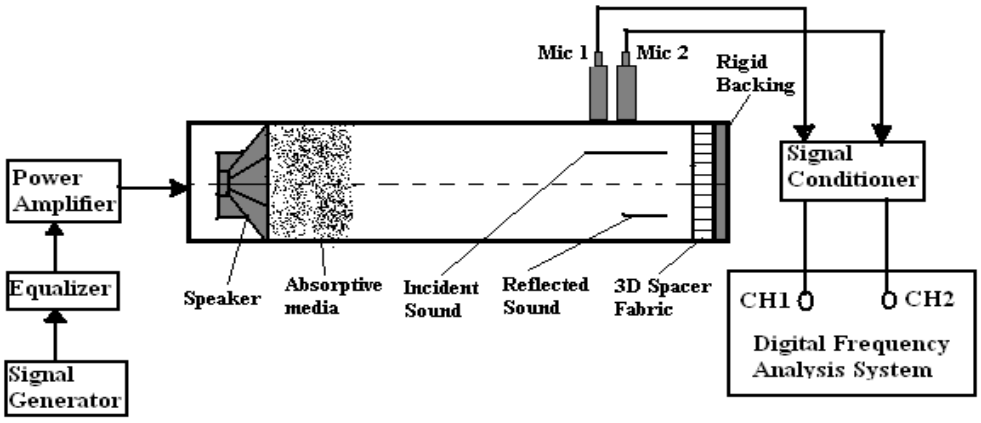

Figure 3.13 Impedance tube method (ASTM E 1050-08)

3.2.4.3.2 Calculation of NRC (Noise Reduction Coefficient)

The "Noise Reduction Coefficient" (NRC) is a measure of how much sound is absorbed by a particular material, and is derived from the measured Sound Absorption Coefficients AT different frequencies (Hertz). The NRC was determined using the following formula (eqn. 3.15).

$$NRC = \frac{\alpha_{250} + \alpha_{500} + \alpha_{1000} + \alpha_{2000}}{4} \quad (3.15)$$

3.2.5 Statistical analysis

Statistical analysis software, QC Expert - Trilobyte was used to conduct all the statistical tests mentioned in this work. Advance statistical evaluation and two-way analysis of variance was used to analyze the significance of various factors on required properties of warp as well as weft knitted spacer fabrics. Also, differences in means between various groups were examined for statistical significance using one-way ANOVA followed by pair comparison using Scheffe's method. For all the statistical tests, differences were considered significant at $P < 0.05$. Data were reported as mean ± standard error of mean, unless otherwise stated.

Chapter 4 - Results and discussions

4.1 In-plane shear behavior of 3D spacer fabrics

The in-plane shear properties of both warp and weft knitted spacer fabrics have been carefully evaluated using experimental and image analysis method and discussed in this section.

4.1.1 Image analysis method

The picture frame test method was verified for the 3D spacer fabrics under consideration. Figure 6 shows the array of images for a 3D spacer fabric specimen captured during the loading process at each 5mm displacement for every 30 sec. In the beginning, (Figure 4.1a), there is no shearing. Subsequently the shear deformation resistance was mainly from the friction between the wale and course direction loops before reaching the limiting locking angle. The limiting locking angle was the ultimate shear deformation observed by means of local wrinkling. Based on the deformed configuration of the fixture, shear angle was calculated using the relationship shown in equation 3. A vertical displacement of 40 mm, which corresponds to a shear angle of around 45^{o} was found to be the maximum displacement but the pre-buckling occurs after 20 mm displacement with shear angle ranging between $20\text{-}30^{o}$ (Figure 4.1 e). The local buckling is calculated using image analysis software. Figure 4.2 presents the linear fit curve between time and displacement.

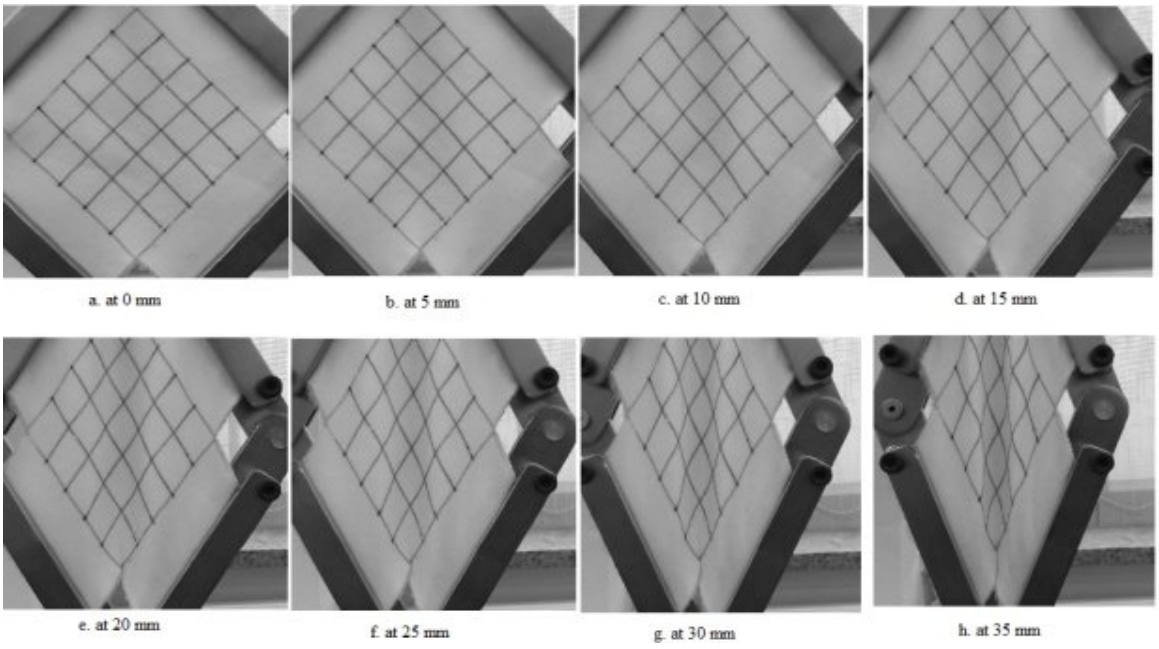

Figure 4.1 Shear deformation of specimen at different displacement levels

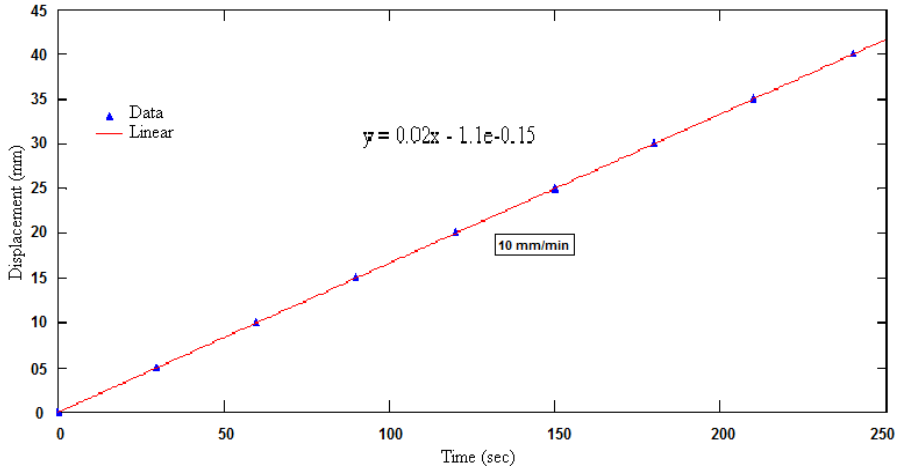

Figure 4.2 Linear fit curve between time and displacement (10 mm/min)

Figure 4.3 shows the image of a fabric specimen captured during the loading process without displacement. This image was analyzed to obtain shear angle of the specimen during the shear displacement. The image file string was examined and then the appropriate image reading function was called by MATLAB imread. The image was then converted to a gray image and then normalized to a matrix of values ranging from zero to one. This matrix was returned by the function in the variable I. Image analysis can aid in the determination of the shear angle and displacement at any particular point on the surface of fabric specimen. Grid pattern was applied on the specimen surface before the test and used as the reference points of image analysis. Around 16 points (25 square cells (4cm^2 each) with 90^o angle at 4 points) can be chosen on a 100 mm x 100 mm specimen for image analysis to determine the displacements and shear angles at the chosen points. First, by manually choosing the points on a reference image, the X and Y coordinates of each point can be determined in pixel as shown in Figure 11. The difference of X and Y coordinates of each chosen point between the reference image and the image chosen for analysis represents the displacements in X and Y directions. Figure 4.4 shows the main idea of Hough transform applied to find the shear angle in image analysis technique. The Hough transform is widely used in image analysis, computer vision and digital image processing. It is a technique used to find shapes in a binary digital image. This approach is preferred when the objective is to find lines or curves in an image. The parameter ρ represents the distance between line and origin, θ is the angle of the vector from origin to this point. Figure 4.5 shows the points where the lines intersect giving the distance and angle. This distance and angle indicate the line which bisects the points being tested after each 5 mm displacement at every 30 sec interval. It helps researchers to understand more about detection of angles using Houghs transform. It clearly shows that detected points for two different levels of displacement are widely different, at 0 mm (θ=90^o) and at 10 mm (θ= around 80^o). Figure 4.5(a & b) show behavior of specimen during application of axial force by considering bucking effects. At 10 mm displacement the lines detected on surface of the specimen clearly indicate that the buckling has not happened

because of regular intersection of lines (Fig 4.4a). But in case of 25 mm displacement, the irregular intersections of lines have occurred due to its wrinkling effects (buckling). The bucking starts at 20 mm displacement and having maximum buckling at 35 mm. The determination of shear angle for both warp and weft knitted spacer fabrics using image analysis are discussed and presented clearly in the following section.

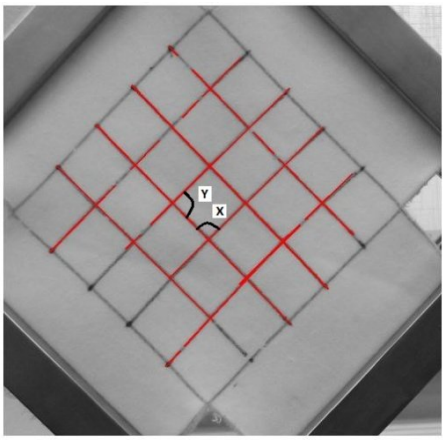

Figure 4.3 Determination of shear angle using image analysis

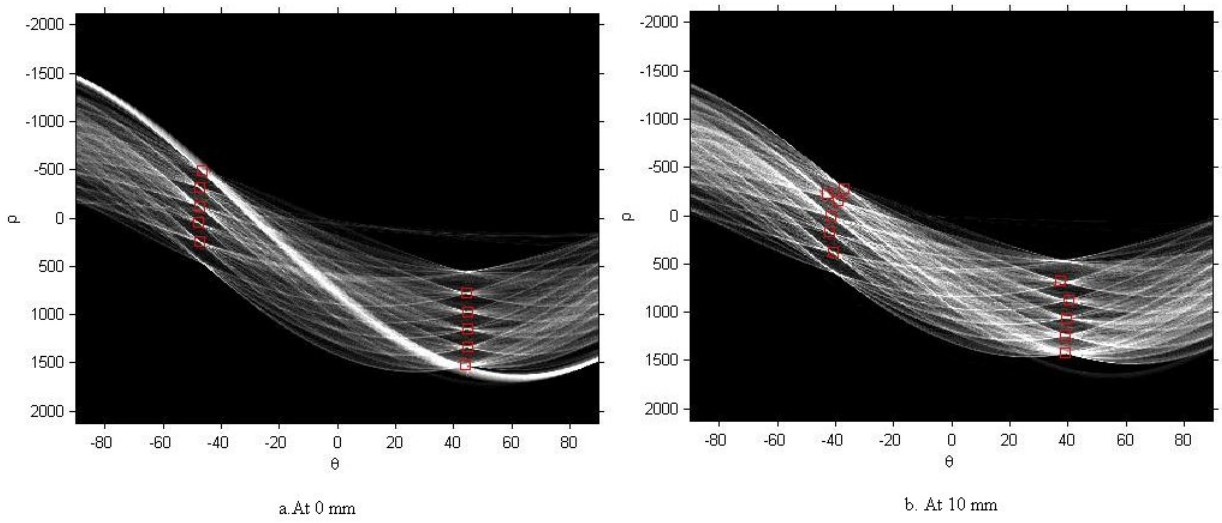

Figure 4.4 Detected lines and points in Hough's histogram at two displacement levels

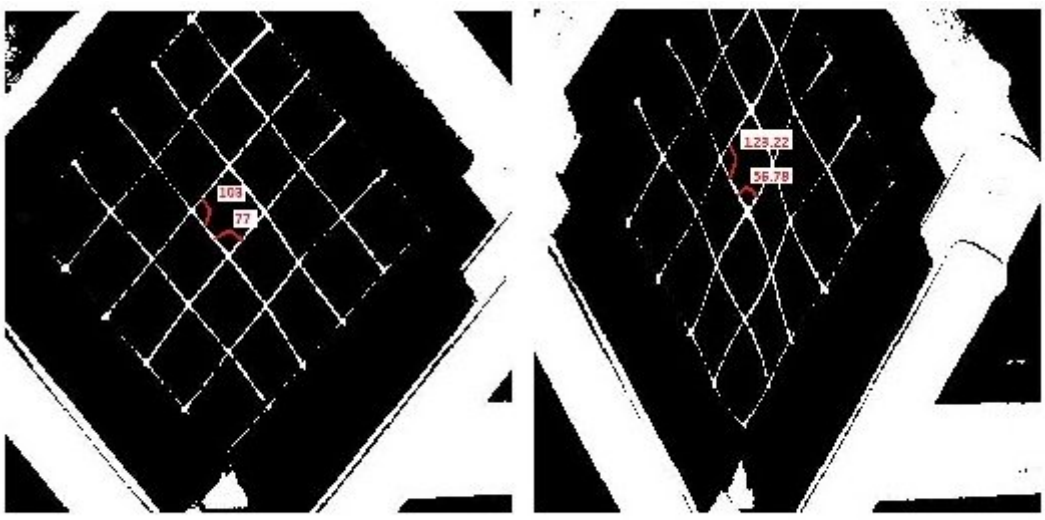

a. At 10 mm (Without Buckling) b. At 25 mm (With Buckling)

Figure 4.5 Gray image of shear angle at two displacement levels, considering buckling effects

4.1.2 Experimental evaluation of in-plane shear behavior of warp knitted spacer fabrics

The experimental evaluation of shear stress, shear strain and shear angle of warp knitted spacer fabrics are explained in this section.

4.1.2.1 Influence of thickness on in-plane shear behavior of warp knitted spacer fabrics

In this section, the effect of thickness on in-plane shear behavior of warp knitted spacer fabrics has been evaluated with respect to different structural parameters. First group of six spacer fabrics (WAS 1 – WAS 6) were produced with same outer layer structure (Lock knit) and stitch density but with different thickness (1.5, 2.5 & 3.5mm). As shown in Figs. 4.6a & b, the stress-strain curve reveals that the shear resistance decreases with increase in thickness. It can be seen that, the samples have almost similar behavior as they behave linearly in surface extension stage due to same surface structure and density. In next stage of shear deformation, the compressive stress also played a vital role to make the fabrics resist shear force. It was also observed that the thicker fabric has ability to undergo larger deformation in both shear and compression conditions. It was found that the hexagonal net structure fabrics (WAS 7 - WAS 12) show similar trend as the lock knit structures (Figures 4.6c & d). The stress–strain curves show that, shear resistance is indirectly proportional to thickness of the spacer fabrics. From this observation, it is suggested that the fabrics with different thicknesses have different ranges of applications. The thickness of the fabric should be selected according to the amount of the energy to be absorbed and allowed shear stress level. The shear stress–strain behavior of spacer fabrics appears to change significantly with an appreciable decrease in spacer thickness.

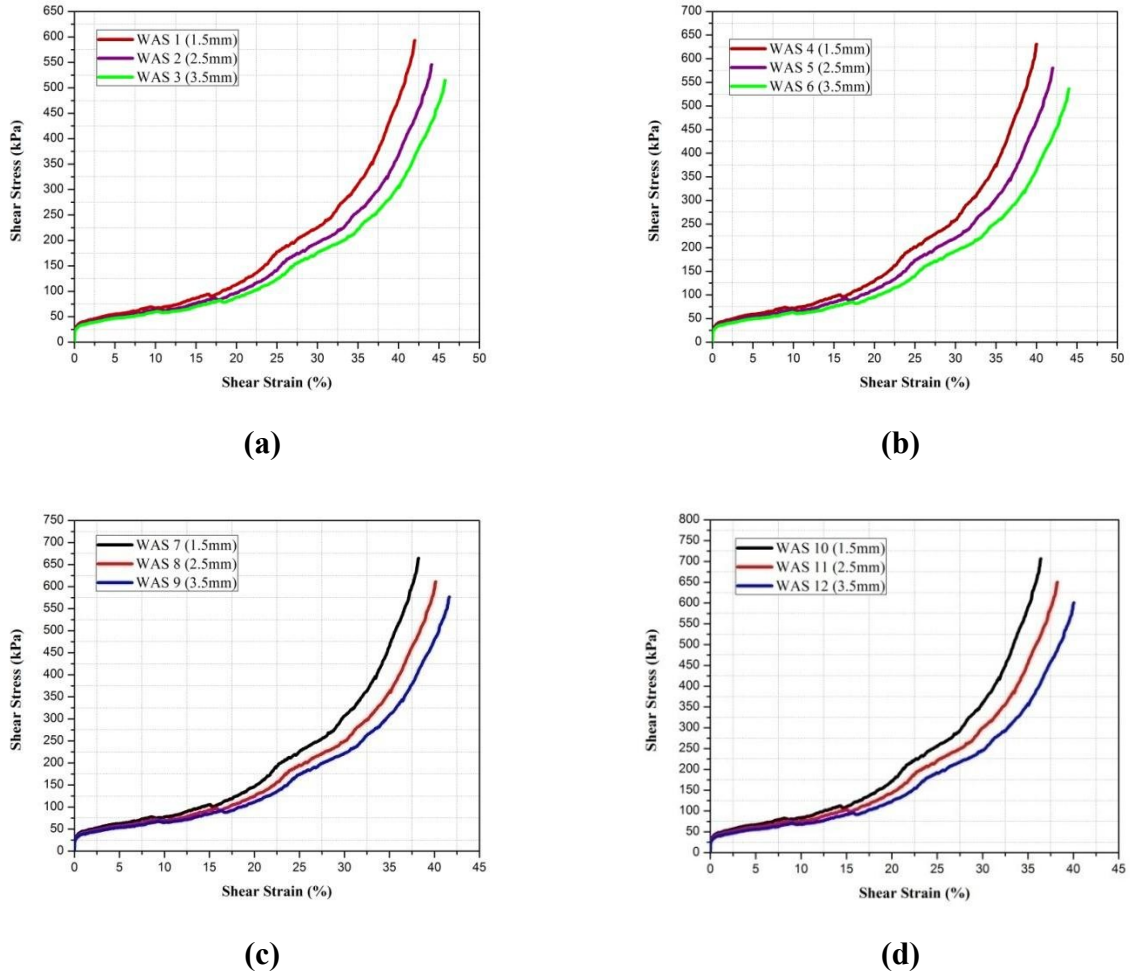

Figure 4.6 Influence of thickness on shear behavior of warp knitted spacer fabrics

4.1.2.2 Influence of spacer yarn on in-plane shear behavior of warp knitted spacer fabrics

In both sets of spacer fabrics (lock knit and hexagonal net), two types of spacer yarn with different linear density (33 & 108 dtex) and diameter (0.055 & 0.1 mm) were used for convenient analysis of its effect on in-plane shear. Normally the spacer yarns are monofilament which connect surface layers and keep them apart. The spacer yarns act as linear springs which offer more resistance towards compression, result in higher shear stress as compared to other type of materials in specific applications. The angles between spacer yarn and surface layer can be varied by means of needle under lapping. In this study, spacer yarn angles (84^o – 86^o) of different samples have been maintained. From the Figures 4.7(a)&4.7(b), it is observed that, the shear stress is high for the fabrics with coarser spacer yarn for both types of structures. In surface elongation and compression (1^{st} stage), a higher shear force was observed in the fabrics with coarser spacer yarn as compared to the fabrics made up of finer spacer yarns. It might be the fact that the large diameter and linear density of the coarse spacer yarns have higher ability to resist compressive stress than the fabrics made up of finer spacer yarn. In stage 2, the pre–buckling

was observed after 20% of shear strain because the surface layers come in contact with each other leading to a locking effect. The fabrics have almost identical stress-strain curves with same thickness for both lock knit and hexagonal spacers in stage 1 region. However, a significant difference in the shear stress-strain behavior was obtained in the densification stage. It was due to the fact that the internal surface and spacer layer experience a closer compaction which depends on the thickness, the surface structure and spacer yarn properties.

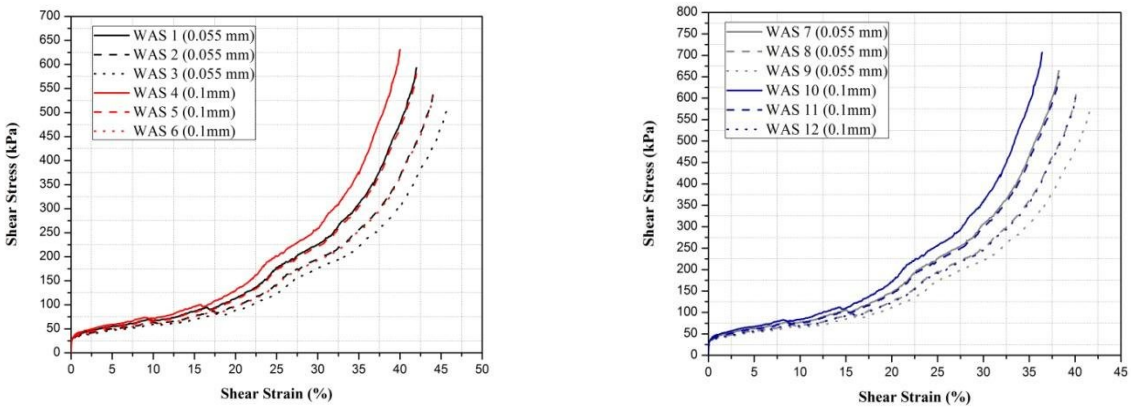

(a) **(b)**

Figure 4.7 Influence of spacer yarn linear density on shear behavior of warp knit spacer fabrics

4.1.2.3 Influence of surface structure on shear behavior of warp knit spacer fabrics

The in-plane shear behaviors of spacer fabric are also greatly influenced by their surface structures. The outer layer structure affects the monofilament yarn inclination, binding condition with surface, distribution and multifilament stitches in surface layers. The surface layers with these structures are shown in Table 3.1, from which the stitch density, spacer yarn angle and size of the stitches in the outer layers can be clearly observed. It has been found that the surface structures could slightly affect the stitch density of the outer layers and the spacer yarn inclination angle, although these parameters are maintained the same during knitting. As shown in Figure 4.8, the shear stress-strain behavior for both the structures (Lock knit and Hexagonal net) exhibits almost same load and deformation in stage 1. In stage 2, it is found that the Hexagonal-mesh fabric offers higher shear resistance than that of lock knit structures. All the samples have almost close value in the surface elongation region and the differences could be observed when the fabric undergoes lateral compression in stage 2. It might be due to those insignificant differences in the stitch density in surface deformation stage and thickness and spacer yarn properties influences in compression stage. In stage 3, the lock knit fabrics (WAS 1 – WAS 6) undergo large shear deformation for the same shear stress.

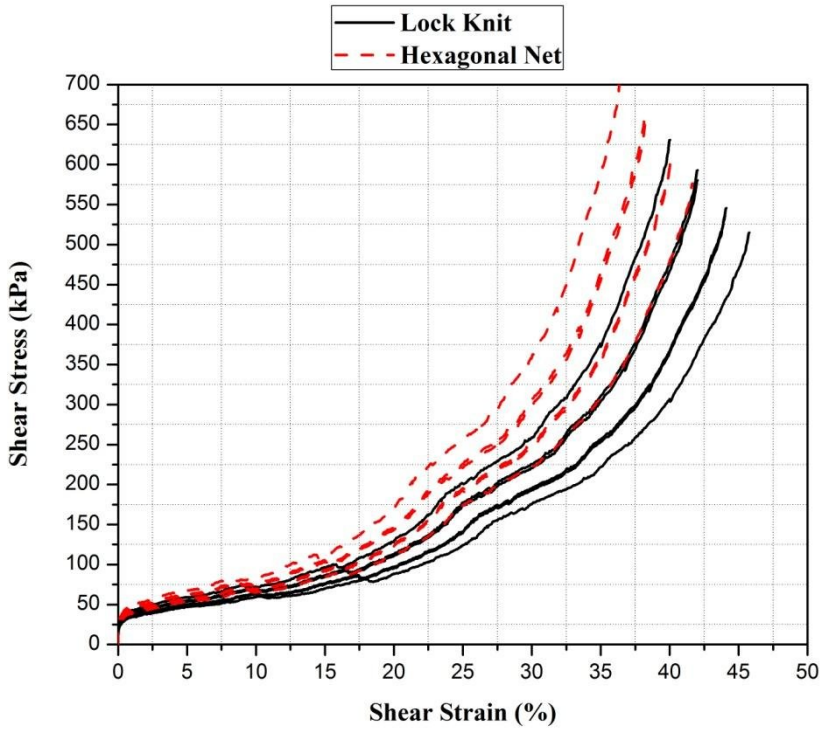

Figure 4.8 Influence of surface structure on shear behavior of warp knit spacer fabrics

4.1.2.4 In-plane shear work done of warp knit spacer fabrics

Figure 4.9 (a – d) presents the work done on all spacer fabrics under in-plane shear load and it also compares the response shear stress with effect of deformation and structural characteristics. The figures reveal that thicker fabrics have higher work done than that of thin fabrics when it undergoes compression. Irrespective of the structural variation (lock knit and hexagonal net), the shear work done shows same trend for all the samples. Overall, the work done values were higher for the fabrics made up of hexagonal net structure on face side than that of lock knit fabrics. Also, it can be seen that fabrics with finer spacer yarn have low work done when compared to other fabrics; it might be due to finer spacer yarn offers low resistance towards compression. Figure 4.10 and Figure 11 present the graphical analysis of shear stress versus absorbed energy versus efficiency. It is obtained from the Figure 6, the shear work done of lock knit spacer fabrics (WAS 1 – WAS 6) linearly increases with the stress in the surface extension and compression stage. The marginal differences in work done between the samples can be seen when the shear stress reaches towards the stage 2 for both the structures. At the start of densification stage, the rapid increases in stress results in small deformation and work done. From the energy absorption graph, it is easy to find the stress associated with the required amount of energy to be absorbed. So, it is more convenient to select the suitable spacer fabrics for car seat and back support application with optimum in-plane shear performance. As it is observed from the Figure 4.10, the fabric with hexagonal net structure shows similar tendency in energy absorption and efficiency with regards to thickness and spacer yarn. The maximum

energy-absorption efficiency is obtained at the end of the densification stage. As noticed in the densification stage from Figures 4.10 & 4.11, efficiency becomes almost constant with increase in stress level. It may also be because of locking of the spacer yarn and with the yarns in the surface structure of spacer fabrics. The point at the maximum energy-absorption efficiency can be considered a critical point in the densification zone. Overall, it was observed that the shear work done and efficiency is higher for the thin fabrics with low density. Also, it was found that fabrics with finer spacer yarns undergoes large amount of work done as well as high efficiency during shearing mechanism.

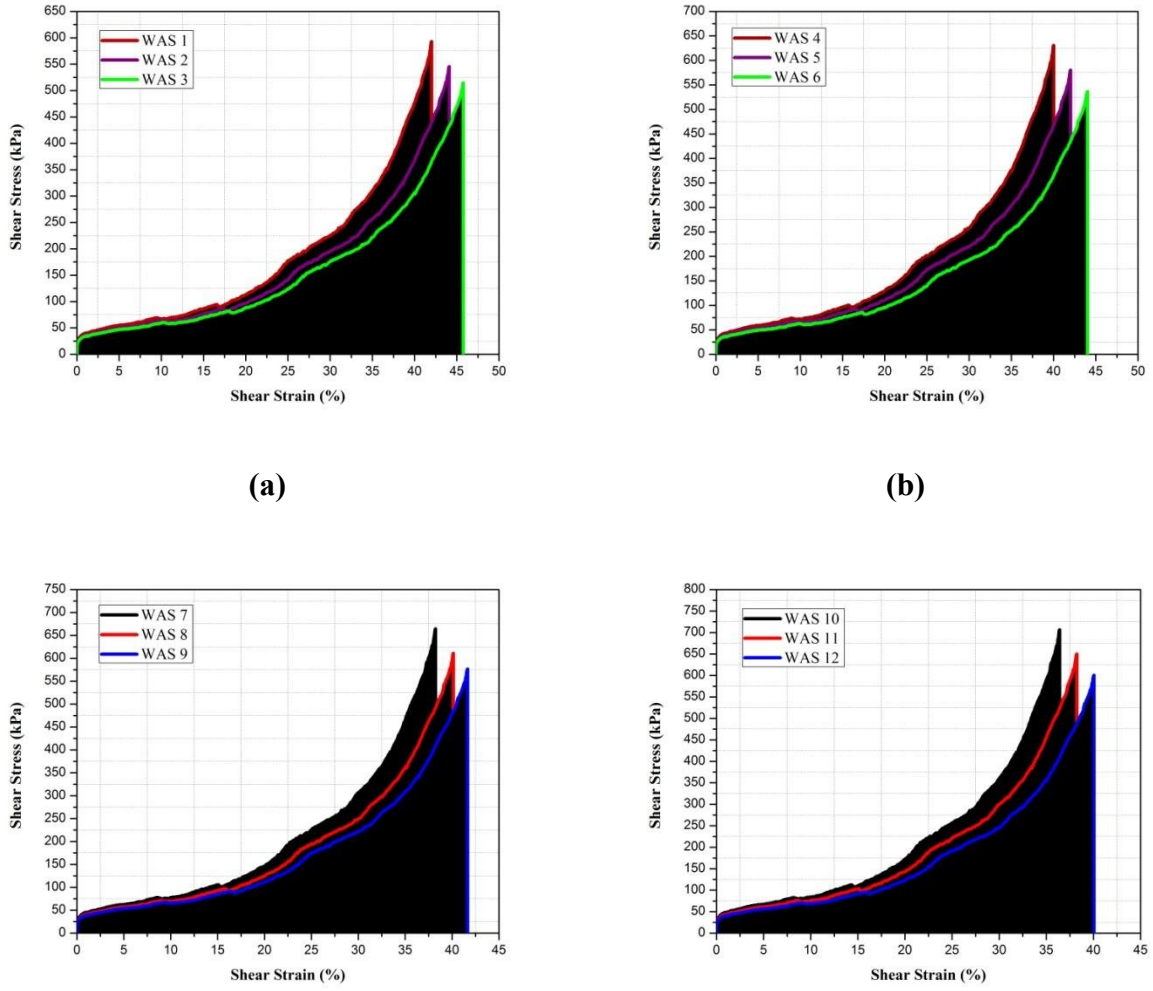

Figure 4.9 Work done during shearing of warp knit spacer fabrics

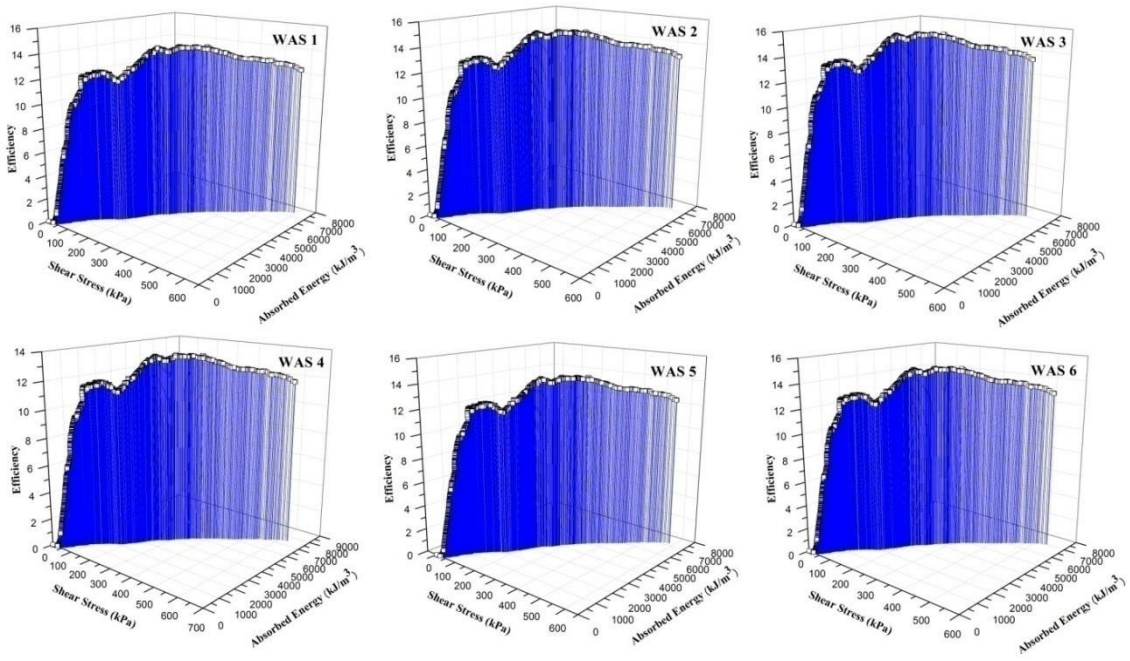

Figure 4.10 In-plane shear energy absorption and efficiency of lock knit spacer fabrics

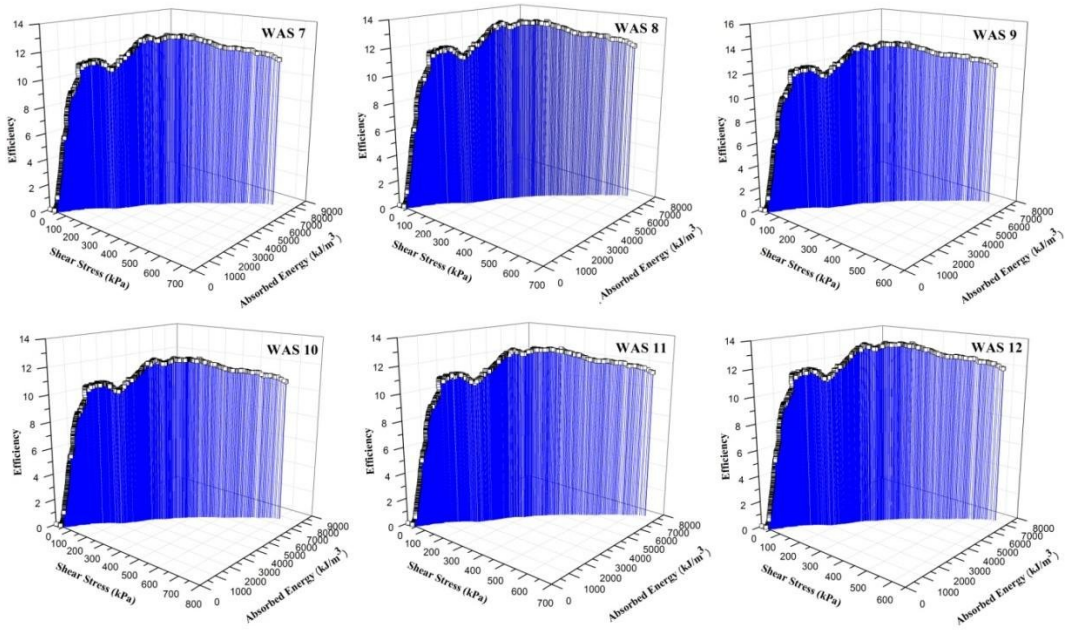

Figure 4.11 In-plane shear energy absorption and efficiency of hexagonal net spacer fabrics

4.1.2.5 Relation between shear angle versus shear force of warp knit spacer fabrics

The in-plane shear angle versus shear stress of 12 warp knitted spacer fabrics were carefully evaluated and presented in the Figure 4.12. It is observed from the graph that the thin hexagonal net spacer fabric with coarser spacer yarn (WAS 10) offers more resistance towards shear

deformation than that of other fabrics. The thick lock knit fabrics with low linear density spacer yarn (WAS 3) have ability to undergoes high shear angle with low shear stress

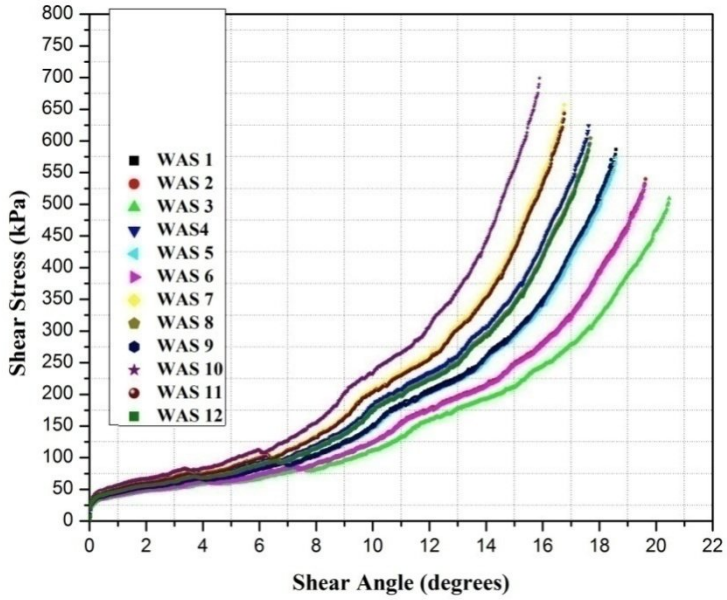

Figure 4.12 Experimental determination of shear force and shear angle of warp knit spacer fabrics

4.1.2.6 Regression model for shear deformation of warp knitted spacer fabrics

Linear relationship between two variables x and y is a common concept, in which effective and easy assumptions helps to deduct relationship between them.

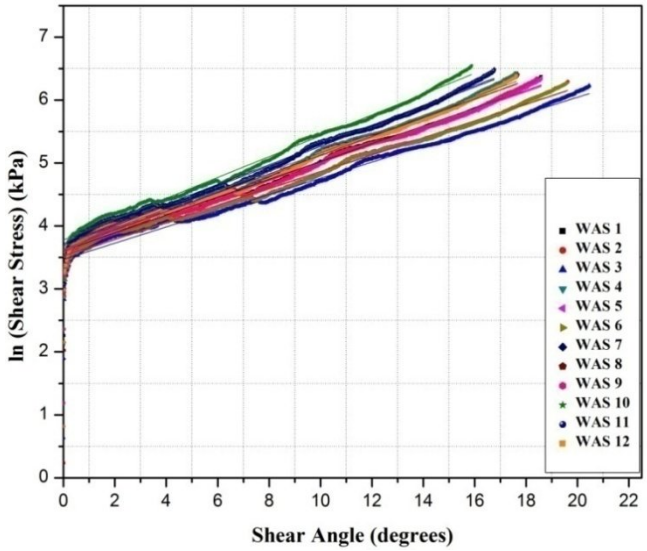

Figure 4.13 Linear regression fit of experimental shear stress of warp knit spacer fabrics as a function of shear angle

The average of in-plane stress responses against shear angle obtained for each spacer fabrics samples was fitted in the general form of linear fit (Figure 4.13). To obtain highly fitted linear equation and R^2 value, the dependent variable values (shear stress) were transformed using log-transformation. Response fit analyses, regression coefficient estimations and model significance evaluations were conducted. The estimated coefficient of determination and fitted linear regression equation are given in Table 4.1. The adequacy of the models was tested using residuals sum of squares and probability.

Table 4.1 Prediction of experimental shear strength of warp knit spacer fabrics using linear regression model

Equation		**y = a + b*x**					
DF		**Model - 1, Error - 926, Total - 926 - 927**					
Weight		**No Weighting**					
Sample Nos.			**Value**	**Standard Error**	**Residual Sum of Squares**	**F Value**	**Prob>F**
ln(Shear Strength)	**WAS 1**	Intercept	3.611	0.007			
		Slope	0.141	0.001	11.837	41678.774	0.000
	WAS 2	Intercept	3.529	0.007			
		Slope	0.134	0.001	13.309	37124.890	0.000
	WAS 3	Intercept	3.470	0.008			
		Slope	0.129	0.001	16.564	29911.002	0.000
	WAS 4	Intercept	3.671	0.007			
		Slope	0.149	0.001	12.088	40814.370	0.000
	WAS 5	Intercept	3.588	0.008			
		Slope	0.141	0.001	13.950	35438.801	0.000
	WAS 6	Intercept	3.510	0.008			
		Slope	0.134	0.001	15.042	32910.134	0.000
	WAS 7	Intercept	3.719	0.008			
		Slope	0.157	0.001	15.121	32725.172	0.000
	WAS 8	Intercept	3.635	0.009			
		Slope	0.149	0.001	18.338	27052.690	0.000
	WAS 9	Intercept	3.584	0.007			
		Slope	0.142	0.001	11.382	43314.790	0.000
	WAS 10	Intercept	3.778	0.008			
		Slope	0.165	0.001	15.815	31309.158	0.000
	WAS 11	Intercept	3.695	0.008			
		Slope	0.157	0.001	16.971	29212.851	0.000
	WAS 12	Intercept	3.620	0.008			
		Slope	0.149	0.001	14.202	34815.729	0.000

4.1.2.7 Statistical evaluation – in-plane shear behavior of warp knit spacer fabrics

In this section, two -way ANOVA is discussed. The selected value of significance for all statistical tests in the study is 0.05 levels. Analysis of different combination of factors on shear work done is presented in Table 4.2. The factors mainly considered were thickness, spacer yarn diameter and structure which strongly influence the shear behavior and energy absorption of the three-dimensional spacer fabrics.

Table 4.2 Statistical evaluation for in-plane shear behavior of warp knit spacer fabrics

ANOVA Table

Source of variability	*Sum of squares*	*Mean square*	*Degrees of freedom*	*Standard deviation*	*F-statistic*	*Critical quantile*	*Conclusion*	*p-value*
Influence of spacer yarn diameter and thickness on shear work done - lock knit								
Thickness	199036.55	99518.27	2.00	315.47	83.16	19.00	Significant	0.011882
Spacer Yarn Diameter	6868.82	6868.82	1.00	82.88	5.74	18.51	Insignificant	0.13884
Interaction	1695.60	1695.60	1.00	48.92	2.43	161.45	Insignificant	0.3631136
Residuals	697.78	697.78	1.00	26.42				
Total	208298.75	41659.75	5.00	204.11				
Influence of spacer yarn dia and thickness on shear work done - Hexogonal net								
Thickness	206704.21	103352.11	2.00	321.48	83.12	19.00	Significant	0.0118881
Spacer Yarn Diameter	7132.91	7132.91	1.00	84.46	5.74	18.51	Insignificant	0.138906
Interaction	1761.48	1761.48	1.00	49.87	2.43	161.45	Insignificant	3.63E-01
Residuals	725.40	725.40	1.00	26.93				
Total	216324.00	43264.80	5.00	208.00				
Influence of structure and thickness on shear work done for spacer yarn dia (0.055 mm)								
Structure	28576.03	28576.03	1.00	169.04	3818.59	18.51	Significant	0.0002618
Thickness	167843.18	83921.59	2.00	289.69	11214.38	19.00	Significant	8.92E-05
Interaction	14.97	14.97	1.00	3.87	35386.51	161.45	Significant	3.38E-03
Residuals	0.000	0.000	1.000	0.021				
Total	196434.17	39286.83	5.00	198.21				
Influence of structure and thickness on shear work done for spacer yarn dia (0.1 mm)								
Structure	29112.10	29112.10	1.00	170.62	2681.85	18.51	Significant	0.0003727
Thickness	242741.17	121370.58	2.00	348.38	11180.82	19.00	Significant	8.94E-05
Interaction	21.71	21.71	1.00	4.66	228306.94	161.45	Significant	0.0013324
Residuals	0.000	0.000	1.000	0.010				
Total	271874.98	54375.00	5.00	233.18				

The critical quantile ($F_{critical}$) values were obtained for factor A - 18.51, Factor B – 19.00 and Interaction – 161.45 with respect to degrees of freedom. The value of $F_{critical} < F_{statistic}$ proved that the changes in the thickness and surface layer structure of warp-knitted spacer fabric has significant influence on the above-mentioned fabric shear properties. Even the minor changes in the fabric thickness resulted in significant impact on the shear behavior. Interaction factors thickness – spacer yarn diameter with in both lock knit and hexagonal net structure doesn't have

significant influence ($p > 0.05$) on shear behavior. The plot of means visually compares the response values for each combination of factor levels (or each cell). In Figure 4.14a, the circle stands for mean value of 5 observations. Diameter of the circle is roughly proportional to the response. Differences between levels and interactions can be seen on this plot. The residuals versus prediction plot show the quality of fit of the model. From the Figure 4.14b it is observed, closer are the points to the line $y = x$, the more significant the model is. If the lines for factor A are similar for each level of the factor B, then the factor A is probably significant. If the lines have rather opposite direction, then there is probably strong interaction between the factors. If the lines are shaped rather randomly, then the influence and significance of the respective factor is probably low. The plot is only a qualitative visual tool and cannot fully replace the F-test. Figures 4.14c and d show that the lines of factor – thickness are looks merely same trend, not just opposite to the factor – spacer yarn diameter, hence it reveals that there is no interaction between these two factors.

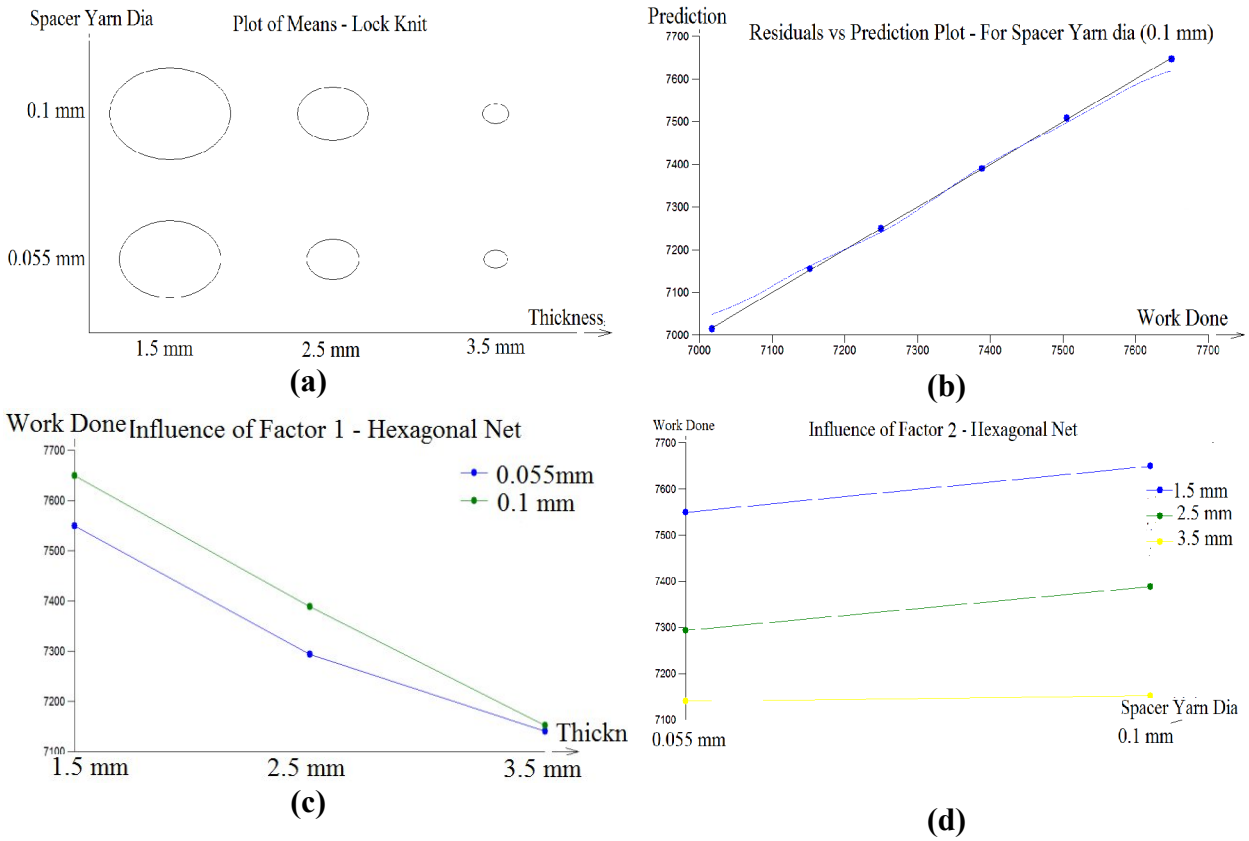

Figure 4.14 Graphical output – Statistical evaluation for in-plane shear behavior response of warp knit spacer fabrics

4.1.2.8 Determination of shear angle of warp knit spacers using image analysis method

The shear angle of warp knitted spacer fabrics was determined using image analysis method at different displacement levels and presented in the Figures 4.15a & b. In both the cases (lock knit

and hexagonal structures), the spacer fabric samples (WAS 1 – WAS 12) have smooth and linear increases in shear angle till 25mm displacement. The irregular trend in shear angle observed after 25 mm displacement may be due to the fact that spacer fabric undergoes compaction which leads to buckling. In the buckled fabric, it is extremely complex to find the same shear angle at different points using Hough transformation image analysis method. The image analysis shear angle is plotted against the shear strain for both the structures such as lock knit (WAS 1 – WAS 6) and hexagonal net (WAS 7 – WAS 12) as given in the Figure 4.16 Also, the linear model fit was presented in figures with shear strain as independent variable and shear angle as dependent variable. The regression equation for all the samples are given in the Table 4.3.

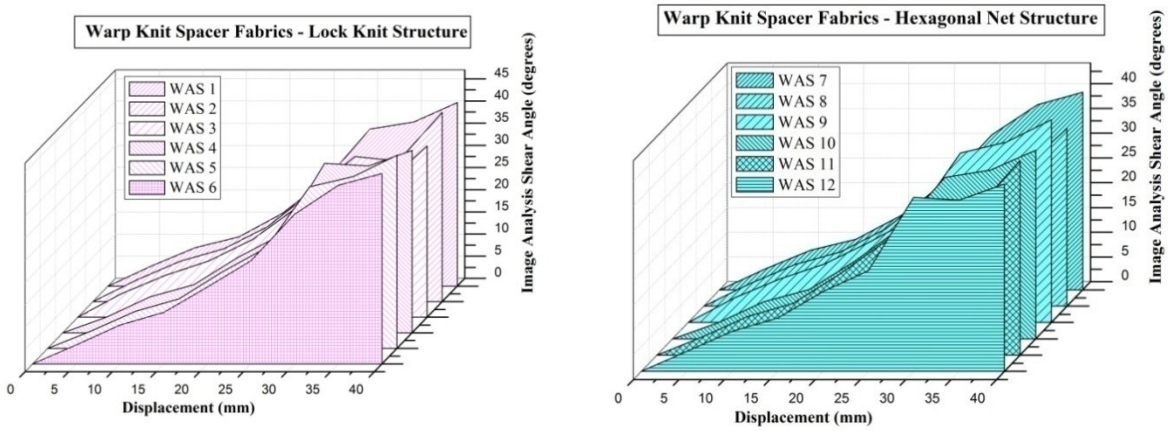

(a) **(b)**

Figure 4.15 Determination of shear angle of warp knit spacers using Image Analysis method

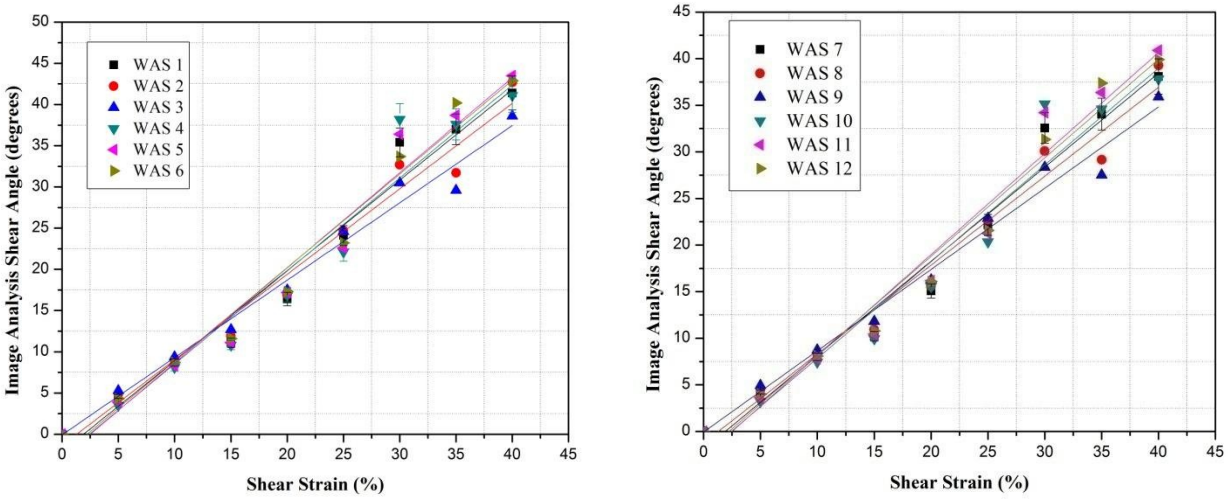

(a) **(b)**

Figure 4.16 Linear regression fit of shear angle using image analysis as a function of strain of warp knit spacer fabrics (a) Lock knit structure (b) hexagonal net structure

4.1.2.9 Comparative discussion of shear behavior of warp knitted spacer fabrics using different methods

The shear angles are calculated by considering sample length as a substitute for L in Equation 2 and it is further used for calculation of shear force. Figure 4.17 shows the comparison of shear angles between image analysis and both experimental measurements for all 12 specimens.

Table 4.3 Prediction of shear angle using image analysis as a function of shear strain of warp knit spacers

Warp Knit Spacer Fabrics - Lock Knit Structure						
Equation	**y = a + b*x**					
DF	**Model - 1 , Error - 7, Total - 8**					
Sample Nos.		**Value**	**Standard Error**	**Residual Sum of Squares**	**F Value**	**Prob>F**
WAS 1	**Intercept**	-2.091	1.668	51.552	245.259	0.000
	Slope	1.097	0.070			
WAS 2	**Intercept**	-1.347	1.474	40.269	280.577	0.000
	Slope	1.037	0.062			
WAS 3	**Intercept**	-0.071	1.097	22.283	414.594	0.000
	Slope	0.938	0.046			
WAS 4	**Intercept**	-2.736	2.229	92.088	144.907	0.000
	Slope	1.127	0.094			
WAS 5	**Intercept**	-2.884	1.859	64.069	218.124	0.000
	Slope	1.154	0.078			
WAS 6	**Intercept**	-2.516	1.561	45.129	300.433	0.000
	Slope	1.136	0.066			
Warp Knit Spacer Fabrics - Hexagonal Net Structure						
WAS 7	**Intercept**	-1.924	1.535	43.633	245.259	0.000
	Slope	1.010	0.064			
WAS 8	**Intercept**	-1.239	1.356	34.084	280.577	0.000
	Slope	0.954	0.057			
WAS 9	**Intercept**	-0.066	1.020	19.272	414.594	0.000
	Slope	0.872	0.043			
WAS 10	**Intercept**	-2.517	2.051	56.340	144.907	0.000
	Slope	1.037	0.086			
WAS 11	**Intercept**	-2.711	1.748	56.611	218.124	0.000
	Slope	1.084	0.073			
WAS 12	**Intercept**	-2.339	1.451	39.032	300.433	0.000
	Slope	1.057	0.061			

The differences between image analysis and calculated shear angle using sample length at the chosen points are relatively small. It does not show any significant difference until pre-buckling occurs but significant difference occurs after 20 mm displacement.

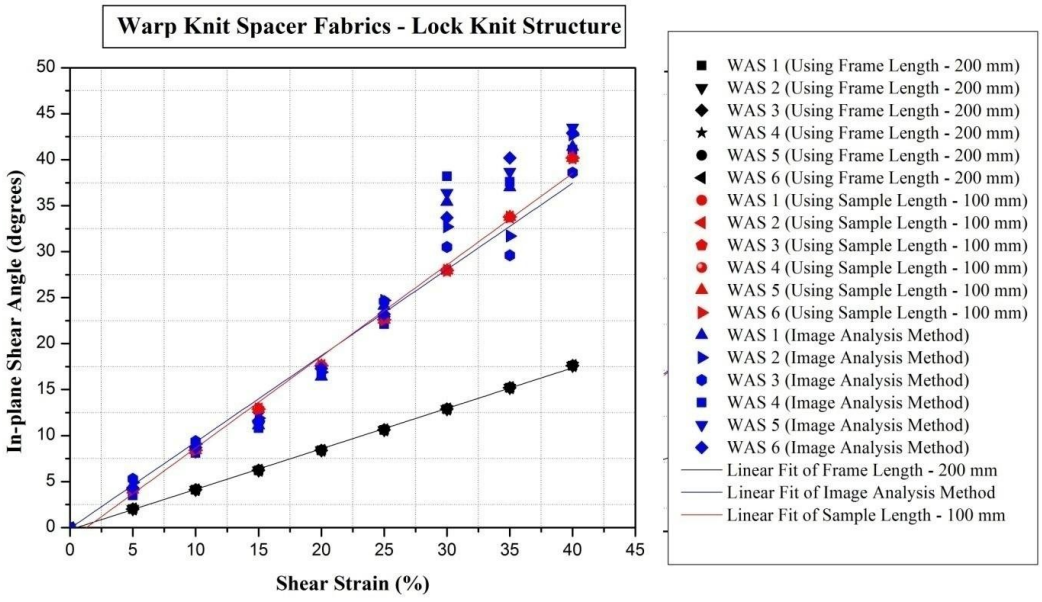

(a)

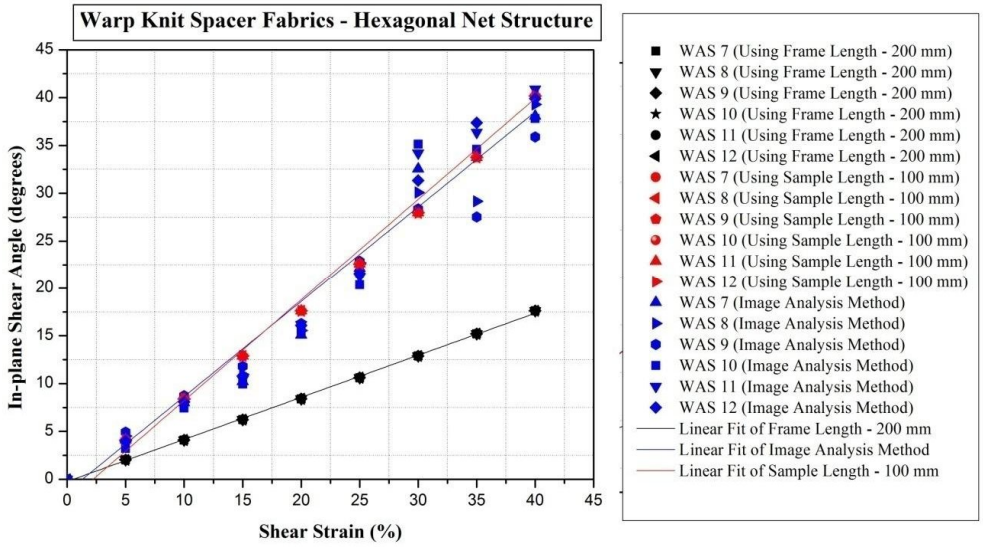

(b)

Figure 4.17 Comparison of shear behavior of warp knit spacer fabrics using different test methods (a) Lock knit structure (b) Hexagonal net structure

It was also believed that during image processing in MATLAB, detection of X and Y coordinates on the image was not accurate due to wrinkling in the central zone of samples. Also, it was noted that dimension of the frame rig length can cause big difference in shear angle as shown in Figure 4.17. Further study is required on the effect of different frame rig length and ratio of frame length to specimen size on in-plane shear behavior of 3D warp spacer fabrics. The comparative linear regression is given in the Table 4.4 as a function of shear strain. The regression equations

for all three methods are also given.

Table 4.4 Prediction of shear stress of warp knit spacer as a function of shear strain using different methods

Warp Knit Spacer Fabrics - Lock Knit Structure						
Equation	y = a + b*x					
DF	**Model - 1 , Error - 7, Total - 8**					
Methods		**Value**	**Standard Error**	**Residual Sum of Squares**	**F Value**	**Prob>F**
Using Frame Length	**Intercept**	-0.236	0.101	0.188	10820.581	2.00E-12
	Slope	0.440	0.004			
Using Sample Length	**Intercept**	-1.297	0.641	7.607	1367.847	2.75E-09
	Slope	0.046	0.027			
Image Analysis Method	**Intercept**	-0.071	1.097	22.283	414.594	1.73E-07
	Slope	0.046	0.046			
Warp Knit Spacer Fabrics - Hexagonal Net Structure						
Using Frame Length	**Intercept**	-0.236	0.101	0.188	10820.581	2.00E-12
	Slope	0.440	0.004			
Using Sample Length	**Intercept**	-1.297	0.641	7.607	1367.847	2.75E-09
	Slope	0.995	0.027			
Image Analysis Method	**Intercept**	-2.339	1.451	39.032	300.433	5.23E-07
	Slope	1.057	0.061			

4.1.2.10 Prediction of shear stress using Finite Element Method

The spacer structures were made using solidworks45 and were imported into ANSYS platform for mesh generation. The number of nodes in unit cell was 2130. Material properties e.g. tensile modulus, tensile strength, strain rate, Poisson's ratio etc. were used. Shear stress at various displacements were simulated. The results are shown in figure 4.18 and 4.19.

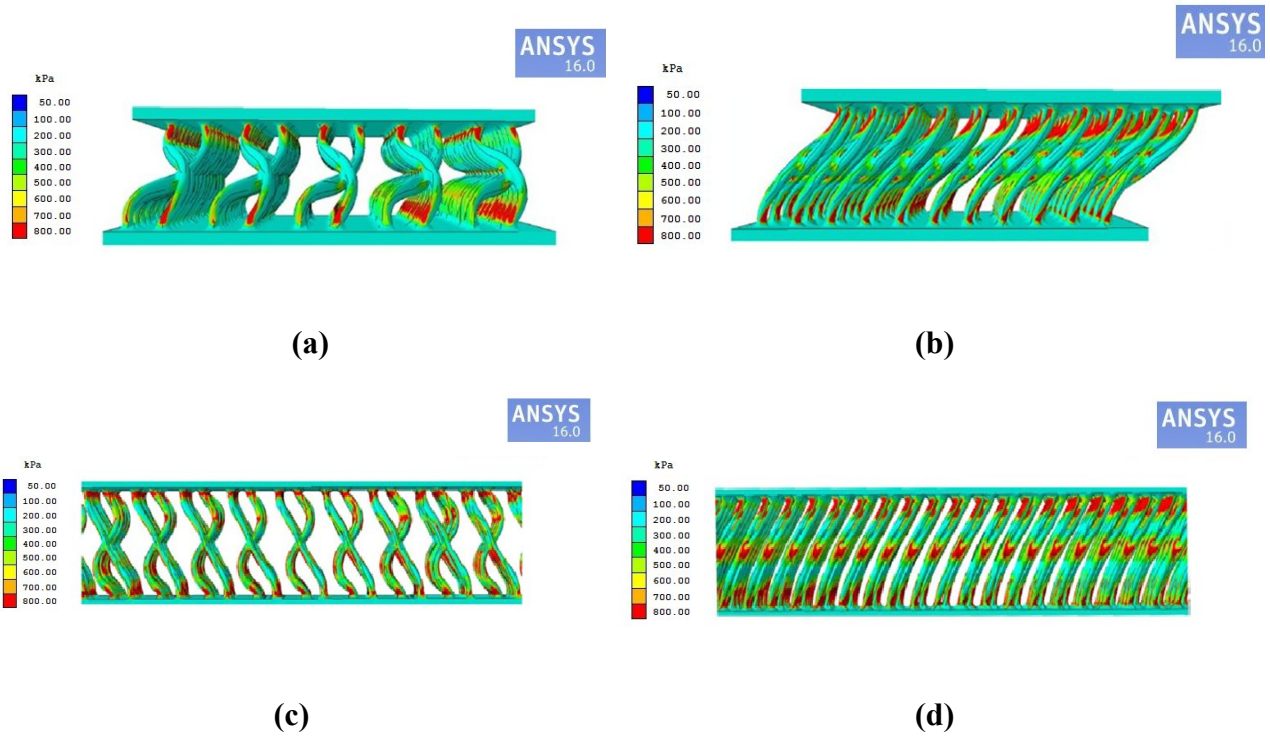

Figure 4.18 (a) Lock knit spacer before shear, (b) Lock knit spacer after shear, (c) Hexagonal net spacer before shear and (d) Hexagonal net spacer after shear

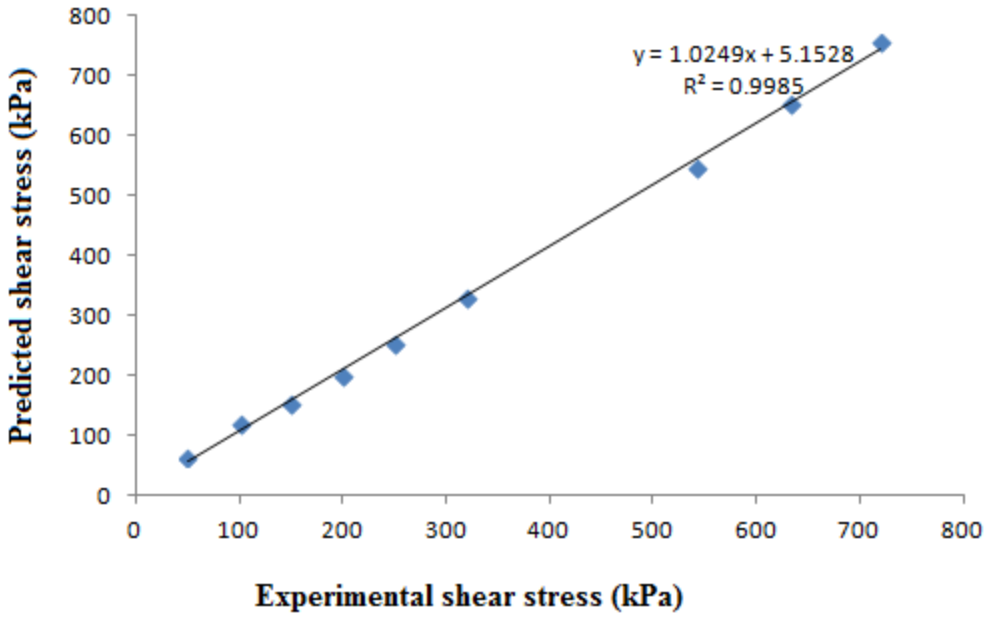

Figure 4.19 Correlation of simulated and experimental shear stress

The predicted shear stress was well correlated with experimental values obtained.

4.1.3 Experimental evaluation of in-plane shear behavior of weft knitted spacer fabrics

4.1.3.1 Effect of fabric characteristics on in-plane shear behavior of weft knit spacer fabrics

There is no shearing in the beginning of axial displacement of frame. Subsequently, the shear deformation resistance was mainly from the friction between the wale and course direction loops before reaching the limiting locking angle. The limiting locking angle is the ultimate shear deformation observed by means of local wrinkling. Based on the deformed configuration of the fixture, shear angle was calculated using the relationship shown in equation 3.5. A vertical displacement of 40 mm, which corresponds to a shear angle of around 50^o was found to be the maximum displacement but the pre-buckling occurs after 20 mm displacement with shear angle range of $20\text{-}30^o$. The local buckling is calculated using image analysis software. The effect of thickness and types of spacer yarn on in-plane shear behavior of weft knitted spacer fabrics have been carefully evaluated and analyzed with respect to different structural parameters. As shown in Figs. 4.20 & 4.21, the fabric samples (WES 1 and WES 2) offers higher resistance to shear than that of other fabrics. Also, the stress-strain curve reveals that the shear deformation is high is high for the fabric samples WES 4 to WES 6. It might be due to the two reasons that, fabrics (WES 4 – WES 6) made up of 6% lycra yarn on the surface layer which results large deformation during initial surface elongation. Also the sample with monofilament spacer yarn (WES 1 & WES 4) offers more resistance to compressive force results high shear resistance during the lateral compression stage.

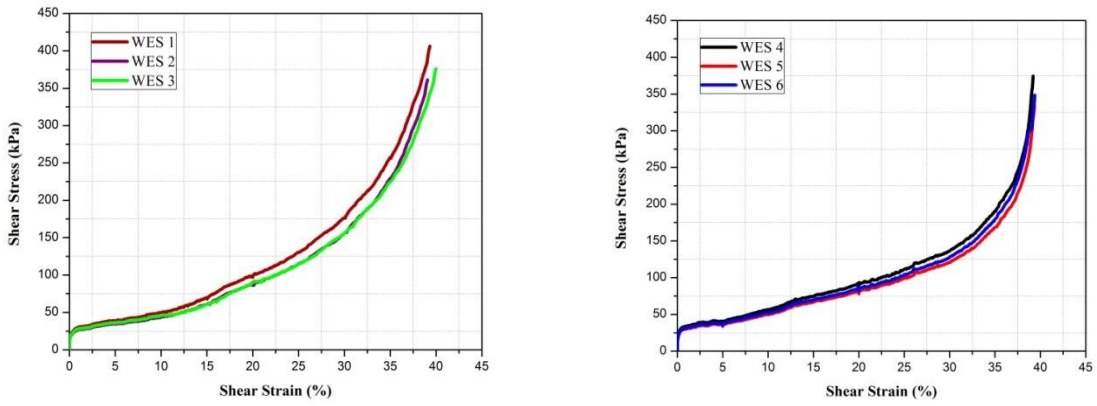

(a) **(b)**

Figure 4.20 Influence of thickness on shear behavior of weft knit spacer fabrics

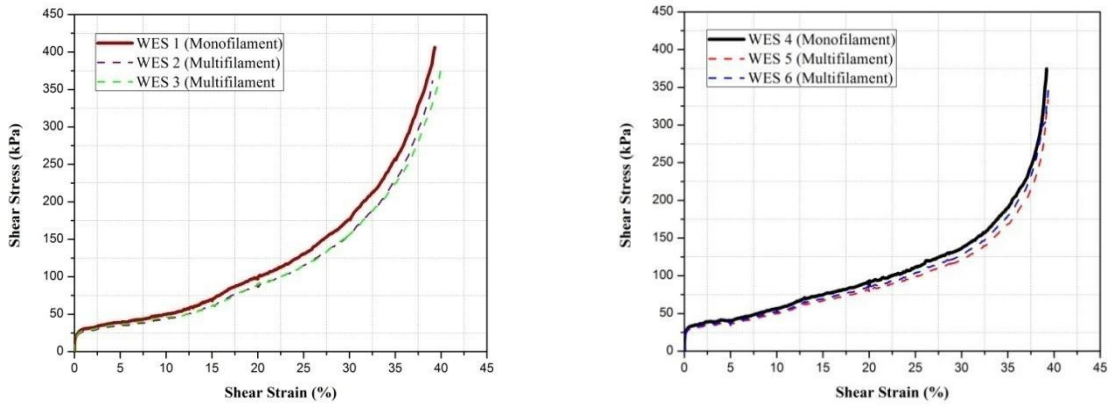

(a) **(b)**

Figure 4.21 Influence of types of spacer yarn on shear behavior of weft knit spacer fabrics

There was no marginal differences in shear stress between the samples in stage 1 (surface extension and lateral compression), but significant differences was seen immediately before pre-buckling and stage 3 (densification). From this observation, it is suggested that the fabrics with different thicknesses have ability to undergo different shear stress. The thickness of the fabric should be selected according to the amount of the energy to be absorbed and the allowed stress level.

4.1.3.2 In-plane shear work done of weft knit spacer fabrics

Figure 4.22a and b presents the work done of all spacer fabrics under in-plane shear load and also it compares the response shear stress with effect of deformation and structural characteristics. The figures reveal that fabrics WES 1 and WES 4 have higher work done than that of other fabrics when it undergoes in-plane shear. Irrespective of the surface structural variation (stitch density, thickness and types of spacer yarn), the shear work done shows same trend for all the samples. Over all work done values are higher for the fabrics made up of monofilament spacer yarn and without lycra on the face side than that of other fabrics. Also, it can be seen that fabrics with multifilament spacer yarn have low work done when compared to other fabrics; it might be due to multifilament spacer yarn has ability to undergo large deformation during surface elongation and lateral compression. Figure 4.23 presents the graphical analysis of shear stress versus absorbed energy versus efficiency. It is obtained from the Figure 4.23, the shear work done of weft knit spacer fabrics (WES 1 –WES 6) linearly increases with the stress in the surface extension and compression stage. The marginal differences in work done between the samples can be seen when the shear stress reaches towards the stage 2. At the start of densification stage, the rapid increases in stress results in small deformation and work done.

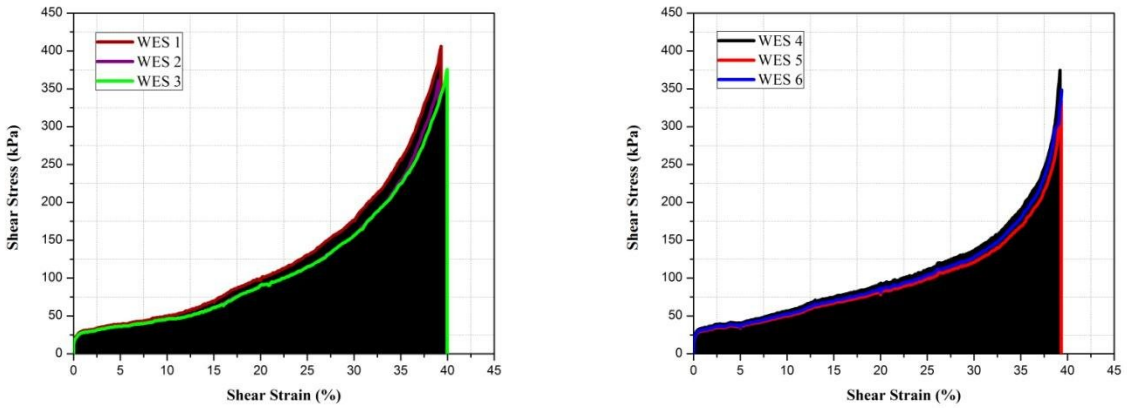

(a) **(b)**

Figure 4.22 Work done during shearing of weft knit spacer fabrics

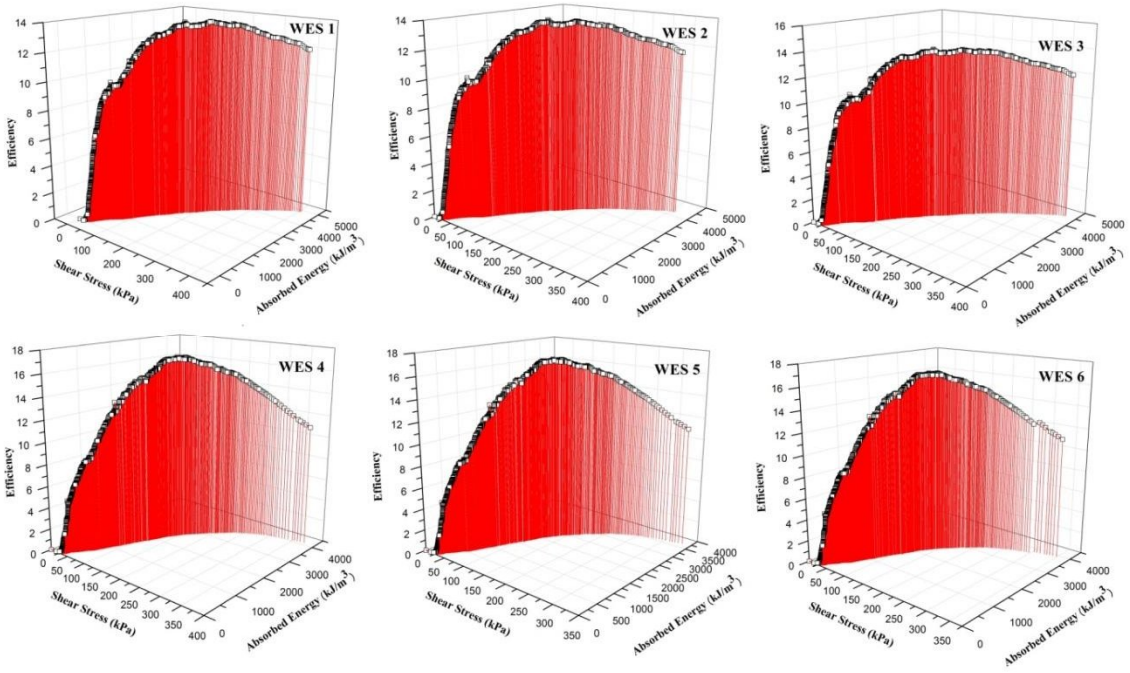

Figure 4.23 In-plane shear energy absorption and efficiency of weft knit spacer fabrics

The maximum energy-absorption efficiency is obtained at the end of the densification stage. The point at the maximum energy-absorption efficiency can also be considered a critical point in the densification zone. As noticed from the Figure 4.23, in the densification stage, efficiency becomes almost constant for fabrics without lycra (WES 1 – WES 3) with increase in shear stress level. It is due to locking of the spacer yarn and with the yarns in the surface structure of spacer fabrics. But for fabrics with lycra on surface (WES 4 –WES 6) shows decreasing trend after critical point, it might be due to the elastic nature of lycra yarn. Overall it is observed that the

shear work done and efficiency is higher for the thick fabrics made up of monofilament spacer yarn with low density. Also it is found that fabrics with multifilament yarns undergoes large amount of shear deformation during shearing mechanism. From the energy absorption graph, it is easy to find the stress associated with the required amount of energy to be absorbed. So, it is more convenient to select the suitable spacer fabrics for car seat and back support application with optimum in-plane shear performance.

4.1.3.3 Relation between shear angle versus shear force of weft knit spacer fabrics

The in-plane shear angle versus shear stress of six weft knitted spacer fabrics were carefully evaluated and presented in the Figure 4.24. The variation in shear angle mainly depends on the different fabric characteristics in samples like stitch density and thickness. The presence of Lycra yarn has shown a significant difference between Group 1(WES1-WES3) and Group 2(WES4-WES6) samples on their in-plane shear performance because of elastic nature. It was observed from the graph that the spacer fabric without lycra on the surface with monofilament spacer yarn (WES 1) offers more shear resistance than that of other fabrics. The thick spacer fabric with lycra on surface with multifilament spacer yarn (WES 5) have ability to undergoes high shear angle with low shear stress. In order to observe the wrinkling more distinctly, the curves of shear force– shear angles were plotted (Figure 4.24). There were significant differences between the six curves due to the different fabric densities and thickness. In the case of 3D spacer fabrics, fabric width decreases rapidly during shear mechanism which results in the spacer yarns being compressed into flat form. Thus, the shear deformation is influenced also by the presence of spacer yarns in the z direction. It introduces obstacles to the in-plane yarns while shearing. It is apparent that fabrics using monofilament as spacer yarn generally have higher compression resistance than those using multifilament yarn because the behavior of monofilament yarns is similar to a linear spring when the fabric is compressed. The inherent resilience behavior of multifilament yarns was less than the monofilament. When the results for spacer fabrics using the monofilament and multifilament spacer yarn were compared, it was found that the shear angle of a sample is closely related to the types of spacer yarn as shown in Figure 4.25. During the shear process, the gap between the yarns vanished gradually and the adjacent yarns contact each other. However, the width of yarn almost does not decrease. The width of yarn starts to decrease under lateral compression after the limiting locking angle during the large shear deformation, which can offer more space for the fabric to be sheared before wrinkling. The wrinkles occur in the central zone of the sample along the load direction due to the lateral compression from the left and right joints of picture frame. The in-plane shear deformation of 3D fabrics is still predominated by the deformation mode.

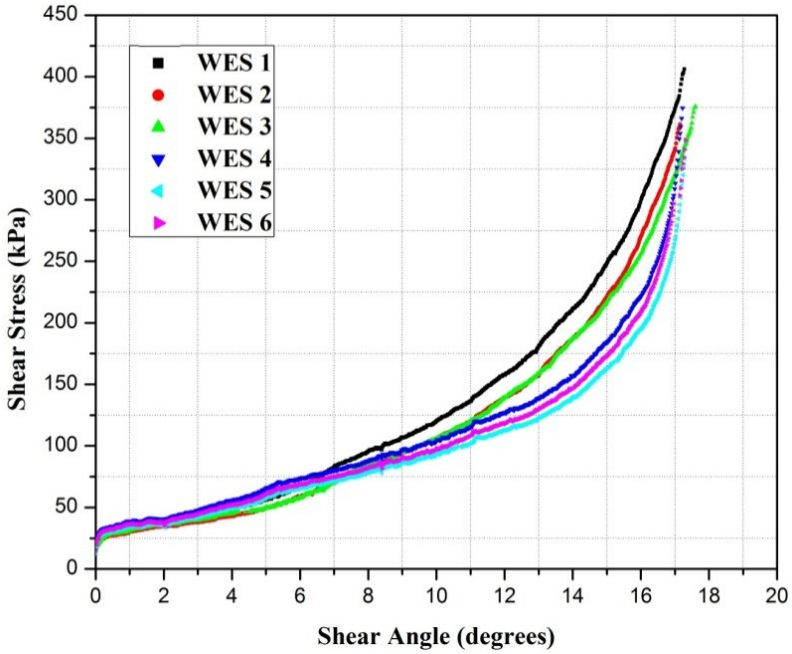

Figure 4.24 Experimental determination of shear force and shear angle of weft knit spacer fabrics

4.1.3.4 Regression model for shear deformation of weft knitted spacer fabrics

The average of in-plane stress responses against shear angle obtained for each spacer fabrics samples was fitted in the general form of linear fit (Figure 4.25).

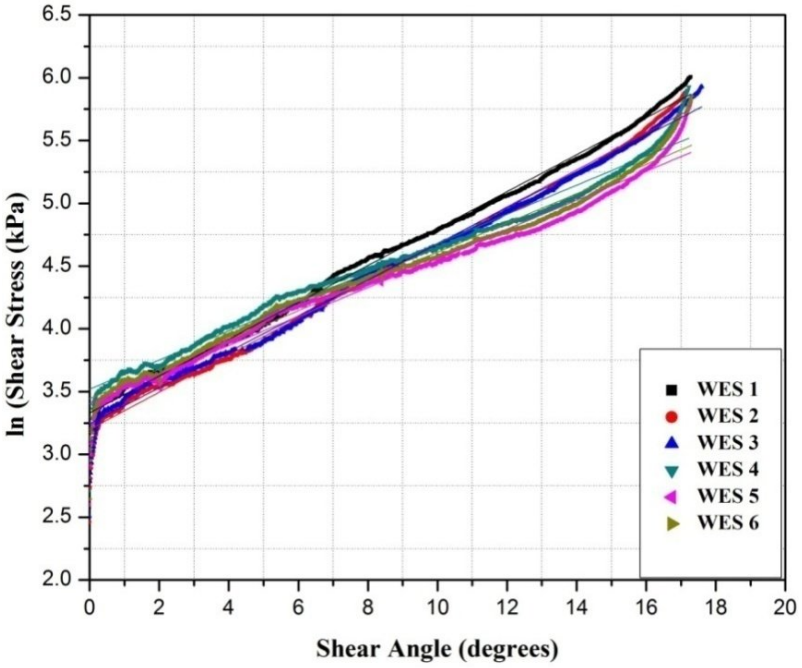

Figure 4.25 Linear regression fit of experimental shear stress of weft knit spacer fabrics as a function of shear angle

Table 4.5 Prediction of experimental shear strength of weft knit spacer fabrics using linear regression model

Equation		y = a + b*x					
DF		Model - 1 , Error - 910, Total - 911					
Weight		No Weighting					
Sample Nos.			Value	Standard Error	Residual Sum of Squares	F Value	Prob>F
ln (Shear Stress)	WES 1	Intercept	3.330	0.003			
		Slope	0.147	0.000	2.615	169893.047	0.000
	WES 2	Intercept	3.201	0.003			
		Slope	0.148	0.000	2.847	155905.056	0.000
	WES 3	Intercept	3.244	0.004			
		Slope	0.143	0.000	2.990	147895.851	0.000
	WES 4	Intercept	3.520	0.005			
		Slope	0.116	0.001	5.544	49779.348	0.000
	WES 5	Intercept	3.405	0.005			
		Slope	0.116	0.001	5.566	49599.977	0.000
	WES 6	Intercept	3.445	0.005			
		Slope	0.117	0.001	5.396	51150.606	0.000

The estimated regression coefficients of the fitted linear regression equation as well as the correlation coefficients for each model are given in Table 4.5. The adequacy of the models was tested using residuals sum of squares and probability.

4.1.3.5 Statistical evaluation – in-plane shear behavior of weft knit spacer fabrics

The above-mentioned results are confirmed by analysis of variance (ANOVA), and the result is significant influence of the surface structure, types of spacer yarn and thickness on fabric properties. In this section, one-way ANOVA is described and the selected value of significance for all statistical tests in the study is α = 0.05 levels. The null sampling distribution of the F-statistic for given one-way ANOVA is the F-distribution with numerator degrees of freedom equal to $df_{between}$ = k-1 and denominator degrees of freedom equal to df_{within} = N- k. The degree of freedom is 1, 8, the $F_{critical}$ is 5.318, and degree of freedom 3, 16, the $F_{critical}$ is 3.239. If the statistic is smaller than the critical value, we retain the null hypothesis because the p-value must be bigger than α, and if the statistic is equal to or bigger than the critical value, we reject the null hypothesis because the p-value must be equal to or smaller than α. Also pair wise comparison using Scheffé's method and Z score was calculated and presented in Table 4.6. The results of the ANOVA are listed in Table 4.6, which analyses the effect of groups of thickness and surface characteristics and types of spacer yarn of spacer fabric samples with in-plane shear

stress. The value of $F_{critical}<F_{actual}$ proves that the changes in the thickness, types of spacer yarn and surface layer structure (stitch density) of warp-knitted spacer fabric results is highly significant on the above-mentioned fabric in-plane shear stress.

Table 4.6 Statistical evaluation for in-plane shear behavior of weft knit spacer fabrics

One Way Anova - Influence of various factors on shear stress of weft knit spacer fabrics									
Test of factor influence : Influence of monofilament spacer yarn between both the groups									
		F_{cri}	F_{cal}	Prob.	Conclusion	Z-score (95% interval)	Pairwise comparison (Scheffé's method)		
							Compared Pair	Prob.	Significance
a	Without Lycra	5.318	25.205	0.0010	Significant	1.255	a-b	1.03E-03	Significant
b	With Lycra					-1.255			
Test of factor influence : Influence of multifilament spacer yarn between both the groups									
a	Without Lycra (Thickness - 2.62mm)	3.239	19.803	2.03E-08	Significant	4.577	a-b	1.34E-01	Insignificant
							a-c	0.001959	Significant
b	Without Lycra (Thickness - 2.74mm)					4.761	a-d	2.21E-01	Insignificant
c	With Lycra (Thickness - 3.5mm)					-4.226	b-c	2.1E-05	Significant
							b-d	0.002302	Significant
d	With Lycra (Thickness - 3.4mm)					-4.416	c-d	1.16E-01	Insignificant
Test of factor influence : Influence of types of spacer yarn within the group - Without Lycra									
a	Monofilament Spacer Yarn (Thickness - 4.4 mm)	5.318	52.654	8.75E-05	Significant	5.883	a-b	8.75E-05	Significant
b	Multifilament Spacer Yarn (Thickness - 2.62 mm)					-5.231			
Test of factor influence : Influence of types of spacer yarn within the group - With Lycra									
a	Monofilament Spacer Yarn (Thickness - 4.4 mm)	5.318	19.902	2.11E-03	Significant	5.591346	a-b	0.002108	Significant
b	Multifilament Spacer Yarn (Thickness - 3.4 mm)					-5.20286			

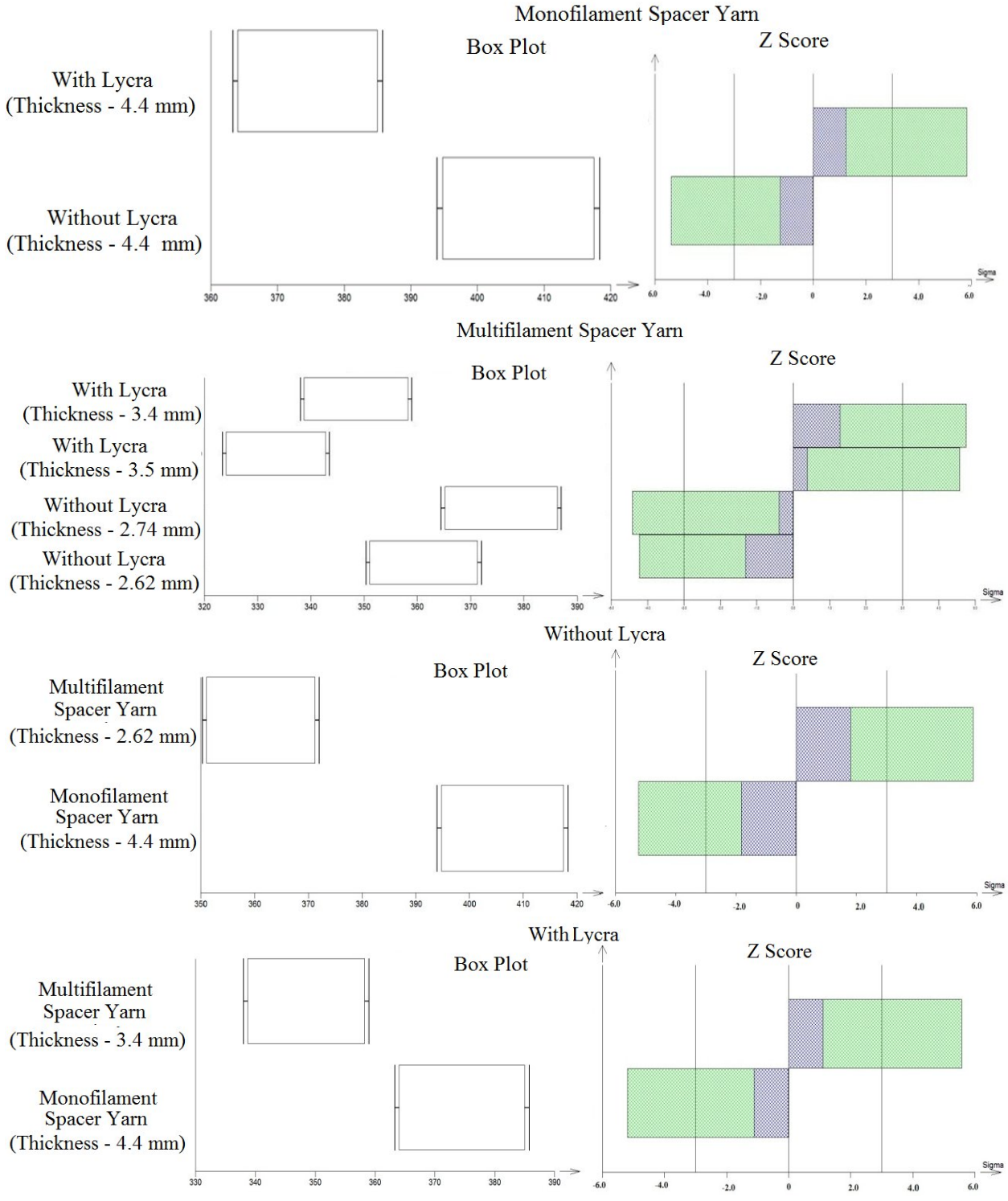

Figure 4.26 Graphical output – Statistical evaluation for in-plane shear behavior response of weft knit spacer fabrics

The pair comparison result shows that the insignificant differences in shear stress within group for the samples made up of multifilament space yarn with same surface yarn with different thickness. But the quite significant values are obtained for the samples with multifilament yarn between the groups. The box plot and a z-score are also known as a standard score and it can be placed on a normal distribution curve as shown in Figure 4.26. The box plots show fairly symmetric distributions with fairly equal spread and also observed that the no outliers. Normally Z-scores range from -3 standard deviations (which would fall to the far left of the normal distribution curve) up to +3 standard deviations (which would fall to the far right of the normal distribution curve).

4.1.3.6 Determination of shear angle of weft knit spacers using image analysis method

The shear angle of weft knitted spacer fabrics was determined using image analysis method at different displacement levels and presented in the Figure 4.27. The spacer fabric samples (WES1 – WES 6) have smooth and linear increases in shear angle till 20mm displacement. The image analysis shear angle is plotted against the shear strain all weft knit spacer samples (WES 1 – WES 6) are given in the Figure 4.28. Also, the linear model fit was presented in figures with shear strain as independent variable and shear angle as dependent variable. The regression equation for all the samples are given in the Table 4.7 to find the degree of linear fit.

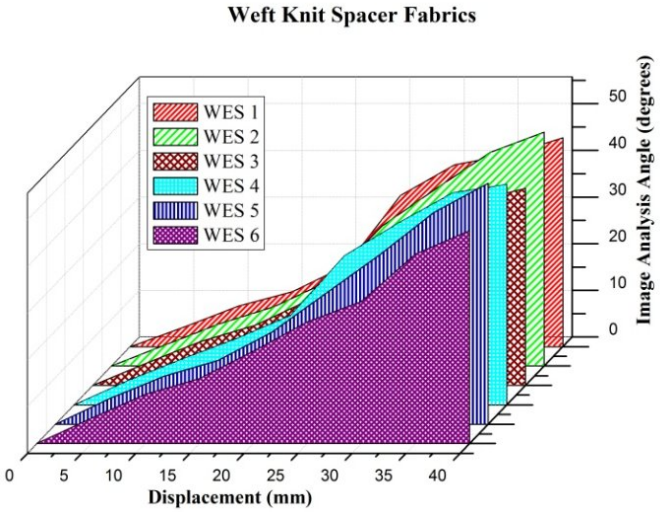

Figure 4.27 Determination of shear angle of weft knit spacers using image analysis method

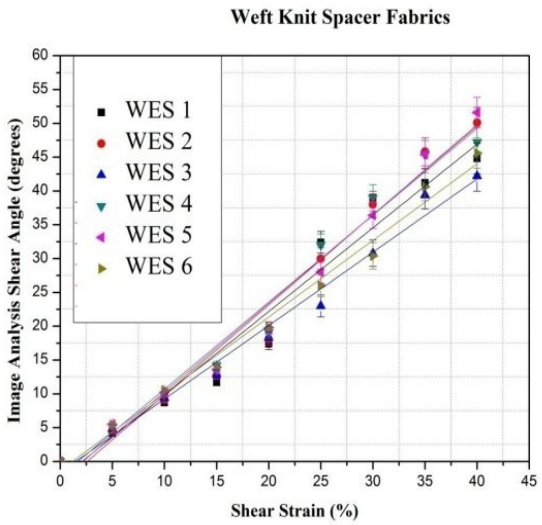

Figure 4.28 Linear regression fit of shear angle using image analysis as a function of strain of weft knit spacer fabrics

Table 4.7 Prediction of shear angle using image analysis as a function of shear strain of weft knit spacers

Equation	**y = a + b*x**					
DF	**Model - 1 , Error - 7, Total - 8**					
Sample Nos.		**Value**	**Standard Error**	**Residual Sum of Squares**	**F Value**	**Prob>F**
WES 1	**Intercept**	-2.593	2.196	89.350	180.101	2.99E-06
	Slope	1.238	0.092			
WES 2	**Intercept**	-3.451	1.862	64.220	289.352	5.95E-07
	Slope	1.330	0.078			
WES 3	**Intercept**	-1.611	1.176	25.630	482.255	1.03E-07
	Slope	1.085	0.049			
WES 4	**Intercept**	-2.162	1.744	56.330	307.898	4.81E-07
	Slope	1.285	0.073			
WES 5	**Intercept**	-2.816	1.618	48.490	371.373	2.52E-07
	Slope	1.310	0.068			
WES 6	**Intercept**	-1.304	1.101	22.460	599.889	4.82E-08
	Slope	1.133	0.046			

4.1.3.7 Comparative discussion of shear behavior of weft knitted spacer fabrics using different methods

Figure 4.29 shows the comparison of shear angles between image analysis and both experimental measurements for all 6 specimens. The differences between image analysis and calculated shear

angle using sample length at the chosen points are relatively small. It did not show any significant difference until pre-buckling occurs but significant difference occurs after 20 mm displacement. It is also believed that during image processing in MATLAB, detection of X and Y coordinates on the image is not accurate due to wrinkling in the central zone of samples. Also, it is noted that dimension of the frame rig length can cause big difference in shear angle as shown in Figure 4.29.

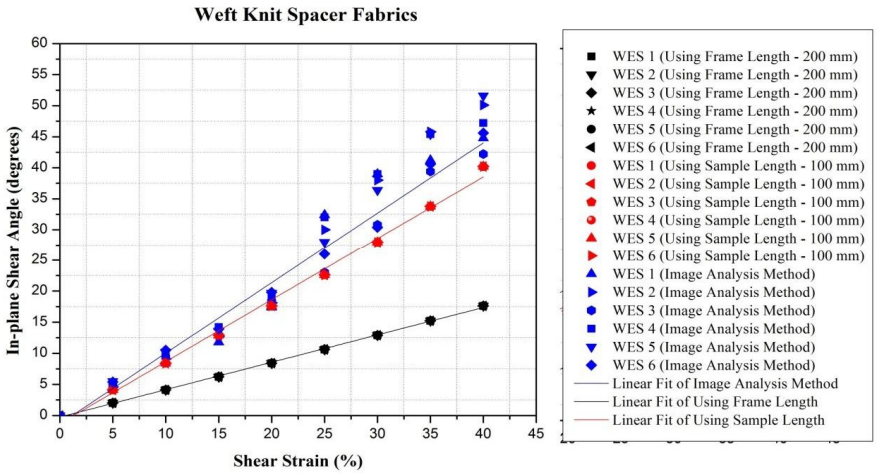

Figure 4.29 Comparison of shear behavior of weft knit spacer fabrics using different test methods

Table 4.8 Prediction of shear stress of weft knit spacer as a function of shear strain using different methods

Equation		y = a + b*x				
DF		**Model - 1 , Error - 7, Total - 8**				
Sample Nos.		**Value**	**Standard Error**	**Residual Sum of Squares**	**F Value**	**Prob>F**
Using Frame Length	**Intercept**	-0.236	0.101	0.188	10820.581	2.00E-12
	Slope	0.440	0.004			
Using Sample Length	**Intercept**	-1.297	0.641	7.607	1367.847	2.75E-09
	Slope	0.995	0.027			
Image Analysis Method	**Intercept**	-1.304	1.101	22.469	599.889	4.82E-08
	Slope	1.133	0.046			

Further study is required on the effect of different frame rig length and ratio of frame length to specimen size on in-plane shear behavior of 3D spacer fabrics. The comparative linear regression is given in the Table 4.8 as a function of shear strain.

4.1.3.8 *Prediction of shear stress using Finite Element Method*

The FEM analysis was also employed for predicting shear stress for both categories of weft knitted spacer fabrics. Results are shown in figures 4.30 and 4.31.

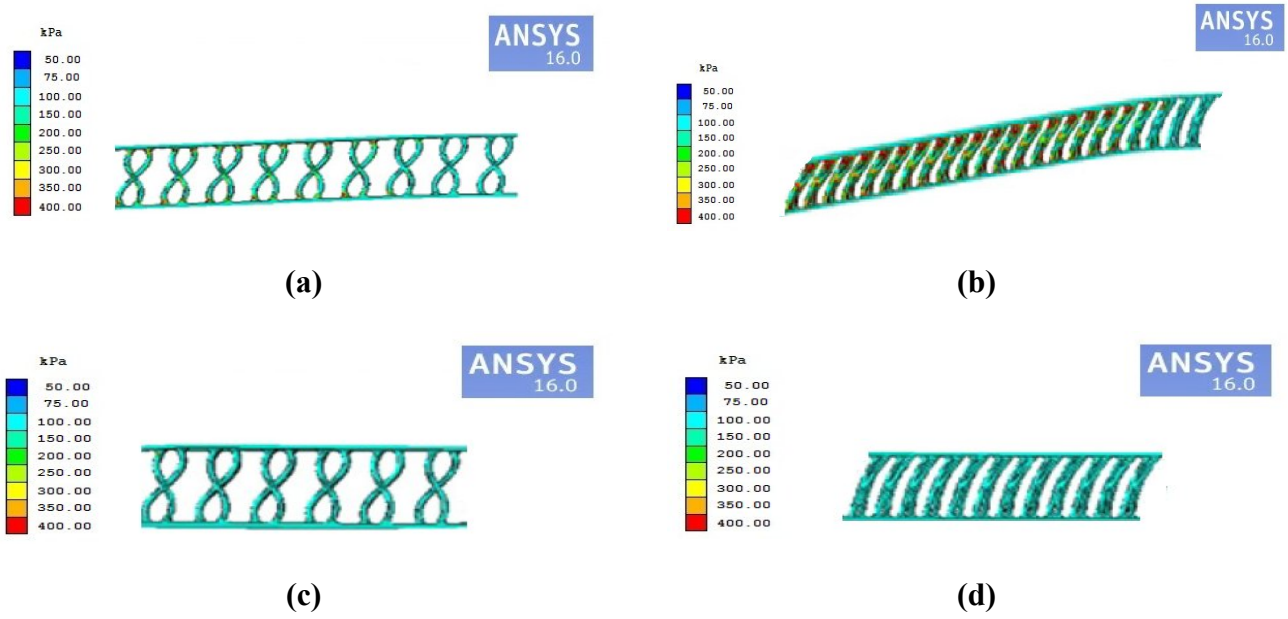

Figure 4.30 Weft knitted spacer (a) without Lycra before shear (b) without Lycra after shear (c) with Lycra before shear and (d) with Lycra after shear

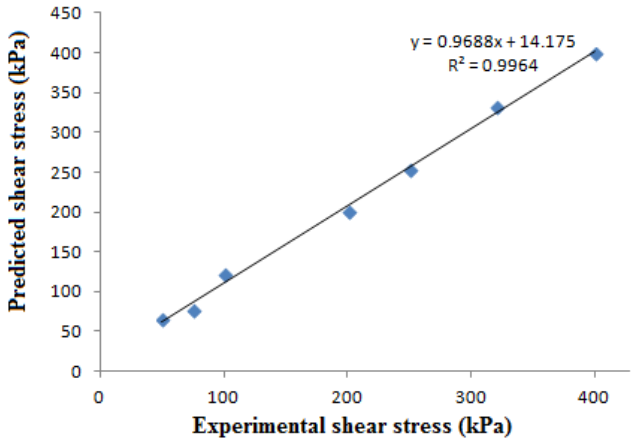

Figure 4.31 Correlation of shear stress predicted vs experimental

4.2 Compression behavior of spacer fabrics

The compression properties of both warp and weft knitted spacer fabrics was carefully evaluated using experimental method is discussed in this section.

4.2.1 Compression behavior of warp knitted spacer fabrics

4.2.1.1 Influence of thickness on compression behavior of warp knit spacer fabrics

In this section, the effect of thickness on compressive behavior of warp knitted spacer fabrics have been carefully evaluated and analyzed with respect to different structural parameters. As shown in Figures 4.32 a & 3b, the stress-strain curve reveals that the compressive resistance decreases with increase in thickness. It can be seen that, the samples have almost same at linear stage due to same surface structure and density.

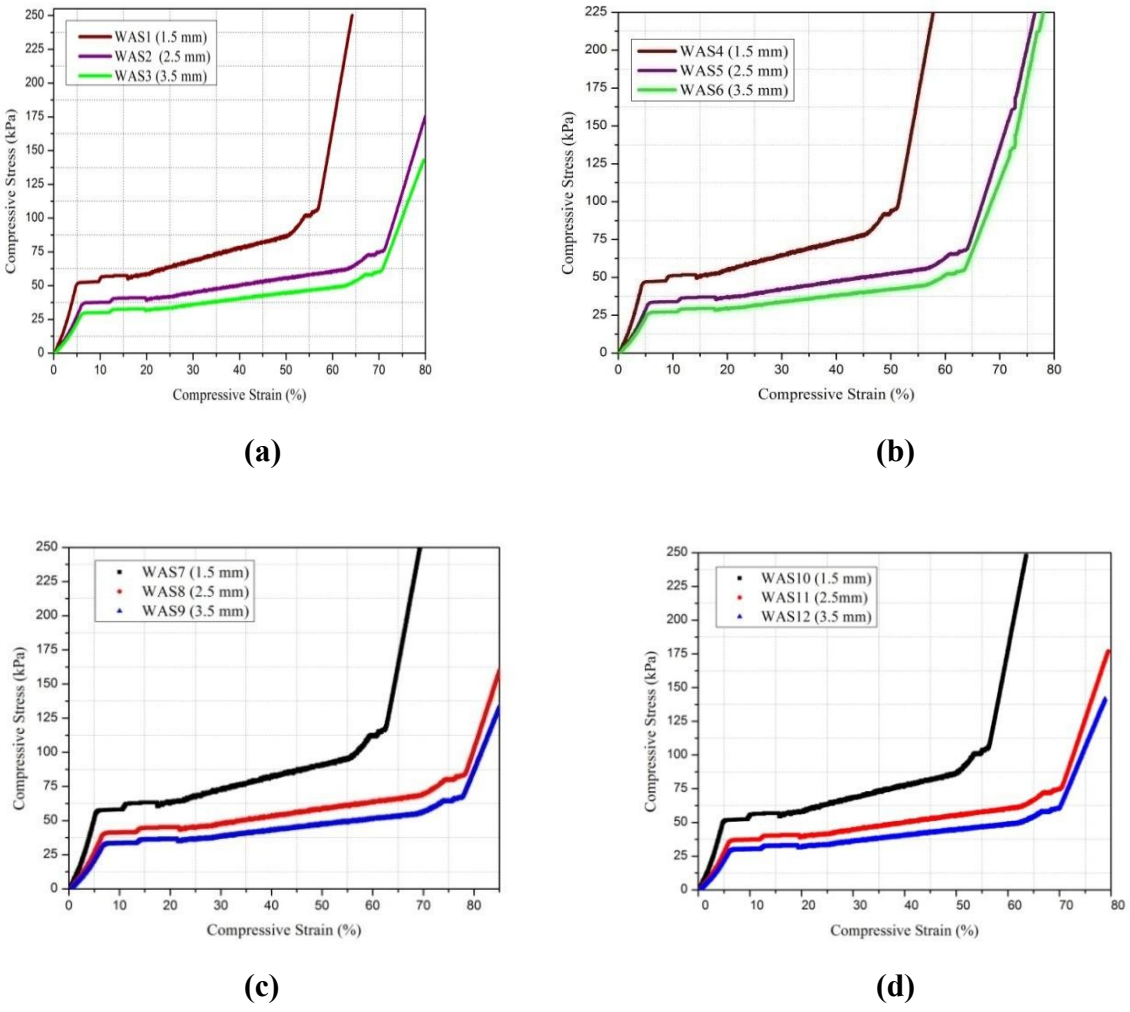

Figure 4.32 Influence of thickness on compressive behavior of warp knit spacer fabrics

In stage two (elastic), the compressive stress of all fabrics was directly proportional to the strain.

It was also observed that the thicker fabric had the ability to undergo larger deformation under low loading condition. It was also found that the hexagonal net structure fabrics (WAS 7 - WAS 12) have the same trend as the lock knit structure fabrics (Figure 4.32(c) & Figure 4.32(d)). The stress – strain curve shows that, compressive resistance is indirectly proportional to thickness of the spacer fabrics in this investigation. From this observation, it is suggested that the fabrics with different thicknesses have different ranges of applications. The thickness of the fabric should be selected according to the amount of the energy to be absorbed and the allowed stress level.

4.2.1.2 Influence of spacer yarn on compression behavior of warp knit spacer fabrics

In both sets of spacer fabrics (lock knit and hexagonal net), two types of spacer yarn with different linear density (33 & 108 dtex) and diameter (0.055 & 0.1 mm) were used for convenient analysis of its effect on compression. Normally the spacer yarns are monofilament which connected surface layers and kept each other apart. The spacer yarns act as a linear spring which offers more resistance towards compression as compared to other type of materials in cushioning applications. The angles between spacer yarn and surface layer can be varied by means of needle under lapping, but in this study, spacer yarn angles (84^o–86^o) of different samples have been observed almost same. From the Figures 4.33a & b, it is observed that, the compressive resistance is high for the fabrics with coarser spacer yarn for both the structures. In plateau region (3^{rd} stage), the fabrics have almost identical stress-strain behavior with same thickness for both lock knit and hexagonal spacers. But in stage 4, the lower deformation was observed in the fabrics with coarser spacer yarn than the fabrics made up of finer spacer yarn. It might be the fact that the large diameter and linear density of the coarse spacer yarns comes in to contact with each other also makes locking effect with surface structure sooner as compared to other samples.

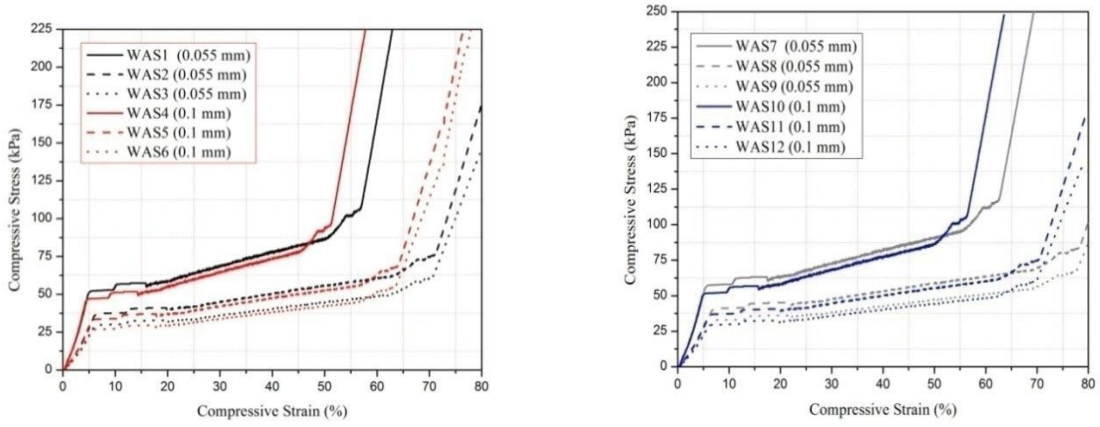

(a) **(b)**

Figure 4.33 Influence of spacer yarn on compressive behavior of warp knit spacer fabrics

4.2.1.3 Influence of surface structure on compression behavior of warp knit spacer fabrics

The surface structure of the spacer fabrics plays a vital role during compression. The outer layer structure affects the monofilament yarn inclination, binding condition with surface, distribution and multifilament stitches in surface layers. In this regard, among 12 spacer fabric samples, first set of six fabrics were produced with lock knit structure on both the surface, latter six samples were knitted using Hexagonal net structure on face side and lock knit on bottom surface to investigate the effect of surface layer structure on compressive behavior. The surface layers with these structures are shown in Table 3.1, from which the stitch density, spacer yarn angle and size of the stitches in the outer layers can be clearly observed. It has been found that the outer layer structures could slightly affect the stitch density of the outer layers and the spacer yarn inclination angle, although these parameters are maintained the same during knitting. As shown in Figure 4.34, the compression stress-strain behavior for both the structures (Lock knit and Hexagonal net) exhibits same load and deformation in initial stage. In linear elastic stage, it was found that the Hexagonal-mesh fabric offers lowest compression resistance than that of lock knit structures. All the samples had almost close value in the plateau region irrespective of other structural parameters such as thickness and spacer yarn properties. Also, it might be due to insignificant differences in stitch density. In stage 4, the Hexagonal net fabrics (WAS 7 – WAS 12) undergo large deformation for the same compression stress.

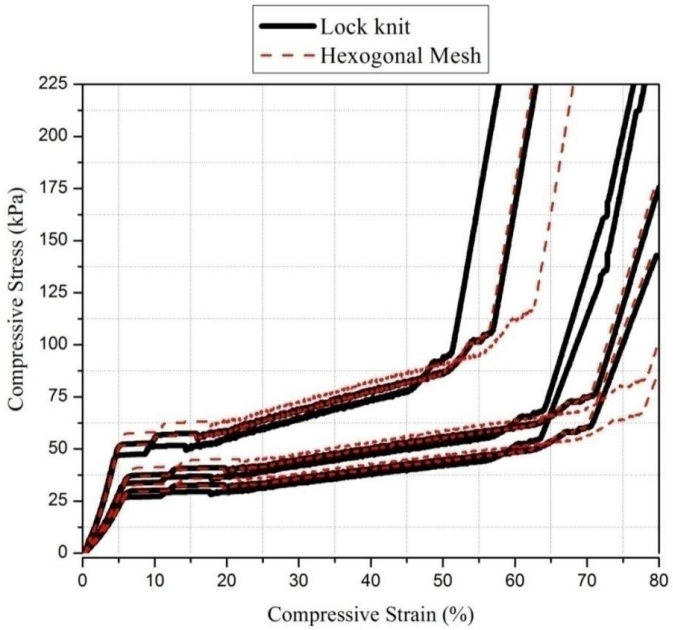

Figure 4.34 Influence of surface structure on compressive behavior of warp knit spacer fabrics

4.2.1.4 Compressive energy absorption of warp knit spacer fabrics

The compression curves reveal long deformation plateaus, suggesting that three-dimensional spacer fabrics may potentially be good compressive energy absorbing materials. Figure 4.35 (a – d) presents the work done of all spacer fabrics under compression load and also it compares the response compressive stress with effect of deformation and structural characteristics. The figures reveal that thicker fabrics have higher work done than that of thin fabrics when it undergoes compression. Irrespective of the structural variation (lock knit and hexagonal net), the compressive work done shows same trend for all the samples. Over all, the work done values are higher for the fabrics made up of hexagonal net structure on face side than that of lock knit fabrics. Also, it can be seen that fabrics with coarser spacer yarn have low work done when compared to other fabrics, it might be due to coarser yarn offers more resistance towards compression. The density of spacer fabric is also plays a vital role in compressive behavior, negative linear correlation was observed between density and compressive work done.

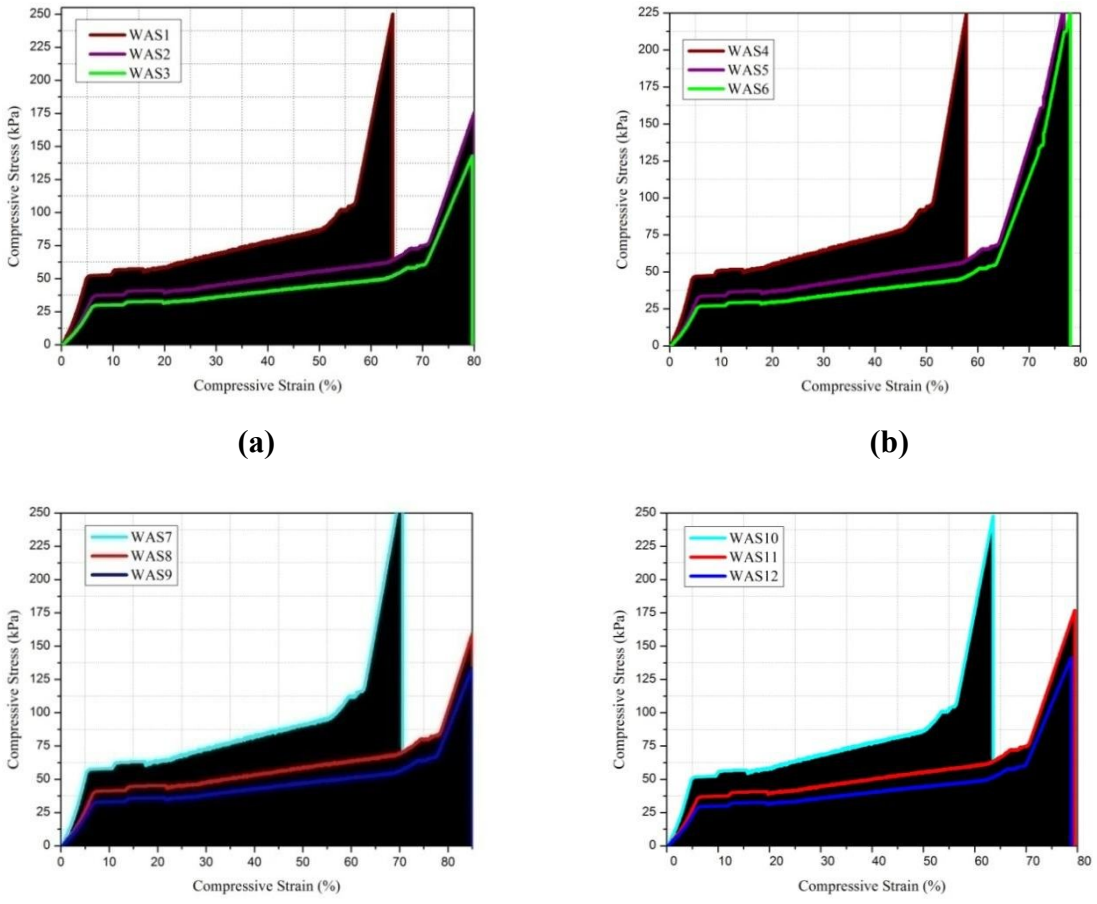

(a) **(b)**

(c) **(d)**

Figure 4.35 Energy absorption during compression of warp knit spacer fabrics

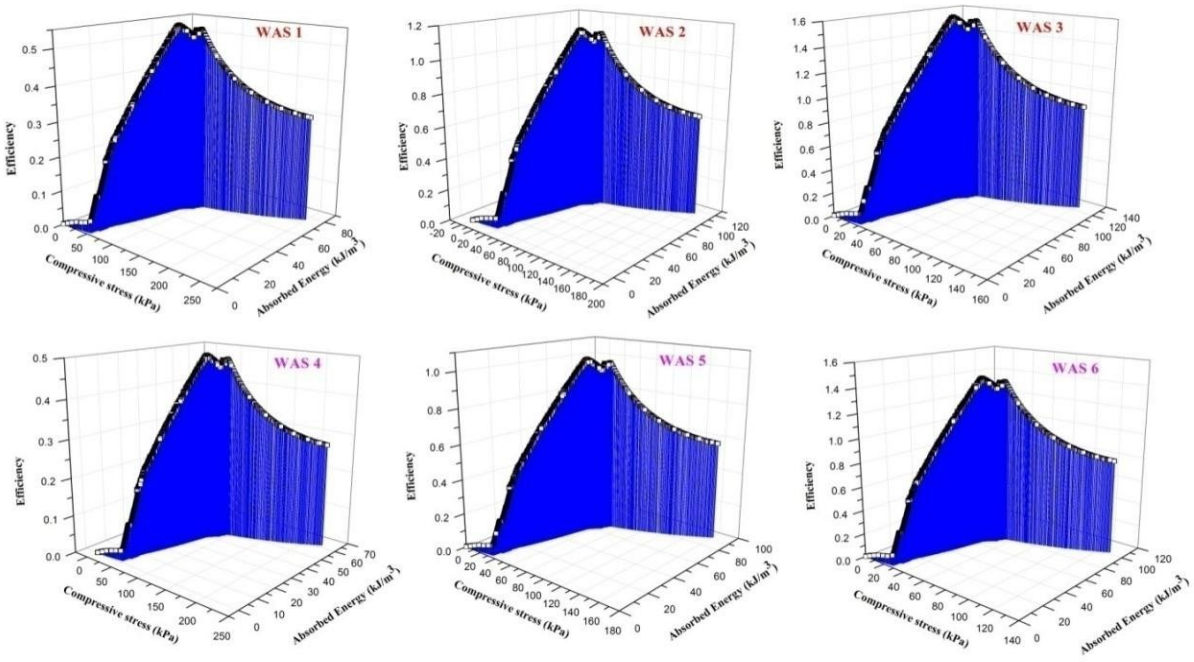

Figure 4.36 Energy absorption and efficiency of lock knit spacer fabrics

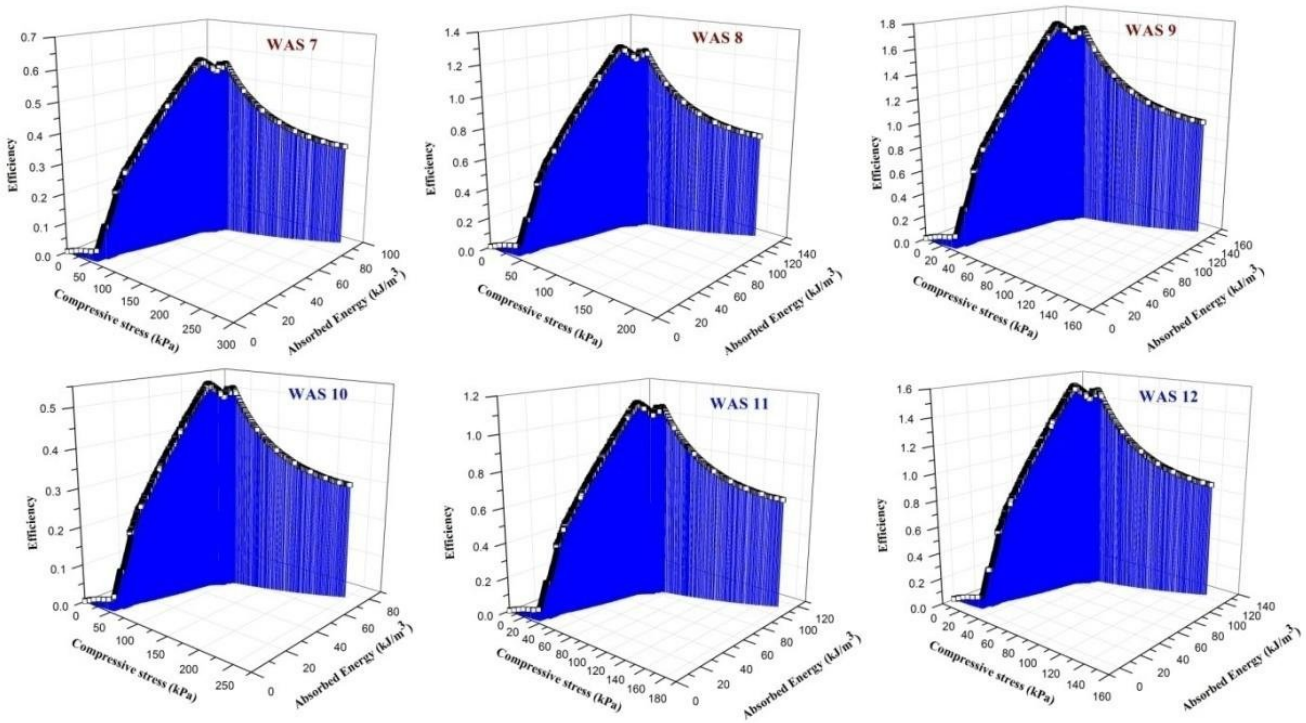

Figure 4.37 Energy absorption and efficiency of hexagonal net spacer fabrics

Figure 4.36 and Figure 4.37 present the graphical analysis of compressive stress – absorbed energy – efficiency. As is visible from the Figure 4.32, the absorbed energy of lock knit spacer

fabrics (WAS 1 – WAS 6) linearly increases with the stress in the initial stage of compression. The marginal differences in energy absorption between the samples can be seen when the compressive stress reaches towards the third stage for both the structures. At the start of densification stage, the rapid increases in stress results in small deformation and energy absorption. From the energy absorption graph, it is easy to find the stress associated with the required amount of energy to be absorbed. So, it is more convenient to select the suitable spacer fabrics for cushioning application with optimum compressive performance. As observed in Figure 4.37, the fabric with hexagonal net structure also shows the same tendency in energy absorption and efficiency with the effect of thickness and spacer yarn. Similar tendency was observed for the efficiency- stress curve until the densification stage starts as like energy absorbed for the spacer samples. The maximum energy-absorption efficiency was obtained at the end of the plateau stage. As noticed from the Figure 4.36 and Figure 4.37, efficiency decreases with rapid increase in stress level in the densification stage. It was also due to dramatic increase in volume density of the spacer fabrics. The point at the maximum energy-absorption efficiency can also be considered a critical point between the plateau zone and the densification zone. Overall it was observed that the compressive energy and efficiency is higher for the thicker fabrics with low density. Also it was found that fabrics with finer spacer yarns undergoes large amount of work done as well as high efficiency during compression mechanism.

4.2.1.5 Regression model for compressibility of warp knitted spacer fabrics

Linear relationship between two variables x and y is one of the most common concept, in which effective and easy assumptions helps to make relationship among them. The true relationship between two variables is more complex than that, and this is when polynomial regression comes in to help. The Polynomial curves can be used as a sort of replacement for transformations of x.

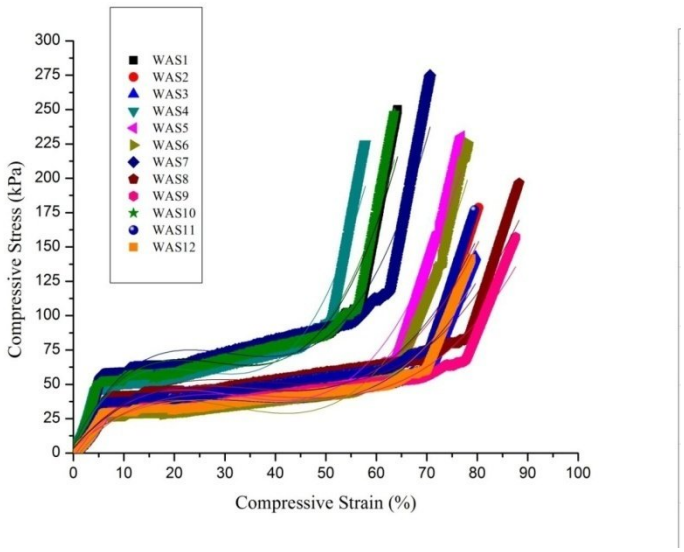

Figure 4.38 Third order polynomial regression fit for compressibility of warp knit spacer fabrics

Table 4.9 Prediction of compressive stress of warp knit spacer fabrics using polynomial regression model

Model			Polynomial				
Equation			$y = Intercept + B1x + B2x^2 + B3x^3$				
	Warp Knit Spacer Sample Nos.		Value	Standard Error	Residual Sum of Squares	F Value	Prob>F
Compressive Stress	WAS 1	Intercept	4.576	0.936	291173.900	10909.738	0
		B1	7.579	0.125			
		B2	-0.289	0.004			
		B3	0.003	0.000			
	WAS 2	Intercept	3.269	0.669	148558.100	10910.738	0
		B1	4.331	0.071			
		B2	-0.132	0.002			
		B3	0.001	0.000			
	WAS 3	Intercept	2.615	0.535	95077.180	10911.738	0
		B1	3.493	0.058			
		B2	-0.108	0.002			
		B3	0.001	0.000			
	WAS 4	Intercept	4.119	0.843	235850.800	10912.738	0
		B1	7.579	0.125			
		B2	-0.322	0.005			
		B3	0.004	0.000			
	WAS 5	Intercept	-3.036	0.736	202133.900	17542.797	0
		B1	5.488	0.082			
		B2	-0.193	0.002			
		B3	0.002	0.000			
	WAS 6	Intercept	-5.978	0.718	199599.900	17012.842	0
		B1	5.100	0.079			
		B2	-0.183	0.002			
		B3	0.002	0.000			
	WAS 7	Intercept	5.034	1.030	352320.400	10912.738	0
		B1	7.579	0.125			
		B2	-0.263	0.004			
		B3	0.003	0.000			
	WAS 8	Intercept	3.596	0.736	179755.300	10913.738	0
		B1	4.331	0.071			
		B2	-0.120	0.002			
		B3	0.001	0.000			
	WAS 9	Intercept	2.876	0.589	115043.400	10914.738	0
		B1	3.493	0.058			
		B2	-0.098	0.002			
		B3	0.001	0.000			
	WAS 10	Intercept	4.530	0.927	285379.500	10915.738	0
		B1	7.579	0.125			
		B2	-0.292	0.005			
		B3	0.004	0.000			
	WAS 11	Intercept	3.236	0.662	145601.800	10916.738	0
		B1	4.331	0.071			
		B2	-0.134	0.002			
		B3	0.001	0.000			
	WAS 12	Intercept	2.589	0.530	93185.140	10917.738	0
		B1	3.493	0.058			
		B2	-0.109	0.002			
		B3	0.001	0.000			

The average of compressive stress responses against strain obtained for each spacer fabrics samples was fitted in the general form of third order polynomial (Figure 4.38). Response fit analyses, regression coefficient estimations and model significance evaluations were conducted. The estimated regression coefficients of the fitted polynomial equation as well as the correlation coefficients for each model are given in Table 4.9. The adequacy of the models was tested using residuals sum of squares and probability.

4.2.1.6 Statistical evaluation for compressive behavior response of warp knit spacer fabrics

In this section, two-way ANOVA is analyzed and the selected value of significance for all statistical tests in the study is 0.05 levels. Analysis of different combination of factors on compressive work done is presented in Table 4.10. The factors mainly considered are thickness, spacer yarn diameter and structure which strongly influence the compressive behavior and energy absorption of the three-dimensional spacer fabrics. The critical quantile ($F_{critical}$) values obtained for factor A-18.51, 19, Factor B–19 and Interaction–161.45 with respect to degrees of freedom.

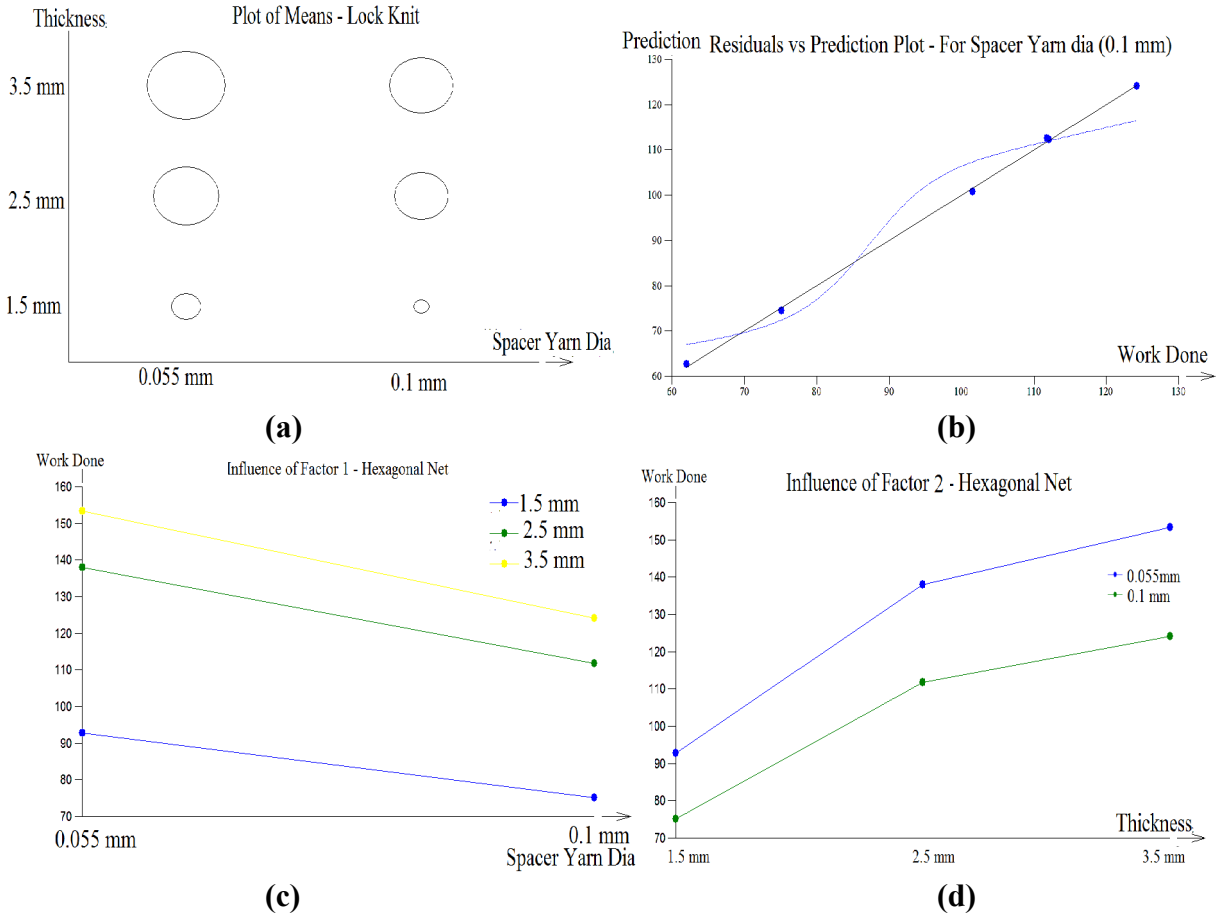

Figure 4.39 Graphical output – Statistical evaluation for compressive behavior response of warp knit spacer fabrics

Table 4.10 Statistical evaluation for compression behavior of weft knit spacer fabrics

ANOVA Table

Influence of spacer yarn dia and thickness on energy absorption - lock knit

Source of variability	Sum of squares	Mean square	Degrees of freedom	Std deviation	F-statistic	Critical quantile	Conclusion	p-value
Spacer Yarn Diameter	289.94	289.94	1	17.028	399.858	18.513	Significant	0.0024916
Thickness	2743.96	1371.98	2	37.04	1892.078	19	Significant	0.0005282
Interaction	0.1	0.1	1	1.204	0.077	161.448	Insignificant	0.8275701
Residuals	1.35	1.35	1	1.16				
Total	3035.35	607.07	5	24.639				

Influence of spacer yarn dia and thickness on energy absorption - Hexogonal net

Spacer Yarn Diameter	887.57	887.57	1	29.79	49.54	18.51	Significant	0.0195932
Thickness	3251.63	1625.82	2	40.32	90.75	19	Significant	0.0108991
Interaction	35.83	35.83	1	5.99	5.54141E+13	161.45	Significant	8.55E-08
Residuals	0	0	1	0				
Total	4175.04	835.01	5	28.9				

Influence of structure and thickness on energy absorption for spacer yarn dia (0.055 mm)

Structure	740.68	740.68	1	27.22	49.61	18.51	Significant	0.0195683
Thickness	3311.36	1655.68	2	40.69	110.89	19	Significant	0.0089373
Interaction	29.86	29.86	1	5.46	93824837.28	161.45	Significant	6.57E-05
Residuals	0	0	1	0				
Total	4081.9	816.38	5	28.57				

Influence of structure and thickness on energy absorption for spacer yarn dia (0.1 mm)

Structure	208.77	208.77	1	14.45	206.12	18.51	Significant	0.0048165
Thickness	2689.96	1344.98	2	36.67	1327.91	19	Significant	0.0007525
Interaction	0.71	0.71	1	1.42	0.54	161.45	Insignificant	0.5978509
Residuals	1.32	1.32	1	1.15				
Total	2900.75	580.15	5	24.09				

The value of $F_{critical} < F_{statistic}$ proves that the changes in the thickness, spacer yarn linear density and surface layer structure of warp-knitted spacer fabric significantly influences the above-mentioned fabric compression properties. Even a minor change in the fabric thickness results in significant impact on the compression behavior. Interaction factors structure–thickness with spacer yarn diameter (0.1mm) and spacer yarn diameter–thickness in lock- knit structure don't have significant influence ($p > 0.05$) on compression behavior. In Fig. 4.39a, circle stands for mean value of 5 observations. Diameter of the circle is roughly proportional to the response. Differences between levels and interactions can be seen on this plot. The residuals versus prediction plot show the quality of fit of the model. From the Fig. 4.39b it is observed, closer are the points to the line $y = x$, the more significant the model is. Plot of the influence of a given factors at separate levels of the other factor. If the lines for factor A are similar for each level of

the factor *B*, then the factor A is probably significant. If the lines have rather opposite direction, then there is probably strong interaction between the factors. If the lines are shaped rather randomly, then the influence and significance of the respective factor is probably low. The plot is only qualitative visual tool and cannot fully replace the F-test. Fig.s4.39c and 4.39d show that the lines of factor–thickness are just opposite to the factor–spacer yarn diameter, so it proves that the strong interaction between these two factors.

4.2.2 Compression behavior of weft knitted spacer fabrics

4.2.2.1 Effect of fabric characteristics on compression behavior of weft knit spacer fabrics

As shown in Figure 4.40a, the compressive stress-strain curve reveals that the compressive resistance of spacer fabric without lycra made up of monofilament yarn is low in linear and elastic stage, but sudden increase in compressive stress observed in plateau and densification stage. From Figure 4.40b, spacer fabrics with lycra made up of monofilament spacer yarn constantly offers high compression resistance in all four stages. Among the fabrics made up of multifilament spacer yarn, the compressive stress – strain curve showed that, compressive resistance has indirectly proportional to thickness of the spacer fabrics. It was observed that the denser fabrics require higher compressive stress to undergo same compressive deformation than the fabric with low density. It was also observed that the thicker fabric has ability to undergo larger deformation under low loading condition. The thickness of the fabric should be selected according to the amount of the energy to be absorbed and the allowed stress level. In both the set of spacer fabrics (without lycra and with lycra), two types of spacer yarn such as monofilament and multifilament spacer yarns were used for convenient analysis of its effect on compression. Normally the monofilament spacer yarns act as a linear spring which offers more resistance towards compression as compared to other type of materials in cushioning applications. From the Figure 4.41, it is observed that, the compressive resistance is high for the fabrics with monofilament yarn for both the groups than that of fabric with multifilament spacer yarn. In plateau region (3^{rd} stage), the marginal differences has been observed between the fabrics made up of monofilament spacer yarn (WES 1 & WES 4) in both the groups. It might be due to the fact that the large differences in density between these two samples. But the fabrics with multifilament spacer yarn (WES 2, 3 & WES 5, 6) don't show significant differences in compressive strength because the densities of these samples have almost closer to each other. It has also been found that the outer layer structures could affects the stitch density of the fabrics. The stitch density on the surface layer directly affects the compressive strength of the spacer fabrics. The compressive resistance increases with increase in stitch density. The lower stitch density on the surface of the fabric results in large surface deformation. In stage 4, the lower deformation was observed in the fabrics with monofilament spacer yarn than the fabrics made up of multifilament spacer yarn. It might be the fact that the spacer yarns have comes in to contact with each other and also makes locking effect with surface structure as quick as possible.

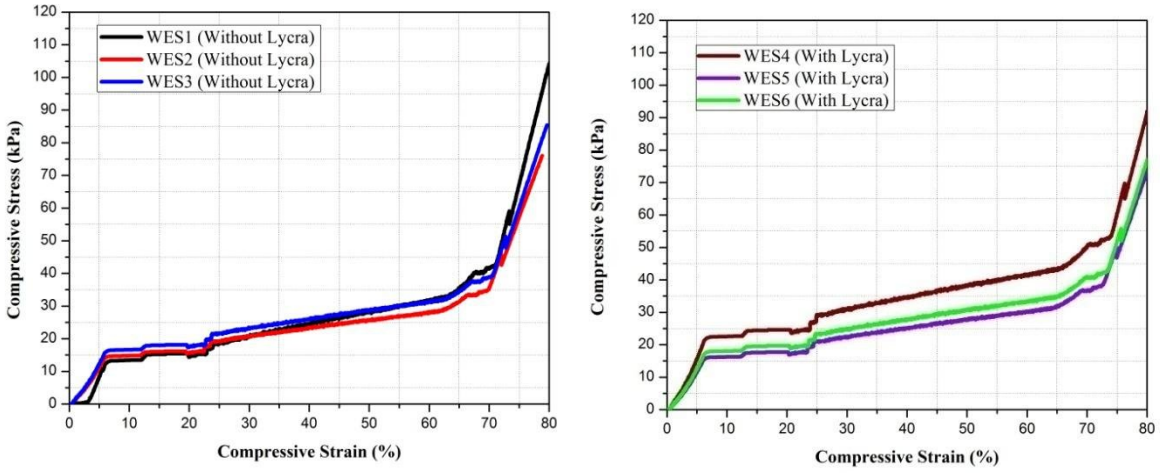

(a) **(b)**

Figure 4.40 Influence of thickness on compressive behavior of weft knit spacer fabrics

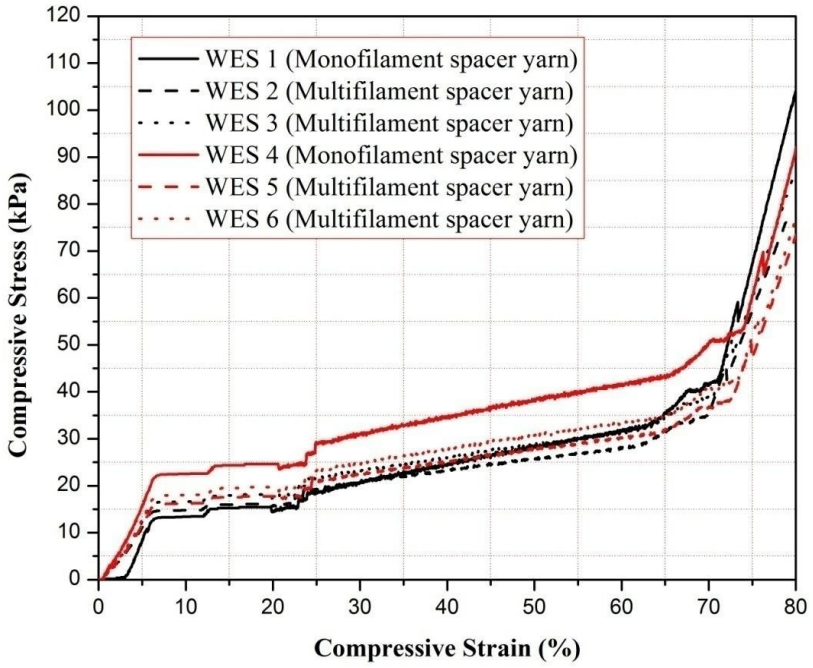

Figure 4.41 Influence of spacer yarn on compressive behavior of weft knit spacer fabrics

4.2.2.2 Compressive energy absorption of weft knit spacer fabrics

Figure 4.42 (a & b) presents the work done of all spacer fabrics under compression load and also it compares the response compressive stress with effect of deformation and structural

characteristics. The figures reveal that thicker spacer fabrics with monofilament spacer yarn have higher work done than that of thin fabrics with multifilament spacer yarn when it undergoes compression. Irrespective of the structural variations, the compressive work done shows same trend for all the samples. In both the groups, over all work done values are higher for the spacer fabrics made (WES 1 & WES 2) up of monofilament yarn. The density of spacer fabric also plays a vital role in compressive behavior, negative linear correlation was observed between density and compressive work done. Figure 4.43 presents the graphical analysis of compressive stress – absorbed energy – efficiency. It is observed from the figure that the absorbed energy of weft knit spacer fabrics (WES 1 –WES 6) linearly increases with the stress in the initial stage of compression. The marginal differences in energy absorption between the samples can be seen when the compressive stress reaches towards the third stage for both the groups. At the start of densification stage, the rapid increases in stress results in small deformation and energy absorption. From the energy absorption graph, it is easy to find the stress associated with the required amount of energy to be absorbed. So, it is more convenient to select the suitable spacer fabrics for car seat and back support application with optimum compressive performance. As noticed from the Figure 4.43, in the densification stage, efficiency decreases with rapid increase in stress level. It is also because of dramatic increase in volume density of the spacer fabrics. The point at the maximum energy-absorption efficiency can also be considered a critical point between the plateau zone and the densification zone. Overall it is observed that the compressive energy and efficiency is higher for the thicker fabrics made up of monofilament spacer yarn with low density. Also it is found that fabrics with finer spacer yarns undergoes large amount of work done as well as high efficiency during compression mechanism.

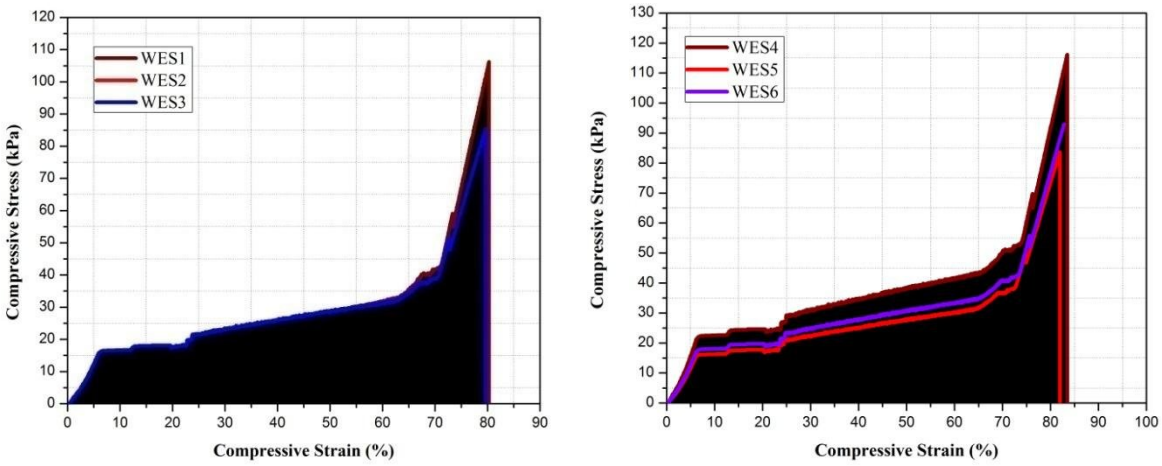

(a) **(b)**

Figure 4.42 Compressive energy absorption of weft knit spacer fabrics

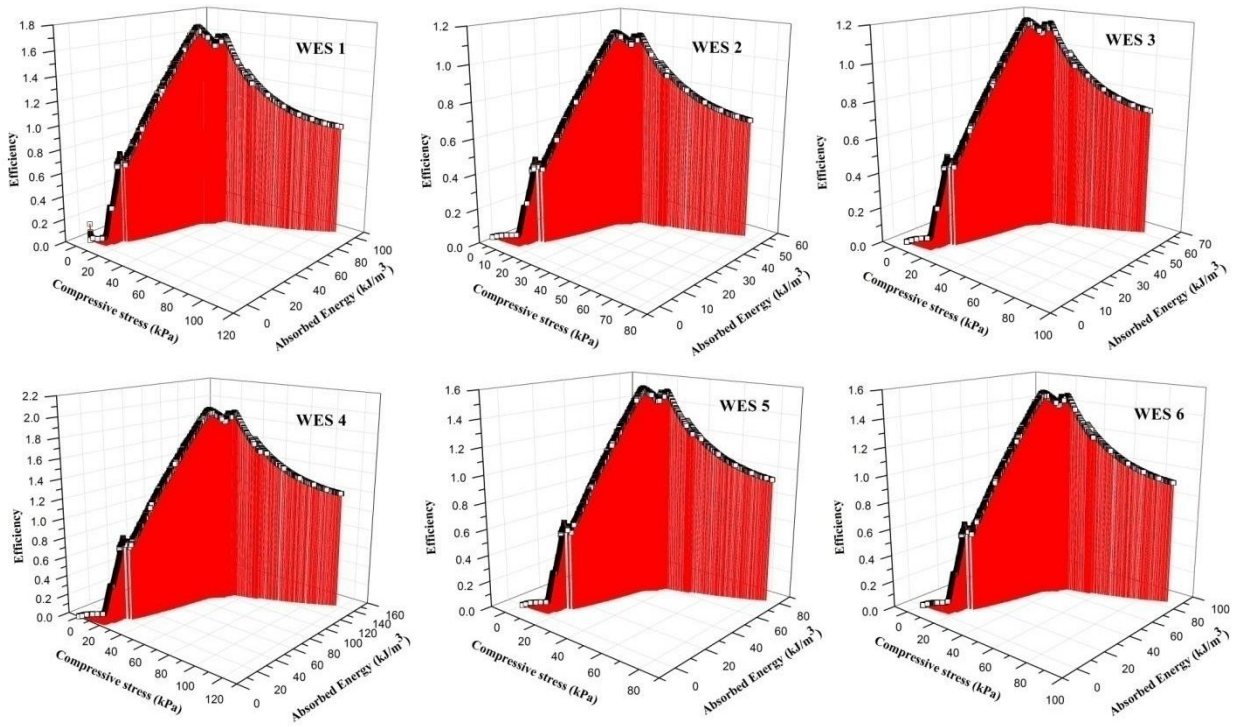

Figure 4.43 Energy absorption and efficiency of weft knit spacer fabrics

4.2.2.3 Regression model for compressibility of weft knit spacer fabrics

The average of compressive stress responses against strain obtained for each spacer fabrics samples was fitted in the general form of third order polynomial (Figure 4.44). Response fit analyses, regression coefficient estimations and model significance evaluations were conducted. The estimated regression coefficients of the fitted polynomial equation as well as the correlation coefficients for each model are given in Table 4.11. The adequacy of the models was tested using residuals sum of squares and probability.

4.2.2.4 Statistical evaluation for compressive behavior response of weft knit spacer fabrics

In this section, one-way ANOVA is analyzed and the selected value of significance for all statistical tests in the study is α = 0.05 levels. The degree of freedom is 1, 8, the F_{critic}al is 5.318, and degree of freedom 3, 16, the $F_{critical}$ is 3.239. If the statistic is smaller than the critical value, we retain the null hypothesis because the p-value must be bigger than α, and if the statistic is equal to or bigger than the critical value, we reject the null hypothesis because the p-value must be equal to or smaller than α. Also pair wise comparison using Scheffé's method and Z score was calculated and presented in Table 4.12. The results of the ANOVA are listed in Table 4.12, which analyses the effect of groups of thickness and surface characteristics and types of spacer yarn of spacer fabric samples with compressive stress.

Table 4.11 Prediction of compressive stress of weft knit spacer fabrics using polynomial regression model

Model			Polynomial				
Equation			$y = Intercept + B1x + B2x^2 + B3x^3$				
Weight			No Weighting				
	Sample Nos.		Value	Standard Error	Residual Sum of Squares	F Value	Prob>F
Compressive Stress	WES 1	Intercept	-5.123	0.413	56756.200	12126.867	0.000
		B1	2.450	0.044			
		B2	-0.073	0.001			
		B3	0.001	0.000			
	WES 2	Intercept	0.473	0.270	24157.850	12940.484	0.000
		B1	1.835	0.029			
		B2	-0.054	0.001			
		B3	0.001	0.000			
	WES 3	Intercept	0.531	0.303	30483.590	12940.484	0.000
		B1	2.040	0.033			
		B2	-0.059	0.001			
		B3	0.001	0.000			
	WES 4	Intercept	0.722	0.412	56274.350	12940.484	0.000
		B1	2.644	0.042			
		B2	-0.073	0.001			
		B3	0.001	0.000			
	WES 5	Intercept	0.520	0.296	29172.620	12940.484	0.000
		B1	1.939	0.031			
		B2	-0.055	0.001			
		B3	0.001	0.000			
	WES 6	Intercept	0.578	0.329	36015.580	12940.484	0.000
		B1	2.132	0.034			
		B2	-0.059	0.001			
		B3	0.001	0.000			

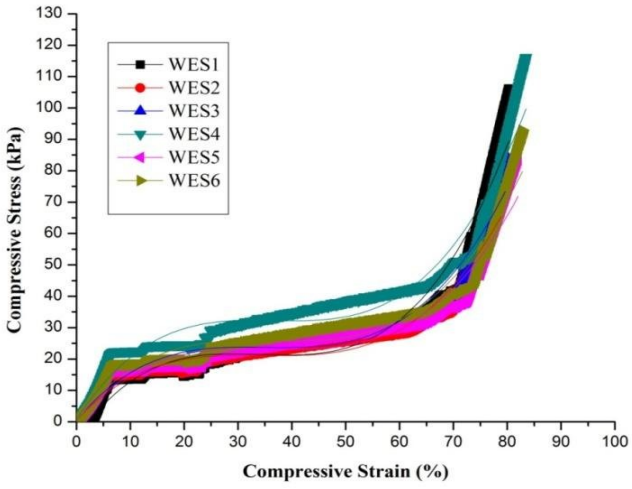

Figure 4.44 Third order polynomial regression fit for compressibility of weft knit spacers

Table 4.12 Statistical evaluation for compressive behavior of weft knit spacer fabrics

One Way Anova - Influence of various factors on compression stress of weft knit spacer fabrics									
Test of factor influence : Influence of monofilament spacer yarn between both the groups									
		F_{cri}	F_{cal}	Prob.	Conclusion	Z-score (95% interval)	Pairwise comparison (Scheffé's method)		
							Compared Pair	Prob.	Significance
a	Without Lycra	5.318	30.520	0.0006	Significant	-2.859	a-b	5.57E-04	Significant
b	With Lycra					3.126			
Test of factor influence : Influence of multifilament spacer yarn between both the groups									
a	Without Lycra (Thickness - 2.62mm)	3.239	92.238	2.03E-08	Significant	-1.974	a-b	4.98E-05	Significant
b	Without Lycra (Thickness - 2.74mm)					2.217	a-c	0.000561	Significant
							a-d	2.22E-08	Significant
c	With Lycra (Thickness - 3.5mm)					-2.169	b-c	0.614266	Insignificant
							b-d	0.000637	Significant
d	With Lycra (Thickness - 3.4mm)					2.410	c-d	5.59E-05	Significant
Test of factor influence : Influence of types of spacer yarn within the group - Without Lycra									
a	Monofilament Spacer Yarn (Thickness - 4.4 mm)	5.318	409.016	3.73E-08	Significant	3.138	a-b	3.73E-08	Significant
b	Multifilament Spacer Yarn (Thickness - 2.62 mm)					-2.248			
Test of factor influence : Influence of types of spacer yarn within the group - With Lycra									
a	Monofilament Spacer Yarn (Thickness - 4.4 mm)	5.318	187.617	7.78E-07	Significant	3.215	a-b	7.78E-07	Significant
b	Multifilament Spacer Yarn (Thickness - 3.4 mm)					-2.572			

The value of $F_{critical}<F_{actual}$ proves that the changes in the thickness, types of spacer yarn and surface layer structure (stitch density) of warp-knitted spacer fabric have significant influence on the above-mentioned fabric compressive stress. The insignificant difference in compressive stress is obtained between the pair, sample made up of multifilament spacer yarn without lycra on surface and with lycra. But the quite significant values are obtained in compressive stress between the other samples with multifilament spacer yarn. The box plot and a z-score are also known as a standard score and it can be placed on a normal distribution curve as shown in Figure

4.45. The box plots show fairly symmetric distributions with fairly equal spread and also observed that the no outliers. Normally Z-scores range from -3 standard deviations (which would fall to the far left of the normal distribution curve) up to +3 standard deviations (which would fall to the far right of the normal distribution curve).

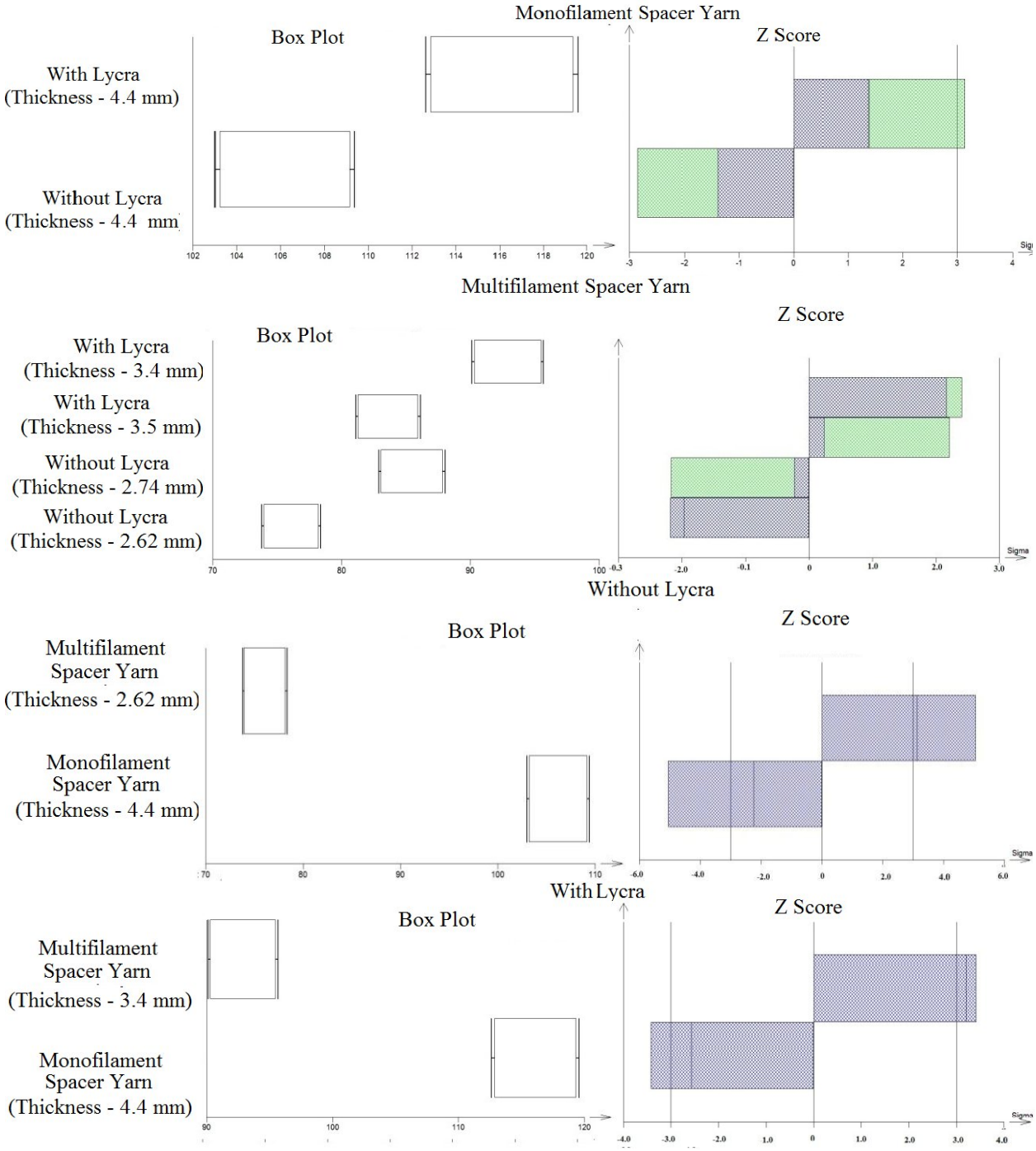

Figure 4.45 Graphical outputs – Statistical evaluation for compressive behavior response of weft knit spacer fabrics

4.3 Thermo-physiological behavior of spacer fabrics

The thermal and physiological property of both warp and weft knitted spacer fabrics have been evaluated using experimental method is discussed in this section.

4.3.1 Thermo-physiological properties of warp knitted spacer fabrics

4.3.1.1 Porosity and stitch density of warp knitted spacer fabrics

The unique characteristic of spacer fabrics is porosity, which decides air permeability, moisture transmission and thermal comfort. The volume porosity is mostly affected by surface structure, thickness and density. In this study polyester multifilament with same linear density was used in the outer surface layers, polyester monofilament with two different linear densities (33 & 108 dtex) were used in spacer layer. The spacer fabric porosity is directly influenced by vertical gaps created by spacer layer and also depends on bulkiness. The stitch density is the surface characteristics of textile materials, which normally decides the tightness, openness and loop geometry of fabrics. The small variations in stitch density have higher influence on the pore size and volume porosity. In this work, the stitch density kept almost same for all the samples, because the volume porosity is directly affected by varying thickness and areal density.

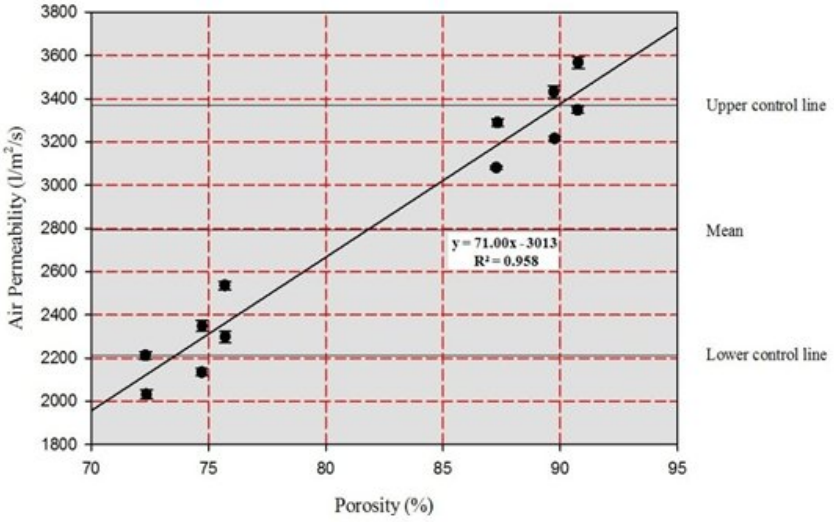

ANOVA	DF	Sum of Squares	Mean Square	F Value	Prob > F
Model	1	3.53E+06	3.53E+06		
Error	10	151994	15199.4	232.5397	2.98E-08
Total	11	3.69E+06			

Figure 4.46 Effect of porosity on air permeability

One way ANOVA was conducted to study the significance of stitch density, it proves that there is no significant differences among the samples with p value greater than 0.05 (p= 0.246). Figure 4.46 proves that the porosity has direct positive correlation with air permeability with R^2 value of 0.958 and also regression relation equation presented in it. The porosity of both structures (lock knit and hexagonal) have almost same, but the significant differences in air-

permeability was observed due to its different surface structure. The increase in porosity can result in a significant increase in air and water vapour permeability.

4.3.1.2 Effect of structural characteristics on air permeability

The cushions are subject to change in air movement and velocity depends on compressive load applied by persons. If the air flow rate is too high or irregular, then local thermal discomfort appears. Thus, it's very important to control the air velocity and the flow direction in the cushioning materials. The air permeability of a fabric is closely related to the construction characteristics of the yarns it is made of, in which large volumes are occupied by air. The air permeability of a spacer fabric is a measure of how well it allows the passage of air through it. The air transmission is of importance for a number of spacer fabric end uses. There are several factors affecting the air permeability of the fabric, such as fabric's structure, thickness, porosity, surface characteristics, etc. The air permeability of fabric is highly correlated with fabric areal density and thickness, which are related to fabric tightness. The results show that fabric thickness has a significant effect on the air permeability values of the spacer fabric, as air permeability tended to increase as thickness decreased, irrespective of yarn linear density and stitch density. As shown in Figure 4.47, the lower thickness and mass per square meter also facilitate the passage of air through the fabric. It is also noticed from the graph, the denser fabrics offers more resistant towards air to pass from one surface to other. Also it is observed from the Figure 4.47, porous with lower areal density fabrics offers more permeable to air. Lock knit fabrics (WAS 1 – WAS 6) have tighter surface structure because it inter-loops the filament very close to each other, So, it is resistant to air flow. Comparison between all the samples show the hexagonal net fabrics have more air permeability than lock knit fabrics with respect to thickness and areal density. Hexagonal knit fabrics (WAS 7 – WAS 12) produces more open structure on surface, it produce more gaps which results in highly permeable to air. All these factors contribute towards the higher air permeability.

4.3.1.3 Influence of structural characteristics on thermal properties

Thermal resistance is a measure of a material's ability to prevent heat from flowing through it. Thermal conductivity and resistance are immensely influenced by the fabric structure and thickness. Increase in fabric thickness will result in increase in thermal insulation, as there will be a decrease in heat losses for the space insulated by the textile. Thermal resistance is a function of the thickness and thermal conductivity of a fabric. To study the thermal performance of the above samples, characterization and analysis of thermal properties such as thermal conductivity and thermal resistance are discussed in this section.

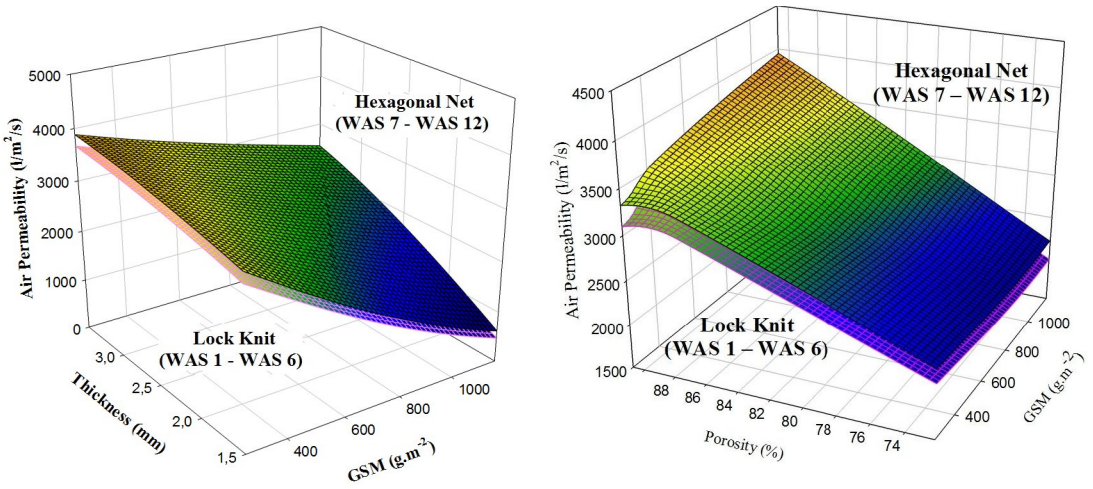

(a) **(b)**

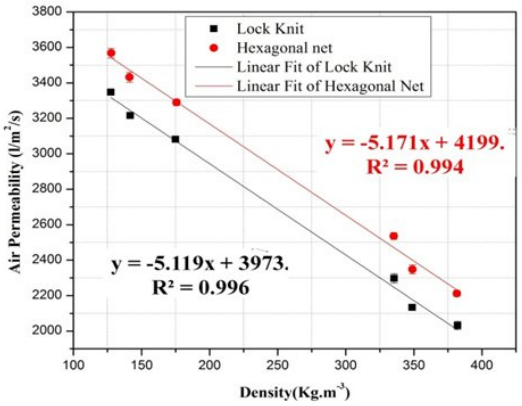

	ANOVA	DF	Sum of Squares	Mean Square	F Value	Prob > F
Lock Knit	Model	1	1.75E+06	1.75E+06	1056.4929	5.34E-06
	Error	4	6634.3417	1658.5854		
	Total	5	1.76E+06			
Hexagonal	Model	1	1.78E+06	1.78E+06	747.54169	1.06E-05
	Error	4	9536.979	2384.2448		
	Total	5	1.79E+06			

(c)

Figure 4.47 Influence of structural parameters on air permeability of warp knit spacer fabrics

Figure 4.48a & b demonstrates the influence of thickness and areal density on thermal properties of all the samples. It is reported that the thermal conductivity decreases with increase in thickness and areal density for both the structures. The major factors influencing the thermal behavior of fabrics are density, porosity and air permeability. As shown in Figure 4.49a &b, the thermal conductivity of spacer fabrics significantly increased with increase in density and decrease in air permeability. Also it is observed that, hexagonal net fabrics (WAS 7- WAS 12) have ability to resist more heat than the fabrics with lock knit structure on the surface (WAS 1 – WAS 6). Because, the open surface pores in hexagonal fabrics results in higher air permeability makes thermally resistant materials comparatively. It is also proved from Figure 4.49c, spacer

fabrics with low porosity results in high thermal conductivity, due to fabrics act s a barrier for air permeability. Overall results give in the way that comparatively higher fabric thickness of a spacer fabric entraps more air within the middle layer and therefore cause higher thermal resistance with lower thermal conductivity. The amount of air entrapped in denser fabrics (WAS 4 –WAS 6 & WAS 10 – WAS 12) is high and it allows conduction of heat causing higher thermal conductivity. Figure 4.49 also presents the regression model for thermal conductivity with the effect of density and air permeability. The thermal conductivity of warp knitted spacer fabric has positive linear correlation with density and negative correlation with porosity and air permeability with the coefficient of determinant of more than 0.9.

4.3.1.4 Effect of structural parameters on water vapour permeability

The transmission of heat through compressible and cushion are additionally disturbed by the occupant's temperature control system, that is, perspiration. These properties are required in the materials mainly mattress, shoe insole, seat and back supports should be characterized by its ability to transport moisture, independently of whether it maintains appropriate thermal properties. The moisture transport behavior is based on absorbing moisture by the material, and afterwards by carrying it out to the environment. The physiological properties of seat materials are formed by two factors, first is ability to accumulate moisture and transmission of water vapour. The porous and elastic cushions are subject to undergo multidirectional stresses of compression and relaxation due to vibrations caused by car's motion. It results in carrying out of water vapour from one medium to another medium by means of pump effect. So, in this section the ability of spacer fabrics to transport water vapour and evaporative resistance were carefully measured and discussed. Figure 4.50 (a & b) demonstrates the influence of thickness and areal density on physiological properties of all the samples. It is reported that the relative water vapour permeability decreases with increase in thickness and areal density for all the fabrics. The pore characteristics in the cushioning fabrics are important factor in which diffusion of water vapour happens.

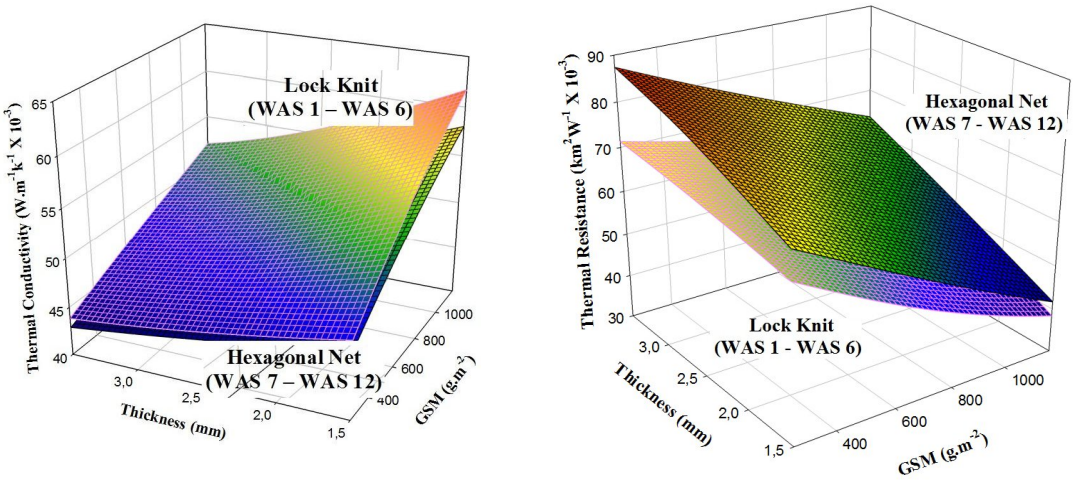

(a) **(b)**

Figure 4.48 Effect of gsm and thickness on thermal properties of warp knit spacer fabrics

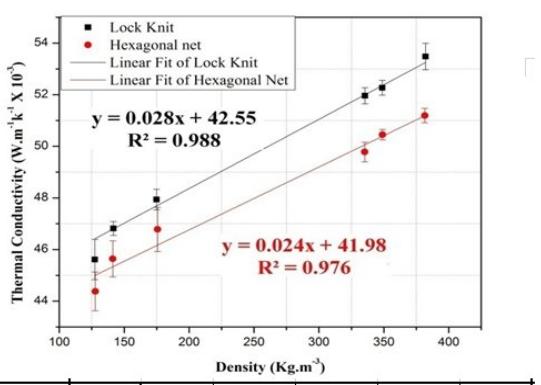

	ANOVA	DF	Sum of Squares	Mean Square	F Value	Prob > F
Lock Knit	Model	1	5.35E+01	5.35E+01	355.27414	4.67E-05
	Error	4	0.60253	0.15063		
	Total	5	5.41E+01			
Hexagonal	Model	1	3.86E+01	3.86E+01	166.06597	2.09E-04
	Error	4	0.92908	0.23227		
	Total	5	3.95E+01			

(a)

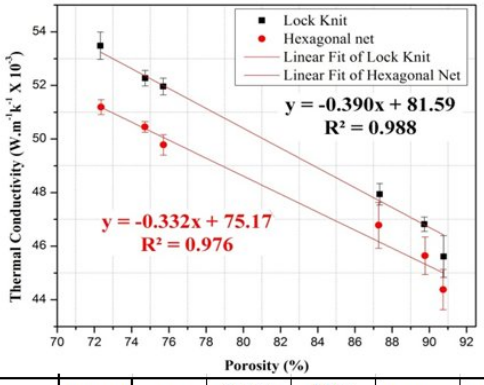

	ANOVA	DF	Sum of Squares	Mean Square	F Value	Prob > F
Lock Knit	Model	1	5.35E+01	5.35E+01	355.27414	4.67E-05
	Error	4	0.60253	0.15063		
	Total	5	5.41E+01			
Hexagonal	Model	1	3.86E+01	3.86E+01	166.06597	2.09E-04
	Error	4	0.92908	0.23227		
	Total	5	3.95E+01			

(b)

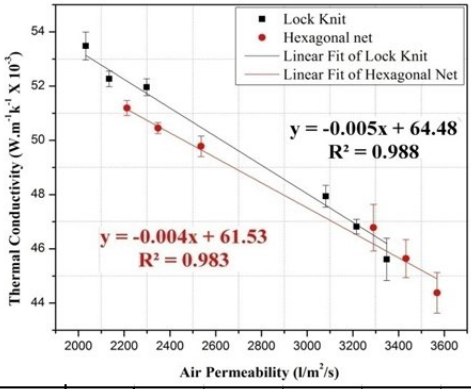

	ANOVA	DF	Sum of Squares	Mean Square	F Value	Prob > F
Lock Knit	Model	1	5.35E+01	5.35E+01	334.33428	5.26E-05
	Error	4	0.63982	0.15996		
	Total	5	5.41E+01			
Hexagonal	Model	1	3.89E+01	3.89E+01	240.412	1.01E-04
	Error	4	0.64647	0.16162		
	Total	5	3.95E+01			

(c)

Figure 4.49 Effect of structural characteristics and linear regression model for thermal conductivity of warp knit spacer fabrics

As shown in Figure 4.51(a) & (b), the evaporative resistance is lower for the porous spacer fabrics with high air permeability. It is also proved that, spacer fabrics with low density results in higher water vapour permeability. Overall it is observed from that the evaporative resistance decreases with increase in porosity and decrease in thickness, density and areal density of spacer fabrics. It was also noticed that, hexagonal net fabrics (WAS 7- WAS 12) have ability to pass more water vapour than the fabrics with lock knit structure on the surface (WAS 1 – WAS 6).

Because, the open surface pores in hexagonal fabrics results in porous nature makes material with higher water vapour permeability.

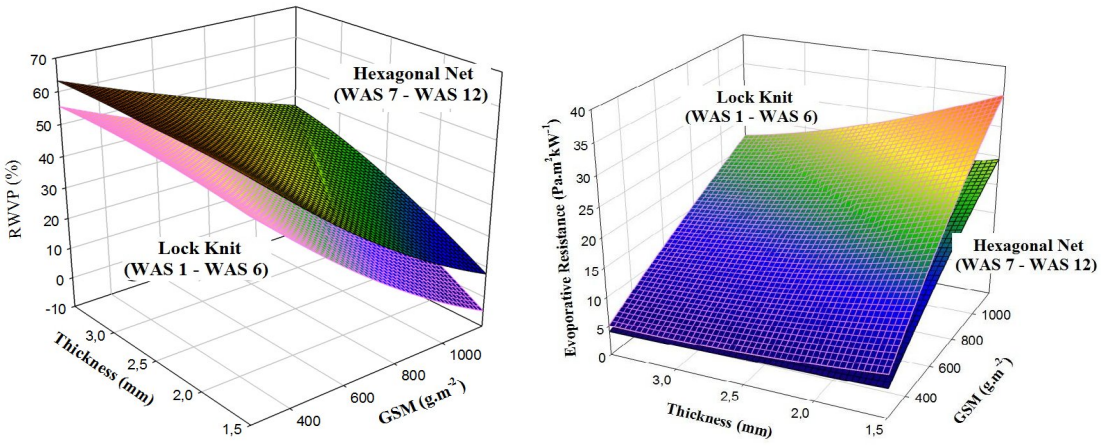

(a) **(b)**

Figure 4.50 Effect of thickness and areal density on water vapour permeability

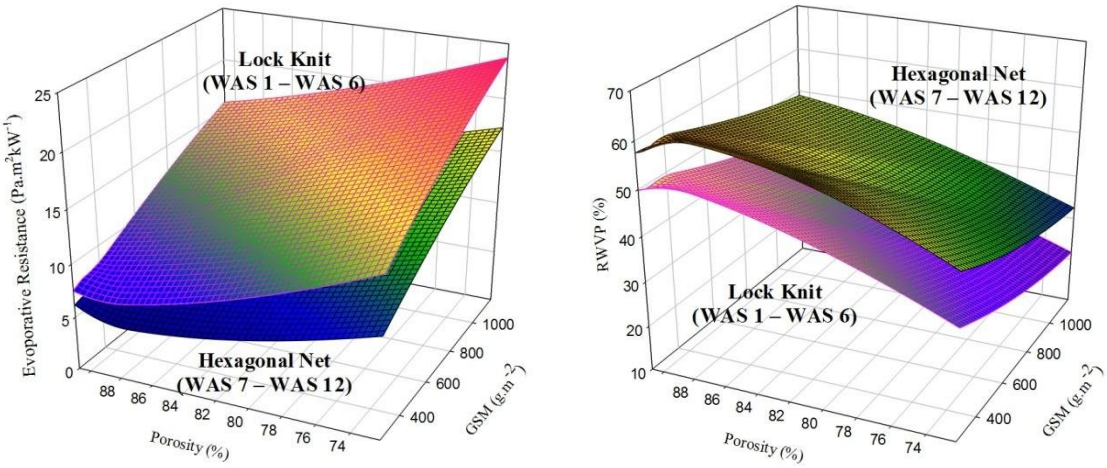

(a) **(b)**

Figure 4.51 Influence of structural characteristics on water vapour permeability

The results obtained shows that, the thick spacer fabric with high density have higher evaporative resistance (Figure 4.52a & b). The increase in thickness of middle (spacer) layer has ability to entrap more air therefore cause higher evaporative resistance with lower water vapour permeability. The spacer fabrics (WAS 1 – WAS 3 & WAS 7 – WAS 9) show relatively lower density and higher porosity; therefore allow water vapour to pass through easily. It is observed from the figure 4.52c, the water vapour permeability depends not only air permeability, it depends surface structure structural pores, thickness and density. Figure 4.52 also presents the regression model for water vapour permeability with the effect of density, porosity and air

permeability. The water vapour permeability of warp knitted spacer fabric has negative linear correlation with density and positive correlation with air permeability and porosity with R^2 value more than 0.9.

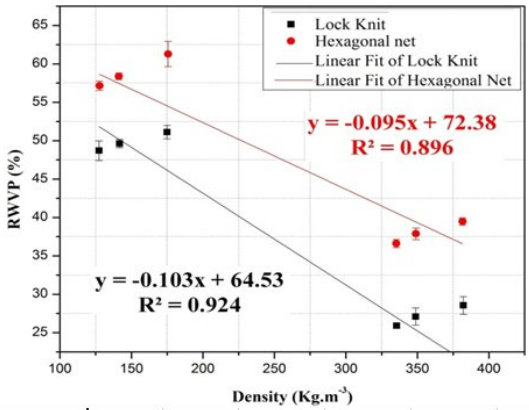

	ANOVA	DF	Sum of Squares	Mean Square	F Value	Prob > F
Lock Knit	Model	1	7.15E+02	7.15E+02	48.73043	2.21E-03
	Error	4	58.71211	14.67803		
	Total	5	7.74E+02			
Hexagonal	Model	1	6.02E+02	6.02E+02	34.67824	4.16E-03
	Error	4	69.43936	17.35984		
	Total	5	6.71E+02			

(a)

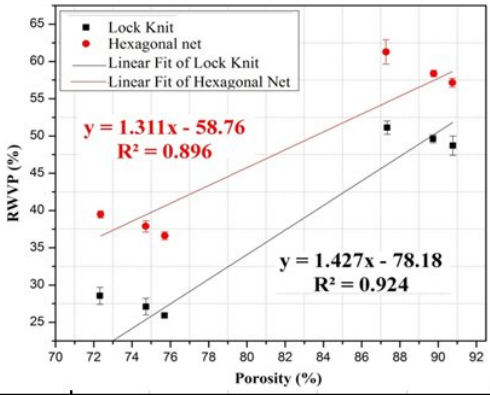

	ANOVA	DF	Sum of Squares	Mean Square	F Value	Prob > F
Lock Knit	Model	1	7.15E+02	7.15E+02	48.73043	2.21E-03
	Error	4	58.71211	14.67803		
	Total	5	7.74E+02			
Hexagonal	Model	1	6.02E+02	6.02E+02	34.67824	4.16E-03
	Error	4	69.43936	17.35984		
	Total	5	6.71E+02			

(b)

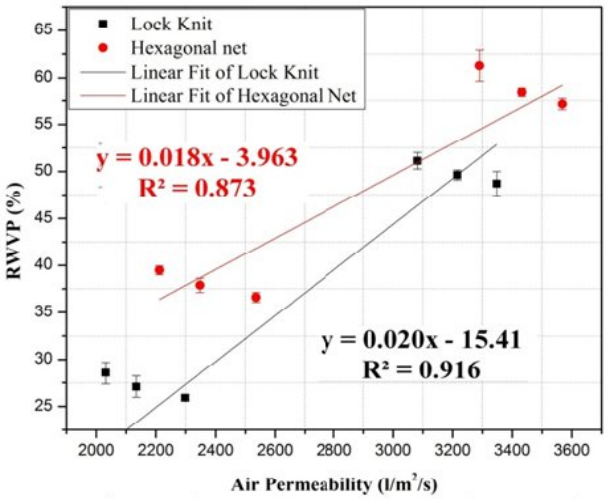

	ANOVA	DF	Sum of Squares	Mean Square	F Value	Prob > F
Lock Knit	Model	1	7.09E+02	7.09E+02	43.76966	2.70E-03
	Error	4	64.80923	16.20231		
	Total	5	7.74E+02			
Hexagonal	Model	1	5.87E+02	5.87E+02	27.65371	6.26E-03
	Error	4	84.8492	21.2123		
	Total	5	6.71E+02			

(c)

Figure 4.52 Linear regression model for water vapour permeability

4.3.1.5 Statistical evaluation for thermo-physiological behavior of warp knit spacer fabrics.

The test results were evaluated using the advanced statistical software QC EXPERT.

Table 4.13 Statistical evaluation for thermo-physiology properties of warp knit spacer fabrics

TWO WAY ANOVA								
Effect of Structure and Thickness on Air permeability								
Source of variability	**Sum of squares**	**Mean square**	**Degrees of freedom**	**Std deviation**	**F-statistic**	**Critical quantile**	**Conclusion**	**p-value**
Structure	69122.7	69122.7	1	262.9119	3703	18.5128	Significant	0.00027
Thickness	73989.3	36994.7	2	192.34	1981.86	19	Significant	0.0005
Interaction	36.1151	36.1151	1	6.110101	29.6465	161.448	Insignificant	0.11563
Residuals	1.21819	1.21819	1	1.103718				
Total	143149	28629.9	5	169.2036				
Effect of Structure and Thickness on Thermal Conductivity								
Structure	2.12415	2.12415	1	1.457446	3267.92	18.5128	Significant	0.00031
Thickness	5.5969	2.79845	2	1.672857	4305.31	19	Significant	0.00023
Interaction	0.00124	0.00124	1	0.036056	20.5853	161.448	Insignificant	0.13811
Residuals	6.02E-05	6.02E-05	1	0.007761				
Total	7.72235	1.54447	5	1.242767				
Effect of Structure and Thickness on Thermal Resistance								
Structure	165.585	165.585	1	12.86799	23.9144	18.5128	Significant	0.03936
Thickness	51.0137	25.5069	2	5.050432	3.6838	19	Insignificant	0.2135
Interaction	13.3868	13.3868	1	3.721308	29.0159	161.448	Insignificant	0.11685
Residuals	0.46136	0.46136	1	0.679235				
Total	230.447	46.0894	5	6.788916				
Effect of Structure and Thickness on Relative Water Vapour Permeability								
Structure	124.944	124.944	1	11.17784	303.508	18.5128	Significant	0.00328
Thickness	11.1185	5.55927	2	2.35781	13.5043	19	Insignificant	0.06895
Interaction	0.80228	0.80228	1	0.907377	38.1072	161.448	Insignificant	0.10224
Residuals	0.02105	0.02105	1	0.145097				
Total	136.886	27.3772	5	5.232321				
Effect of Structure and Thickness on Evaporative Resistance								
Structure	7.61627	7.61627	1	2.759758	676	18.5128	Significant	0.00148
Thickness	2.6284	1.3142	2	1.146386	116.645	19	Significant	0.0085
Interaction	0.00725	0.00725	1	0.150111	0.47394	161.448	Insignificant	0.61617
Residuals	0.01529	0.01529	1	0.123644				
Total	10.2672	2.05344	5	1.432983				

The study for each thermo-physiological property (air permeability, thermal resistance, thermal conductivity, water vapour permeability and evaporative resistance) was examined by two-way analysis of variance (ANOVA) with a confidence level of 95%. In this section, the statistical significance of fabric characteristics is presented (Table 4.13). Statistical analysis also indicates that the structure and thickness of warp knit spacer fabrics are significantly influence on air permeability, thermal conductivity and evaporative resistance with $F_{critical} < F_{static}$. But the insignificant differences are observed in the interaction on fabric properties. The plot of means visually compares the response values for each combination of factor levels (or each cell). In Figure 4.53, circle stands for mean value of 5 observations. Diameter of the circle is roughly proportional to the response. Differences between levels and interactions can be seen on this plot. The residuals versus prediction plot show the quality of fit of the model. From the Fig. 4.53, it is observed, closer are the points to the line $y = x$, the more significant the model is.

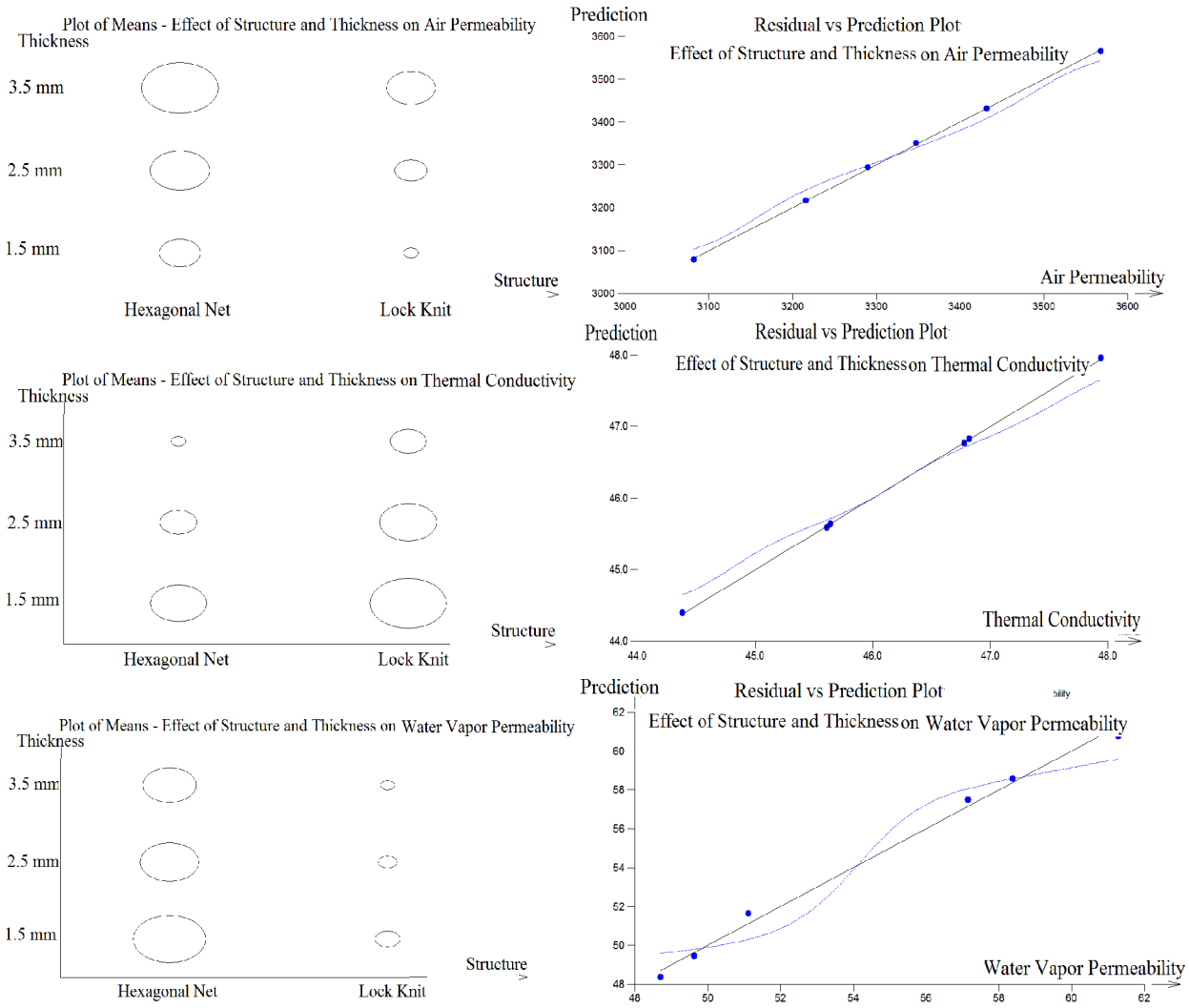

Figure 4.53 Graphical outputs – Statistical evaluation for thermo-physiology properties response of warp knit spacer fabrics

4.3.2 Thermo -physiological properties of weft knitted spacer fabrics

4.3.2.1 Porosity and stitch density of weft knitted spacer fabrics

The stitch density is the surface characteristics of textile materials, which normally decides the tightness, openness and loop geometry of fabrics. The small variations in stitch density have higher influence on the pore size and volume porosity. In this work, the stitch density differs for all weft knit fabrics. Also, the volume porosity was calculated and presented in this section since it directly affected by varying thickness and areal density. One way ANOVA was conducted to study the significance of stitch density and porosity between the two group samples (without lycra and with lycra). The result proves that there is significant differences between the groups with p value less than 0.05 (p= 0.0088). The volume porosity has no significant differences between the two groups of weft knit spacer fabrics with p value greater than 0.05 (0.296).

4.3.2.2 Influence of structural parameters on air permeability

Air permeability is the rate of air flow passing perpendicularly through a known area under a prescribed air pressure differential between the two surfaces of a material. Figure 4.54 shows that fabric thickness has a significant effect on the air permeability values of the spacer fabric, as air permeability tended to increase as thickness decreased, irrespective of yarn linear density and stitch density. The areal density has high influences on air permeability, higher air permeability observed with low areal density of weft knit spacer fabrics. The lower thickness and mass per square meter also facilitate the passage of air through the fabric. As observed in Figure 4.55 (a & b), in both groups of spacer fabrics, the lower air permeability values were obtained with samples WES 3 in group 1 and WES 6 in group 2 because of higher fabric density. Among the samples, the presence of lycra causes decrease in air permeability. The reduction in the fabric air permeability with lycra content can be attributed to the higher bulk, compactness, and the fabric thickness which offer resistance to the passage of air. On the other hand, the air permeability of fabric depends on the number and size of pores through which most of the airflow occurs. In general 3D spacer fabrics are more breathable, so it shows higher air permeability than 2D fabrics. Also, the structure and surface characteristics of spacer fabric affects the nature of air permeability. It is clear that, the air permeability of the spacer fabric increases with the decrease of stitch density percent in the surface. Normally lower stitch density results more permeable to air owing to their higher porosity compared with higher density of stitches. But, the reverse trend was observed for the samples (WES 1 and WES 4), it might be due to fabrics made up of monofilament as spacer yarn offers more air to trap inside the structure than the fabrics made up of multifilament yarn. So the air permeability of 3D spacer fabrics not only depends on surface characteristics such as stitch density and roughness, also depends on thickness, density and type of spacer yarn. As it can be observed in Figure 4.55aand was confirmed by ANOVA analysis, there is a significant influence of the density on air permeability and also linear correlation coefficient (0.947) with regression equation is given. The porosity of both groups has no significant differences, but the significant differences in air-permeability were observed due to

its different surface characteristics (Figure 4.55b). The increase in porosity can result in a significant increase in air permeability. The porosity has direct positive correlation with air permeability with R^2 value of 0.947 and also regression relation equation presented in it.

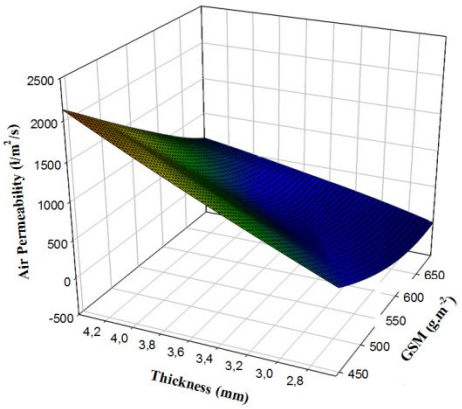

Figure 4.54 Influence of structural parameters on air permeability of weft knit spacer fabrics

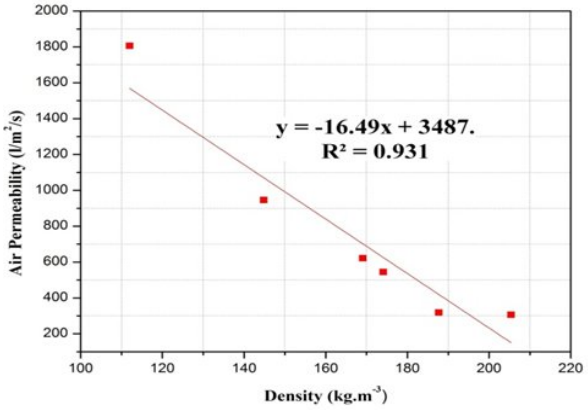

ANOVA	DF	Sum of Squares	Mean Square	F Value	Prob > F
Model	1	1.49E+06	1.49E+06	54.26128	1.81E-03
Error	4	109570.3	27392.57		
Total	5	1.60E+06			

(a)

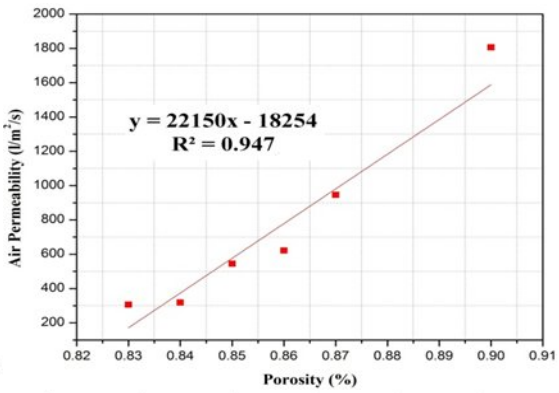

ANOVA	DF	Sum of Squares	Mean Square	F Value	Prob > F
Model	1	3.07E+01	3.07E+01	222.6534	1.17E-04
Error	4	0.55086	0.13771		
Total	5	3.12E+01			

(b)

Figure 4.55 Effect of structural characteristics and linear regression model for air permeability of warp knit spacer fabrics

4.3.2.3 Influence of fabric characteristics on thermal properties

The properties mentioned above are considered most important for thermal comfort inside vehicles. Table 3.6 shows thermal properties of the six spacer fabric samples. The thermal comfort of materials depends not only on the thermal properties of fabrics but other properties

are also important, for instance their density, porosity and thickness. A higher mass and thickness generally results in better thermal insulation of fabrics. Nevertheless, higher mass and thickness can lead to a worsening of utility comfort, especially the freedom of movement. The three dimensional structure of a spacer fabric has higher thickness and lower mass which leads to trapping of huge amount of air in the fabric structure. If the fabric is in contact with air from one side, the trapped air will circulate between the upper and bottom layers because of the high air permeability in these fabrics. This feature helps in transfer of moisture and heat from skin surface through the circulating air (Gross, 2003)**.** Figure 4.56a & b shows that, the spacer fabrics with more space to trap air inside the structure have relatively lower thermal conductivity value (0.053 – 0.066 W/mK).

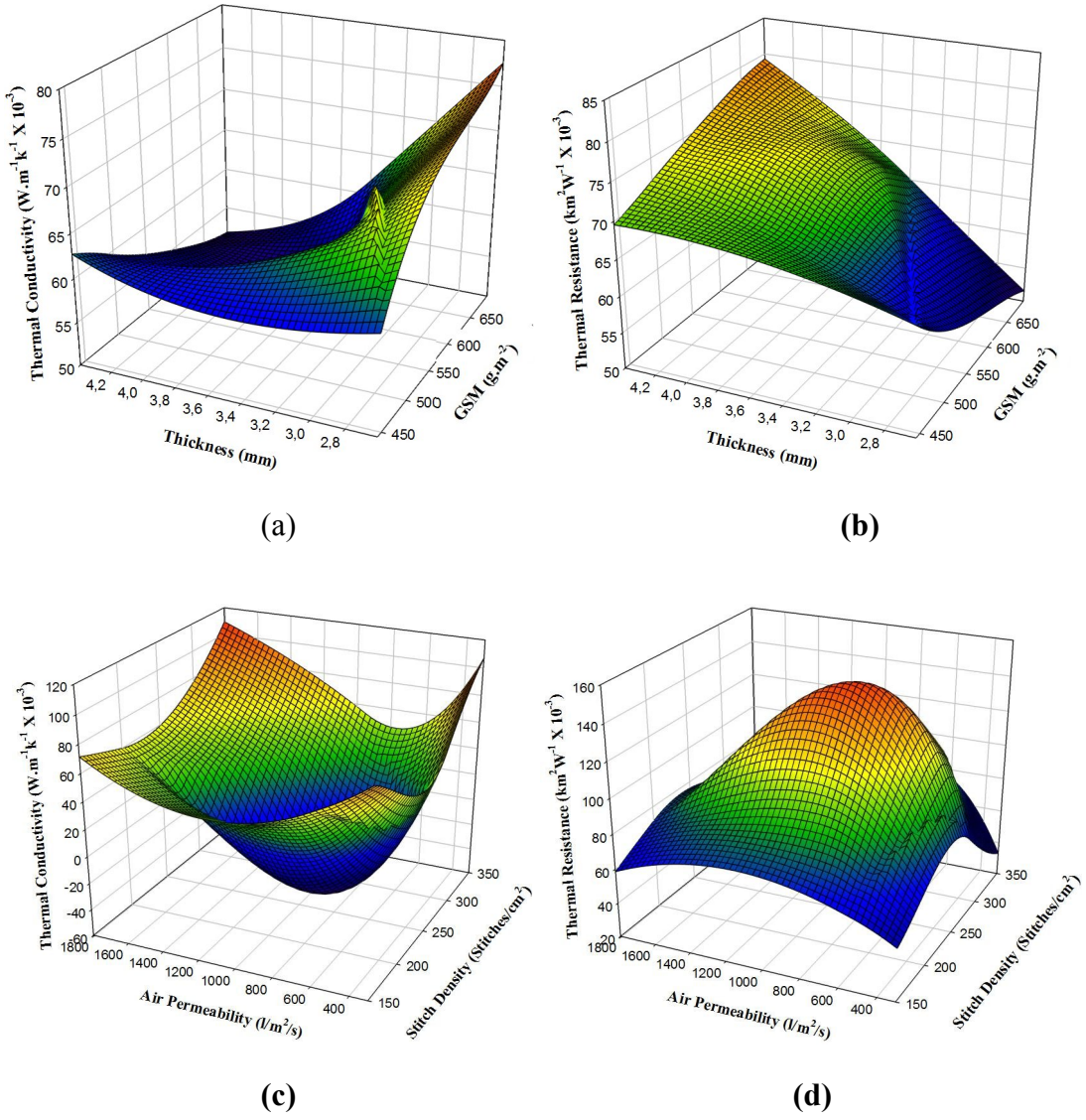

Figure 4.56 Influence of structural parameters on thermal properties of weft knit spacer fabrics

Since a lower value of thermal conductivity indicates a lower heat transfer from the skin to the fabric surface, this is usually associated with a warm feeling. The thickness is also a significant factor which influences the thermal resistance of spacer fabrics, higher thickness leads to higher thermal resistance. Also it is observed that, thick spacer fabric with low areal density leads the fabric to resist the heat to conduct. This study also found that, the thick fabrics with low density and higher air permeability exhibit relatively lower thermal conductivity for both the group of samples (Figure 4.56c &d). Also denser fabric has better thermal conductivity. It is also found that the spacer fabrics composed of monofilament spacer yarn (WES 1 & WES 4) have higher capacity to resist conduction of heat as compared to fabrics with multifilament spacer yarn (WES 2, WES 3 & WES 5, WES 6). It is mainly because monofilament spacer yarns make the fabric more bulky with lower density which offers more space to entrap air between the face and back layer. A remarkable difference between the heat transfer rates of group 1 and 2 fabrics are also justified here. It is also observed that fabrics made up of 6% of lycra yarn in the face layers (WES 4, WES 5 & WES 6) have lower thermal conductivity value than group 1 samples without lycra (WES 1, WES 2 & WES 3). The air trapped within the fabric structure starts to circulate and that's why the heat transfer rate of Group 2 is lower than that of Group 1. Due to higher stitch density and lycra based filament yarns on the surface layers, these spacer fabrics have lower air permeability value and consequently a lower thermal conductivity. Thermal resistance is a very important parameter from the point of view of thermal insulation; it is directly proportional to the fabric density and inversely proportional to air permeability (Figure 4.56c). Due to increase in density between the samples WES 1 to WES 3 and WES 4 to WES 6, one can observe the increase in thermal conductivity and decrease in resistance value.

4.3.2.4 Effect of fabric characteristics on water vapour permeability

The water vapour permeability of fabric depends upon a number of factors including thickness and density of fabrics, wetting and wicking behavior of yarns, and the relative humidity and temperature of the atmosphere. Figure 4.57 a & b demonstrates the influence of thickness and areal density on physiological properties of all the samples. It is reported that the relative water vapour permeability decreases with increase in thickness and areal density for all the fabrics with multifilament spacer yarn. The thick spacer fabric made up of monofilament spacer yarn has ability to transfer high amount of water vapour from one surface to another (Figure 4.53a &b). It is also observed from Figure 4.53c and Table 3.6 that the water vapour permeability increases as the stitch density of the spacer fabric increases in both the group of samples. But the trend is reversed in the case of evaporative resistance as shown in Figure 4.57d. Also, From the Figure 4.57, the fabrics made up of multifilament as spacer yarn offers more resistant towards permeability of water vapour. It might be due to the fabrics with multifilament spacer yarn has higher density. It is greatly reduced by the presence of 6% of lycra in group 2 samples as shown in Figure 4.57. Variation in the fibre composition ratio between polypropylene and polyester shows significant effect in both water vapour permeability and evaporative Resistance. It is also seen that with the increasing density of samples in a dry state, the relative water vapour

permeability increases in all samples. The research also showed that with a reduction in the percentage of polyester fibre content, the ability to transmit water vapour decreases. But the trend is reversed in the case of evaporative Resistance. So, the results demonstrate the apparent influence of fibre composition and density on the water vapour permeability of spacer knitted fabrics.

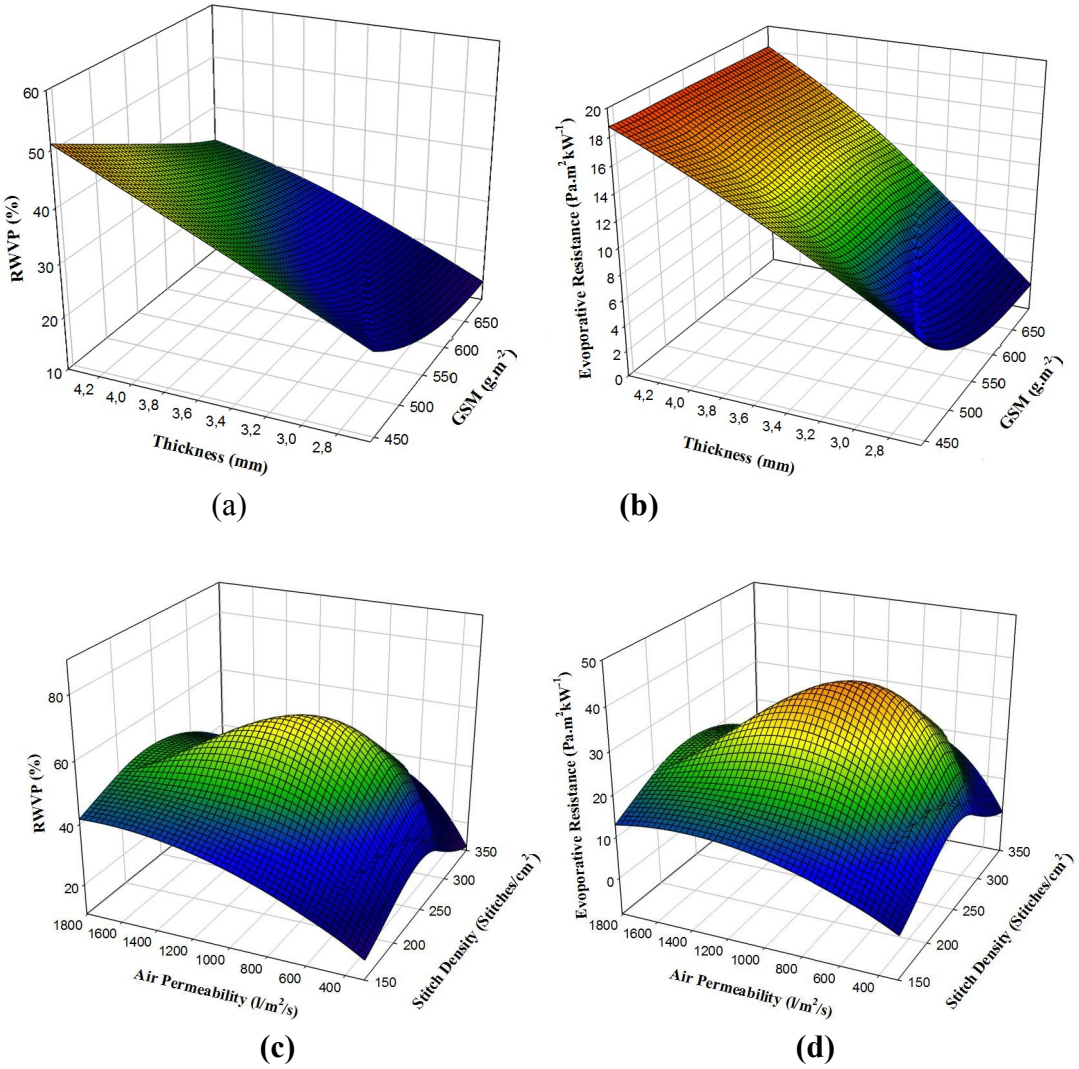

Figure 4.57 Influence of structural parameters on thermal properties of weft knit spacer fabrics

4.3.2.5 Statistical evaluation for thermo-physiological behavior of weft knit spacer fabrics

The above-mentioned results are confirmed by analysis of variance (ANOVA), and the result is significant influence of the surface structure, types of spacer yarn and thickness on fabric thermo-physiological properties. The three main properties which are essential for thermo-

physiology comfort for mattress, insole, mats and automobiles upholsteries are considered such as air permeability, thermal conductivity and water vapour permeability for statistical analyzes. In this section, one-way ANOVA is analyzed and the selected value of significance for all statistical tests in the study is α = 0.05 levels. The null sampling distribution of the F-statistic for given one-way ANOVA is the F-distribution with numerator degrees of freedom equal to $df_{between}$ = k-1 and denominator degrees of freedom equal to df_{within} = N- k. The degree of freedom is 1, 8, the $F_{critical}$ is 5.318, and degree of freedom 3, 16, the $F_{critical}$ is 3.239. If the statistic is smaller than the critical value, we retain the null hypothesis because the p-value must be bigger than α, and if the statistic is equal to or bigger than the critical value, we reject the null hypothesis because the p-value must be equal to or smaller than α. Also pair wise comparison using Scheffé's method and Z score was calculated and presented in Table 4.14, 4.15 & 4.16. The box plot and a z-score are also known as a standard score and it can be placed on a normal distribution curve as shown in Figure 4.58-4.60. The box plots show fairly symmetric distributions with fairly equal spread and also observed that the no outliers.

Table 4.14 Statistical evaluation for air permeability of weft knit spacer fabrics

One Way Anova - Influence of various factors on air permeability of weft knit spacer fabrics									
Test of factor influence : Influence of monofilament spacer yarn between both the groups									
		F_{cri}	F_{cal}	Prob.	Conclusion	Z-score (95% interval)	Pairwise comparison (Scheffé's method)		
							Compared Pair	Prob.	Significance
a	Without Lycra	5.318	8519.710	2.12E-13	Significant	6.039	a-b	2.12E-13	Significant
b	With Lycra					-3.326			
Test of factor influence : Influence of multifilament spacer yarn between both the groups									
a	Without Lycra (Thickness - 2.62mm)	3.239	2600.272	1.03E-21	Significant	4.106	a-b	1.48E-11	Significant
b	Without Lycra (Thickness - 2.74mm)					2.674	a-c	8.99E-20	Significant
							a-d	1.56E-20	Significant
c	With Lycra (Thickness - 3.5mm)					-2.363	b-c	2.67E-17	Significant
							b-d	2.32E-18	Significant
d	With Lycra (Thickness - 3.4mm)					-2.953	c-d	1.15E-05	Significant
Test of factor influence : Influence of types of spacer yarn within the group - Without Lycra									
a	Monofilament Spacer Yarn (Thickness - 4.4 mm)	5.318	15358.872	2.01E-14	Significant	5.96184	a-b	2.01E-14	Significant
b	Multifilament Spacer Yarn (Thickness - 2.62 mm)					-3.63892			
Test of factor influence : Influence of types of spacer yarn within the group - With Lycra									
a	Monofilament Spacer Yarn (Thickness - 4.4 mm)	5.318	15712.763	1.83E-14	Significant	4.235	a-b	1.83E-14	Significant
b	Multifilament Spacer Yarn (Thickness - 3.4 mm)					-3.375			

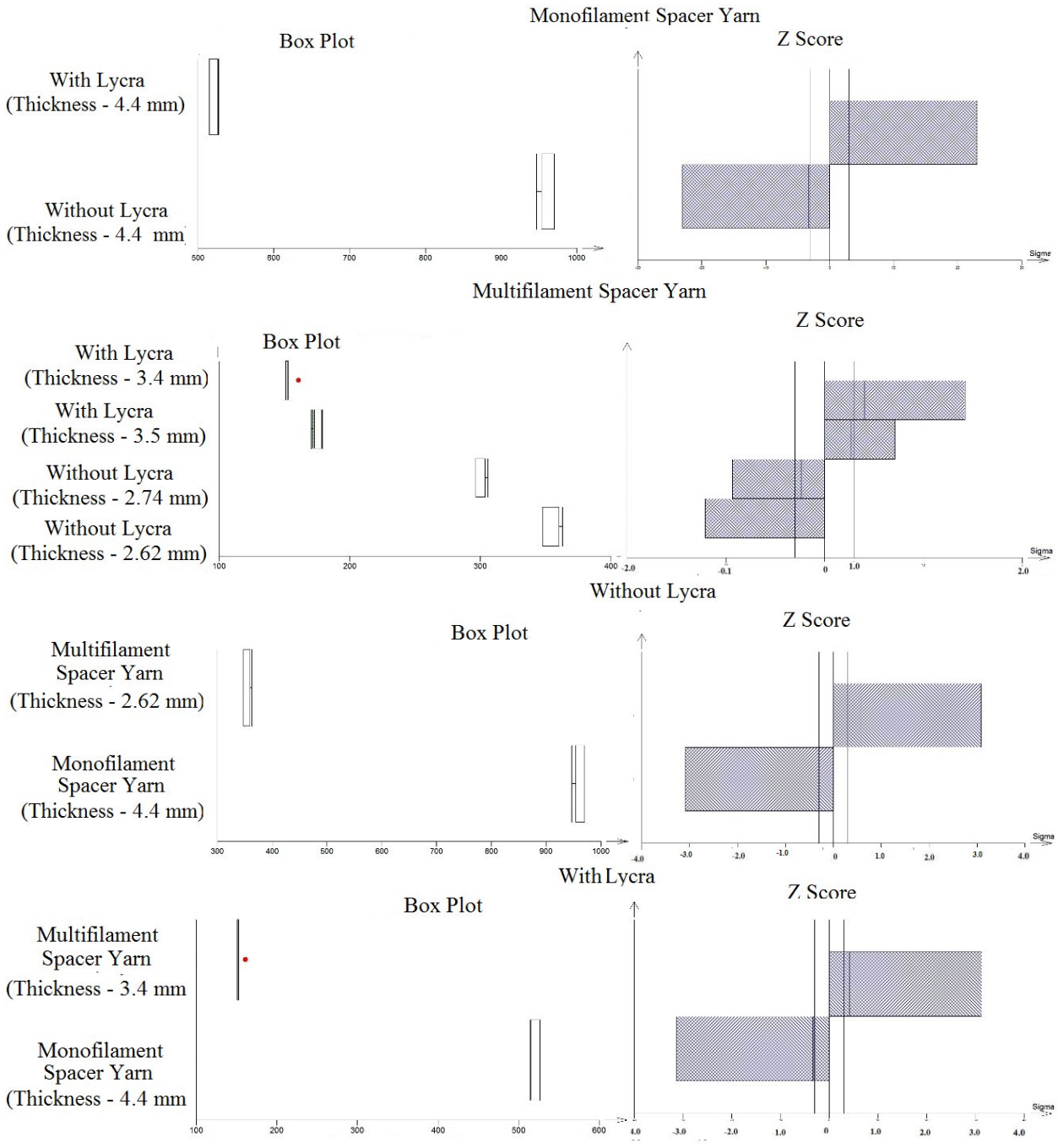

Figure 4.58 Graphical outputs – Statistical evaluation for air permeability response of weft knit spacer fabrics

Table 4.15 Statistical evaluation for thermal properties of weft knit spacer fabrics

One Way Anova - Influence of various factors on thermal conductivity of weft knit spacer fabrics									
Test of factor influence : Influence of monofilament spacer yarn between both the groups									
		F_{cri}	F_{cal}	Prob.	Conclusion	Z-score (95% interval)	Pairwise comparison (Scheffé's method)		
							Compared Pair	Prob.	Significance
a	Without Lycra	5.318	205.247	5.5E-07	Significant	3.582	a-b	5.50E-07	Significant
b	With Lycra					-3.582			
Test of factor influence : Influence of multifilament spacer yarn between both the groups									
a	Without Lycra (Thickness - 2.62mm)	3.239	142.469	3.27E-02	Significant	-0.155	a-b	4.98E-05	Significant
							a-c	4.49E-07	Significant
b	Without Lycra (Thickness - 2.74mm)					3.635	a-d	8.17E-01	Insignificant
c	With Lycra (Thickness - 3.5mm)					-3.667	b-c	9.6E-12	Significant
							b-d	5.77E-07	Significant
d	With Lycra (Thickness - 3.4mm)					0.187	c-d	1.24E-07	Significant
Test of factor influence : Influence of types of spacer yarn within the group - Without Lycra									
a	Monofilament Spacer Yarn (Thickness - 4.4 mm)	5.318	6.648	3.73E-08	Significant	-1.547	a-b	0.032699	Significant
b	Multifilament Spacer Yarn (Thickness - 2.62 mm)					1.579			
Test of factor influence : Influence of types of spacer yarn within the group - With Lycra									
a	Monofilament Spacer Yarn (Thickness - 4.4 mm)	5.318	318.126	1.00E-07	Significant	-1.412	a-b	1E-07	Significant
b	Multifilament Spacer Yarn (Thickness - 3.4 mm)					1.631			

The study for each thermal property (air permeability, thermal resistance, thermal conductivity, water vapour permeability and evaporative resistance) was examined by one-way analysis of variance (ANOVA) with a confidence level of 95%. Statistical analysis also indicates that the results are significant for air permeability, thermal resistance and thermal conductivity and water vapour permeability of the fabrics.

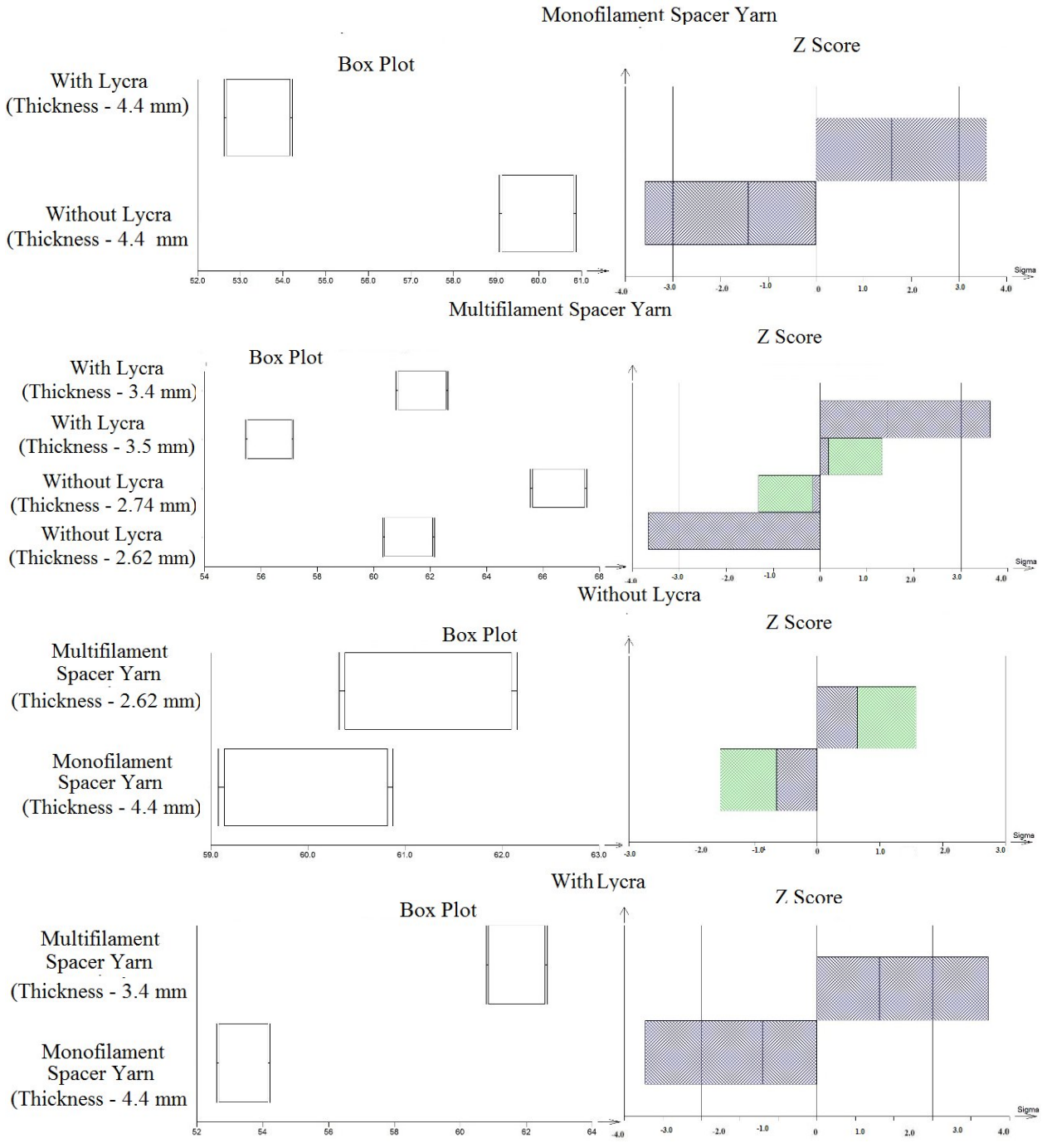

Figure 4.59 Graphical outputs – Statistical evaluation for thermal properties response of weft knit spacer fabrics

Table 4.16 Statistical evaluation for water vapor permeability of weft knit spacer fabrics

One Way Anova - Influence of various factors on water vapor permeability of weft knit spacer fabrics

		F_{cri}	F_{cal}	Prob.	Conclusion	Z-score (95% interval)	Pairwise comparison (Scheffé's method)		
							Compared Pair	Prob.	Significance
Test of factor influence : Influence of monofilament spacer yarn between both the groups									
a	**Without Lycra**	5.3177	28.8751	0.000667	Significant	2.912	a-b	6.67E-04	Significant
b	**With Lycra**					-3.217			
Test of factor influence : Influence of multifilament spacer yarn between both the groups									
a	**Without Lycra (Thickness - 2.62mm)**	3.239	5.876	6.65E-03	Significant	1.956	a-b	4.92E-02	Significant
							a-c	0.883705	Insignificant
b	**Without Lycra (Thickness - 2.74mm)**					-1.799	a-d	2.56E-02	Significant
c	**With Lycra (Thickness - 3.5mm)**					1.148	b-c	0.188543	Insignificant
							b-d	0.987781	Insignificant
d	**With Lycra (Thickness - 3.4mm)**					-1.067	c-d	1.07E-01	Insignificant
Test of factor influence : Influence of types of spacer yarn within the group - Without Lycra									
a	**Monofilament Spacer Yarn (Thickness - 4.4 mm)**	5.318	223.864	1.59E-05	Significant	3.377	a-b	3.93E-07	Significant
b	**Multifilament Spacer Yarn (Thickness - 2.62 mm)**					-1.612			
Test of factor influence : Influence of types of spacer yarn within the group - With Lycra									
a	**Monofilament Spacer Yarn (Thickness - 4.4 mm)**	5.318	84.444	7.78E-07	Significant	3.686	a-b	1.59E-05	Significant
b	**Multifilament Spacer Yarn (Thickness - 3.4 mm)**					-0.869			

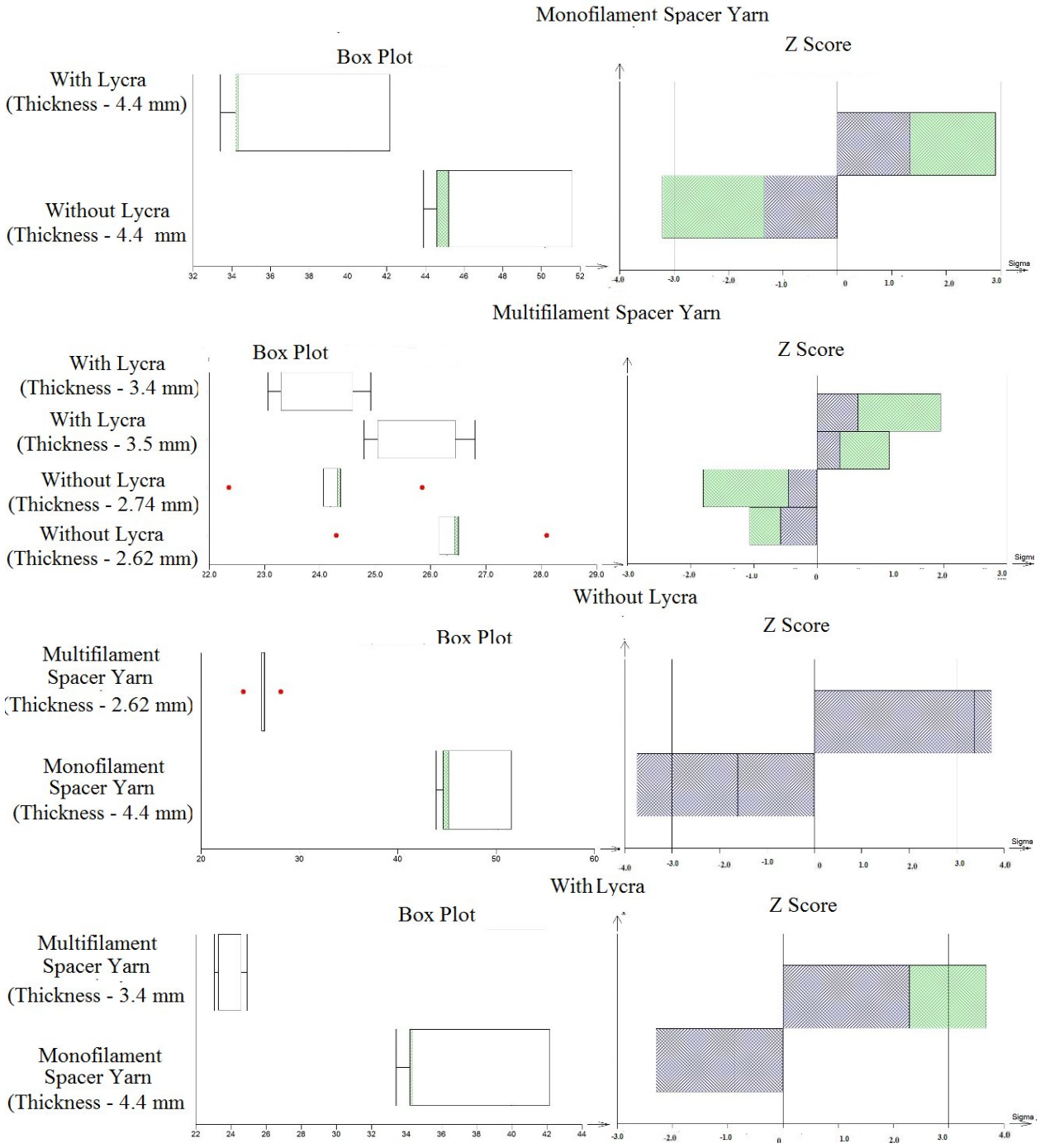

Figure 4.60 Graphical outputs – Statistical evaluation for water vapour permeability response of weft knit spacer fabrics

4.4 Acoustic properties of spacer fabrics

The acoustic properties of both warp and weft knitted spacer fabrics has been carefully evaluated using experimental method and is discussed in this section.

4.4.1 Acoustic properties of warp knitted spacer fabrics

4.4.1.1 Influence of materials parameters on tortuosity of warp knit spacer fabrics

In this section the effect of material parameters on tortuosity has been discussed thoroughly. Also both analytical and experimental data of both lock knit (WAS 1 –WAS 6) and hexagonal net (WAS 7 – WAS 12) warp knit spacer fabrics were presented and compared in the Figure 4.61(a &b). It clearly shows that there is strong significant difference between these two methods for the samples with lower thickness (WAS 1, WAS 4, WAS 7 and WAS 10). Also tortuosity values show significant difference between the samples (WAS 1 -WAS 6 and WAS 7 – WAS 12). As compared both the structure of samples, no differences is observed in tortuosity for the samples with almost same stitch density and massivity. So, tortuosity is highly dependent on the thickness, massivity and inner geometry for the spacer fabrics. A small variation in thickness causes a huge impact on tortuosity of air channel in the material. The tortuosity increases with increase in massivity of spacer textile materials.

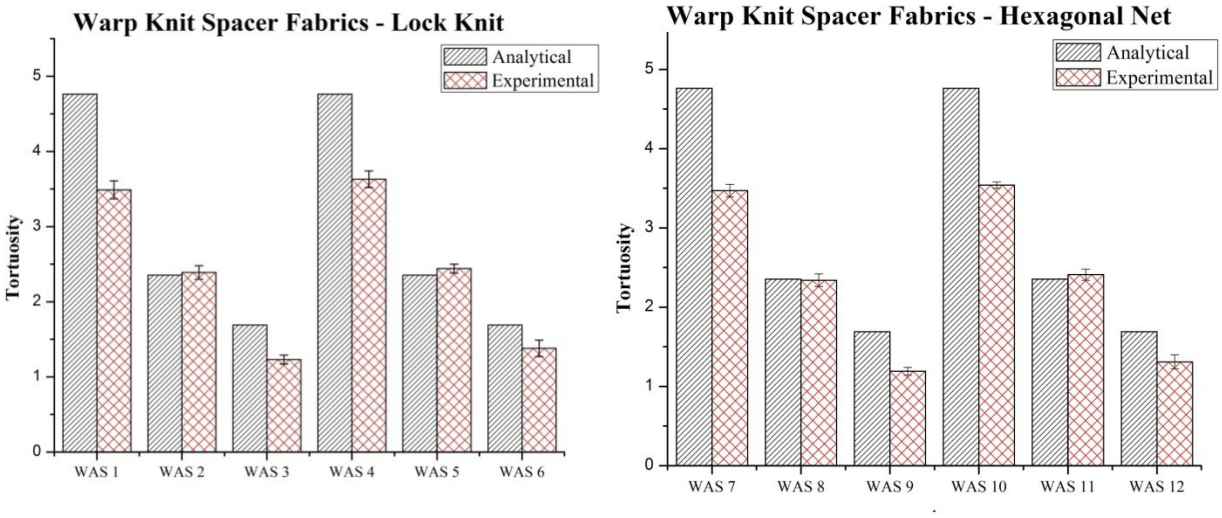

(a) **(b)**

Figure 4.61 Comparison of experimental and analytical tortuosity of warp knit samples

4.4.1.2 Effect of structural characteristics on air flow resistivity of warp knit spacer fabrics

The flow resistivity of material is majorly decides by the characteristics such as density, massivity or porosity and tortuosity. In this section effect of these three characteristics on air flow resistivity of warp knitted spacer fabrics are clearly discussed and presented in Figure 4.62. The results show that fabric density has a significant effect on the air flow resistivity values of the spacer fabric, as air flow resistivity tended to increase as density increased, irrespective of yarn linear density and stitch density. As shown in Figure 4.62a, the denser fabrics offer more resistant towards air to pass from one surface to other.

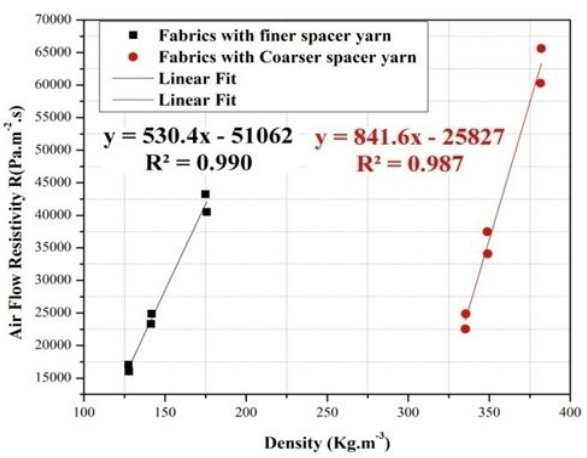

	ANOVA	DF	Sum of Squares	Mean Square	F Value	Prob > F
Finer spacer yarn	Model	1	6.77E+08	6.77E+08	415.0868	3.43E-05
	Error	4	6.52E+06	1.63E+06		
	Total	5	6.83E+08			
Coarser spacer yarn	Model	1	1.62E+09	1.62E+09	303.3484	6.38E-05
	Error	4	2.13E+07	5.33E+06		
	Total	5	1.64E+09			

(a)

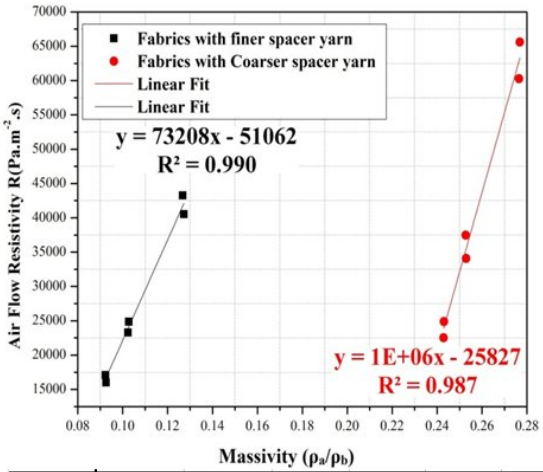

	ANOVA	DF	Sum of Squares	Mean Square	F Value	Prob > F
Finer spacer yarn	Model	1	6.77E+08	6.77E+08	415.0868	3.43E-05
	Error	4	6.52E+06	1.63E+06		
	Total	5	6.83E+08			
Coarser spacer yarn	Model	1	1.62E+09	1.62E+09	303.3484	6.38E-05
	Error	4	2.13E+07	5.33E+06		
	Total	5	1.64E+09			

(b)

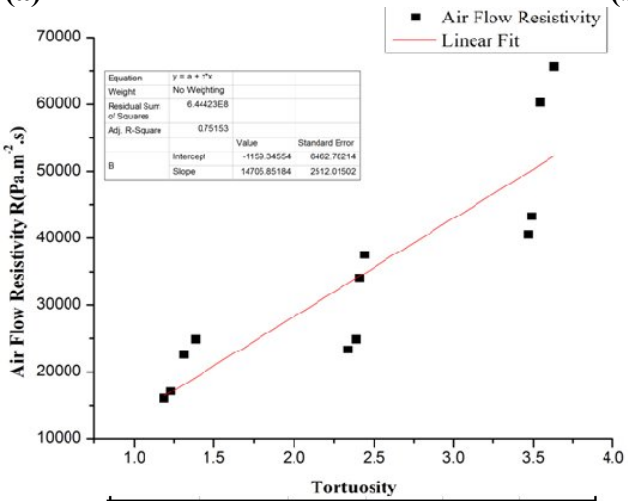

ANOVA	DF	Sum of Squares	Mean Square	F Value	Prob > F
Model	1	2.21E+09	2.21E+09	34.27172	1.61E-04
Error	10	6.44E+08	6.44E+07		
Total	11	2.85E+09			

(c)

Figure 4.62 Effect of structural characteristics and linear regression model for air flow resistivity of warp knit spacer fabrics

Also it was observed from the Figure 4.62 b, porous with lower massivity of fabrics offers more permeable to air. Lock knit fabrics (WAS 1 – WAS 6) have tighter surface structure because it inter-loops the filament very close to each other, So, it is resistant to air flow. It was also noticed that the spacer fabrics with finer spacer yarn offers lower resistance to air due to lower density. As shown in Figure 4.62c, the torturous (high tortuosity) fabrics results high air flow resistivity because it is obvious that, when the material has more tortuous path, it resists the fluid to flow

freely. The positive linear correlation was found between tortuosity and flow resistivity with R^2 value of 0.895. Comparison between all the samples shows the lock knit fabrics have higher flow resistance than the hexagonal net fabrics. Hexagonal fabrics (WAS 7 – WAS 12) produces more open structure on surface, it produce more gaps which results in highly permeable to air. All these factors contribute towards the higher air flow resistance.

4.4.1.3 Influence of structural properties on sound absorption of warp knit spacer fabrics

The sound absorbencies of the warp knit spacer fabrics were measured with a two-microphone impedance tube according to the ISO 10534-2 standard. The effect of structural properties such as thickness, density, massivity (or porosity) and airflow resistivity parameters of the tuck spacer fabrics on their sound absorbency are analyzed in this section. For the range of considered porosity, the influence on the sound absorption is complicated. As shown in Figure 4.63 a & b, porosity increases from 72 to 90 % for both the structures (lock knit and hexagonal net) warp knit spacer fabrics, the changes on sound absorption is insignificant for low frequency range (50 Hz to 2000 Hz). In middle frequency range, 2000 -4500 Hz, the absorption coefficient increases drastically when the porosity decreases because of increases in air-flow resistivity. For frequency range above 4500Hz (high frequency), the significant differences in sound absorption value between the samples can be observed clearly from the Figure 4.63, it might be due to the variation in flow resistivity and the thickness.

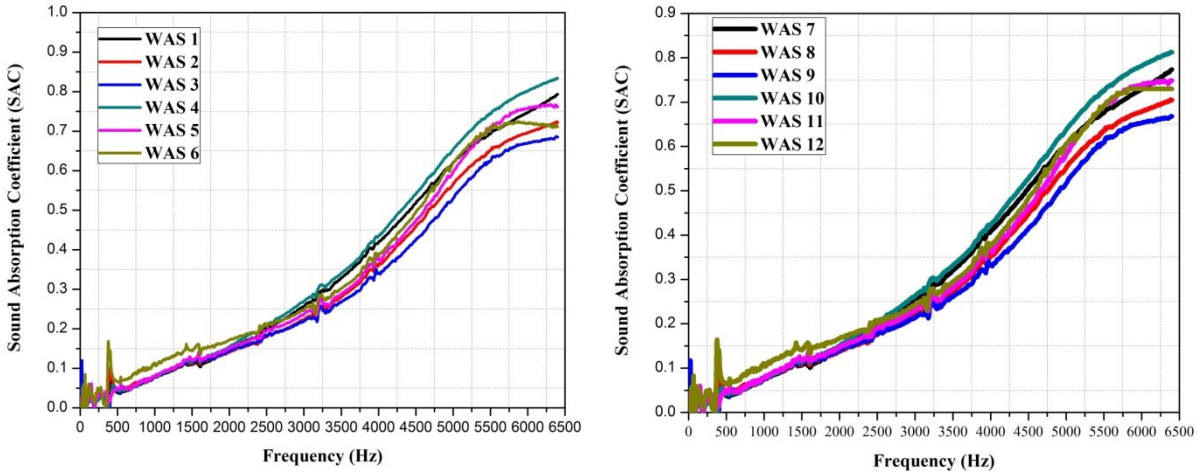

(a) **(b)**

Figure 4.63 Effect of structural properties on sound absorption behavior of warp knit spacer fabrics

The results obtained show that the thin spacer fabric with high density have higher air flow resistance. The increase in torturous path of middle (spacer) layer has ability to entrap more air therefore cause higher flow resistance with more sound absorption. The spacer fabrics (WAS 4 –

WAS 6 & WAS 10 – WAS 12) are relative shows higher density and lower porosity; allows sound waves to attenuate easily. It was noticed from the figure 4.63, the sound absorption capacity of spacer fabrics depends not only air flow resistivity, it depends surface structure structural pores, thickness and density. In case of spacer fabric samples with hexagonal net (WAS 7 – WAS 12), the sound absorption is comparatively lower than samples with lock knit (WAS 1 and WAS 6) because of surface pore characteristics. This is mainly because of surface roughness and stitch density of the spacer fabrics which causes sound waves to reflect more on the surface itself. Variations of porosity in the range of 10 or 15 % have major influence on the acoustic behavior of spacer fabrics. Figures 4.64 indicate that the noise reduction coefficient of the spacer fabrics increase with the increase of airflow resistivity. Moreover, an increase in airflow resistivity gives rise to a reduction in porosity; thus, the sound absorbency of the fabric increases with the reduction in its porosity. The effect of airflow resistivity has a greater effect on the sound absorbency of the warp knit spacer fabric than its thickness. Moreover, as shown in figure 6.64, the airflow resistivity is more or less inversely proportional to the porosity or directly proportional to massivity of the fabric; the effect of massivity thus has a greater effect on its sound absorbency. Further, this would result in the sound absorbency of these fabrics increasing with density.

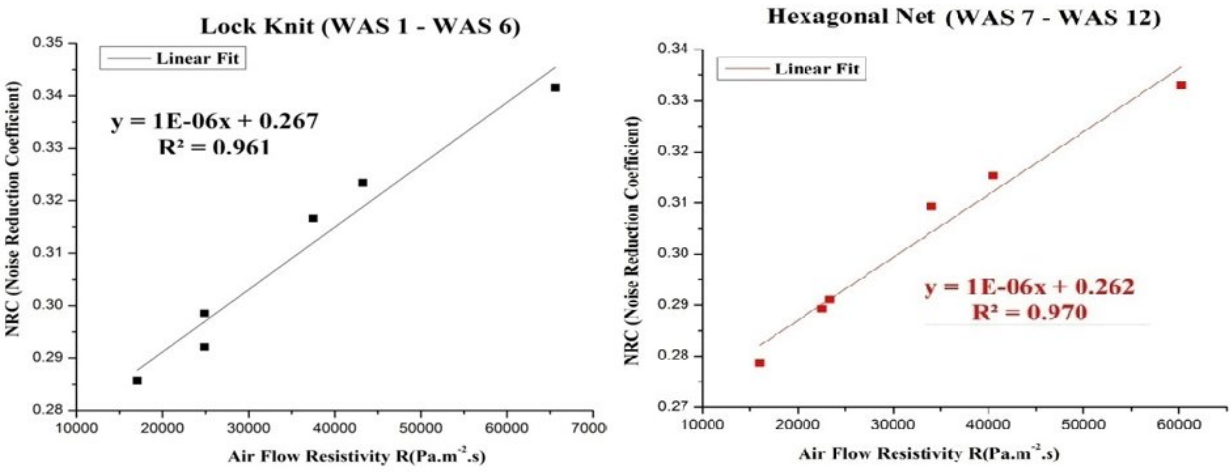

	ANOVA	DF	Sum of Squares	Mean Square	F Value	Prob > F
Lock Knit	Model	1	2.17E-03	2.17E-03	99.56072	5.67E-04
	Error	4	8.74E-05	2.18E-05		
	Total	5	2.26E-03			
Hexagonal	Model	1	1.96E-03	1.96E-03	130.9826	3.33E-04
	Error	4	5.99E-05	1.50E-05		
	Total	5	2.02E-03			

Figure 4.64 Influence of air flow resistivity on noise reduction coefficient and its linear regression model of warp knit spacer fabrics

Figure 4.64 also presents the regression model for noise reduction coefficient with the effect of air flow resistivity. The noise reduction coefficient (NRC) of warp knitted spacer fabric has positive linear correlation with flow resistivity with the correlation coefficient of more than 0.9.

4.4.1.4 Statistical evaluation for sound-absorption behavior of warp knit spacer fabrics.

In this section, two-way ANOVA is carried out and the selected value of significance for all statistical tests in the study is 0.05 levels. Analysis of different combination of factors on air flow resistivity and noise reduction coefficient is presented in Table 4.17. The factors mainly considered are structure and density which strongly influence the acoustic properties of the three-dimensional spacer fabrics.

Table 4.17 Statistical evaluation for acoustic properties of warp knit spacer fabrics

Two Way ANOVA Table

Influence of Structure and Density on Air Flow Resistivity

Source of variability	Sum of squares	Mean square	Degrees of freedom	Std deviation	F-statistic	Critical quantile	Conclusion	p-value
Structure	22531048	22531048	1	4746.6881	19.410204	6.607891	Significant	0.0069846
Density	2.825E+09	564927223	5	23768.198	486.67742	5.0503291	Significant	1.03E-06
Interaction	5243226.3	5243226.3	1	2409.1323	37.405376	7.7086474	Significant	0.003619
Residuals	560692.27	140173.07	4	374.39694				
Total	**2.853E+09**	**259361007**	**11**	**16104.689**				

Influence of Structure and Density on NRC

Structure	0.0001944	0.0001944	1	0.0139419	396.23513	6.607891	Significant	5.91E-06
Density	3.80E-03	7.60E-04	5	0.0275615	1548.5042	5.0503291	Significant	5.74E-08
Interaction	9.05E-07	9.05E-07	1	0.0015661	2.3407916	7.7086474	Insignificant	0.200767
Residuals	1.55E-06	3.87E-07	4	0.000622				
Total	**3.99E-03**	**3.63E-04**	**11**	**1.91E-02**				

The critical quantile ($F_{critical}$) values obtained for factor A – 6.60, 19, Factor B – 5.05 and Interaction – 7.70 with respect to degrees of freedom. The value of $F_{critical} < F_{statistic}$ proves that the changes in the density and surface layer structure of warp-knitted spacer fabric results is highly significant on the above-mentioned fabric compression properties. Even the minor changes in the fabric densities results in significant impact on the flow resistivity and NRC. But the insignificant differences are observed in the NRC for the interaction with $p > 0.05$. The plot of means visually compares the response values for each combination of factor levels (or each cell). In Figure 4.65, circle stands for values of flow resistivity and NRC values without replications. Diameter of the circle is roughly proportional to the response. Differences between levels and interactions can be seen on this plot. The residuals versus prediction plot show the quality of fit of the model. From the Fig. 4.65 it is observed, closer are the points to the line $y = x$, the more significant the model is.

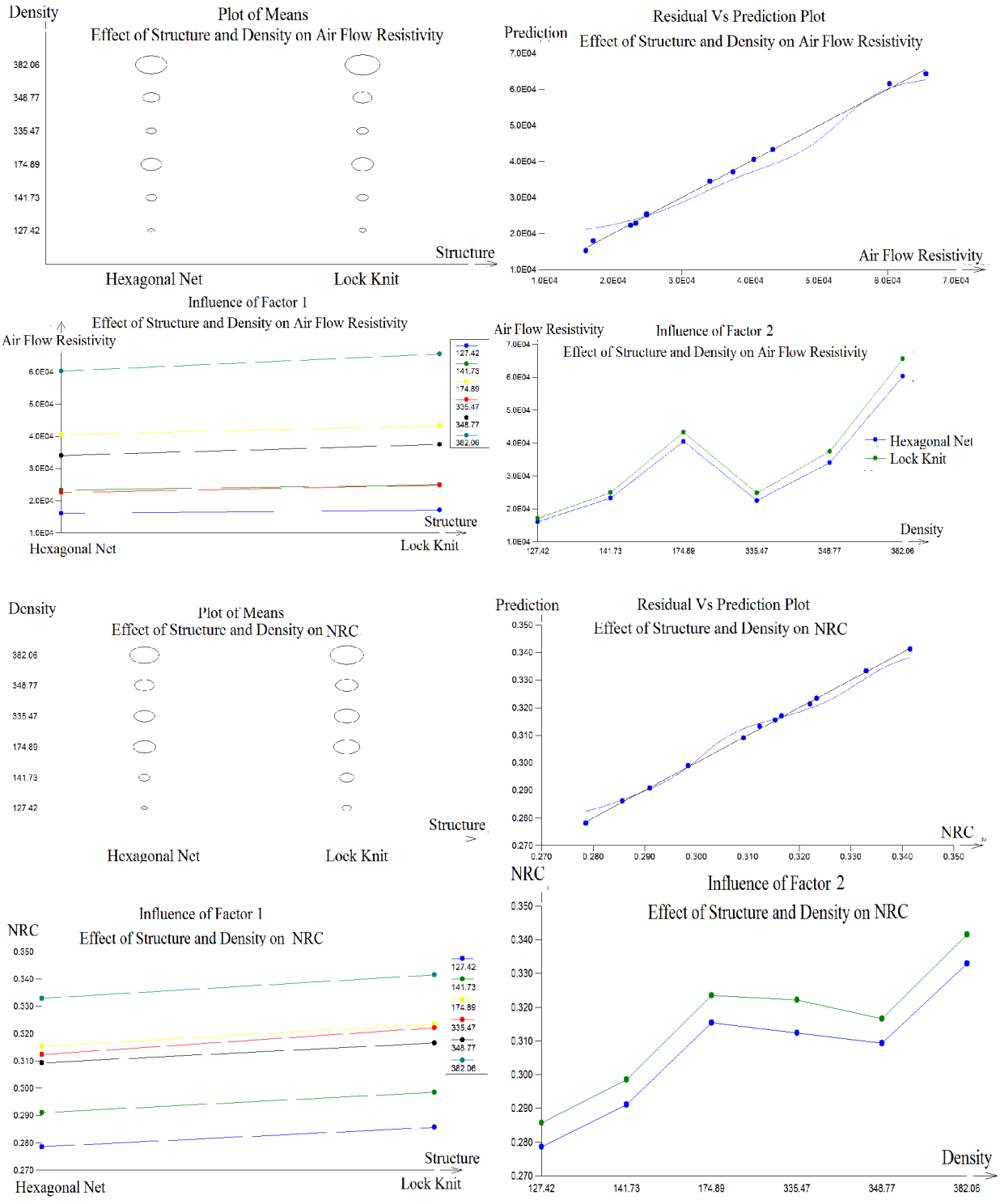

Figure 4.65 Graphical outputs – Statistical evaluation for acoustic properties response of warp knit spacer fabrics

Plot of the influence of a given factors at separate levels of the other factor. If the lines for factor A are similar for each level of the factor *B*, then the factor A is probably significant. If the lines

have rather opposite direction, then there is probably strong interaction between the factors. If the lines are shaped rather randomly, then the influence and significance of the respective factor is probably low. Figure 4.65 shows that the lines of factor –structure is not exactly same to the factor–density, so it proves that some interactional effects exist between these two factors on flow resistivity. Similar trends in NRC show no interactional effect.

4.4.2 Acoustic properties of weft knitted spacer fabrics

The acoustic properties of weft knitted spacer fabrics are discussed in this section with the careful evaluation and analysis of various characteristics and its influences on sound absorption behavior

4.4.2.1 Effect of materials parameter on tortuosity of weft knit spacer fabrics

Basically tortuosity is the measure of non-straightness of pore structure in given material. If the path is more complex, the sound wave takes longer time to pass through the structure and remains in contact with the constituent material for a longer duration. In this section the effect of material parameters on tortuosity has been discussed thoroughly. Also both analytical and experimental data of each sample (WES 1 to WES 6) were presented and compared in the Figure 6.66. It clearly shows that there is no significant difference between these two methods. But the tortuosity values show significant difference between the samples (WES 1 -WES 6). As per both the group of samples, there is significant difference because of the variation in stitch density and related roughness on the surface of the materials. A small variation in thickness causes a huge impact on tortuosity of air channel in the material. The tortuosity depends on the inner geometry apart from the porosity, tortuosity increases with increase in massivity of spacer textile materials.

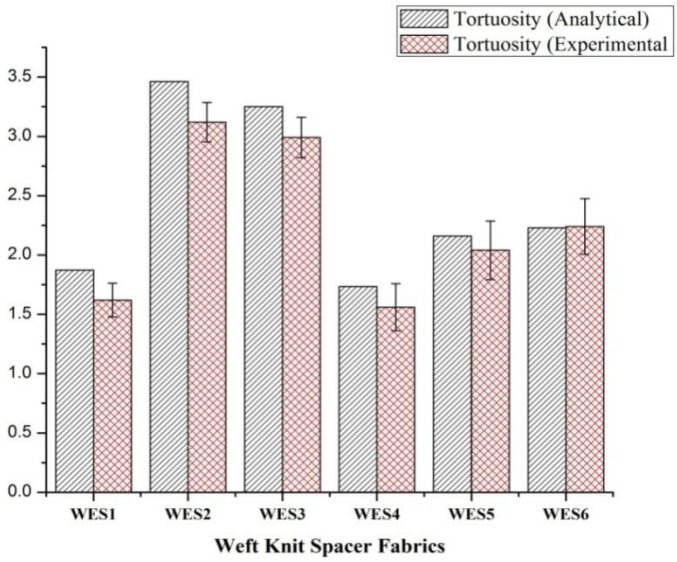

Figure 4.66 Comparison of experimental and analytical tortuosity of weft knit spacer fabrics

4.4.2.2 Influence of structural parameters on air flow resistivity of weft knit spacer fabrics

In this study, six spacer fabrics of different materials, stitch density, thickness and spacer yarns were chosen to study the effect of material characteristics. Maximum 2% variation is observed in flow resistivity values for all the tested samples. The percentage deviation of flow resistivity for sample WES 1 and sample WES 2 is 5-35%. Figure 4.67 shows the flow resistivity values for different samples (WES 1 – WES 6) with respect to density, massivity and tortuosity. The variation in flow resistivity with respect to thickness of samples has not been discussed because only approximately 1-2% variation in thickness is observed between the samples of both the groups. The investigation of air flow resistivity for spacer fabrics made up of monofilament and multifilament spacer yarns has been carried out and described in this section. It was observed that the flow resistance is significantly lower in case of spacer fabrics made up of monofilament spacer yarn compared to multifilament spacer yarn.

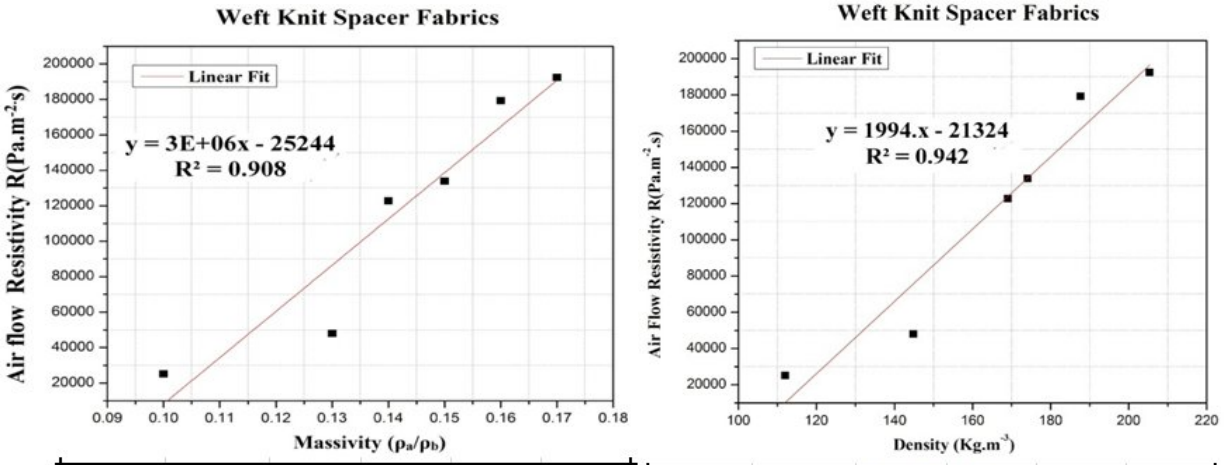

ANOVA	DF	Sum of Squares	Mean Square	F Value	Prob > F
Model	1	2.10E+10	2.10E+10	39.80997	3.23E-03
Error	4	2.11E+09	5.26E+08		
Total	5	2.31E+10			

(a)

ANOVA	DF	Sum of Squares	Mean Square	F Value	Prob > F
Model	1	2.17E+10	2.17E+10	65.33096	1.27E-03
Error	4	1.33E+09	3.33E+08		
Total	5	2.31E+10			

(b)

Figure 4.67 Effect of structural characteristics and linear regression model for air flow resistivity of weft knit spacer fabrics.

The same trend was observed in both the group of samples (group 1 and group 2), it is because of the samples (WES 1 & WES 4) fabrics made up of monofilament spacer yarns have more open structure as compared to samples (WES 2, WES 3 & WES 5, WES 6 respectively). Also, it was observed that group 2 samples have significantly higher flow resistance than group 1 samples because of closeness of structure (higher stitch density) of the samples on the outer surface to resist air to move inside the material. As shown in Figure 4.67b, the density of the material has a strong influence on the air flow inside the material. It is obvious that the increase in density leads to increase in flow resistance. The correlation between density and air flow resistivity was also calculated and mentioned in figure. In both the group of samples the air flow resistance increases

with increase in massivity. So, positive linear correlation trend was found between these two parameters with correlation coefficient of 0.94 as shown in Figure 4.67b.In case of group 2, the samples show higher resistance to air flow on the surface because of tightness of the fabrics (high stitch density). It is also observed that samples with lycra content on surface layer exhibit increased tortuosity along with increase in air flow resistivity. It is obvious that, when the material has more tortuous path, it resists the fluid to flow freely. It is also observed that spacer fabric with monofilament has more open channel for free flow of fluid than multifilament spacer yarns.

4.4.2.3 Influence of fabric properties on sound absorption properties of weft knit spacer fabrics

For the range of considered porosity, the influence on the sound absorption is complicated. When porosity increases from 85 to 90 % for group 1 samples, the changes on sound absorption is insignificant for low frequency range (50 Hz to 2000 Hz). But for frequency range above 2000 Hz, the absorption coefficient decreases drastically when the porosity increases to 90%. This is mainly because of too much space between the two layers in spacer fabrics which entraps excess of air, hence, the sound energy dissipation is substantially weaken, especially when the porosity is higher than 90%. In case of group 2 samples with porosity (83 to 87%), there is significant sound absorption both in low and high frequency ranges. It is mainly due to dissipation of sound waves between the layers having relatively lower volume of air trapped inside the structure. In case of spacer fabric samples with monofilament (WES 1), the sound absorption is comparatively lower than samples with multifilament (WES 2 and WES 3) because of high porosity. In contrast, the trend is reversed for group 2 samples; S4 shows higher sound absorption than WES 5 and WES 6, though the porosity is higher (87%) for WES 4. This is mainly because of surface roughness and stitch density of the spacer fabrics which causes sound waves to reflect more on the surface itself. Variations of porosity in the range of 2 or 3 % have minor influence on the acoustic behavior of spacer fabrics (Figure 4.68). The effect of tortuosity on sound absorption coefficient of the spacer fabrics are analyzed and reported in this section. As can be seen, sound absorption coefficient increases with increase in the tortuosity values for both the group of samples (WES 1 to WES 6) for middle and high frequency ranges. It appears that the optimum sound absorption performed by the highly tortuous material, it is also due to increase in fabric thickness as areal density. At higher values of the tortuosity, the behavior shifts towards higher values of sound absorption. The thickness of the porous material layer has a great influence on the position of the peak value in the frequency spectrum. It is also observed that at low frequency, sound absorption has a direct relationship with thickness and at high frequency; the thickness has a modest effect on sound absorption. Thicker the layer of the porous material, lower is the frequency at which the peak occurs. Also, the material thickness is about one tenth of the wavelength of incident sound waves, which is the limit value for the porous material to achieve effective sound absorption (Figure 4.68).

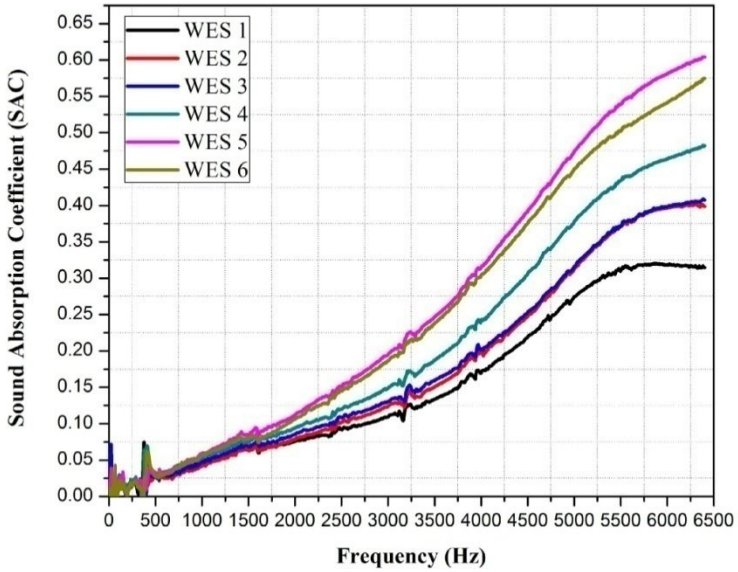

Figure 4.68 Effect of structural characteristics on sound absorption behavior of weft knit spacer fabrics

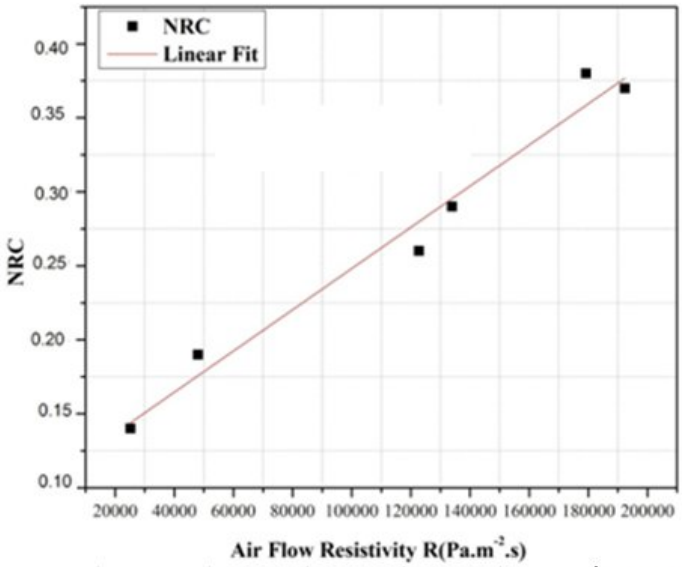

ANOVA	DF	Sum of Squares	Mean Square	F Value	Prob > F	Intercept	Slope
Model	1	4.47E-02	4.47E-02	155.7713	2.37E-04	3.09E-01	1.39E-06
Error	4	1.15E-03	2.87E-04				
Total	5	4.59E-02					

Figure 4.69 Influence of air flow resistivity on noise reduction coefficient and its linear regression model for weft knit spacer fabrics

The effect of air flow resistivity on sound absorption values has also been reported. At low and

mid frequencies, variations of flow resistivity between samples have no noticeable effect on the absorption coefficient. In contrast, there is significant difference in high frequency ranges. It has also been observed that the variation in flow resistivity with respect to thickness and tortuosity for sample with monofilament spacer yarn WES 4 is higher as compared to sample WES 1. This variation might be due to stitch density (surface friction), anisotropic and in-homogeneous nature of spacer fabrics. Moreover, decrease in porosity is also associated with increase in airflow resistivity, along with increase in tortuosity values as well. The airflow resistivity has a strong direct influence on the sound absorbency of the weft knit spacer fabric than other properties. The airflow resistivity is more or less inversely proportional to the porosity or directly proportional to massivity of the fabric; the effect of massivity thus has a greater effect on its sound absorbency. Figure 4.69 also presents the regression model for noise reduction coefficient with the effect of air flow resistivity. The noise reduction coefficient (NRC) of weft knitted spacer fabric has positive linear correlation with flow resistivity with the coefficient of determinant of about 0.975. Overall it is observed that, at higher frequencies, spacer fabrics have ability to absorb around 40-60% of sound due to its 3-dimensional bulk structure. But it has less absorption in both mid and low frequencies. These discussions on sound absorption suggest that, spacer fabrics can achieve substantial sound absorption by modifying its spacer layer structure and material parameters.

4.4.2.4 Statistical evaluation for sound absorption behavior of weft knit spacer fabrics

The main properties which are additional requirement for cushioning materials are considered such as noise reduction coefficient for statistical analyzes. In this section, one-way ANOVA is analyzed and the selected value of significance for all statistical tests in the study is α = 0.05 levels.

Table 4.18 Statistical evaluation for NRC of weft knit spacer fabrics

One Way Anova - Influence of various factors on acoustic properties of weft knit spacer fabrics									
Test of factor influence : Influence of surface properties on NRC between both the groups									
		F_{cri}	F_{cal}	Prob.	Conclusion	Z-score (95% interval)	Pairwise comparison (Scheffe's method)		
							Compared Pair	Prob.	Significance
a	Without Lycra	7.708	16.100	0.0159	Significant	-0.19212	a-b	0.0159	Significant
b	With Lycra					0.325323			

The null sampling distribution of the F-statistic for given one-way ANOVA is the F-distribution with numerator degrees of freedom equal to $df_{between}$ = k-1 and denominator degrees of freedom equal to df_{within} = N- k. If the statistic is smaller than the critical value, we retain the null hypothesis because the p-value must be bigger than α , and if the statistic is equal to or bigger than the critical value, we reject the null hypothesis because the p-value must be equal to or smaller than α . Also pair wise comparison using Scheffe's method and Z score was calculated and presented in Table 4.17. The box plot and a z-score are also known as a standard score and it

can be placed on a normal distribution curve as shown in Figure 4.70.

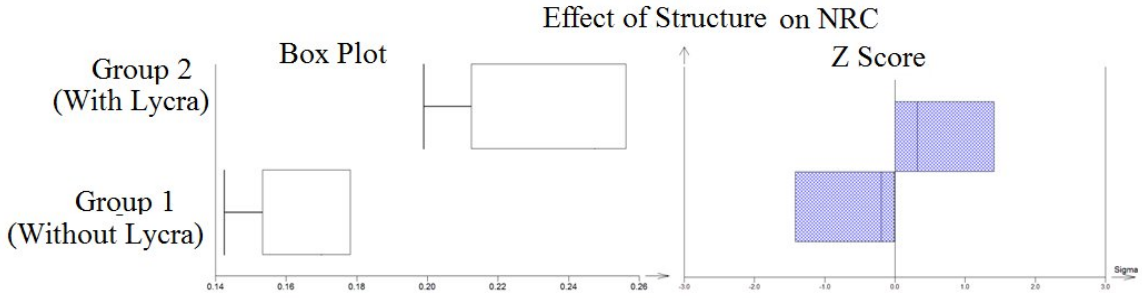

Figure 4.70 Graphical outputs – Statistical evaluation for sound absorption response of weft knit spacer fabrics

Chapter 5 Summary and conclusions

This chapter summarizes the research that was carried out in this thesis. In this study, the in-plane shear, compressibility, thermo-physiology and acoustic properties of both warp and weft knitted spacer fabrics were evaluated. The three-dimensional spacer fabric for the cushioning application is considered to create a comfortable material that improves the shear and compression, thermal performance and additionally good noise absorption capability.

The shear behavior of 3D spacer fabrics was investigated by using a picture frame fixture. Three different methods were used to find the shear angle during loading rate of 10mm/min. All the tests were recorded by a CCD monochrome camera. The images acquired during loading process were used for analysis in order to obtain the displacement and shear angles at chosen points on the surface of test specimen. The image analysis procedure can provide much detailed information about the shear behavior of the fabric than stroke measurement. The displacement data, and change in shear angles during loading process can aid in the understanding of the shear behavior of the fabric. The in-plane shear behavior of spacer fabrics are greatly influenced by their surface structures, type of spacer yarn and the fabric stitch density. The outer layer structure affects the monofilament yarn inclination, binding condition with surface, distribution and multifilament stitches in surface layers. The non-linearity of shear deformation increases after limiting locking angle which initiates the buckling of the sample. Overall, work done was higher for the fabrics made up of hexagonal net structure on face side than that of lock knit fabrics and weft spacers. It was also found that spacer fabrics with multifilament spacer yarn have lower work done when compared to other fabrics. Shear stress was higher for the fabrics with coarser spacer yarns among all the fabrics samples. The significant differences in the shear stress-strain curve were obtained in the densification stage. It was due to the inter-surface and spacer layer comes in to closer compaction varies depends on thickness surface structure and spacer yarn properties. Finite element based shear prediction showed good correlation with experimental results.

Compressive behavior, energy absorption and efficiency of both warp and weft knitted spacer fabrics made from different filament spacer yarn were studied. The compression deformation mechanism of the fabric was identified based on the analyses of the compression load-displacement curve. The 3D spacer fabrics were more resilient towards compression stress. Indeed, this structure enables a vertical alignment of spacer yarn; this z axis yarn has the ability to provide maximum compression recovery to the fabric. On the other hand, it has been shown that the spacer fabrics dissipate sufficient energy in compression. Overall it was observed that the compressive energy and efficiency is higher for the thicker spacer fabrics with low density. Also it is found that fabrics with finer spacer yarns show large amount of work done as well as high efficiency during compression mechanism. The spacer fabric with large compressive deformation, high efficiency and energy absorption until plateau stage is the suitable solution for the materials especially for cushions.

The three-dimensional spacer fabric for the cushioning application is considered to create a comfortable material that improves the thermal performance with compression caused by occupants. The knitted spacer fabrics have significant effect on air permeability when the fabric parameters like density, thickness and structure change. The porosity of both structures (lock knit and hexagonal) is almost similar, but significant differences in air-permeability were observed due to its different surface structure. The spacer fabric offers lower thermal conductivity due to the characteristics such as bulkiness, lower density and air layer in the middle part. Also, due to porous and highly permeable nature, the warp knit spacer fabrics have lower thermal conductivity and consequently a lower water evaporative resistance than the weft knitted spacer fabrics. It is also noticed that, hexagonal net fabrics have ability to pass more water vapour than the fabrics with lock knit structure on the surface. The ANOVA confirmed that the thickness and surface structure have significant impact on the thermal comfort properties of spacer fabric. After deeper consideration of all the properties required for mattress, insole, car seats etc. the spacer fabric with hexagonal net structure on the face are recommended due to their optimum water and air permeability with good thermal conductivity.

The sound absorption coefficient of spacer fabrics with different material parameters was measured using impedance tube method. Also the material characteristics which influence the thermo-acoustic behavior were examined carefully using both experimental and theoretical techniques. It has been found that, spacer fabrics made up of monofilament yarns have lower air flow resistance compared to multifilament yarns because of more open structure. Also weft knit spacer fabrics have higher air flow resistivity because of closeness of structure on the outer surface which resists air from passing through the material. The experimental and theoretical investigation has been carried out to find the tortuosity of spacers. The results show there is no significant difference between these two methods. The tortuous path of the material is greatly influenced by small variation in thickness as well as surface property of the materials. The spacer fabrics have too much air in the pores, hence, sound energy dissipation may weaken when the porosity is nearly 0.9. The air flow resistivity is inversely proportional to the porosity of the spacer fabrics; therefore, the sound absorption can increase with decrease in porosity and increases with air flow resistivity. The weft knit spacer fabrics have more tortuous path but still lower sound absorption because incident sound energy may get reflected away from the top layer and does not penetrate in to the fabric. The thickness of the porous material layer has also a great influence on the position of the peak value in the frequency spectrum. But the effect of density and flow resistivity is more predominant in terms of sound absorbency as compared to effect of thickness and tortuosity in case of both warp and weft knit spacer fabrics.

These findings are important requirements for designing knitted spacer fabrics as an innovative cushion material in the applications such as mattress, car seats, pillows insole, back supports etc.

5.1 Scope for Future Work

The ideas, experiments and data generated as part of this research, have added to the knowledge base that could be useful to define the future direction and provide insightful references to researchers. The potential of this research can be realized by pursuing further studies into areas given below:

- The developed FEM model can be extended to other types of spacer fabrics and other properties such as compression, thermo-physiology and acoustic behavior.
- Conduct compression creep study for various spacer fabrics.
- Comparatives study of in-plane shear and compression behavior of both knitted and woven spacer fabrics.
- Develop analytical model to predict compression and shear properties of knitted spacer fabrics, by taking in to account of spacer yarn properties.
- Performing a series of tests with the human subjects in multiple test sessions.
- The image analysis of shear behavior of spacer fabrics can be further improved with suitable function to identify the perfect shear angle after wrinkling.

References

1. Fung, W. and Hardcastle, M.: Product engineering – Interior trim, Textiles in automotive engineering, In: Textiles in automotive engineering. The Textile Institute, 2001, pp 194-211, Woodhead Publishing Limited, ISBN 1 85573 493 1, Cambridge, England
2. Deng, R., Davies, P. and Bajaj. K.: Flexible polyurethane foam modelling and identification of viscoelastic parameters for automotive seating applications. Journal of Sound and Vibrations, 2003, vol. 262, no. 3, 391– 417.
3. Gibson, L. J. and Ashby, M. F.: Cellular Solid Structure and Properties, Pergamon Press, New York, 1988.
4. Pajon, M., Bakacha, M. Pignede, D. and Van, P. Effenterre,: Modeling of P.U. Foam Behavior – Applications in the Field of Automotive Seats, Bertrand Faure Equipments S.A., SAE 960513, International Congress and Exposition Detroit, Michigan, February 1996
5. Blair, G. R., Milivojevich, A. and Van Heumen, J. D.: Automotive Seating Comfort: Investigating the Polyurethane Foam Contribution - Phase I, SAE Paper No. 980656, Detroit, Michigan, 1997.
6. Ebe, K.: Effect of Thickness on Static and Dynamic Characteristics of Polyurethane Foam, International Congress of Noise Control Engineering, Yokohama, 1994.
7. Kolich, M., Essenmacher, S. D. and McEvoy, J. T.: Automotive seating. the effect o f foam physical properties on occupied vertical vibration transmissibility.Journal of Sound and Vibrations, 2005, vol. 281, no. 1– 2, pp. 409–416.
8. Hopkins, J.: A comparative analysis of laminating automotive textiles to foam. Journal of coated fabrics, 1995, 250-267.
9. Pfeifer, R. A.: Evaluation of textile fabric properties Utilized in foam-in-place head restraints. Master Thesis, Eastern Michigan University October 12, 2005.
10. Njeugna, N., Schacher, L., Adolphe, D. C., Schaffhauser, J. B. and Strehle, P.: Development of a New 3D Nonwoven for Automotive Trim Applications, New trends and developments in automotive industry, 323 – 346, January 2011, I SBN: 978 - 953 - 307 - 999 - 8, InTech .
11. Wu, X., Rakheja, S., Boileau, P.: Distribution of human-seat interface pressure on a soft automotive seat under vertical vibration. International Journal of Industrial Ergonomics, 1999, vol. 24, 545-557.
12. Hostens, G. Papajoannou, A., Spaepen, and Ramon, H.: Buttock and back pressure distributio n tests on seats o f mobile agricultural machinery. Applied. Ergonomics, 2001, vol. 32, no. 4, 347– 55..
13. Cengiz, T.G. and Bablik, F. C.: In on -the-road experiment into the thermal comfort of car seats.Applied. Ergonomics, 2007, vol. 38, no. 3, pp. 337– 47.
14. Hilyard, N. C. and Collier, P.: Effect of vehicle seat cushion material on ride comfort, ” Paper presented at Plastic on the Road, The Plastic and Rubber Institute International Conference, London, 1984.

15. Liu, Y. and Hu, H.: Compression property and air permeability of weft□knitted spacer fabrics. Journal of the Textile Institute, 2011, vol. 102, no. 44, 366-372.
16. Liu, Y., Lv, L., Sun, B., Hu, H. and Gu, B.: Dynamic response of 3d biaxial spacer weft-knitted composite under transverse impact. Journal of Reinforced Plastics and Composites, 2006, vol. 25, no.15, 1629-1641.
17. Liu, Y., Hu, H., Zhao, L. and Long, H.: Compression behavior of warp-knitted spacer fabrics for cushioning applications. Textile Research Journal, 2012, vol. 82, no. 1, 11-20.
18. Li, M., Wang, S., Zhang, Z. and Wu, B.: Effect of structure on the mechanical behaviors of three-dimensional spacer fabric composites. Applied Composite Materials, 2008, vol. 16, 1-14.
19. Yip J, and Ng S.: Study of three-dimensional spacer fabrics: Physical and mechanical properties. Journal of Materials Processing Technology, 2008, vol. 206, no. 1-3, 359-364.
20. D. Gross, 3D spacer knit fabrics for medical applications, Journal of Textile Apparel Technology Management. 2003, vol. 4, 26-28.
21. Ionesi, D., Ciobanu, R., Vircan, A., Blaga, M. and Budulan, C.: Three - dimensional knitted fabric with technical destination, Universitatea Tehnică „Gheorghe Asachi" din Iaşi Tomul LVI (LX), Fasc. 3, 2010, 29-37.
22. Ciobanu, L.: Development of 3D Knitted Fabrics for Advanced Composite Materials, Advances in Composite Materials - Ecodesign and Analysis, Dr. Brahim Attaf (Ed.), ISBN: 978-953-307-150-3, 2011, InTech,
23. Bruer, S. H., Powel, N., Smith, G.: Three dimensionally knit spacer fabrics: A review of production techniques and applications, Journal of Textile Apparel Technology Management, 2005, vol. 4, 1-31.
24. Darlington, K. D.: The productions of Raschel crochet fabric, Knit Outwear Times, 1968, vol. 22, 42–45.
25. Wheatley, B.: Development of tricot and Raschel machinery over the past 50 years. Knit Outwear. Times Y'r Bk, 1968, 242-57.
26. http://www.textileworld.com/textile-world/knitting-apparel/2015/03/the-wide-world-of-knits/
27. Palanirajan, T., Ramakrishnan, G., Sundaresan, S. and Kandhavadivu, P.: The influence of fabric parameter on low-stress mechanical properties of polyester warp-knitted spacer fabric. International Journal of Fashion Design, Technology and Education, 2016, http://dx.doi.org/10.1080/17543266.2016.1177738.
28. Liu, Y., and Hu, H., Three-dimensional knitted textiles, Advances in 3D Textiles, Edited by Xiaogang Chen, The Textile Institute, Wood head, Cambride, 125 – 152, 2015.
29. Fung, W. and Hardcastle, M.: Textile and automotive engineering. The Textile Institute, Woodhead Publishing Ltd., 2001
30. Fung, W.: Coated and laminated textile. The Textile Institute, Woodhead Publishing, 2002.

31. Liu, Y., and Hu, H.: Vibration Isolation Performance of Warp-knitted Spacer Fabrics. fiber Society spring conference, Honkong, China, 2011, 23−25 May, 63–64.
32. Smith, G. : Industrial fabric products review. Buyers Guide, 2004, vol. 60, no.10, 42-44.
33. Iyer, C., Mammel, B. and Schach, W.: Circular knitting. Germany: Meisenbach, 1992.
34. Ertekin, G. and Marmarali, A.: Heat, Air and Water Vapor Transfer Properties of Circular Knitted Spacer Fabric.Textil ve Konfeksiyon, 2011, vol. 4, 369-373.
35. Abounaim, M..: Process development for the manufacturing of flat knitted innovative 3D spacer fabrics for high performance composite applications. PhD. Thesis, Technical University of Dresden, Germany, 2011.
36. De Araujo, M., Fangueiro, R., Cataring, A. and Hong, H.: Recent developments in weft - knitting science and technology: the way a head in the new millennium. Revista Romana de Textile - Pielarie, 2001, 1, 61-66, ISSN1453-5424.
37. Liu, Y. P., Hu, H., Long, H., Zhao, L.: Compression behavior of warp-knitted spacer fabrics for cushioning application, Textile Research Journal, 2012, vol. 82, 21-26.
38. Yip J, and Ng S.: Study of three-dimensional spacer fabrics: Physical and mechanical properties. Journal of Materials Processing Technology, 2008, vol. 206, no. 1-3, 359-64.
39. Liu, Y. P., Hu, H., Long, H., Zhao, L.: Impact compressive behavior of warp-knitted spacer fabrics for protective applications, Textile Research Journal, 2012, vol. 82, 773 – 288.
40. Liu, Y., Hu, H. and Au, W. M.: Effect of structural parameters and lamination Protective properties of warp-knitted spacer fabrics under impact in hemispherical form. Part II.Textile Research Journal , 2013, DOI: 10.1177/0040517513495942
41. Machova, K., Klug, P., Waldmann, M., Hoftmann, G. and Cherif, C.: Determining of the bending strength of knitted spacer fabric. Melliand Textilberichte, 2006, vol. 87, no. 6, E93.
42. Arumugam, V., Mishra, R., Militky, J., M. Tunak.: In-plane shear behavior of 3d knitted spacer fabrics. Journal of Industrial Textiles, 2016, vol. 46, 868–886.
43. Xu-hong, M., Ming-qiao, G.: The compression behaviour of the warp knitted spacer fabric. Fibers and Textile in Eastern Europe, 2008, vol.16, no.1, 56-61.
44. Arumugam, V., Mishra, R., Militky, J., Salcova, J.: Investigation on Thermo-physiological and Compression Characteristics of Weft Knitted Spacer Fabrics. Journal of Textile Institute, Epub ahead of print 12 August 2016. DOI: 10.1080/00405000.2016.1220035.
45. Dias, T., Monaragala, R., Needham, P. and Lay, E.: Analysis of sound absorption of tuck spacer fabrics to reduce auto-motive noise.Measurement Science and Technology, 2007, vol. 18, no. 8, 2657–2666.
46. Liu, Y. and Hu, H.: Sound Absorption behavior of knitted spacer fabrics. Textile Research Journal, 2010, vol. 80, no. 18, 1949-1947.
47. Sancak, E.: An Investigations of Sound Absorbance Properties of Weft Knitted Spacer Fabrics. International Journal of Acoustics and Vibration, 2015, vol. 20, no. 1, 36-40.

48. Arumugam, V., Mishra, R., Militky, J. and Novak, J.: Thermo - acoustic Behavior of 3D Knitted spacer fabrics, fibers and Polymers, 2015, vol.16, no.11, 2467-2476.
49. Ye, X., Hu, H. and Feng, X.: Development of the warp knitted spacer fabrics for cushion applications. Journal of Industrial Textiles, 2008, vol. 37, no. 3, 213-223.
50. Machova, K., Hoffmann, G. and Cherif, C.: Micro-climate regulation of clothing systems. Melliand Textilberichte Internat Textile Reports German Incl Yellow Engl Tra, 2006, vol. 87, 11-12.
51. Bagherzadeh, M., Gorji, M., Latifi, P., Payvandy and Kong, L. X.: Evalution of Moisture Management Behavior of High-wicking 3D Warp Knitted Spacer Fabrics. Fibers and Polymers, 2012, vol.13, no.4, 529-534.
52. Ye, X., Hu, H., Feng, X.: Development of the warp knitted spacer fabrics for cushion applications. Journal of Industrial Textiles, 2008, vol. 37, 213-223.
53. Anand, S. C.: Recent advances in knitting technology and knitted structures for technical textiles applications. Proceedings from ISTEK 2003.
54. Ye, X., Fangueiro, R., Hu, H. and Araujo, M.: Application of warp-knitted spacer fabrics in car seats. Journal of Textile Institute, 2007, vol. 98, 337–344.
55. Armakan, D. M. and Roye, A.: A study on the compression behavior of spacer fabrics designed for concrete applications. Fibers and Polymers, 2009, vol. 10, 116–123.
56. Mecit, D. and Roye, A.: Investigation of a testing method for compression behavior of spacer fabrics designed for concrete applications. Textile Research Journal, 2009, vol. 79, 867–875.
57. Savci. S., Curiskis, J. I. and Pailthorpe, M.: Knittability of glass fiber weft-knitted preforms for composites. Textile Research Journal, 2001, vol. 71, 15–21.
58. Abounaim, M., Hoffmann, G., Diestel, O. and Cherif C.: 3D spacer fabric as sandwich structure by flat knitting for composites using hybrid yarn. In: Proceedings of the Autex Conference , Izmir, Turkey, 2009, 675-681.
59. Verpoest, I.: Characterisation and development of 3D knitted composites. Katholieke 78 Universitaet Leuven, Department of Material and Metallurgy Engineering Composite Materials Group,1995;.
60. Phillips, D., Verpoest, I. and van Raemdonck, J.: Optimising the mechanical properties of 3D-knitted sandwich structures. Proceedings of the 11th International Conference on Composite Materials, 14– 18 July 1997, 211– 218.
61. Philips, D. and Verpoest, I.: 3D-knitted sandwich structures: production, properties and prospects. Proc. ECCM-8, 8th European Conference on Composite Materials - Science, Technologies and Applications Vol. 1, Italy, 3-6 June 1998, 543-550.
62. Mecit, D. and Marmarali, A.: Application possibilities of 3d weft knitted spacer fabrics in composite structures, AUTEX 2011, 8-10 June 2011, Mulhouse, France
63. Richard, A. Scott.: Textiles for protection, The Textile Institute, Woodhead Publishing Limited, ISBN 1 85573 493 1, Cambridge, England, 2005.

64. Rothe, D.: Warp knitted s pacer fabric—design and application fields, Knitting Technology, 2001, vol. 4, 14–16.
65. Liu, Y., Au, W. M. and Hu, H.: Protective properties of warp-knitted spacer fabrics under impact in hemispherical form. Part I: Impact behavior analysis of a typical spacer fabric, Textile Research Journal, 2014, Vo l. 84, no. 4, 422–434
66. Guo, X. F., Long, H. R. and Zhao, L.: Investigation on the impact and compression-after-impact properties of warp-knitted spacer fabrics. Textile Research Journal, 2013, vol. 83, 904–916.
67. Oglakcioglu. N. and Marmarali. A.: Thermal comfort properties of some knitted structures. Fibers and Textiles in Eastern Europe, 2007, vol. 15, no. 5 – 6, 64 - 65.
68. Ucar, N., and Yilmaz, T.: Thermal Properties of 1x1, 2x2, 3x3 Rib Knit Fabrics.Fibers & Textiles in Eastern Europe, 2004, vol. 3, no. 47, 34-38.
69. Crina, B., Blaga, M., Luminita, V., and Mishra, R.: Comfort properties of functional weft knitted spacer fabrics. TekstiL Ve Konfeksiyon, 2013, vol. 23, no. 2, 220-227.
70. Pause, B.: Thermo-physiological comfort provided by knitted spacer fabrics.Melliand Textileberichte, 2002, vol. 83, no. 3, 134-136.
71. Krel, V., Hoffmann, G., Offermann, P., Machova, K. and Hes, L.: Spacer fabrics for sports clothing with improved comfort. Melliand Textilberichte, 2005, vol. 86, no. 5, E73.
72. Anand, S., and Rebenciuc, C.: Elaboration of a prediction method of the values for some characteristics of the weft knitted fabrics, In "5th International Conference TEXSCI 2003 Proceedings, Liberec, Czech Republic, 2003.
73. Reisfeld, A.: Warp Knit Engineering. National Knitted Outerwear Association, New York, 1990.
74. Rajendran, S. and Anand, S.: Design and development of novel bandages for compression therapy. British Journal of Nursing, 2003, vol. 12, no. 6, S20-9.
75. Davies, A. and Williams, J.: The use of spacer fabrics for absorbent medical applications. Journal of fiber Bioengineering and Informatics, 2009, vol. 1, no. 4, 321-329
76. Miao, X. H. and Ge, M. Q.: The compression behavior of warp knitted spacer fabric. Fibers and Textiles in Eastern Europe, 2008, vol. 16, 90–92.
77. Ting He.: A Study of Three Dimensional Warp Knits for Novel Applications as Tissue Engineering Scaffolds, A master thesis, NC State University, USA, 2011.
78. Lee, G., Rajendran, S. and Anand, S.: New single-layer compression bandage system for chronic venous leg ulcers. British Journal of Nursing, 2009, vol. 18, no.15, S4-18.
79. Moutos, F. T., Estes, B. T. and Guilak, F.: Multifunctional hybrid three-dimensionally woven scaffolds for cartilage tissue engineering. Macromolecular Bio-science, 2010, vol. 10, no. 11, 1355-64.
80. Moutos, F. T, Freed, L. E. and Guilak, F.: A biomimetic three-dimensional woven composite scaffold for functional tissue engineering of cartilage. Natural Materials, 2007, vol. 6, no. 2, 162-167.

81. Rock, M. and Lohmueller, K.: Three dimensional knit spacer fabric for bed pads. US patent No. 5817391, 1998.
82. Bawadi, S.: Development of the weaving machine and 3D woven spacer fabric structures for lightweight composites materials. PhD Dissertation, Technische Universität Dresden, 2007.
83. Unal, A., Hoffmann, G. and Cherif, C.: Development of weft knitted spacer fabrics for composite materials. Melliand Textileberichte, 2006, vol. 4, 49–50.
84. Abounaim, M., Hoffmann, G., Diestel, O. and Cherif, C.: Thermoplastic composite from innovative flat knitted 3D multi-layer spacer fabric using hybrid yarn and the study of 2D mechanical properties. Composite Science and Technology, 2010, vol. 70, 363–370.
85. Gilbert L, Martin NB and Johanne D. Evaluation of bias-extension and picture-frame test methods for the measurement of intra ply shear properties of PP/Glass commingled fabrics. Compos Struct 2003; 61: 341–352.
86. Willems A, Lomov S, Verpoest I and Vandepitte D. Picture frame shear tests on woven, textile composite reinforcements with controlled pretension. In: 10th Esa form conference on material forming, Parts A and B 2007. 999–1004.
87. Avalle, M., Belingardi, G. and Montanini, R.: Characterization of polymeric structural foams under compressive impact loading by means of energy-absorption diagram. International Journal of Impact Engineering, 2001, vol. 25, 455–472.
88. Mareze, P. H., Becker, R. P., Lenzi, A. and Pellegrini, C.: Rigid-Frame Porous Material Acoustic Attenuation on Compressor Discharge. International Compressor Engineering Conference at Purdue July 16-19, 2012.
89. Fohr, F., Parmentier, D., Castagnede, B. and Henry M,.: An alternative and industrial method using low frequency ultrasound enabling to measure quickly tortuosity and viscous characteristic length, Proceedings of Acoustics, 2008.

List of Publications

List of publications in journals

1. **Veerakumar Arumugam,** Rajesh Mishra, Jiri Militky, Maros Tunak, In-plane shear behavior of 3D knitted spacer fabrics, **Journal of Industrial Textile**, Vol-46, Issue-3, p. 868-886, 2016 . **IF- 1.750. WoS and SCOPUS.**
2. **Veerakumar Arumugam**, Rajesh Mishra, Jiri Militky, Blanka Tomkova**,** Noise attenuation performance of warp knitted spacer fabric. **Textile Research Journal,** Accepted, **IF- 1.443**. **WoS and SCOPUS.**
3. **Veerakumar Arumugam**, Rajesh Mishra, Jiri Militky, Maros Tunak, In-plane shear behavior of 3D warp knitted spacer fabrics. Part II – Effects of structural parameters, **Journal of Industrial Textiles**, Accepted, **IF- 1.750**. **WoS and SCOPUS.**
4. **Veerakumar Arumugam**, Rajesh Mishra, Jiri Militky, Louise Davies & Simon Slater. Thermal and Water vapour Transmission through Porous Warp Knitted 3D Spacer Fabrics for Car Upholstery Applications, **Journal of the Textile Institute,** published June 2017 DOI: 10.1080/00405000.2017.1347023, **IF- 1.128. WoS and Scopus**.
5. **Veerakumar Arumugam,** R Mishra, Jiri Militky and Jan Novak Thermo - acoustic Behavior of 3D Knitted Spacer Fabrics, **Fibres and Polymers**, 2015, Vol.16, No.11, 2467-2476. DOI 10.1007/s12221-015-5602-5. **IF- 1.022. WoS and SCOPUS**
6. **Veerakumar Arumugam**, R Mishra, Jiri Militky and Jana Salcova Investigation on Thermo-physiological and Compression Characteristics of Weft Knitted Spacer Fabrics, **Journal of the Textile Institute**, Epub ahead of print 12 August 2016. DOI: 10.1080/00405000.2016.1220035. **IF- 1.128. WoS and Scopus**
7. **V. Arumugam**, R Mishra & J. Militky: Thermo-physiological comfort properties of 3D spacer knitted fabrics, **International Journal of Clothing Science and Technology**, Vol- 28, No. 3, pp- 328-339, 2016. **IF- 0.418. WoS.**
8. **Veerakumar Arumugam,** Rajesh Mishra, Jiri Militky, Maros Tunak, Blanka Tomkova, Study on in-plane shear performance of spacer fabrics in composite forming, **Materials and Technology**, Accepted, **IF – 0.428**.
9. **Veerakumar Arumugam**, Rajesh Mishra, Jiri Militky, Dana Kremenakova, Blanka Tomkova, Mohanapriya Venkatraman, The compressive Behavior of 3d Weft Knitted Spacer Fabrics Designed for Cushioning Applications. **Journal of Fibre Bioengineering and Informatics**, 10 (2), 117-130, 2017, **in SCOPUS.**
10. **Veerakumar Arumugam**, Rajesh Mishra, Maros Tunak, Jiri Militky, Dana Kremenakova & Mohanapriya Venkatraman. Investigation on Intra-Ply Shear Properties of 3d Weft Knitted Spacer Fabrics by Image Analysis, **Journal of Fibre Bioengineering and Informatics,** accepted September 2016. **in SCOPUS**
11. **Veerakumar Arumugam**, Rajesh Mishra, Jiri Militky, Dana Kremenakova Jana Salacova, Mohanapriya Venkatraman & V. B. Raminisanthi Subramanian. Effect of 3-Dimensional Knitted Spacer Fabrics Characteristics on Its Thermal and Compression

Properties,**Vlakna Textil**, published June 2016. **SCOPUS**

12. **Veerakumar Arumugam,** Rajesh Mishra, Jana Salacova, Mohanapriya Venkatraman, Dana Kremenakova, Hafsa Jamshaid, Tao Yang, Xiaoman Xiong, Kasthuri Venkatesh, Jiri Militky, Functional characteristic evaluation of 3-dimensional knitted spacer fabrics, **Vlakna Textil**, published 2017. **SCOPUS**
13. **Veerakumar Arumugam**, Rajesh Mishra, Jiri Militky, Jana Salacova, Effect of 3-Dimensional Knitted Spacer Fabrics Characteristics on Its Thermal and Compression Properties, **International Journal of Industrial and Manufacturing Engineering**Vol:3, No:3, 2016, **International Science Indexed.**
14. **Veerakumar Arumugam,** Rajesh Mishra, Jiri Militky, Dana Kremenakova, Jana Salacova, Mohanapriya Venkatraman. Study on Compression behavior and energy absorption of Warp knitted spacer fabrics for Cushioning applications, **Journal of Textile Institute**, Under Review, **IF- 1.128.**
15. **Veerakumar Arumugam**, Rajesh Mishra, Jiri Militky, Blanka Tomkova, Dana Kremenakova, Mohanapriya Venkatraman, Study of thermo-physiological properties of 3D warp knitted spacer fabrics for car seat application, **Fibres and Polymers**, Under Review, **IF- 1.022.**
16. **Veerakumar A** and Selvakumar N, "A Preliminary Investigation on Kapok/Polypropylene Nonwoven Composite for Sound Absorption", **Indian Journal of fibre and Textile Research**, Vol. 37, pp. 385 – 388, December 2012. **WoS and SCOPUS.**

List of publications in conferences

1. **Veerakumar Arumugam**, Rajesh Mishra, Jiri Militky, Dana Kremenakova & Mohanapriya Venkataraman, Compression Behavior and Energy Absorption of 3d Weft Knitted Spacer Fabrics, TBIS, May 2017, Wuhan, China
2. **Veerakumar Arumugam**, Rajesh Mishra, Jiri Militky, Mohanapriya Venkatraman, Louise Davies and Simon Slater, Investigation of moisture management properties of 3-dimensional warp knitted spacer fabrics, TRS-IIT, December 2016, New Delhi, India
3. **Veerakumar Arumugam**, Rajesh Mishra, Jana Salacova, Mohanapriya Venkatraman, Dana Kremenakova, Hafsa Jamshaid, Tao Yang, Xiaoman Xiong, Kasthuri Venkatesh, Jiri Militky, Functional characteristic evaluation of 3-dimensional knitted spacer fabrics, STRUTEX December 2016, Liberec, Czech Republic
4. **Veerakumar Arumugam**, Rajesh Mishra, Jiri Militky, Louise Davies and Simon Slater: An analysis on the moisture and thermal protective performance of 3-dimensional knitted spacer fabrics, 3D Fabrics and their Applications, September 8-9, ENSAIT, Roubaix, France, 2016.
5. **Veerakumar Arumugam**, Rajesh Mishra, Vignesh Balaji Ramanisanthi Subramanian, Hafsa Jamshaid and Jiri Militky: Bio-composites Reinforced with Flax, Jute and Glass Fabric: Comparative Study of Static, Dynamic-mechanical and Thermal Properties, 3D

Fabrics and their Applications, September 8-9, ENSAIT, Roubaix, France, 2016.

6. **Veerakumar Arumugam**, Rajesh Mishra, Jiri Militky, Dana Kremenakova, Jana Salacova & Mohanapriya Venkataraman and V. B. Ramanisanthi Subramanian,: Effect of 3-Dimensional Knitted Spacer Fabrics Characteristics on its Thermal and Compression Properties, IFATCC XXIV International Congress, June 13-16,Pardubice, Czech Republic, 2016.
7. **Veerakumar Arumugam**, Rajesh Mishra, Maros Tunak, Jiri Militky, Dana Kremenakova, Mohanapriya Venkataraman and V. B. Ramanisanthi Subramanian,:Investigation on Intra-Ply Shear Properties of 3d Weft Knitted Spacer Fabrics by Image Analysis**,** TBIS-APCC, July 12-15, Melborne, Australia 2016
8. Rajesh Mishra, **Veerakumar Arumugam**, Dana Kremenakova & Jiri Militky,: 3D spacer knitted fabrics with advanced characteristics, 8th International Textile, Clothing & Design Conference – Magic World of Textiles October 02- 05th 2016, Dubrovnik, Croatia
9. **Veerakumar Arumugam**, Rajesh Mishra, Jiri Militky, Dana Kremenakova, Jana Salacova & Mohanapriya Venkataraman : Experimental and analytical investigation on thermal and acoustic behavior of 3d spacer knitted fabrics, 90th Textile Institute Conference, April 25-28, Poznan, Poland, 2016
10. **V. Arumugam**, R Mishra & J. Militky: Effect of material parameters on thermo-physiological comfort properties of 3D spacer knitted fabrics, ITTC 2015, October 14-16, Izmir/Turkey, 2015, ISBN 978-975-441-448-6.
11. **Veerakumar Arumugam**, Rajesh Mishra, Jiri Militky & Mohanapriya Venkatraman: Evaluation of thermo - physiological comfort characteristics of 3-dimensional spacer fabrics, CLOTECH 2015, University of Lodz Poland, ISBN 978-83-7283-671-7.
12. **V. Arumugam**, R Mishra, Analysis of air and water vapour transmission through knitted spacer fabrics, STRUTEX 2014, Decemeber 1-2, Liberec, 2014.
13. **Veerakumar Arumugam**: Thermo-acoustic behavior of 3D knitted spacer fabrics, Workshop Světlanka 2015, 22nd-25thSeptember 2015, Rokytnice nad Jizerou, Czech Republic.
14. **Veerakumar Arumugam**, Rajesh Mishra, Jiri Militky, Jana Salacova: Effect of 3-Dimensional Knitted Spacer Fabrics Characteristics on Its Thermal and Compression Properties, 18th International Conference on Textiles and Fashion, Singapore, SG, March 03-04, 2016.
15. **Veerakumar Arumugam**: Experimental analyses of in-plane shear behavior of 3d spacer fabrics using picture frame fixture, Workshop Světlanka, 16th-19th September 2014, Rokytnice nad Jizerou, Czech Republic.
16. **Veerakumar Arumugam**, Rajesh Mishra, Jiri Militky, Mohanapriya Venkatraman: Studies on 3D knitted spacer fabrics: in plane shear and thermal conductivity, Second International Conference on Industrial Textiles – Products, Applications and Prospects (InduTech 2014) 22nd & 23rd August 2014.
17. **Veerakumar Arumugam**, R Mishra, V Saravanan and Jiri Militky, Braided composites

from glass-polypropylene, ICIC 2014, Coimbatore, 29-30 April 2014, ISBN: 9788192375243.

List of book chapters

1. **Veerakumar Arumugam**, Rajesh Mishra, Dana Křemenáková, Jirí Militký, Mohanapriya Venkatraman and Ludmila Koukolíková, 3D warp knitted spacer fabrics for multifunctional applications, Progress in fibrous material science, ISBN 978-80-87269-40-4, 2014.
2. **Veerakumar Arumugam***, Rajesh Mishra, Jana Salcova, Jiri Militky, Dana Kremenakova, Mohanapriya Venkatraman & Vignesh Balaji Ramanisanthi Subramanian: Assessment of the sound absorptive performance of 3-dimensional knitted spacer fabrics, Recent Developments in Fibrous Material Science,ISBN 978-80-87269-45-9.
3. **Veerakumar Arumugam***, Rajesh Mishra, Jana Salcova, Jiri Militky, Dana Kremenakova, Mohanapriya Venkatraman & Vignesh Balaji Ramanisanthi Subramanian: A study on thermo-physiological comfort behavior of 3-dimensional spacer knitted fabrics, Recent Developments in Fibrous Material Science,ISBN 978-80-87269-45-9.
4. **Veerakumar Arumugam**, Rajesh Mishra, Dana Kremenakova, Jana Salcova, Jiri Militky, Mohanapriya Venkatraman & Vignesh Balaji Ramanisanthi Subramanian: Knitted spacer fabrics – A review on production techniques, Properties and technical application. In Press.
5. **Veerakumar Arumugam**, Rajesh Mishra, Maros Tunak, Jana Salcova, Jiri Militky, Dana Kremenakova, Mohanapriya Venkatraman & Vignesh Balaji Ramanisanthi Subramanian: Investigation on intra-ply shear properties of 3d knitted spacer fabrics by image analysis, In Press.
6. Rajesh Mishra, Jiri Militky, Vijay B aheti, Juan Huang, Bandu Kale, Mohanapriya Venkataraman, Vijay Bele, Veerakumar **Arumugam,** Guochen Zhu, & Yan Wang, (2014): The production, characterization and applications of nanoparticles in the textile industry. Textile Progress, Taylor& Francis, Vol. 46, No. 2, 133 pp.

List of co-authored publications

1. Rajesh Mishra, Jiri Militky, Mohanapriya Venkataraman and **Veerakumar Arumugam** Functional advantages of 3D woven glass nanocomposites, Vlakna a textil, ISSN 1335-0617, Vol:3, 2014.
2. Mohanapriya Venkataraman, Rajesh Mishra, Jiri Militky, **Veerakumar Arumugam**& Srabani Misra, Thermal properties of high performance nonwoven padding fabrics at sub zero temperatures, Vlakna a textil, ISSN 1335-0617, Vol:3, 2014.
3. Mohanapriya Venkataraman, Rajesh Mishra, Jakub Weiner, Adnan Mazari, Jiri Militky, **Veerakumar Arumugam**, Innovative Techniques for Characterization of Nonwoven Insulation Materials Embedded with Aerogel International Journal of Chemical, Nuclear,

Metallurgical and Materials Engineering Vol:8 No:9, 2014.

4. Mohanapriya Venkataraman, Rajesh Mishra, Jiri Militky and **Veerakumar Arumugam**, Acoustic properties of aerogel embedded nonwoven fabrics, NANOCON, November 5-7, Brno, 2014
5. Rajesh Mishra, Mohanapriya Venkatyaraman, **Veerakumar Arumugam**, Jiri Militky and Srabani Misra, Novel techniques to analyze thermal properties of nonwoven padding fabrics at subzero temperatures, TEXCO International conference, Ruzomberok, Slovakia, ISBN 978-80-8075-660-42, 7-28 August 2014.
6. Mohanapriya Venkataraman, Rajesh Mishra, **Veerakumar Arumugam** and Jiri Militky, Thermal analysis of aerogel treated non woven fabrics, fibre society spring conference, May 21-23, 2014.
7. Rajesh Mishra, B K Behera, Mohanapriya Venkataraman, **Veerakumar Arumugam**, Vijay Baheti and Jiri Militky, Green composites from textile waste: Thermo-mechanical characterization, fibre society spring conference, May 21-23, 2014.
8. Mohanapriya Venkataraman, Rajesh Mishra, **Veerakumar Arumugam** and Jiri Militky, Thermodynamics of aerogel treated non woven fabrics, ICIC 2014, Coimbatore , 29-30 April 2014, ISBN: 9788192375243.
9. Mohanapriya Venkataraman, Rajesh Mishra, Jakub Weiner, Adnan Mazari, Jiri Militky, **Veerakumar Arumugam**, Novel Techniques to Analyze Thermal Performance of Aerogel Blankets under Extreme Temperatures, 7th Textile Bioengineering and Informatics Symposium(TBIS), 2014, ISSN:19423438
10. Mohanapriya Venkataraman, Rajesh Mishra, Jakub Wiener, Marie Štěpánková, **Veerakumar Arumugam**, Jiri Militky, Impact of Laser Thermal Irradiation on Kevlar Embedded with Aerogel Particles, STRUTEX 2014, Decemeber 1-2, Liberec, 2014.
11. Mishra Rajesh, Venkataraman Mohanapriya, Kremenakova Dana, Militky jiri, **Veerakumar Arumugam**, Thermal Properties of High Performance Nonwoven Padding Fabrics at Subzero Temperatures, , 7th International Textile, Clothing & Design Conference (ITC&DC) Conference Procedings with citation Index (CPCI-S), Tekstil, ISBN:978-953-7105-54-9, ISSN 1847-7275.
12. Venkataraman Mohanapriya, Mishra Rajesh, Kremenakova Dana, Militky Jiri, **Veerakumar Arumugam**, Thermodynamical characterization of Aerogel Treated Nonwoven Fabrics, 7th International Textile , Clothing & Design Conference (ITC&DC) Conference Procedings with citation Index (CPCI-S), Tekstil, ISBN:978-953-7105-54-9, ISSN 1847-7275.